

**Oligosaccharides production from pea hull fiber using  
carboxylic acid-catalyzed subcritical water systems**

by

Carla Sofía Valdivieso Ramírez

A thesis submitted in partial fulfillment of the requirements for the degree of

Doctor of Philosophy

in

Food Science and Technology

Department of Agricultural, Food and Nutritional Science  
University of Alberta

© Carla Sofía Valdivieso Ramírez, 2021

## ABSTRACT

Production of pea into pea protein concentrates/isolates has dramatically increased due to changing dietary preferences of consumers, generating substantial amounts of pea hull as an underutilized co-product. Recently, pea hull was labelled as a ‘novel fiber’ by Health Canada due to its proven physiological laxative effect associated with its high content of insoluble dietary fiber. However, its soluble dietary fiber fraction has not been studied in terms of its extractability and utilization for the production of value-added functional ingredients like pectic oligosaccharides (POS). POS, an emerging type of prebiotic, have been obtained by enzymatic or chemical partial hydrolysis of pectin. However, the use of multi-enzyme complexes and extended reaction times as well as the low selectivity of chemical treatments are some of the challenges regarding its potential scale up. In this thesis research, the use of aqueous di- and tri-carboxylic acids under subcritical water (sCW) conditions was investigated as a green catalytic reaction medium for pea fiber conversion into POS.

The first two studies, carried out as a proof-of-concept, investigated the catalytic effect of aqueous malic and citric acids at sCW conditions on the hydrolysis of model pectic systems of linear polygalacturonic acid (PolyGalA) and branched rhamnogalacturonan (RG). For the sCW hydrolysis, temperatures of 125-155°C and reaction times of 10 to 120 min were evaluated at constant pH 2.6 using both carboxylic acids and pressure of 100 bar. The HPSEC-RID and HILIC-ELSD analyses of the corresponding hydrolysates showed that *i*) PolyGalA was hydrolysed in the selected sCW reaction medium at relatively low temperatures (125 or 135°C) and short reaction time (30 min), and that its hydrolytic pattern was characterized by poly/oligogalacturonic acid intermediates with a degree of polymerization (DP) of 8-14 that were subsequently hydrolyzed to oligogalacturonides of 2-7 DP, and *ii*) aqueous carboxylic acids at 125°C/100 bar favored cleavage

of neutral sugar residues from the side chains of RG whereas the scission of RG backbone was evident at 135°C/100 bar where fractions of 4.7 kDa, 2.1 kDa and < 1.4 kDa were prevalent. These results demonstrated that sCW+carboxylic acid systems can catalyze the hydrolysis of pectic model substrates into oligosaccharides.

In the third study, sCW+carboxylic acid systems were used to extract the soluble polysaccharides from pea fiber and further hydrolyze them into oligosaccharides. Aqueous citric acid at 120°C/50 bar and 30 min allowed the extraction of 11.8% (g/100 g starting pea fiber) of pea fiber soluble polysaccharides with 17.4% of galacturonic acid content and esterification degree of 50.9%. Then, the addition of citric and malic acids favored break down of the extracted pea pectic substrate into oligosaccharides at temperatures higher than 125°C and 100 bar. However, the yields of released 2 -6 DP gluco-oligosaccharides were the highest (20.4%) at 135°C/100 bar/120 min. In addition, a hydrolytic stepwise pattern was observed for pea fiber soluble polysaccharides in aqueous citric acid at sCW conditions.

The last study focused on the scale up of the process for the sCW production of pea soluble-fiber-derived oligosaccharides at lab scale as well as on the downstream processing of pea soluble-fiber-derived oligosaccharides. Pea soluble-fiber-derived oligosaccharides were successfully produced on a large-scale (600 mL reactor) as their chemical composition and yield were not compromised. Further concentration of oligosaccharides was achieved by tangential-flow ultrafiltration followed by conventional freeze and spray drying and pressurized gas-expanded liquid drying to obtain pea soluble-fiber-derived oligosaccharides in powder form.

Overall, the findings provide new insights about the use of carboxylic acid-catalyzed sCW systems within a potential pea hull fiber biorefinery as well as for valorization of similar pectin-rich agro-industrial co-products.

## PREFACE

This thesis is an original work done by Carla Sofia Valdivieso Ramírez under the supervision of Dr. Marleny D.A. Saldaña and Dr. Feral Temelli. This thesis has seven chapters. In Chapter 1, the rationale of this research and its objectives are presented. Chapter 2 includes a literature review on structure, functionality, characterization, and manufacture of pectin and pectic oligosaccharides.

Chapter 3 is *In Press* as Carla S. Valdivieso Ramirez, Jose Edwin Sanchez, Michael Gänzle, Feral Temelli and Marleny D.A. Saldaña. Carboxylic acid-catalysed hydrolysis of polygalacturonic acid in subcritical water in the *Journal of Supercritical Fluids* (2020). As the first author, I was responsible for the experimental design, performing the experiments, analytical characterization, data analysis, modeling and writing the first draft of the manuscript. Dr. Sanchez helped with modifications of the Parr reactor and the kinetic modeling. Dr. Saldaña, Dr. Temelli, and Dr. Gänzle provided insightful comments on discussion of results as well as in the revision of the manuscript. Dr. Saldaña is the corresponding author, who was responsible for the experimental design, revisions, and submission of the manuscript.

Chapter 4 was submitted to the *Journal of Supercritical Fluids* for consideration for publication as Carla S. Valdivieso Ramirez, Feral Temelli and Marleny D.A. Saldaña. Carboxylic acid-catalysed hydrolysis of rhamnogalacturonan in subcritical water media. As the first author, I was responsible for the experimental design, performing the experiments, analytical characterization, data analysis and writing the first draft of the manuscript. Dr. Saldaña and Dr. Temelli provided insightful comments on discussion of experimental design and results as well as in the revision of the manuscript. Dr. Saldaña is the corresponding author and was responsible for the experimental design, revisions, and submission of the manuscript.

Chapter 5 was submitted for consideration for publication as Carla S. Valdivieso Ramirez, Feral Temelli and Marleny D.A. Saldaña. Production of soluble pea fiber-derived oligosaccharides using subcritical water with carboxylic acids. As the first author, I was responsible for the experimental design, performing the experiments, analytical characterization, data analysis and writing the first draft of the manuscript. Dr. Saldaña and Dr. Temelli provided insightful comments on discussion of experimental design and results as well as in the revision of the manuscript. Dr. Saldaña is the corresponding author and was responsible for the experimental design, revisions, and submission of the manuscript.

Chapter 6 dealt with the scale-up of soluble pea fiber-derived oligosaccharides production, and further downstream processing and drying of soluble pea fiber hydrolysates, and in Chapter 7, key findings and suggestions for future work were summarized.

*This thesis is dedicated to my beloved parents Nelly and Luis for being examples of love, kindness, righteousness, and dedication to me and to my kind-hearted siblings, Linda and Santiago.*

## ACKNOWLEDGEMENTS

I would like to thank my Lord almighty for the everyday blessing and care during this amazing scientific and life-enriching journey.

I am forever grateful to my dear supervisors Dr. Marleny D.A. Saldaña and Dr. Feral Temelli for their support, kind care, insightful advice, and guidance throughout my PhD studies. Thank you very much for encouraging me to keep up and for being my inspiration to bring out my best and love for what I do.

I am deeply thankful to Dr. Michael Gänzle, Dr. Kelvin Lien and Dr. Curtis for providing guidance and invaluable help with the analytical methods and instrumentation required to complete my research studies.

I feel blessed and very thankful to all my friends, colleagues, and professors whom I was able to meet during these years. You are like a second family to me! Once again, thanks to all of you who made my PhD studies a wonderful and enjoyable life experience.

I would like to thank Alberta Innovates, Alberta Pulse Growers and New Leaf Essentials Ltd. (2017F083R), and Natural Sciences and Engineering Research Council of Canada (NSERC, #04371-2019, Discovery Grant of Dr. Saldaña) for their financial support to conduct this research. I also thank Dr. Mehmet C. Tulbek from AGT Food and Ingredients Inc. (Saskatoon, SK, Canada) for providing the pea hull fiber concentrate.

## TABLE OF CONTENTS

Chapter 1: Introduction and thesis objectives .....	1
Chapter 2: Literature review .....	6
2.1 Introduction.....	6
2.2 Pectic polysaccharides .....	7
2.2.1 Structure.....	7
2.2.2 Sources and functionality.....	10
2.2.3 Subcritical water for extraction and hydrolysis .....	12
2.3 Pectic oligosaccharides .....	15
2.3.1 Definition and functionality.....	15
2.3.2 Homogeneous acid catalysis .....	16
2.3.3 Production and characterization.....	19
2.3.4 Purification of pectic oligosaccharides .....	22
2.3.5 Drying of pectic oligosaccharides.....	28
Chapter 3: Carboxylic acid-catalysed hydrolysis of polygalacturonic acid in subcritical water medium .....	34
3.1 Introduction.....	34
3.2 Materials and Methods.....	36
3.2.1 Materials .....	36
3.2.2 Subcritical water hydrolysis of polygalacturonic acid.....	36
3.2.3 Characterization of the hydrolysates.....	40
3.2.3.1 Molecular weight distribution of polygalacturonic acid hydrolysates.....	40
3.2.3.2 Determination of oligogalacturonides in polygalacturonic acid hydrolysates.....	40
3.2.4 Kinetics and modelling of polygalacturonic acid hydrolysis.....	42
3.2.5. Statistical analysis.....	45
3.3 Results and discussion .....	46
3.3.1 Molecular weight distribution of polygalacturonic acid hydrolysates.....	46
3.3.2 Oligogalacturonides distribution in polygalacturonic acid hydrolysates.....	49
3.3.3 Kinetics and modelling of polygalacturonic acid hydrolysis.....	58
3.4 Conclusions.....	61
Chapter 4: Carboxylic acid-catalyzed hydrolysis of rhamnogalacturonan in subcritical water medium .....	62

4.1 Introduction.....	62
4.2 Materials and Methods.....	63
4.2.1 Materials .....	63
4.2.2 Subcritical water hydrolysis of rhamnogalacturonan .....	64
4.2.3 Characterization of rhamnogalacturonan hydrolysates.....	65
4.2.3.1 Fourier transform infrared (FT-IR) spectroscopy analysis .....	65
4.2.3.2 Molecular weight distribution.....	65
4.2.3.3 Determination of oligosaccharides .....	66
4.2.3.4 Neutral sugar analysis .....	66
4.3 Results and discussion .....	67
4.3.1 Characterization of rhamnogalacturonan by ATR-FTIR analysis.....	67
4.3.2 Characterization of rhamnogalacturonan hydrolysates.....	71
4.3.2.1 Molecular weight distribution.....	71
4.3.2.2 Determination of oligosaccharides .....	82
4.4 Conclusions.....	89
Chapter 5: Production of soluble pea fiber-derived oligosaccharides using subcritical water with carboxylic acids .....	90
5.1 Introduction.....	90
5.2 Materials and Methods.....	93
5.2.1 Materials .....	93
5.2.2 Characterization of raw material.....	93
5.2.2.1 Proximate composition analysis .....	93
5.2.2.2 Total starch and dietary fiber analyses.....	94
5.2.2.3 Neutral sugars analysis .....	94
5.2.2.4 Galacturonic acid analysis .....	95
5.2.3 Subcritical water extraction and characterization of soluble polysaccharides from pea fiber.....	96
5.2.3.1 sCW extraction.....	96
5.2.3.2 Characterization of sCW pea fiber extract and residue .....	98
5.2.3.2.1 Fourier transform infrared (FT-IR) spectroscopy analysis .....	98
5.2.3.2.2 Morphology analysis.....	98
5.2.3.2.3 Degree of esterification analysis.....	100

5.2.4 Subcritical water hydrolysis of pea fiber soluble polysaccharides into oligosaccharides and their characterization.....	101
5.2.4.1 sCW hydrolysis.....	101
5.2.4.2 Characterization of sCW hydrolysates.....	102
5.2.4.2.1 Molecular weight distribution.....	102
5.2.4.2.2 Determination of oligosaccharides .....	102
5.3 Results and discussion .....	103
5.3.1 Pea fiber characterization.....	103
5.3.2 Subcritical water extraction of soluble polysaccharides from pea hull fiber.....	105
5.3.3 Characterization of pea hull fiber soluble polysaccharides extract and residue .....	107
5.3.3.1 Morphology analyses .....	107
5.3.3.2 ATR-FTIR and degree of esterification analyses .....	109
5.3.3.3 Neutral sugars and galacturonic acid contents.....	110
5.3.4 Characterization of subcritical water hydrolysates of pea hull fiber soluble polysaccharides.....	112
5.3.4.1 Molecular weight distribution.....	112
5.3.4.2 Determination of oligosaccharides .....	115
5.4 Conclusions.....	121
Chapter 6: Scale-up of soluble pea fiber-derived oligosaccharides production and drying .....	123
6.1 Introduction.....	123
6.2 Materials and Methods.....	124
6.2.1 Materials .....	124
6.2.2 Production of soluble pea fiber-derived oligosaccharides .....	125
6.2.2.1 Subcritical water hydrolysis scale-up .....	125
6.2.2.2 Purification.....	127
6.2.3 Characterization of pea soluble fiber hydrolysate .....	128
6.2.3.1 Molecular weight distribution analysis.....	128
6.2.3.2 Free sugars analysis .....	128
6.2.3.3 Neutral oligosaccharides analysis.....	129
6.2.4 Drying of soluble pea fiber-derived oligosaccharides .....	130
6.2.4.1 Preparation of dried powders .....	130
6.2.4.1.1 Spray drying.....	130
6.2.4.1.2 Pressurized Gas eXpanded liquid (PGX) drying .....	131

6.2.4.1.3 Freeze drying .....	133
6.2.4.2 Characterization of hydrolysate powders.....	133
6.2.4.2.1 Morphology and water activity .....	133
6.2.4.2.2 Differential scanning calorimetry analysis .....	133
6.2.4.2.3 X-ray diffraction analysis .....	134
6.3 Results and discussion .....	134
6.3.1 Production of soluble pea fiber-derived oligosaccharides .....	134
6.3.1.1 sCW hydrolysis scale-up and neutral oligosaccharides determination.....	134
6.3.1.2 Characterization of sCW hydrolysate .....	138
6.3.1.2.1 Molecular weight distribution and free sugars analyses .....	138
6.3.1.3 Purification.....	140
6.3.2 Drying of soluble pea fiber-derived oligosaccharides .....	141
6.3.2.1 Preparation of dried powders .....	141
6.3.2.2 Characterization of powders .....	144
6.3.2.2.1 Morphology and water activity .....	144
6.3.2.2.2 Differential scanning calorimetry analysis .....	147
6.3.2.2.3 X-ray diffraction analysis .....	151
6.4 Conclusions.....	152
Chapter 7: Conclusions and recommendations.....	154
7.1 Summary of key findings.....	154
7.2 Recommendations.....	161
References.....	163

## LIST OF TABLES

<b>Table 2.1.</b> Extracted rhamnogalacturonans and rhamnogalacturonan-derived fragments. ....	11
<b>Table 2.2</b> Pectic oligosaccharides obtained by hydrothermal hydrolysis of agricultural by-products and pectic substrates.....	21
<b>Table 2.3.</b> Membrane processes for purification and concentration of oligosaccharides and pectic oligosaccharides.....	26
<b>Table 2.4.</b> Effect of carrier agents on yield and $T_g$ of spray-dried oligosaccharides. ....	29
<b>Table 3.1.</b> Effects of temperature and reaction media on polygalacturonic acid hydrolysis at 100 bar/ 60 min. ....	55
<b>Table 3.2.</b> Arrhenius activation energy and rate constants for polygalacturonic acid hydrolysis with citric acid at 125 or 135°C and 100 bar. ....	59
<b>Table 4.1.</b> Molar sugar composition (%) of soybean pectic fragments.....	68
<b>Table 4.2.</b> Released sugars during hydrolysis of rhamnogalacturonan at 135°C, 145°C and 155°C/100 bar/60 min with aqueous citric acid or water. ....	80
<b>Table 5.1.</b> Proximate composition and neutral sugars profile of pea fiber used in this study. ..	104
<b>Table 5.2.</b> Neutral sugars, galacturonic acid and macro-components of pea fiber soluble polysaccharides extracted under sCW. ....	111

## LIST OF FIGURES

**Fig. 2.1.** Chemical structure of pectic fragments: a) homogalacturonan, b) xylooligogalacturonan, c) rhamnogalacturonan-I backbone, and d-e) rhamnogalacturonan side chains. Arrows in colors indicate the action site of pectin-degrading enzymes. Endo-PG: endo-polygalacturonase, exo-PG: exo-polygalacturonase, PME: pectin methylesterase, XGH: xylogalacturonan hydrolase; exo-/endo-RGH: exo/endo RG-galacturonohydrolase, endo-A: endo-arabinases, AF: arabinofuranosides, and exo- $\beta$ -/endo- $\beta$ -GA: endo- $\beta$ -1,4/exo- $\beta$ -1,4 galactanases (Adapted from Bonnin et al. 2014)..... 9

**Fig. 2.2.** Subcritical water region. Colored squares represent some sCW conditions used for pectin extraction from various biomass reported in the literature (Muñoz-Almagro et al., 2019; Ueno et al., 2008; Valdivieso-Ramirez, 2016; X. Wang et al., 2014). Squares in orange (pomegranate rind), in grey (cacao pod), in yellow (citrus flavedo), and in green (apple pomace). ..... 13

**Fig. 2.3.** Temperature dependence curves of the dielectric constant (1), density (2), and ionic product of water (3) at a constant pressure of 240 bar. Source: A A Galkin, V V Lunin, "Subcritical and supercritical water: a universal medium for chemical reactions ", Russ Chem Rev, 2005, 74 (1), 21–35, DOI: <https://doi.org/10.1070/RC2005v074n01ABEH001167>, Reprinted with permission from Turpion-Moscow Ltd., Moskow, Russia.)..... 14

**Fig. 2.4.** Chemical structure of oligogalacturonides..... 16

**Fig. 2.5.** Acid-catalysed hydrolysis of digalacturonic acid by specific-acid catalysis ..... 18

**Fig. 2.6.** Ultrafiltration (UF) coupled to nanofiltration (NF) for oligosaccharides purification... 23

**Fig. 2.7.** Phase diagram of CO<sub>2</sub>–EtOH–H<sub>2</sub>O obtained at 40°C and pressures of 100, 200 and 300 bar reported by Durling et al. (2007) (Reprinted with permission from Elsevier Inc.). ..... 32

**Fig. 3.1.** Parr 4590 system with a 100 mL batch stirred reactor..... 37

**Fig. 3.2.** Temperature and pressure profiles of the Parr reactor set at 125°C/100 bar over 120 min. .... 39

**Fig. 3.3.** Proposed reaction mechanism for polygalacturonic acid hydrolysis under scW conditions. PGa<sub>(n>14)</sub> = polygalacturonic acid with a DP higher than 14, Ga<sub>(8-14)</sub> = poly/oligogalacturonic acids with 8-14 DP, Ga<sub>(2-7)</sub> = oligogalacturonic acid with 2-7 DP and Ga = galacturonic acid monohydrate. .... 42

<b>Fig. 3.4.</b> HPSEC-RID chromatograms of polygalacturonic acid hydrolysates obtained in aqueous citric acid at 125°C/100 bar and reaction times of: a) 10 min, b) 20 min, c) 30 min, d) 40 min, and e) 60 min, and different reaction media: f) aqueous malic acid, and g) water.....	47
<b>Fig. 3.5.</b> Effect of reaction time (10-120 min) on polygalacturonic acid hydrolysis in aqueous citric acid at 100 bar and temperatures of: a) 125°C, and b) 135°C analyzed by HILIC-ELSD. Scale of Fig. 3.5b is 2:1 with respect to Fig. 3.5a. ....	50
<b>Fig. 3.6.</b> HILIC-ELSD chromatograms of polygalacturonic acid hydrolysates obtained at: a) 125°C and b) 135°C, 100 bar and 60 min in different reaction media: 1) aqueous citric acid, 2) aqueous malic acid, and 3) water. ....	53
<b>Fig. 3.7.</b> O-glycosidic bonds $\alpha$ -GalA-(1→4)- $\alpha$ -GalA-(1→2)- $\alpha$ -Rha-(1→4)- $\alpha$ -GalA in polygalacturonic acid. ....	54
<b>Fig. 3.8.</b> Experimental concentrations of released poly/oligogalacturonic acid fragments in aqueous citric acid and their yields at: a) 125°C/100 bar, and 135°C/100 bar. The insets show the yield of poly/oligogalacturonides at 125°C and 135°C. ....	57
<b>Fig. 3.9.</b> Kinetics of polygalacturonic acid hydrolysis with aqueous citric acid at 100 bar predicted by the model at: a) 125°C, and b) 135°C. ....	60
<b>Fig. 4.1.</b> ATR-FTIR spectra of rhamnogalacturonan, polygalacturonic acid and low methoxyl pectin.....	70
<b>Fig. 4.2.</b> HPSEC-RID molecular weight distribution profiles of rhamnogalacturonan hydrolysates obtained in aqueous citric acid at 125°C/100 bar and reaction times of: a) 0 min, b) 10 min, c) 20 min, d) 30 min, e) 40 min, and f) 60 min. Ex <sub>L</sub> : column exclusion limit, and P <sub>L</sub> : column permeation limit. ....	72
<b>Fig. 4.3.</b> Released sugars during rhamnogalacturonan hydrolysis with aqueous citric acid at 125°C/100 bar over 60 min of reaction. ....	73
<b>Fig. 4.4.</b> HPSEC-RID molecular weight distribution profiles of rhamnogalacturonan hydrolysates obtained in aqueous citric acid at 135°C/100 bar and reaction times of: a) 0 min, b) 10 min, c) 20 min, d) 30 min, e) 40 min, f) 60 min, and different reaction media of: g) malic acid, and h) water. Ex <sub>L</sub> : column exclusion limit, and P <sub>L</sub> : column permeation limit. ....	75
<b>Fig. 4.5.</b> Sugars released during rhamnogalacturonan hydrolysis with aqueous citric acid at 135°C/100 bar over 120 min of reaction. ....	77

<b>Fig. 4.6.</b> HPSEC-RID elution profiles of rhamnogalacturonan hydrolysates obtained at 145°C and 155°C/100 bar/60 min within different reaction media: a-c) aqueous citric acid, and d) water. EX <sub>L</sub> : column exclusion limit, and P <sub>L</sub> : column permeation limit. ....	78
<b>Fig. 4.7.</b> Rhamnogalacturonan hydrolysates obtained at 145°C and 155°C/100 bar/60 min within different reaction media: A-C) aqueous citric acid, and D) water. ....	82
<b>Fig. 4.8.</b> Effect of reaction time (10-120 min) on rhamnogalacturonan hydrolysis in aqueous citric acid at 100 bar and temperatures of: a) 125°C and b) 135°C, analyzed by HILIC-ELSD. ....	83
<b>Fig. 4.9.</b> HILIC-ELSD chromatograms of rhamnogalacturonan hydrolysates obtained at 135°C/100 bar/60 min in different reaction media. Glu stands for 2–10 DP gluco-oligosaccharides that elute at the same time as galacto-oligosaccharides. ....	86
<b>Fig. 4.10.</b> Schematic representation of a proposed multi-stage sequential hydrolysis of rhamnogalacturonan with aqueous citric acid at 135°C/100 bar within 120 min of reaction. ....	88
<b>Fig. 5.1.</b> Extraction of soluble polysaccharides from pea fiber under sCW conditions with aqueous 0.2% w/w citric acid at 120°C/50 bar/30 min. ....	99
<b>Fig. 5.2.</b> Scanning electron microscopy images of: (a, b) pea fiber and (c, d) pea fiber residue after sCW extraction with aqueous citric acid at 120°C/50bar/30 min. Scale bars represent 10µm in a) and c), and 1µm in b) and d). ....	108
<b>Fig. 5.3.</b> Helium ion microscopy images of sCW pea fiber dried extract. Scale bars represent 5µm in (a), and 1µm in (b). ....	108
<b>Fig. 5.4.</b> ATR-FTIR spectra of sCW pea fiber extract and standards of rhamnogalacturonan, arabinogalactan and low methoxyl pectin. ....	109
<b>Fig. 5.5.</b> HPSEC molecular weight distribution profile of pea fiber soluble polysaccharides hydrolysates obtained in aqueous citric acid at 125°C/100 bar and reaction times of: a) 0 min, b) 30 min, c) 60 min, and d) 120 min. EX <sub>L</sub> : column exclusion limit, and P <sub>L</sub> : column permeation limit. ....	113
<b>Fig. 5.6.</b> Effect of reaction time (10-120 min) on pea fiber soluble polysaccharides hydrolysis in aqueous citric acid at 100 bar and 2-6 DP gluco-oligosaccharides yield (insets) at temperatures of: a) 125°C and b) 135°C analyzed by HILIC-ELSD. ....	116
<b>Fig. 5.7.</b> HILIC-ELSD chromatograms of pea fiber soluble polysaccharides hydrolysates obtained at 100 bar and 60 min in different reaction media at a) 135°C, b) 145°C and 155°C. (GluOS: gluco-oligosaccharides).....	118

<b>Fig. 5.8.</b> HILIC-ELSD chromatograms of hydrolysates obtained with citric acid at 135°C, 100 bar and 60 min from linear polygalacturonic acid (Chapter 3), branched rhamnogalacturonan-I (Chapter 4), and pea fiber soluble polysaccharides. ....	121
<b>Fig. 6.1.</b> Scheme for the production, drying and characterization of soluble pea fiber-derived oligosaccharides. ....	126
<b>Fig. 6.2.</b> Scheme of the spray drying process of the soluble pea fiber sCW hydrolysate .....	132
<b>Fig. 6.3.</b> Heating and pressure profiles of the Parr 4590 system set at 155°C/100 bar up to 80 min using reactor vessels of 100 mL and 600 mL volume. ....	135
<b>Fig. 6.4.</b> Yield of individual and total gluco-oligosaccharides present in the sCW hydrolysates obtained at 155°C/100 bar/60 min using a reactor vessel of 100 mL (black square) and 600 mL (red circle). ....	137
<b>Fig. 6.5.</b> HPSEC-RID elution profiles of pea soluble fiber hydrolysate obtained at 155°C/100 bar/60 min using a reactor vessel of 600 mL (orange), and xylo-oligosaccharide standard (blue). ....	139
<b>Fig. 6.6.</b> Recovery of free sugars in the retentate and permeate obtained by ultrafiltration of pea soluble fiber sCW hydrolysate using a 1 kDa membrane for 7 h. ....	141
<b>Fig. 6.7.</b> Dry powders obtained from soluble pea fiber sCW hydrolysate (containing pea fiber-derived oligosaccharides) using a) spray drying, b) PGX drying, and c) freeze drying. ....	143
<b>Fig. 6.8.</b> Scanning electron microscopy images of dry powders from pea fiber-derived oligosaccharides obtained by a) spray drying, b) freeze drying, and c) PGX drying. Scale bars represent 50 µm in a1) and c1), 100 µm in b1), 10 µm in a2-c2), and 5µm in a3-c-3). ....	145
<b>Fig. 6.9.</b> DSC thermograms of dried sCW hydrolysates obtained by: a) freeze drying, b) spray drying, and c) PGX drying. ....	148
<b>Fig. 6.10.</b> XRD diffraction pattern of sCW hydrolysate powders obtained by spray drying (orange), freeze drying (black) and PGX drying (blue). ....	151
<b>Fig. 7.1.</b> Scheme of proposed integrated sCW process for the production of pea soluble fiber-derived oligosaccharides followed by ultrafiltration (UF) and drying. ....	160

## ABBREVIATIONS

AG-I	Arabinogalactan type I
AG-II	Arabinogalactan type II
A-I	Arabinan type I
Arb	Arabinose
ATR	Attenuated total reflection germanium crystal cell
$a_w$	Water activity
DE	Degree of esterification
DP	Degree of polymerization
DSC	Differential scanning calorimetry
ELSD	Evaporative light scattering detector
FT-IR	Fourier transform infrared spectroscopy
Fuc	Fucose
GalA	Galacturonic acid
Glu	Glucose
GluOS	Gluco-oligosaccharides
GRAS	Generally recognized as safe solvents
HG	Homogalacturonan
HILIC	Hydrophilic interaction liquid chromatography
HIM	Helium ion microscopy
HPSEC	High pressure size exclusion chromatography
NF	Nano filtration
PG	Polygalacturonase
PGX	Pressurized gas-expanded liquid
POS	Pectic oligosaccharides
RG-I	Rhamnogalacturonan-I
RG-II	Rhamnogalacturonan-II
Rha	Rhamnose
RID	Refractive index detector
SAS	Supercritical anti-solvent

SC-CO <sub>2</sub>	Supercritical carbon dioxide
sCW	Subcritical water
SEDS	Solution enhanced dispersion by subcritical fluids
SEM	Scanning electron microscopy
TGA	Thermogravimetric analysis
UF	Ultra filtration
XG	Xylogalacturonan
XRD	X-ray diffraction
Xyl	Xylose

## **Chapter 1: Introduction and thesis objectives**

Industrial processing of pea into pea protein concentrate and pea protein isolate has dramatically increased worldwide due to consumers emerging dietary preferences towards high-quality plant-based protein. As such, leading companies in the pea protein market, such as Cosucra (Warcoing, Pecq, Belgium), Roquette Freres (Lestrem, France) and Cargill Inc. (Wayzata, MN, USA) have been investing on the expansion of their processing facilities as well as opening new manufacturing plants in Denmark, Canada and USA, respectively (Ahuja and Mamtani, 2020). Production of pea protein, however, generates substantial amounts of underutilized pea hulls as a co-product after the dehulling process (90 kg of hull/ton whole pea) (Ali-Khan, 1993). Efforts have been made towards valorization of this co-product, and pea hull was labelled as a ‘novel fiber’ by Health Canada in 2017 due to its proven physiological laxative effect (Health-Canada, 2017). This physiological effect has been mainly associated to the high content of insoluble dietary fiber present in pea hull. Conversely, the soluble dietary fiber fraction that is also present in pea hull has not been studied yet in terms of its extractability and further depolymerization to obtain value-added products like pea soluble fiber-derived oligosaccharides with potential prebiotic and health-promoting effects.

Recent studies on the structure of soluble polysaccharides extracted from the hull and cell wall of cotyledon of the Leguminosae family members, such as pea and soybean, have revealed the presence of pectic polysaccharides, including rhamnogalacturonan-I (Huisman et al., 2001; Nakamura et al., 2014). In general, pectic polysaccharides embrace a complex and heterogeneous group of acidic polysaccharides characterized by their D-galacturonic acid content, including linear homogalacturonan and branched rhamnogalacturonan-I and rhamnogalacturonan-II (Seymour and Knox, 2002). Pectic polysaccharides, also known as pectin, are classified as soluble

dietary fiber and its utilization has been widely reported in the food industry due to its gelling property. Commercial pectin production, however, has been limited to hot diluted mineral acid extraction from a few agro-industrial co-products, such as citrus pulp, apple pomace and sugar beet pulp. Therefore, commercial extraction of pectin from legume co-products, for example, from pea hulls using emerging technologies and generally recognized as safe (GRAS) solvents, is of great interest; however, the literature lacks information in this regard.

Pectic oligosaccharides (POS) can be obtained by partial breakdown of pectin. The POS are comprised of 2 to 10 monosaccharide units (Moss et al., 1995). Recently, POS have been considered as an emerging type of prebiotic (Babbar et al., 2016; Gullón et al., 2013) due to their strong bifidogenic effect and fermentability in the distal part of the colon in contrast to commercial prebiotics that are prone to be fermented in the proximal colon (Tingirikari, 2018).

Enzymatic, chemical and hydrothermal treatments have been used for partial breakdown of pectic substrates into POS (Babbar et al., 2016). Nonetheless, the use of multi-enzyme mixtures and extended reaction times, the use of inorganic acids and its further neutralization as well as the high temperatures and low selectivity are some of the limitations of these methods. Lately, subcritical water (sCW) technology has been explored as an eco-friendly alternative for the extraction of pectin from agro-industrial co-products (i.e., cacao pod husk, and apple pomace) within short extraction times and without the use of inorganic acids (Muñoz-Almagro et al., 2019; Ueno et al., 2008). Likewise, the use of binary solvent systems such as aqueous citric acid and aqueous ethanol under sCW conditions (120°C/50 bar/30 min) has been also reported to extract pectic polysaccharides from pomegranate rinds (Valdivieso-Ramirez, 2016). In addition, fast sCW hydrolysis of model polygalacturonic acid into POS (oligogalacturonides) has been reported at 180°C-260°C/100 bar/2 min (Miyazawa and Funazukuri, 2004). Although sCW medium has

shown potential to catalyze hydrolytic reactions, selectivity control in such catalytic reactions is still a challenge. Therefore, research is needed on selective catalysis under sCW conditions to obtain POS of targeted chemical composition or degree of polymerization.

The use of aqueous organic acids has been explored as an alternative to inorganic acids in homogeneous catalysis to obtain fermentable sugars from lignocellulosic biomass (Lu and Mosier, 2007). Kim et al. (2013), for example, evaluated the catalytic effect of di-carboxylic acids, such as maleic and oxalic acids versus sulfuric acid on the hydrolysis of hardwood-derived xylo-oligosaccharides into xylose at temperatures of 140-180°C/30 h. It was reported that upon hydrolysis of xylo-oligosaccharides into xylose, aqueous di-carboxylic acids prevented further xylose dehydration to furfural in contrast to sulfuric acid. Thus, it was suggested that aqueous di-carboxylic acids were more selective towards xylose compared to sulfuric acid at temperatures higher than 140°C (Kim et al., 2013). Also, reduced degradation rates of arabinose in aqueous maleic and fumaric acids at 150°C and 170°C/60 min have been reported compared to that in water at either 150°C and 170°C, indicating that the addition of dicarboxylic acids can potentially modify the selectivity in reactions where water at high temperature was used as a reaction medium (Kootstra et al., 2009). Hence, the potential selectivity of di-carboxylic acids for glycosidic bond cleavage has been related to the acidic nature of the core active site of glycosyl hydrolases family (i.e. polygalacturonases and cellulases) as they harbor two amino acids with a carboxylic acid group on their side chain (aspartic and glutamic acids) that facilitate cleavage of the susceptible glycosidic bond via general acid catalysis (Palanivelu, 2006). Nonetheless, dicarboxylic acid-catalyzed hydrolysis under sCW conditions has not been yet investigated for POS manufacture from neither model pectic compounds nor agro-industrial co-products. In addition, due to the complexity of the pectic substrates and the heterogeneous chemical composition of the

hydrolysates that result from their hydrothermal treatment, downstream processes are required for POS isolation and drying. Membrane filtration and spray drying have been reported for purification and drying of various oligosaccharides, respectively (Akin et al., 2012; Aghashahi, 2019; Wrzosek et al., 2013); however, there are limited studies on the membrane purification of POS and no study has been reported on the spray drying of POS.

Overall, no studies focusing on integrated eco-friendly processes for conversion of pectin-rich agro-industrial co-products into dried powders of bioactive pectic oligosaccharides have been reported, and more research is needed to better understand the effect of di-carboxylic acids under sCW conditions on the hydrolysis of pectic substrates. Therefore, it was hypothesized that i) sCW technology can favor extraction of soluble fiber from pea hulls and its further hydrolysis into pectic oligosaccharides, and ii) aqueous di- and tri-carboxylic acids under mild sCW conditions can exert a catalytic effect on hydrolytic cleavage of glycosidic bonds of pectic substrates but minimize monosaccharides degradation.

The overall objective of this research was to study the hydrolysis of pea soluble fiber into pectic-oligosaccharides using sCW with the addition of carboxylic acids as well as to evaluate the use of ultrafiltration for purification and different drying methods to obtain pectic-oligosaccharides in powder form. To accomplish this goal, the specific objectives were:

- i) To investigate whether aqueous di- or tri-carboxylic acids at sCW conditions exert a catalytic effect on the hydrolysis of a model system of linear polygalacturonic acid into oligogalacturonides as well as to determine the kinetics and propose a hydrolysis mechanism (Chapter 3),

- ii) To study the effects of aqueous di- and tri-carboxylic acids at sCW conditions, temperature, and reaction time on the hydrolysis of a model system of branched rhamnogalacturonan into POS (Chapter 4),
- iii) To investigate the effect of aqueous di- and tri-carboxylic acids at various sCW conditions and reaction times on the hydrolysis of pea soluble fiber into POS (Chapter 5), and
- iv) To perform a scale up for sCW production of pea soluble fiber-derived oligosaccharides at lab scale as well as to evaluate ultrafiltration for their purification, and spray drying, freeze drying and pressurized gas-expanded liquid (PGX) drying to obtain POS in powder form (Chapter 6).

## **Chapter 2: Literature review**

### **2.1 Introduction**

Pectic polysaccharides are commercially referred to as pectin and, its use as a hydrocolloid is widely known in the food industry. Also, as pectin is a water soluble dietary fiber, its recognized health claims include the reduction of post-prandial glycaemic response, maintenance of normal blood cholesterol level and increased satiety (Paulionis et al., 2015). Besides, since pectin was first isolated from apple juice by Vauquelin in 1790, research on its fine chemical structure, biochemistry, applications and sources is still ongoing (Ciriminna et al., 2015). Modified pectin, for example, has recently drawn the attention of pharmaceutical industry due to its potential anti-cancer activity, in particular as a natural anti-metastatic compound (Leclere et al., 2013). Modified pectin refers to pectin that has been treated by enzymatic, chemical, or physical means to reduce its molecular weight ( $< 25$  kDa) and tailor its monosaccharide composition to enhance its bioactivity (Staples and Rolke, 2015). Likewise, pectic oligosaccharides originating from partial depolymerization of pectin has been shown to be a potential new class of prebiotic due to its enhanced bifidogenic effect compared to its parent high molecular weight molecule (Olano-Martin et al., 2002). Such effect has been associated to pectic oligosaccharides' low molecular weight, simplified structure and low steric hindrance, which facilitate the action of bacterial enzymes located in the distal part of the colon (Tingirikari, 2018). In addition, alternative pectin sources to citrus peel and apple pomace have been explored, including various agricultural by-products like coffee bean residues, prickly pear peels, sunflower heads, soybean hull, etc. (Ciriminna et al., 2015; Nesterenko et al., 2004). Furthermore, the potential pectin production from orange peel residues biorefinery has also been reported (Balu et al., 2012).

Based on the above, this literature review is focussed on pectin's structure, functionality, and extraction as well as on pectic oligosaccharides' manufacture (hydrolysis, purification and drying) and characterization. In addition, homogeneous acid catalysis and the use of subcritical water technology as an eco-friendly method for biomass conversion are reviewed.

## **2.2 Pectic polysaccharides**

### **2.2.1 Structure**

Pectic polysaccharides are naturally found in the middle lamella and primary cell walls of vascular plants; however, their content can vary according to the plant species (Mohnen, 2008; Voragen et al., 2009). For example, pectic polysaccharides in primary cell wall of dicotyledonous (i.e. apples, oranges and tomatoes) and non-gramineous monocotyledonous plants (i.e. onion and asparagus) can be up to 35%, whereas in woody tissue pectic polysaccharides can be up to 5% (Mohnen, 2008). Pectic polysaccharides are crucial for various plant physiological processes such as growth, hydration, ion transport, fruit ripening, defense towards plant pathogens, etc. (Voragen et al., 2009). Their vital roles within the plant can be related to their versatile structure, known as the most complex among the plant cell wall components. This structurally complex and heterogeneous group of polysaccharides are characterized by their D-galacturonic acid component as well as neutral sugars such as D-galactose, L-arabinose, D-xylose and L-rhamnose. Homogalacturonan (HG), rhamnogalacturonan-I (RG-I) and rhamnogalacturonan-II (RG-II) have been reported as the major pectic structural fractions (Seymour and Knox, 2002). The HG structure is a linear polymer of (1→4)-linked D-galacturonic acid residues (Fig. 2.1a) that can be partially methyl-esterified at C-6 position or O-acetyl-esterified; however, it can also be xylosylated at O-3 position, in which case it is referred to as xylogalacturonan (XG) (Fig. 2.1b). RG-I is a branched structure with a backbone comprised of the repeating disaccharide [→2)-α-L-rhamnose-(1→4)-α-

D-galacturonic acid-(1→]n (Fig. 2.1c). In RG-I structure, the rhamnose residues can be linked at O-4 position to linear or branched arabinans ( $\alpha$ -L-arabinose-(1→5) backbone) (Fig. 2.1d) and/or to galactans ( $\beta$ -D-galactose-(1→4) backbone), which can be also partially substituted with  $\alpha$ -L-fucose residues (Buffetto et al., 2015). In addition, RG-I can also include arabinogalactans as sugar side chains (Fig. 2.1e). Arabinogalactans (AG) are also branched structures containing either a (1→4)- $\beta$ -D-Galp backbone (AG-I) or a (1→3)- $\beta$ -D-Galp backbone (AG-II). AG-I can be substituted at its O<sub>6</sub> or O<sub>3</sub> positions with monomeric  $\alpha$ -L-Araf residues or (1→5)- $\alpha$ -L-Araf linked oligosaccharides, whereas arabinosylated (1→6)- $\beta$ -D-Galp side chains substituted with  $\alpha$ -L-Araf bearing L-Fucp residues are found in AG-II (Buffetto et al., 2015; Choct et al., 2010; Mikshina et al., 2015). Nonetheless, the RG-II, is the most complex pectic structure with a backbone of nearly nine (1→4)-D-galacturonic acid units surrounded by branched side chains, which include approximately 12 different and rare saccharides such as 2-O-methyl xylose, 2-O-methyl fucose, aceric acid, 2-keto-3-deoxy-D-lyxo-heptulosaric acid and 2-keto-3-deoxy-D-manno-octulosonic acid (Ochoa-Villarreal et al., 2012; Seymour and Knox, 2002).

Although the major pectic structures have been generally defined, they can vary depending on the type of substrate (i.e., fruits, vegetables, legumes, or agro-industrial by-products), and the extraction method employed (i.e. chemical, enzymatic, or hydrothermal). As reviewed by Bonnin et al. (2014), various enzymes with different acting sites are needed to cleave the linkages within the complex pectic structures. For example, pectin methylesterases are used to release methanol from methyl-esterified HG whereas endo- and exo-polygalacturonases, pectin and pectate lyases lead to HG depolymerization (Fig. 2.1a).



For depolymerization of RG-I, however, enzymes with acting sites on the RG backbone (i.e. RG-hydrolase and RG-galacturonohydrolase) as well as on the side sugar chains (i.e. endo- and exo-arabinases, arabinofuranosidases, and endo- $\beta$ -1,4 and exo- $\beta$ -1,4 galactanases) are required (Figs. 2.1c-2.1e).

### **2.2.2 Sources and functionality**

The importance of pectin extraction and production relies on its valuable functional and physiological properties. In general, commercial pectin is used in a wide range of applications in the food industry due to its gelling property (Thakur et al., 1997). Such pectin, however, is characterized by its high galacturonic acid content (> 65%) and its exclusively extracted from apple pomace or citrus peel. Also, pectin consumption has shown to have health promoting effects as it is a soluble dietary fiber, such as cholesterol reduction as well as anticancer activity (Leclere et al., 2013; Nesterenko et al., 2004). In addition, pectin has been also explored as a potential biocompatible material for tissue engineering and drug delivery systems as reviewed earlier (Bačáková et al., 2014; Ghai et al., 2012; Munarin et al., 2012). Moreover, as pectin has a saccharide-rich structure due to the rhamnogalacturonans component, it has recently been considered as a promising substrate for the production of bioactive compounds as summarized in Table 2.1. According to Table 2.1, rhamnogalacturonans from various sources such as ginseng, green tea, pumpkin, starfruit, soybean, potato, and potato residues have been isolated, and some of them further hydrolyzed to obtain bioactive polysaccharides, such as arabinogalactans and galactans with diverse bioactivity.

**Table 2.1.** Rhamnogalacturonans and rhamnogalacturonan-derived fragments extracted from different sources reported in the literature.

Plant substrate	Extraction conditions	Pectic structure	Bioactivity	Ref.
Ginseng pectin	0.1 M NaOH/4°C/4 h Endo-PG/50°C/2 h	RG-I, RG-II		(Sun et al., 2019)
Green pepper	H <sub>2</sub> O/100°C/2 h Fehling solution	RG-I (AG-I and AG-II)		(do Nascimento et al., 2017)
Green tea leaves	H <sub>2</sub> O/100°C/2 h	AG-II	anti-diabetic effect	(Wang et al., 2015)
Potato RG-I	RG-lyase/37°C/48 h	RG-I fragment	elicitor activity <sup>a</sup>	(Jiménez-Maldonado et al., 2018)
Potato tuber	0.2 M Na <sub>2</sub> CO <sub>3</sub> +10 mM NaBH <sub>4</sub> /4°C/24 h Endo-PG/35°C/24 h	RG-I		(Øbro et al., 2004)
Potato waste	Endo-PG+oxalic acid/42°C/18 h	RG-I		(Byg et al., 2012)
Prunes	H <sub>2</sub> O/100°C/2 h Fehling solution	RG-I (AG-I)	gastro-protective effect	(Cantu-Jungles et al., 2014)
Pumpkin	1M NaOH	RG-I fragment	galectin-3 inhibitor <sup>b</sup>	(Zhao et al., 2017)
Soybean meal	H <sub>2</sub> O/100°C/2 h	AG-I	gastro-protective effect	(Cipriani et al., 2009)
Starfruit	10% NaOH+ NaBH <sub>4</sub> /100°C/2 h Fehling solution	RG-I (A-I, AG-I)		(Leivas et al., 2015)
Sugar-beet pulp	0.1 M HCl/80°C/72 h	RG-I oligomers		(Renard et al., 1997)

A-I: arabinan type I, AG-I: arabinogalactan type I, PG: polygalacturonase, AG-II: arabinogalactan type II, RG-I: rhamnogalacturonan-I, RG-II: rhamnogalacturonan-II,

<sup>a</sup>Elicitor: molecules that trigger the hypersensitivity response in the plant.

<sup>b</sup>Galectin-3: lectin associated with cancer metastasis.

Agro-industrial co-products from legumes, however, have not been explored as potential sources for commercial production of pectin. In Canada, for example, production of peas as an economic field crop has reached 4.2 million tons in 2019, where Alberta accounted for 41% of the pea production (Canadian Grain Commission, 2020). Peas are valued due to their high-quality protein contents (Nosworthy et al., 2017; Wu et al., 2018); however, the industrial manufacture of pea protein generates substantial amounts of underutilized pea hull as a co-product after the

dehulling process (90 kg hull/ton whole pea) (Ali-Khan, 1993). As pea hull contains a soluble fiber fraction (Reichert, 1981), it is a promising available source for pectin production that is worth to investigate further.

### **2.2.3 Subcritical water for extraction and hydrolysis**

Extraction process is required to isolate pectic polysaccharides or pectin from plant cell walls as they are not in free form but interacting with lignocellulosic and cellulosic material. To overcome some drawbacks associated with the conventional pectin extraction methods, such as the use of mineral acids and further neutralization of the effluents or the use of multienzyme mixtures and extended reaction times, subcritical water (sCW) technology has been explored as an eco-friendly alternative (Valdivieso-Ramirez, 2016). In sCW technology, pressurized liquid water at temperatures between its boiling point (100°C) and its critical point (374°C/221 bar) (Fig. 2.2) is used as a solvent for extraction and as a reaction medium for acid-base catalyzed reactions due to its different physicochemical properties compared to those of hot water at atmospheric pressure (Mollër, et al. 2011). For example, increasing temperature and pressure within the subcritical water region induces structural changes, leading to the disruption of the hydrogen bond network of water and modifying its solvent properties, where its dielectric constant ( $\epsilon$ ) and density ( $\rho$ ) decrease while its ionic product ( $K_w$ ) increases as illustrated in Fig. 2.3 (Galkin and Lunin, 2005). Such reduction in the dielectric constant of water with temperature facilitates solvation of compounds with a broad range of polarity (Galkin and Lunin, 2005; Maguire and O'Donoghue, 2015; Rogalinski et al., 2008; Saldaña and Valdivieso-Ramírez, 2015; Zhao and Saldaña, 2019); whereas, the reduction in density influences the other properties of water like viscosity, heat capacity, and thermal conductivity, which in turn enhance the transport phenomena in aqueous solutions (Galkin and Lunin, 2005). Moreover, as the ionic product of water increases with

temperature and pressure, subcritical water is not limited to act as a protic solvent (source of  $H^+$ ) but also as a self-neutralizing (source of  $OH^-$ ) acid-base catalyst, facilitating ionic reactions including acidic and basic catalysis that involve charged intermediates (i.e., hydrolysis and dehydration reactions) (Galkin and Lunin, 2005; Marshall and Frank, 1981; Park and Park, 2002). Besides, increased ionic strength (a measure of the concentration of ions) and reduced pH have been associated with the increasing ionic product of water in the subcritical water region, and therefore to its catalytic effect (Plaza and Turner, 2015). Likewise, the addition of inorganic and organic acids or bases in sCW can also alter its ionic strength (concentration of ions) and subsequently enhance its catalytic effect (Moll er, et al. 2011; Salak and Yoshida, 2006).

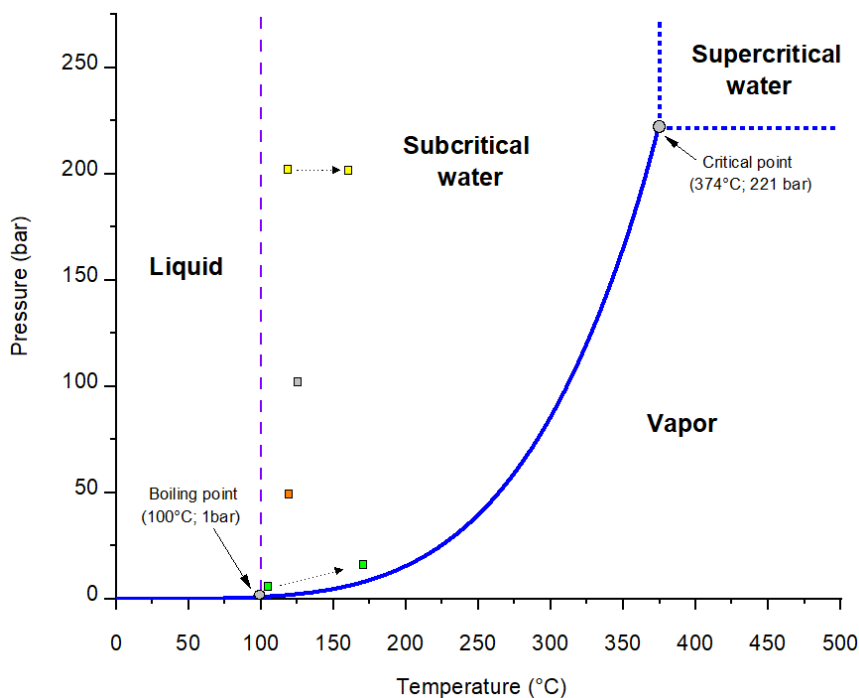


**Fig. 2.2.** Subcritical water region. Colored squares represent some sCW conditions used for pectin extraction from various biomass reported in the literature (Mu oz-Almagro et al., 2019; Ueno et al., 2008; Valdivieso-Ramirez, 2016; X. Wang et al., 2014). Squares in orange (pomegranate rind), in grey (cacao pod), in yellow (citrus flavedo), and in green (apple pomace).

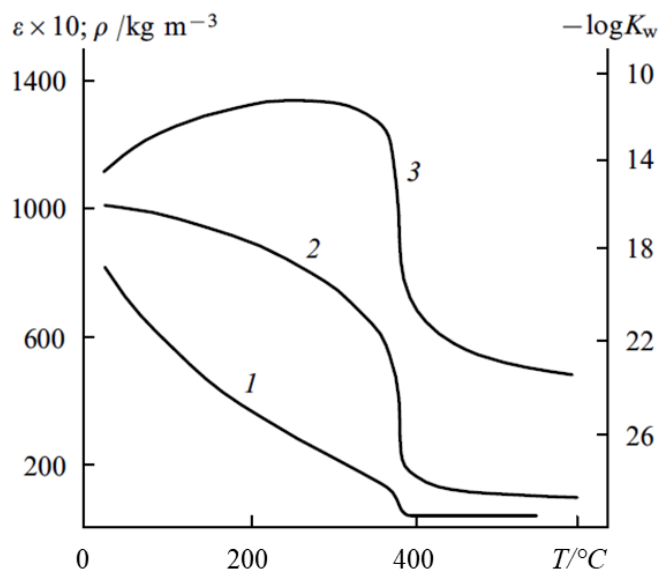


**Fig. 2.3.** Temperature dependence curves of the dielectric constant (1), density (2), and ionic product of water (3) at a constant pressure of 240 bar. Source: Galkin, A and Lunin, V. *Subcritical and supercritical water: a universal medium for chemical reactions*, Russ Chem Rev, 2005, 74 (1), 21–35. DOI: <https://doi.org/10.1070/RC2005v074n01ABEH001167>. (Reprinted with permission from Turpion-Moscow Ltd., Moskow, Russia)

The sCW water medium, in contrast to superheated steam (steam at a temperature higher than the boiling point of water), exhibits moderate enthalpy and entropy at relatively low temperature that can facilitate control of selectivity in reactions as in homogeneous acid catalysis (i.e., hydrolysis of polysaccharides). Conversely, superheated steam at the same moderate temperature exhibits considerably higher enthalpy due to its latent heat of condensation as well as entropy compared to those of sCW, which could make selectivity control of catalytic reactions involving superheated steam more challenging.

Extraction of pectin from various fruit biomass under different sCW conditions has been reported, such as pomegranate peel, cacao pod husk, *Citrus junos* flavedo, and apple pomace/citrus peel at 120°C/50 bar/30 min, 121°C/103.4 bar/30 min, 120-160°C/200 bar and 100-170°C/5 min, respectively (Muñoz-Almagro et al., 2019; Ueno et al., 2008; Valdivieso-Ramirez, 2016; Wang et

al., 2014). The sCW extraction conditions used in these studies were depicted in Fig. 2.2 to provide an insight about the sCW region that has been explored for pectin extraction from fruit residues. Nonetheless, sCW extraction of pectic polysaccharides from legume residues like the hulls has not been yet explored. The use of sCW as a reaction medium to hydrolyze pectic substrates into pectic oligosaccharides is detailed later in Section 2.3.3.

## **2.3 Pectic oligosaccharides**

### **2.3.1 Definition and functionality**

Oligosaccharides are defined by the IUPAC as saccharides with generally 2 to 10 monosaccharide units linked together by glycosidic bonds (McNaught, 1996). In the case of pectic oligosaccharides (POS), however, it can be inferred that the saccharides containing 2 to 10 units are pectin derived. POS are generally obtained from partial depolymerization of pectin. Consequently, due to the complexity of pectin structure, POS can be grouped into acidic POS (homogalacturonan derived) and neutral POS (rhamnogalacturonan derived). Acidic POS are referred to as oligogalacturonides (OGalA) (Fig. 2.4), while neutral POS are classified according to the neutral sugar backbone, such as arabino-oligosaccharides (AraOS), galacto-oligosaccharides (GOS), and oligorhamnogalacturonides (ORham) (Onumpai et al., 2011).

Pectic oligosaccharides have been shown to have *in vitro* and *in vivo* prebiotic and biological effects as reviewed earlier (Babbar et al., 2016; Gullón et al., 2013; Holck et al., 2014). It was reported that POS enzymatically obtained from high and low-methoxyl apple pectin exhibited protective properties towards Shiga-like toxins from *Escherichia coli* O157:H7 in the human colonic cell line HT29 (Olano-Martin et al., 2003), while POS from carrots exhibited anti-adhesive properties towards *E. coli* in uroepithelial cells (Guggenbichler et al., 1997). Likewise, POS were reported to have an *in vitro* anti-proliferative effect on human colonic adenocarcinoma HT29 cells

(Olano-Martín et al., 2003) and a cholesterol-lowering effect in mice (Li et al., 2010). In addition, among the POS, AraOS obtained from sugar beet pulp have been shown to have an *in vitro* selective bifidogenic effect on human gut microbiota (Holck et al., 2011). Conversely, OGalA has been reported as an anti-aging agent in dermatological care (Lubrano et al., 2004). Besides the benefits that OGalA can exert in humans, OGalA has been also shown to be beneficial for plants due to its shoot growth stimulating effect, as a plant elicitor (pathogen signal metabolites that trigger plant defenses) and natural fungicide (Suzuki et al., 2002; Van Aubel et al., 2014).

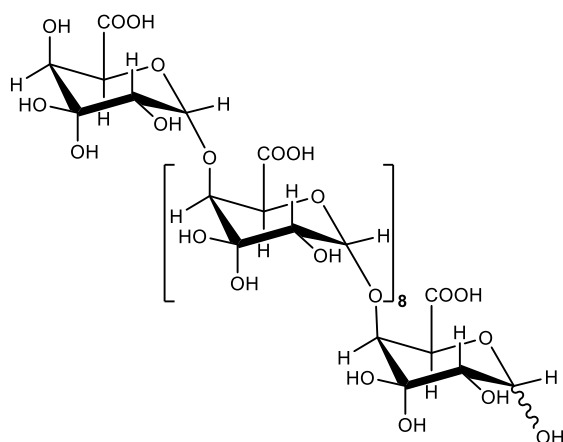


**Fig. 2.4.** Chemical structure of oligogalacturonides.

### 2.3.2 Homogeneous acid catalysis

A catalytic process aims to increase the rate of a chemical reaction by the means of a catalyst. Catalysts are defined by the IUPAC as compounds that increase the rate of a reaction without modifying the overall standard free-energy change ( $\Delta G^\circ$ ) in the reaction (Moss et al., 1995). In homogeneous catalysis, the catalyst and the reactants are in the same phase, commonly gas or liquid. Protic acids in solution are widely used in homogeneous catalysis, especially in organic chemistry, as they can catalyse various reactions, such as hydrolysis, dehydration, substitution,

elimination, and rearrangements (Molnár, 2011). Among protic acids are sulfuric, hydrochloric and trifluoroacetic acids. In homogeneous acid catalysis, the reactions are initiated by a proton transfer reaction and according to the proton transfer rate, the catalytic mechanism can be described by either the specific-acid catalysis or the general-acid catalysis pathway. Specific-acid catalysis is common for strong acids in polar solvents (fast proton transfer), whereas general-acid catalysis can occur for weak acids (slow proton transfer) and during enzymatic reactions (Molnár, 2011).

Pectic polysaccharides, as other polysaccharides, are comprised of a large number of monosaccharide units linked together via glycosidic bonds. A glycosidic bond, however, is a type of acetal bond as it is formed between the OH group of the anomeric carbon of a hemiacetal or hemiketal function of a cyclic sugar or a saccharide, and the OH group of another saccharide, which results in the formation of an acetal, and the release of one water molecule. Consequently, the hydrolysis of a glycosidic bond can resemble that of an acetal or ketal. Acetals and ketals are stable in neutral or basic conditions, but they are susceptible to nucleophilic attack in acidic conditions, so its hydrolysis is generally acid catalyzed. Likewise, hydrolysis of polysaccharides is also an acid-catalyzed reaction (Biermann, 1988; Cordes and Bull, 1974).

Based on the above, Fig. 2.5 summarizes the possible mechanism of the acid catalyzed hydrolytic cleavage of an  $\alpha$ -(1→4) glycosidic bond between two D-galacturonic acid residues, commonly found in pectic substrates. According to this mechanism of catalysis, the oxygen involved in the glycosidic bond is first protonated by a strong acid in solution prior to the nucleophilic attack of water on the carbocation, leading to an oxonium ion that is further deprotonated by water, generating the monomeric galacturonic acid.

The use of protic acids such as hydrochloric, nitric and trifluoroacetic acids as catalysts has been reported to hydrolyze pectic substrates into low molecular weight pectic fragments and pectic oligosaccharides (Cano et al., 2020). However, controlling the catalytic activity of such strong acids to minimize degradation products is still a challenge. Therefore, the use of weak acids as homogeneous catalysts for controlled hydrolytic cleavage of different glycosidic bonds present in pectic substrates could be of great interest.

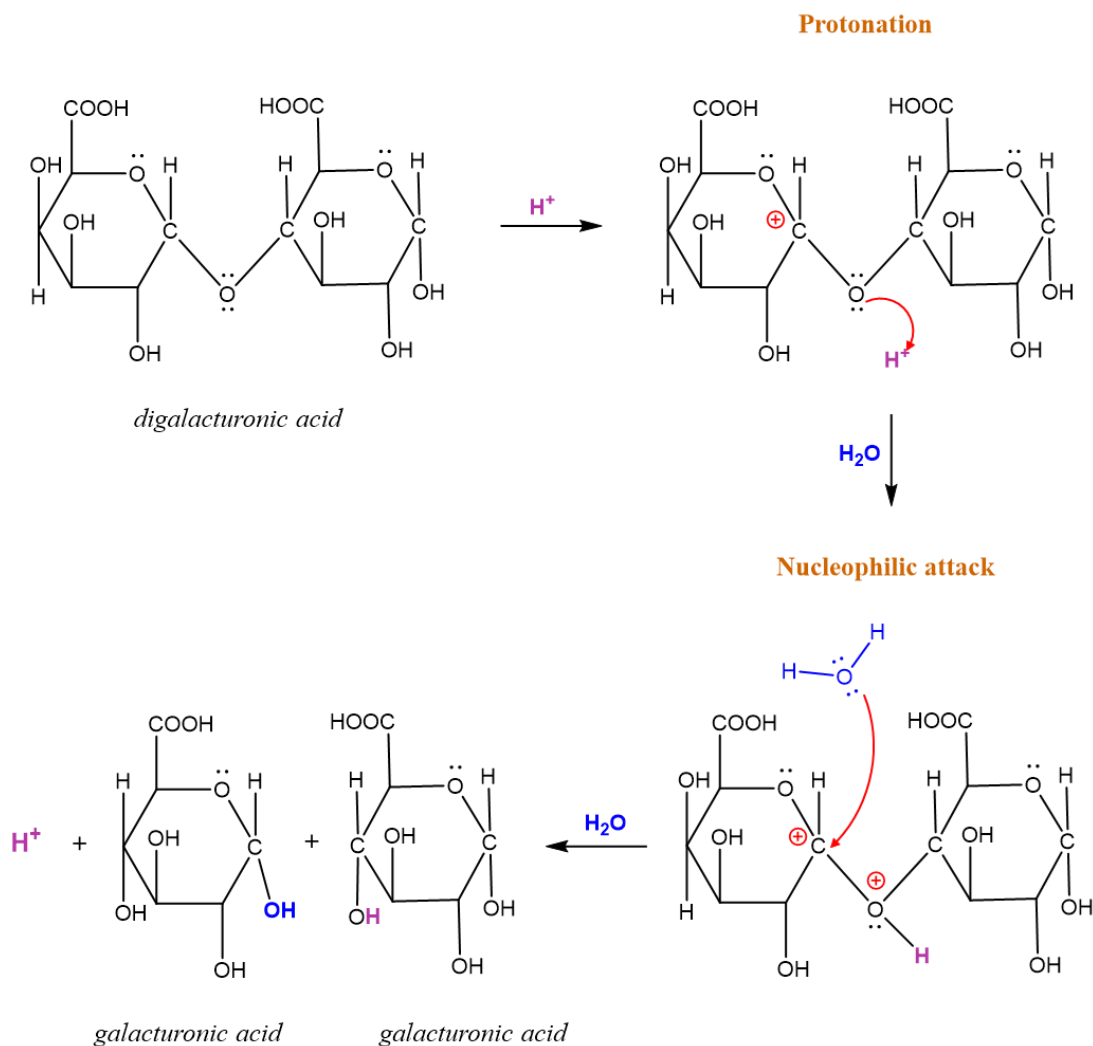


**Fig. 2.5.** Acid-catalysed hydrolysis of digalacturonic acid by specific-acid catalysis

### 2.3.3 Production and characterization

Pectic oligosaccharides have been produced at lab scale mostly by enzymatic and/or chemical partial hydrolysis of various pectic substrates as reviewed earlier (Babbar et al., 2016; Gullón et al., 2013). Enzymatic treatments were characterized by the use of complex mixtures of homogalacturonan- and rhamnogalacturonan-degrading enzymes together with long reaction times, whereas the chemical treatments involved the use of mineral acids (HCl, HNO<sub>3</sub> or TFA) or bases as homogeneous catalysts to enhance hydrolysis of the pectic substrates. Mineral acids as catalysts, however, lack the selectivity favoring not only hydrolytic cleavage of glycosidic bonds but side dehydration reactions. Nonetheless, efforts has been made to improve the selectivity of the homogeneous acid catalysts and studies on the use of di- and tri-carboxylic acids for hemicellulosic biomass hydrolysis into fermentable sugars have been performed (Kim et al., 2013; Kootstra et al., 2009; Lu and Mosier, 2007). These studies have found that indeed aqueous di-carboxylic acids were more selective towards sugars rather than towards degradation products compared to the conventional sulfuric acid. The product selectivity of the catalyst is referred to as the yield ratio of the desired product to the undesired product (Butt, 1964). Recently, the potential selectivity of di-carboxylic acids towards glycosidic bond cleavage has been related to the acidic nature of the core active site of glycosyl hydrolases family (i.e. polygalacturonases and cellulases) as they harbor two amino acids with a carboxylic acid group on their side chain (aspartic and glutamic acids) that facilitate cleavage of the susceptible glycosidic bond via general acid catalysis (Palanivelu, 2006). Nonetheless, dicarboxylic acid-catalyzed hydrolysis under sCW conditions has not been yet investigated for POS manufacture from neither model pectic compounds nor agro-industrial co-products.

Hydrothermal treatments have been also explored as an eco-friendly alternative to chemical hydrolysis for POS production from agro-industrial residues as summarized in Table 2.2. According to Table 2.2, neutral and acidic POS have been obtained by either steam at 170°C or pressurized hot water at a temperature range of 150-260°C within short reaction times. Also, reactors with a range of volumes of 125 mL to 100 L were tested, suggesting its potential for scale-up. Besides hydrothermal treatments, the use of dynamic high-pressure micro-fluidization (Chen et al., 2013) and photochemical reaction (UV/TiO<sub>2</sub>) (Burana-Osot et al., 2010) has been also reported for POS production.

POS have been obtained from diverse pectic substrates, including pure citrus and apple pectins as well as agricultural residues such as orange and passion fruit peels, sugar beet and potato pulps, bergamot peel and onion skins as reviewed by Gómez et al. (2014). However, agro-industrial co-products from legumes, for example, from pea hull have not been explored as a potential pectic substrate for POS production.

Due to the complexity of the resulting pectic hydrolysates, various analytical techniques have been employed for POS characterization and quantification (Table 2.2). Among such techniques, high performance liquid chromatography (HPLC) with *p*-aminobenzoic ethyl ester pre-derivatization was used for the quantification of released neutral sugars and galacturonic acid. Also, semi-preparative ion exchange chromatography (IEC) and adsorption chromatography using Amberlite XAD-16 resin were reported for the separation of neutral POS from acidic POS prior to their quantification by either high-performance anion-exchange chromatography with pulsed amperometric detection (HPAEC-PAD) or hydrophilic interaction liquid chromatography with evaporative light scattering detection (HLIC-ELSD).

**Table 2.2** Pectic oligosaccharides obtained by hydrothermal hydrolysis of agricultural by-products and pectic substrates.

Substrate	Reactor system (volume)	Hydrolytic conditions		Characterization method	Conversion	Ref.
		Temperature/time	Pressure			
Olive pomace	Batch (100 L)	170°C <sup>a</sup> /15 min	3 -10 bar	HPLC (ABEE) Adsorption-XADC HPSEC ESI-MS/MS	13.8% OGalA (> 3 kDa)	(Lama-Muñoz et al., 2012)
Passion fruit peel	Batch (0.125 L)	100-245°C 150°C/4.5 min <sup>b</sup> 175°C/5.5 min <sup>b</sup>	n.r.	HPLC (PMP) HPSEC	21% OS <sup>c</sup> 0.9% 5-HMF	(Klinchongkon et al., 2017)
Lemon waste peel	Batch (3.5 L)	150-180°C <sup>d</sup> Ro:161-1038 min	n.r.	HPAEC-PAD LP-IEC	18.3% OGalA 4.9% AraOS 1.9% GOS	(Gómez et al., 2013)
Orange waste peel	Batch (3.5 L)	160°C <sup>d</sup> Ro: 326 min	n.r.	IEC HPLC-RID HPAEC-PAD HPSEC HILIC-ELSD MALDI-TOF-MS GC	37.8% OGalA 18% AraOS 12% GOS	(Gómez et al., 2014)
Polygalacturonic acid	Semi-batch	180-260°C/2 min	100 bar	HPLC-RID ESI-TOF	22.1% OGalA 11.4% DP 1	(Miyazawa and Funazukuri, 2004)

a: steam, b: optimum conditions, c: total neutral and acidic oligosaccharides, d: autohydrolysis (10-35 bar), Ro: severity factor in min, OS: oligosaccharides, OGalA: oligogalacturonides, AraOs: arabino-oligosaccharides, GOS: galacto-oligosaccharides, DP 1: monosaccharides, 5-HMF: 5-Hydroxymethylfurfural, HPLC: high pressure liquid chromatography, HPSEC: high pressure size exclusion liquid chromatography, HPAEC: High-performance anion-exchange chromatography, HILIC: hydrophilic interaction liquid chromatography, IEC: semi preparative ion exchange chromatography, LP-IEC: low pressure anion-exchange chromatography, PAD: Pulsed amperometric detector; RID: refractive index detector, ESI: electrospray ionization, MS/MS: tandem mass spectrometry, ESI-TOF: electrospray time-of-flight mass spectrometer, MALDI: matrix-assisted laser desorption ionization, PMP: 1-phenyl-3-methyl-5-pyrazolone derivatization, ABEE: p-aminobenzoic ethyl ester derivatization

Moreover, electrospray ionization (ESI) with tandem mass spectrometry (MS/MS) and matrix-assisted laser desorption/ionization time-of-flight mass spectrometry (MALDI-TOF) were required to study the fine chemical structure and the mass-to-charge ratio of ions from the different types of POS generated as summarized in Table 2.2.

#### **2.3.4 Purification of pectic oligosaccharides**

As partial enzymatic or chemical hydrolysis of pectic substrates leads to complex mixtures, the resulting pectic oligosaccharides are in solution together with other reduced low molecular weight saccharides of diverse chemical composition as well as various monosaccharides (Cano et al., 2020). To obtain a concentrated pectic oligosaccharides fraction out of this complex mixture, envisioning a high-quality functional product, purification processes are required. Membrane technology, for example, has been widely used in the food industry to concentrate and purify a variety of products (i.e. dairy ingredients, sugars, and fruit juices) (Muralidhara, 2010) as well as functional ingredients and nutraceuticals (i.e. phospholipids, tocopherols, proteins and polyphenols) (Akin et al., 2012). Membrane technology allows physical separation of solutes from a solution by means of a semi-permeable membrane driven by gradients in pressure, concentration, or electrical potential (Mulder, 1996). Among membrane processes, micro-, ultra- and nano-filtration are pressure driven, and are characterized by a low energy input (i.e. feed pumping), versatile membrane configuration (i.e. plate-and-frame, spiral wound, hollow-fiber and tubular) (Berk et al., 2009), and ease of control of operational parameters (i.e. temperature, pressure, pH and feed flow rate) (Pinelo et al., 2009).

As reviewed by Akin et al. (2012), ultrafiltration (UF) and nanofiltration (NF) have been a feasible alternative for purification of various types of oligosaccharides like fructooligosaccharides (FOS), xylooligosaccharides (XOS), galactooligosaccharides (GOS), pectate

oligosaccharides (POS), milk oligosaccharides (MOS), etc. For example, UF or UF+NF within various module configurations, such as stirred cells, spiral modules, plate-and-frame modules, and tubular units, used in single and double stages were reported for purification of MOS, FOS, and GOS as well as for the fractionation and concentration of XOS from hydrolysates of corn cob and almond shells by the removal of monosaccharides (Akin et al., 2012). The general mechanism of oligosaccharides purification by UF and NF can be summarized as depicted in Fig. 2.6

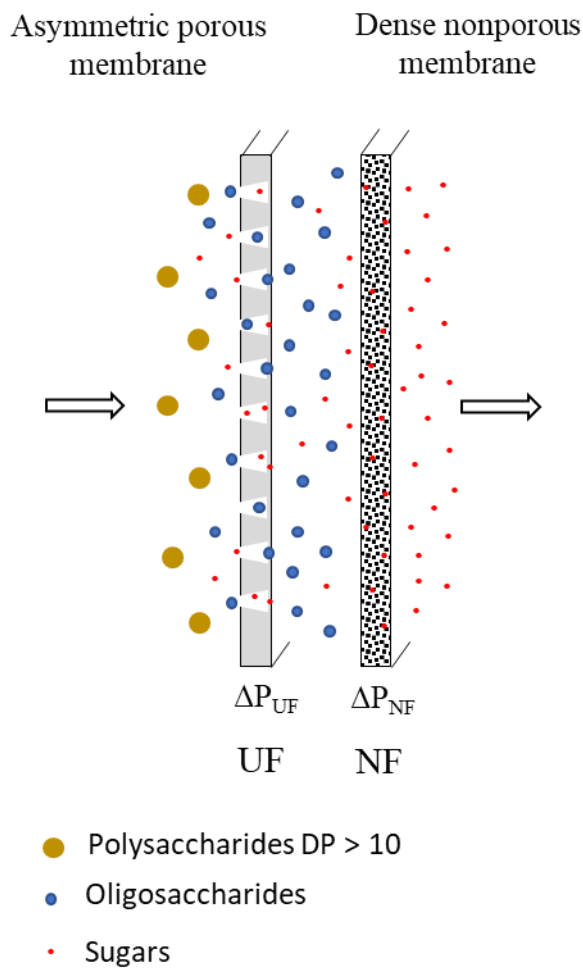


**Fig. 2.6.** Ultrafiltration (UF) coupled to nanofiltration (NF) for oligosaccharides purification.

According to Fig. 2.6, oligosaccharides and sugars are separated from polysaccharides by passing through an asymmetric porous UF membrane (pore-flow mechanism) (Baker, 2004), while sugars are separated from oligosaccharides by diffusion through a dense nonporous NF membrane, leading to a final retentate rich in oligosaccharides. As UF membranes have fixed pores of 2-100 nm and are commonly less compact than NF membranes (network structure with pores < 2 nm), the required pressure gradient for UF is less than that of NF membranes ( $\Delta P_{NF} > \Delta P_{UF}$ ).

As pectic oligosaccharides are an emerging type of oligosaccharides, studies on membrane utilization for their purification, considering the impact of various operating parameters are limited. Table 2.3 summarises the characteristics of membranes, module configuration, operating conditions, and yield of reported membrane processes for purification of hydrolysates (enzymatically produced) from pectic substrates. Kamada et al. (2002), for example, explored the feasibility of using a sequential UF + NF process within a plate-and-frame membrane module with recirculation of the retentate in each batch step to purify and concentrate a 2.5% solution of a commercial mixture of oligosaccharides from chicory rootstock. They used a polysulfone UF membrane of 20 kDa as well as polyamide composite NF membranes with different salt rejection percentages (3% to 65%). Their results showed that UF + NF process had an overall yield of 63.1%, where 52.3% rejection of the total saccharides occurred during the UF step. In addition, Kamada et al. (2002) found that a NF membrane with 30% salt rejection allowed removal of 6.4% of the initial mono- and di-saccharides. Conversely, Gómez et al. (2014) studied the effect of two different filtration modes (dead-end and cross flow) on the purification of POS from orange peel waste hydrolysate as part of their scale-up process. Their diafiltration and concentration experiments were carried out using a tight UF membrane of 1 kDa within a Amicon stirred cell of 400 mL capacity (dead-end) and a Prep/Scale spiral wound module (cross flow) equipped with a

30 L feed tank. Their results showed that dead-end filtration mode favored the removal of high molecular weight compounds from the feed solution while the recovery of neutral and acidic POS (91.8% AraOS, 92.9% GOS, and 95.4% OGalA) was maximized compared to that of the cross-flow mode (Table 2.3). Besides the variation in the recovery, a difference in the molecular weight distribution profile of the permeate obtained from the spiral wound module compared to that of the permeate obtained from the Amicon cell was reported, suggesting that research is needed to gain more insights on the optimization and scale-up of POS membrane purification.

The use of membrane reactors has been explored to improve the productivity of POS manufacture as reaction and separation steps are merged into one unit (Mulder, 1996). As such, Baldassarre et al. (2018) used an enzyme membrane reactor (EMR) for the continuous production and purification of POS from onion skin pectin. They selected a multienzyme complex (Viscozyme L) with concentrations of 82.7, 41.4 and 20.7 U/mL, to induce hydrolysis of the onion skin pectin, followed by a cross flow 10 kDa hollow fiber cartridge to achieve the separation. In their set up, the reactor was sequentially connected to the UF module, and the retentate stream was recycled back to the reactor for complete hydrolysis, while the permeate, containing compounds with reduced molecular weight, oligo- and mono-saccharides, was collected. Their results showed that after 15 min of reaction, the yield of POS of 2-8 DP and monosaccharides was 60% and 25%, respectively, indicating the feasibility of the process.

**Table 2.3.** Membrane processes for purification and concentration of oligosaccharides and pectic oligosaccharides.

Substrate	Membrane process	Module configuration (mode)	Membrane		Operating conditions		Recovery (%)	Membrane rejection R (%)	Ref.
			Type	MWCO	T / pH	Pressure			
Commercial chicory rootstock oligosaccharides	UF+NF	Plate-and-frame (cross flow+R)	UF: polysulfone NF: polyamide composite	20 kDa ≤ 700 Da	30°C 25°C	3.5 bar 40 bar	63.1%	UF: 52% DP > 1 NF: 23% DP 1, 51% DP 2, 88% DP>4	(Kamada et al., 2002)
Pectate hydrolysate	UF+NF	(cross flow)	UF: polysulfone NF: polyamide composite	50 kDa 100 Da–5 kDa	25°C	1.5 bar 5 bar	nr.	UF: ~100% DP>5 NF: 0% DP 1, 8% DP 2, 58% DP 3, 96% DP>5	(Iwasaki and Matsubara, 2000)
Soybean oligo-saccharides <sup>a</sup> (SBOS)	UF+NF	Flat sheet membrane (cross flow)	UF: nr. NF: polyamide composite	100 kDa 100 Da–5 kDa	20°C 20°C	15 bar	83.2%	NF: 52% lactose, 86% glucose, 96% SBOS	(Li et al., 2018)
Lemon peel waste	DF+UF	Amicon stirred cell (dead-end)	DF/UF: regenerated cellulose	1 kDa	nr.	3 bar	96% OGalA <sup>b</sup> 76% AraOS <sup>b</sup>	nr.	(Gómez et al., 2013)
Orange peel waste	DF+UF	Prep/Scale Spiral Wound TFF-6 Module (cross flow)	DF/UF: regenerated cellulose	1 kDa	nr.	4 bar	74% OGalA <sup>b</sup> 79% AraOS <sup>b</sup> 77% GOS <sup>b</sup> 26% DP 1	nr.	(Gómez et al., 2014)

MWCO: Molecular weight cut-off, UF: ultrafiltration, NF: nanofiltration, DF: diafiltration, T: temperature, SBOS: soybean oligosaccharides, a: stachyose + gossypose + verbascose + lactose + glucose, b: part of pectic oligosaccharides, POS: pectic oligosaccharides, R: retentate recycle; FEMR: free enzyme membrane reactor; EMR: enzyme membrane reactor, DP: degree of polymerization, DP1: various monosaccharides, OGalA: oligogalacturonides, AraOS: arabinooligosaccharides, XOS: xylooligosaccharides, GOS: galactooligosaccharides, and sCW: subcritical water technology.

**Table 2.3.** Continued.

Substrate	Membrane process	Module configuration (mode)	Membrane		Operating conditions		Yield (%)	Membrane rejection R (%)	Ref.
			Type	MWCO	T / pH	Pressure			
Apple pectin	FEMR-UF	Prep/Scale spiral wound (cross flow+R)	polysulfone	10-50 kDa	48°C/4.8	0.35 bar	nr.	60% DP 1	(Rodriguez-Nogales et al., 2008a)
Onion skins pectin	EMR-UF	Romicon 1” Hollow fiber cartridge (cross flow+R)	polysulfone	10 kDa	45°C/4.5	0.5 bar	60% POS 25% DP>1	nr.	(Baldassarre et al., 2018)
Sugar beet pectin	EMR-UF	Romicon 1” Hollow fiber cartridge (cross flow+R)	polysulfone	10 kDa	45°C/4.5	nr.	83% POS 16% DP>1	nr.	(Elst et al., 2018)
Barley bran sCW hydrolysate	UF	Minimate cassette system (tangential cross flow)	polyethersulfone	1 kDa	22°C	1.4 bar	81% XOS	nr.	(Aghashahi, 2020)

MWCO: Molecular weight cut-off, UF: ultra filtration, NF: nanofiltration, DF: diafiltration, T: temperature, SBOS: soybean oligosaccharides, a: stachyose + gossypose + verbascose + lactose + glucose, b: part of pectic oligosaccharides, POS: pectic oligosaccharides, R: retentate recycle; FEMR: free enzyme membrane reactor; EMR: enzyme membrane reactor, DP: degree of polymerization, DP 1: various monosaccharides, XOS: xylooligosaccharides, and sCW: subcritical water technology.

According to Table 2.3, integrated UF + NF is a feasible approach for fractionation, purification and concentration of POS from enzymatically obtained pectic-derived mixtures; however, studies on membrane purification of pectic-derived mixtures obtained by acid catalysis and hydrothermal treatments as well as the separation of neutral POS from acidic POS are still required.

### **2.3.5 Drying of pectic oligosaccharides**

Once the pectic oligosaccharides are concentrated and purified, a drying step is needed to obtain pectic oligosaccharides in a more stable powder form. Nonetheless, accomplishing this downstream step represents a challenge as pectic oligosaccharide solutions are comprised of low molecular weight saccharides with low glass transition temperatures ( $T_g$ ). It has been reported that drying of solutions and food products containing low molecular weight saccharides and their mixtures (Simperler et al., 2006), like sugarcane, fruit juices and fructo-oligosaccharides has not been an easy task (Goula and Adamopoulos, 2010; Papadakis et al., 2007; Polamarasetty et al., 2009; Truong et al., 2005; Wrzosek et al., 2013). During spray drying, for example, drying temperatures can easily exceed the  $T_g$  of low molecular weight saccharides like fructose (5°C), galactose (30°C), glucose (31°C), sucrose (62°C), lactose (101°C), etc., leading to sticky precipitated particles that are more prone to adhere to the surface of the drying chamber and be burnt, reducing the yield and the quality of the final product (Boonyai et al., 2004; Chiou et al., 2008; Jaya and Das, 2009; Jouppila and Roos, 1994; Muzaffar, 2015; Shishir and Chen, 2017; Verma et al., 2020). The addition of carrier agents to the feed solutions prior to spray drying has been reported to improve the yield and stability of powdered products as their  $T_g$  is increased, and therefore their stickiness and hygroscopicity are reduced (Shishir and Chen, 2017). Among carrier agents, maltodextrins and gum arabic have been commonly used to aid spray drying of fruit juices

due to their increased molecular weight and high glass transition temperatures of 100-243°C and 126°C, respectively (Shishir and Chen, 2017). Maltodextrins and other carrier agents have also been added to fructo-, galacto-, and xylo-oligosaccharide solutions prior to spray drying to increase the yield, as well as  $T_g$  and flowability of powders (Amrutha et al., 2014; Sosa et al., 2016; Wrzosek et al., 2013; Zhang et al., 2018) as summarized in Table 2.4.

More recently, non-conventional methods for drying water-soluble saccharides have been reported, such as supercritical CO<sub>2</sub> (SC-CO<sub>2</sub>) drying. In SC-CO<sub>2</sub> drying, CO<sub>2</sub> at supercritical conditions ( $T > 31.1^\circ\text{C}$  and  $P > 73.8$  bar) is used as the drying medium as its distinctive physical properties (i.e. increased density, diffusivity and solubility in water) facilitate heat and mass transfer phenomena involved in the drying mechanism (Benali et al., 2014).

**Table 2.4.** Effect of carrier agents on the yield and  $T_g$  of spray dried oligosaccharides.

Oligosaccharide solution	Spray drying conditions			Powder		Ref.
	Inlet temperature	Outlet temperature	Carrier agent	$T_g$	Yield	
FOS	100-140°C	80-95°C	0%	nr.	23%	(Amrutha et al., 2014)
			GC	nr.	20%	
			2% MgO	nr.	43%	
FOS	110°C	78°C	25% MD	nr.	47%	(Wrzosek et al., 2013)
			50% MD	nr.	62%	
GOS	180°C	75-80°C	0%	40°C <sup>a</sup>	nr.	(Sosa et al., 2016)
			50% MD	60°C <sup>a</sup>	nr.	
XOS	160°C	76	0%	42.5°C	24%	(Zhang et al., 2018)
			36% MD	90°C	72%	
XOS	115°C	54°C	0%	23°C <sup>b</sup>	92% <sup>b</sup>	(Zhang et al., 2019)
			MD:GA (44:6)	47°C	68%	

FOS: fructo-oligosaccharides; GOS: galacto-oligosaccharides; XOS: xylo-oligosaccharides; MD: maltodextrin; GC: gum acacia; GA: gum arabic; MgO: magnesium oxide; a:  $T_g$  at 20% relative humidity, b: XOS control obtained by freeze-drying, and nr: not reported.

The difference between SC-CO<sub>2</sub> drying and spray drying or freeze drying relies on the water removal mechanism. As such, in SC-CO<sub>2</sub> drying, water is dissolved in SC-CO<sub>2</sub> and exits as a mixture of SC-CO<sub>2</sub> + water, whereas water evaporation and sublimation takes place in spray drying and freeze drying, respectively (Benali et al., 2014; Bourdoux et al., 2016). Although SC-CO<sub>2</sub> drying is advantageous as water is removed at relative low temperatures and moderate pressures and no liquid-gas phase change occurs, the nonpolar nature of CO<sub>2</sub> and the low solubility of water in SC-CO<sub>2</sub> are some limitations of this method, which is reflected in the massive amounts of CO<sub>2</sub> and extended drying times required for drying aqueous solutions (Temelli, 2018).

Bouchard et al. (2008), for example, explored SC-CO<sub>2</sub> drying as an alternative to spray drying to obtain powders from low molecular weight saccharides and their mixtures, including di- and tri-saccharides as well as cyclodextrin, low molecular weight dextran and inulin. In the reported process, however, ethanol (EtOH) was added as a co-solvent to enhance water solubility in SC-CO<sub>2</sub>. Their experiment was carried out at 37°C and 100 bar and the experimental variables were the saccharides concentration (10-30%) and the mass flow rate ratio in g/min of CO<sub>2</sub>:EtOH:saccharide aqueous solution (250:20:0.5 to 420:40:0.5) (Bouchard et al., 2008). The reported results showed that the combination of low saccharides concentration and a CO<sub>2</sub>:EtOH:saccharide aqueous solution flow rate ratio of 420:20:0.25 led to amorphous powders with the highest T<sub>g</sub> values. However, it is noticeable that, based on the flow rate ratios reported, a huge amount of CO<sub>2</sub> was needed to remove a very small amount of water from the samples, which is a shortcoming of this technique. In addition, it was also reported that di- and tri-saccharides exhibited an unexpected residual ethanol content of 6 to 7.5% after 4 months of storage, which indicates that the ethanol removal step still needs to be optimized. Although this study showed that SC-CO<sub>2</sub> drying could be a feasible approach to obtain relatively stable powders free from carrier

agents from saccharides with low  $T_g$ , the efficiency of the process based on the drying yield and drying times were not reported for comparison purposes. Therefore, more research is needed to quantify the impact of using low mass flow rate of saccharide aqueous solutions on the efficiency of the SC-CO<sub>2</sub> drying process.

Different configurations of supercritical fluid-assisted processes for particle formation have been reported by Jung and Perrut (2001) and Saldaña et al. (2015). In general, these processes have been grouped based on the various roles of the supercritical fluid, such as a solvent, antisolvent, solute or a co-solute (Jung and Perrut, 2001; Temelli, 2018). Among the anti-solvent processes, the supercritical anti-solvent (SAS) and the solution enhanced dispersion by subcritical fluids (SEDS) methods have been reported (Hanna and York, 1996; Jung and Perrut, 2001; Saldaña et al., 2015). In the SAS process, for example, a mix of SC-CO<sub>2</sub> and a co-solvent, generally ethanol, is used to saturate the polar solvent in which the solute is dissolved, and dramatically decrease its solvent power, causing the desirable precipitation of the solute (Jung and Perrut, 2001). The SAS is a multi-step process and involves atomization of the feed solution, similar to that of spray-drying process, as the feed solution is pumped through a nozzle and sprayed as small droplets into a high-pressure vessel filled with the supercritical fluid. The aim of this step is to enhance the dissolution of the supercritical fluid (SC-CO<sub>2</sub>+ethanol) in the feed solution, and consequently lead to solute supersaturation within the droplets, causing its precipitation as small particles (Jung and Perrut, 2001). Next, the precipitated particles are collected on a filter placed at the bottom of the vessel while the supercritical fluid enriched in the solvent flows continuously towards a depressurization tank for gas-liquid separation. Finally, once the feed solution has been sprayed completely, SC-CO<sub>2</sub> alone is passed through the vessel to ensure complete removal of ethanol and the solvent (Jung and Perrut, 2001). For the SAS process, the solubility of the solute in the solvent and not in

the supercritical fluid is required as well as the miscibility of both, the solvent and the supercritical fluid under the set operating conditions (De Marco and Reverchon, 2012). For example, for particle formation of water-soluble saccharides by SAS, water, and the supercritical fluid ( $\text{CO}_2$  + ethanol) must remain as a single phase under the set pressure and temperature. According to the ternary phase diagram of  $\text{CO}_2$ -ethanol-water (Fig. 2.7) reported by Durling et al. (2007) obtained at  $40^\circ\text{C}$  and pressures of 100 to 300 bar, only small molar fractions of water are required to operate within the supercritical fluid region (bottom right corner of the phase diagram, below the mixture critical point). Then, drying of polysaccharides can be limited due to the low mass flow rate of the aqueous solution that can be employed in the SAS process.

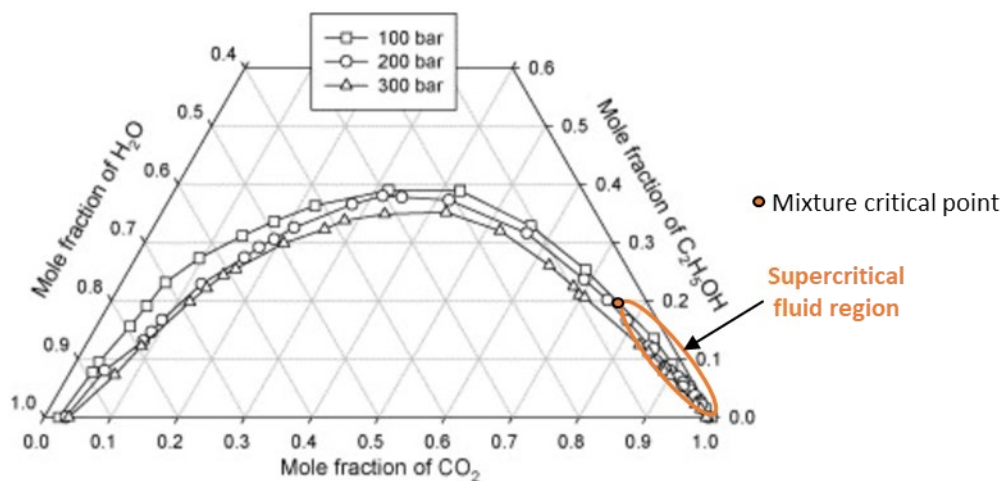


**Fig. 2.7.** Phase diagram of  $\text{CO}_2$ -EtOH- $\text{H}_2\text{O}$  obtained at  $40^\circ\text{C}$  and pressures of 100, 200 and 300 bar reported by Durling et al. (2007) (Reprinted with permission from Elsevier Inc.).

More recently, pressurized gas-expanded liquid (PGX) process has been used to obtain dry particles with large surface areas of high molecular weight water-soluble polysaccharides at relatively low temperature of  $40^\circ\text{C}$  and 100 bar (Couto et al., 2020; Liu, 2019; Temelli and Seifried, 2016). The principle of the PGX process is based on the anti-solvent effect of  $\text{CO}_2$ +ethanol to decrease the solvent power of water and cause precipitation of the solute.

However, the main difference between PGX and SC-CO<sub>2</sub> drying and SAS processes relies on the fact that the mixture of drying fluid (CO<sub>2</sub>+ethanol) and water form a gas-expanded liquid in the single liquid phase region of the ternary phase diagram (Temelli, 2018), located above the phase boundary (Fig. 2.7). The advantage of working inside the gas-expanded liquid region of the ternary phase diagram of CO<sub>2</sub>–EtOH–H<sub>2</sub>O is that large molar fractions of water can be used, and therefore larger mass flow rates of the aqueous solutions can be mixed with the drying fluid compared to the case of operating in the supercritical region (Temelli and Seifried, 2016). Couto et al. (2020), for example, tested a range of mass flow rate (g/min) ratios of aqueous solution:EtOH:CO<sub>2</sub> (1:15:5 to 10:30:10) for PGX-drying of gum arabic, but yield was not reported. Their results showed that flow rate ratios of aqueous solution:EtOH:CO<sub>2</sub> of either 5:30:10 or 1:15:5 (upper right zone of the ternary phase diagram) led to gum arabic powders with a spherically shaped morphology and the highest surface area of 13.6 and 64.7 m<sup>2</sup>/g, respectively, which could be used as a substrate for delivery systems. Similarly, Liu (2019) also explored different flow rate ratios (g/min) of aqueous solution:EtOH:CO<sub>2</sub> (1:6:2, 4:15:5, and 1:3:1) for PGX drying of sodium alginate. The PGX-dried sodium alginate obtained at a ratio of aqueous solution:EtOH:CO<sub>2</sub> of 4:15:5 exhibited an ordered and highly porous structure with the highest surface area of 164.5 m<sup>2</sup>/g but no yield was reported. Although, the studies mentioned above showed that the PGX process is a feasible alternative to obtain powders with desirable physical properties from high molecular weight water-soluble polysaccharides, research focused on the experimental drying yield as well as on the feasibility of drying low molecular weight saccharides is still required.

## Chapter 3: Carboxylic acid-catalysed hydrolysis of polygalacturonic acid in subcritical water medium\*

### 3.1 Introduction

Pectic polysaccharides, commonly referred to as pectin, are comprised of a heterogeneous group of plant cell wall acidic polymers characterized by a backbone structure that is rich in D-galacturonic acid residues linked together via  $\alpha$ -(1 $\rightarrow$ 4)-glycosidic bonds. Different pectic fragments have been identified, including linear homogalacturonan and branched rhamnogalacturonan-I and rhamnogalacturonan-II (Thakur et al., 1997). Homogalacturonan is the most abundant fragment in pectin that has been defined as a homopolymer of (1 $\rightarrow$ 4)-linked D-galacturonic acid, which can be partially methyl-esterified at carbon C-6 or O-acetyl-esterified (Ralet et al., 2016). Pectin is classified as high-methoxyl pectin with a degree of esterification (DE) of 55-75% or low-methoxyl pectin (DE 20-45%); however, when homogalacturonan in pectin is completely de-esterified to polygalacturonic acid, it is known as pectic acid or pectate (Proseus and Boyer, 2012; Seymour and Knox, 2002; Thakur et al., 1997).

As reviewed in Chapter 2 (Section 2.3.1), POS have been shown to exert various benefits for human health promotion as well as in plants. Therefore, POS are an emerging type of natural compound with a wide range of potential industrial applications; however, versatile, and feasible production processes are required. To date, enzymatic, chemical and mechanical processes or their combinations have been reported for pectin depolymerization into POS (Chen et al., 2013; Gullón et al., 2013). However, utilization of multi-enzyme cocktails requires long reaction times. The use of mineral acids such as hydrochloric acid, sulfuric acid and trifluoroacetic acid, or the use of

---

\* A version of this Chapter is In Press as Carla S. Valdivieso Ramirez, Jose Edwin Sanchez, Michael Gänzle, Feral Temelli and Marleny D.A. Saldaña. Carboxylic acid-catalysed hydrolysis of polygalacturonic acid in subcritical water in the *Journal of Supercritical Fluids* (2020).

hydrogen peroxide at elevated pH requiring subsequent neutralization, formation of degradation products such as furfural and organic acids as well as release of pectic fragments with a wider degree of polymerization are some of the drawbacks associated with these methods (Garna et al., 2006; Zhang et al., 2018).

In an effort to overcome these drawbacks, hydrothermal treatments have been explored for pectic-oligosaccharides production. Miyazawa and Funazukuri (2004), for example, used subcritical water (sCW) at temperatures between 180 and 260°C and a pressure of 100 bar as the reaction medium to hydrolyze polygalacturonic acid into oligogalacturonides. The highest oligogalacturonide yield reported was 22% at 260°C. Further, the catalytic influence of CO<sub>2</sub> addition to sCW media on citrus pectin hydrolysis into POS has been reported at temperatures between 100 and 150°C and pressures between 100 and 300 bar (Takahashi et al., 2011). The addition of carboxylic acids has also been considered as a potential approach to enhance the selectivity of hydrothermal treatments as the catalytic effect of these acids has been related to the acidic composition of the core active site of the glycoside hydrolase family of enzymes (i.e. polygalacturonases and cellulases), which hold two amino acid motifs with a carboxylic acid group on its side chain (aspartic and glutamic acids) that allow cleavage of glycosidic bonds (Palanivelu, 2006). Maleic and oxalic acids increased the selectivity of hydrothermal treatments towards monosaccharide production from biopolymeric matrices while minimizing the formation of degradation products like furfural and humic substances (Kim et al., 2013; Lu and Mosier, 2007). Nonetheless, carboxylic acid-catalyzed hydrolysis has not been investigated for POS production. Therefore, an objective of this thesis project was to investigate whether di- or tri-carboxylic acids exert a catalytic effect via general acid catalysis or induce selectivity during pectic polysaccharides hydrolysis under sCW conditions. Due to the complex nature of pectic polysaccharides, the

hydrolysis of polygalacturonic acid (linear pectic fragment) as a model substance was targeted in this first study. The hydrolysis was carried out in a batch mode at relatively low temperatures of 125 and 135°C/100 bar and reaction times of 10 to 120 min to evaluate the catalytic effect of carboxylic acids. A possible mechanism and a kinetic model for polygalacturonic acid hydrolysis under subcritical fluid conditions were proposed.

## **3.2 Materials and Methods**

### **3.2.1 Materials**

Polygalacturonic acid (code number 81325,  $\geq 90\%$  purity, enzymatic), citric acid ( $>99.5\%$ , ACS grade) and malic acid ( $>99.5\%$ , ACS grade) from Sigma Aldrich (Oakville, ON, Canada) as well as water from the Milli-Q system (18.2 M $\Omega$ .cm, Millipore, Bellerica, MA, USA) and nitrogen gas (99.9% purity) from Praxair (Edmonton, AB, Canada) were used for the hydrolysis experiments in sCW.

For the analytical procedures, sodium nitrate, ammonium formate, formic acid, acetonitrile, and standards of mono-galacturonic acid, di-galacturonic acid, tri-galacturonic acid, polygalacturonic acid, glucose, D-galactose, D-arabinose, D-xylose, D-fucose and L-rhamnose were acquired from Sigma Aldrich (Oakville, ON, Canada). Dextrans with molecular weights of 1.2, 3, 5, 25 and 72 kDa were obtained from the American Polymer Standards Corporation (Mentor, OH, USA) and HPLC-water was purchased from Fisher Scientific (Ottawa, ON, Canada).

### **3.2.2 Subcritical water hydrolysis of polygalacturonic acid**

A Parr 4590 system (Parr Instrument Company, Moline, IL, USA) designed to withstand pressures and temperatures up to 200 bar and 350°C, respectively, was used to hydrolyze polygalacturonic acid under sCW conditions. The Parr 4590 system was equipped with a 100 mL batch stirred reactor, a nitrogen cylinder, a temperature controller, a thermocouple placed inside

the reactor and a heating mantle (525 W), a pressure gauge, a computer to record temperature and pressure data, a stirring system, and high-pressure valves (Fig. 3.1). The parameters of the controller were fine tuned to minimize temperature fluctuation. The optimized proportional (P), integral (I) and derivative (D) parameters for the controller were  $P = 21$ ,  $I = 500$  and  $D = 71$ . The heating setting was on full power position and the stirring speed was kept constant at 1 ½ position.

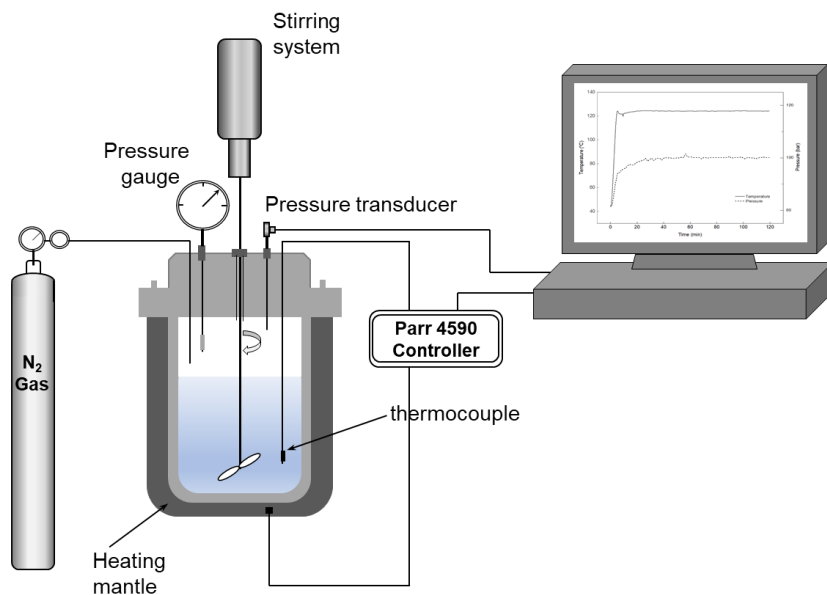


**Fig. 3.1.** Parr 4590 system with a 100 mL batch stirred reactor.

The input variables for the sCW hydrolysis experiments were temperature (125 and 135°C), reaction time (10, 20, 30, 40, 60 and 120 min) and the number of carboxyl groups of the organic acids (tri-carboxylic acid, citric acid and di-carboxylic acid, malic acid) used in the reaction media. An aqueous solution of either 0.20% w/w of citric acid or 0.27% w/w of malic acid was used as the reaction medium to reach a constant pH of 2.6 in both cases. The pH of the reaction medium was selected based on previous studies that reported the use of aqueous malic acid (pH 1.7-2.2) and aqueous oxalic acid (pH 1.5-2.2) as an alternative to inorganic acids in homogeneous catalysis

to obtain fermentable sugars from lignocellulosic biomass (Lu and Mosier, 2007; Kim et al., 2013). In such cases, the hydrothermal treatment was carried out at temperatures between 140°C and 180°C and 30 h, where sulphuric acid at pH 1.3-2.2 was used as the control inorganic acid catalyst (Kim et al., 2013). Therefore, in the present study, a mild pH was selected as the starting point due to the different nature of the substrate and the unknown behavior of malic and citric acids under sCW conditions. In addition, a moderate pressure of 100 bar was selected and kept constant in the system due to the reported enhancing effect of pressure on chemical reactions (i.e. ionic process) that involve negative activation volumes, which are associated to molar volume contraction (Eldik et al., 1989; Martínez et al., 2010). As the first ionization of aqueous citric acid and self ionization of water have exhibited negative reaction volumes of -10.7 and -22.1 cm<sup>3</sup>/mol, respectively (Chen et al., 2017; Martinez-Monteagudo and Saldaña, 2014), hydrolysis of polygalacturonic acid (containing ionizable carboxylic groups) in aqueous citric acid was also expected to be favored by pressure (Ciftci and Saldaña, 2015; Cybulska et al., 2014; Demazeau, 2006). The experiments were performed in duplicates and water was used as the control reaction medium.

For the batch hydrolysis, a start-up run loaded with 40 g of water at set temperature and pressure for 60 min was first carried out to stabilize the temperature of the reaction system to further ensure reproducibility of operating conditions in the experimental runs. The reactor load was selected considering a headspace to prevent overpressure due to thermal expansion of water. The concentration of the starting polygalacturonic acid solution was kept constant at 0.5% w/w. Briefly, for experimental runs, 200 mg of polygalacturonic acid and 40 g of citric acid solution (0.2% w/w) were sequentially loaded into the reactor, which was then assembled into the system. Next, nitrogen gas was used to flush out the entrapped air from the reaction vessel. Once the solution was purged for 12 min under constant stirring, it was pressurized with nitrogen gas to

either 83 or 80 bar and then heated up to 125 or 135 °C, respectively. After reaching the set temperature and pressure of 100 bar, the reaction time was started. Temperature and pressure profiles were automatically recorded for every run (Fig. 3.2). The come-up times for the reactions at 125 and 135 °C were registered as  $5.3\pm 0.2$  and  $5.8\pm 0.4$  min, respectively. Although the come-up time based on the temperature parameter was shorter than the come-up time based on the pressure parameter (26 min), the first was selected for further kinetic calculations as the influence of temperature on the rate of reaction is known to be predominant compared to the effect of pressure. At the end of the targeted reaction time, the heating mantle was turned off and the reactor was immediately quenched to 60°C using a cold-water bath. Subsequently, the reactor was slowly depressurized and unplugged from the system. The resulting polygalacturonic acid hydrolysate was collected and stored frozen at -18°C until further HPLC analysis.

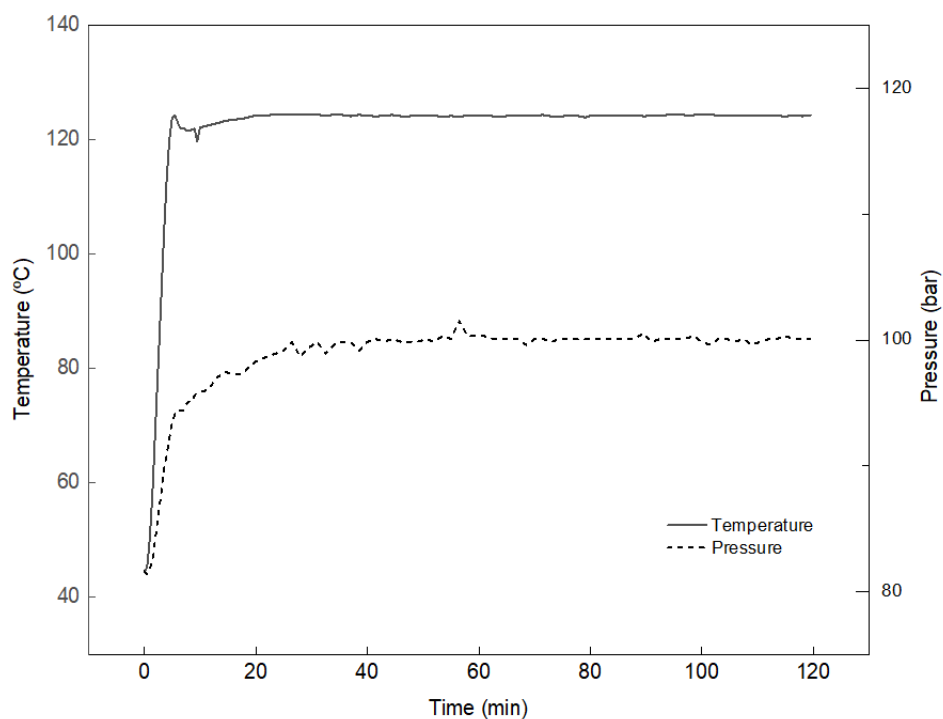


**Fig. 3.2.** Temperature and pressure profiles of the Parr reactor set at 125°C/100 bar over 120 min.

### **3.2.3 Characterization of the hydrolysates**

#### **3.2.3.1 Molecular weight distribution of polygalacturonic acid hydrolysates**

High performance size exclusion chromatography (HPSEC) was used to monitor polygalacturonic acid hydrolysis under subcritical fluid conditions. The molecular weight (MW) distribution of polygalacturonic acid hydrolysates was determined using a Shimadzu 10-A HPLC system (Shimadzu Corporation, Kyoto, Japan) equipped with a refractive index detector RID-10A (Shimadzu Corporation, Kyoto, Japan). The separation was performed on an Ultrahydrogel 250 column (7.8 x 300 mm, 6  $\mu\text{m}$  particle size) (Waters, Milford, MA, USA) with an exclusion limit of  $8 \times 10^4$  g/mol. The elution was carried out at 40°C with 0.05 M sodium nitrate (pH 6.8) as the mobile phase at 0.5 mL/min for 30 min. Dextrans with molecular weights of 1.2, 3, 5, 12, 25 and 72 kDa at concentrations between 1.5 and 4 mg/mL were used as standards and the calibration curve (log (MW) vs elution time) was fitted to a third order polynomial regression equation (Diaz et al., 2007). Dextran standards and polygalacturonic acid hydrolysates were diluted with the mobile phase at a 1:2 v/v ratio and then passed through a syringe filter (0.45  $\mu\text{m}$ , PVDF Target 2) prior to their injection to the column.

#### **3.2.3.2 Determination of oligogalacturonides in polygalacturonic acid hydrolysates**

Hydrophilic interaction liquid chromatography (HILIC) was used to characterize the oligogalacturonides (OGs) released during the polygalacturonic acid hydrolysis according to the methodology described by Leijdekkers et al. (2011). The analysis was performed on a Shimadzu SPD-20A HPLC system equipped with a binary pump, autosampler and a column heater (Shimadzu Corporation, Kyoto, Japan) coupled to an evaporative light scattering detector (3300 Alltech ELSD, BÜCHI Labortechnik. AG, Flawil, Switzerland). Samples were separated on an Amide VanGuard pre-column (4.6 x 5 mm, 3.5  $\mu\text{m}$  particle size, Waters Corporation, Milford,

MA, USA) connected in series to a XBridge Amide column (4.6 x 250 mm, 3.5  $\mu$ m particle size, Waters Corporation, Milford, MA, USA). The elution of oligogalacturonides was carried out at 35°C and a flow rate of 1 mL/min for 40 min. The composition of mobile phases used for the elution were: (A) 80:20 (v/v) acetonitrile/10 mM ammonium formate buffer pH 3, and (B) 20:80 (v/v) acetonitrile/ammonium formate buffer pH 3. The ammonium formate buffer was prepared using a 10 mM ammonium formate solution and 0.2% (v/v) of formic acid was added to reach a pH of 3. The elution gradient was: 0-1 min, isocratic 100% A; 1-2 min, linear from 0 to 30% B; 2-31 min, linear from 30 to 80% B; followed by a column re-equilibration elution gradient: 31-32 min, linear from 20 to 100% A and, 32-40 min, isocratic 100% A. The injection volume was 15  $\mu$ L and the composition of the needle wash solvent was 75:25 v/v acetonitrile/water. The ELSD detection was performed with nitrogen gas as the carrier at a flow rate of 1.75 L/min and the temperature of the drift tube was 50°C.

Standards and samples from polygalacturonic acid hydrolysates were diluted in a 1:2 (v/v) ratio with 50:50 (v/v) acetonitrile/water and then passed through a syringe filter (0.45  $\mu$ m, PVDF Target 2) prior to their injection to the column. Standard solutions of mono-, di- and tri-galacturonic acids with concentrations between 0.1 and 1.5 g/L were injected to obtain a calibration curve, which was fitted to a power model regression curve. In addition, the amounts of oligogalacturonides with a degree of polymerization DP higher than 3 were estimated according to the method described by Leijdekkers et al. (2011) that considers the average response factor of the ELSD detector obtained from the individual power functions of mono-, di- and tri-galacturonic acid standards. The equation generated is provided in Eq. (3.1). In addition, neutral sugar standards, such as glucose, galactose, arabinose, xylose, rhamnose and fucose, were also injected to determine their retention times.

$$\text{Concentration (g/L)} = e^{\left[\frac{\ln(\text{ELSD peak area}/4 \times 10^6)}{1.5713}\right]} \quad (\text{Eq. 3.1})$$

### 3.2.4 Kinetics and modelling of polygalacturonic acid hydrolysis

The rate of hydrolysis of polygalacturonic acid under sCW conditions was determined based on the change in the concentrations of components with time. The intermediate components were selected according to the results obtained from the HILIC-ELSD analysis, where polygalacturonic acid-derived compounds with a degree of polymerization (DP) between 14 and 1 were identified. Then, 8-14 DP and 2-7 DP fractions were selected as the main reactant groups involved in the hydrolysis to satisfy a simplified hydrolysis mechanism proposed in this study (Fig. 3.3). The proposed mechanism, depicted in Fig. 3.3, was based on two competitive reactions with reaction rate constants of  $k_1$  and  $k_2$ , and two consecutive reactions with reaction rate constants of  $k_3$  and  $k_4$ .

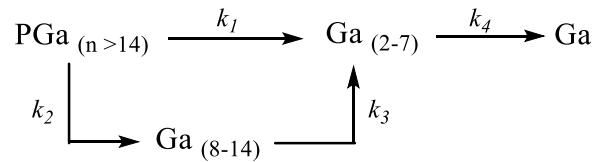


**Fig. 3.3.** Proposed reaction mechanism for polygalacturonic acid hydrolysis under scW conditions.  $\text{PGa}_{(n > 14)}$  = polygalacturonic acid with a DP higher than 14,  $\text{Ga}_{(8-14)}$  = poly/oligogalacturonic acids with 8-14 DP,  $\text{Ga}_{(2-7)}$  = oligogalacturonic acid with 2-7 DP and  $\text{Ga}$  = galacturonic acid monohydrate.

A kinetic model based on irreversible first-order reactions was used to describe the hydrolysis of polygalacturonic acid under sCW conditions because: *i*) experimental data showed an initial linear behavior when the natural logarithm of polygalacturonic acid concentration was plotted as a function of time, and *ii*) first-order reactions have been used since 1945 to successfully describe hydrolysis of plant cell wall components, such as cellulose and lignocellulose, after thermal treatments with dilute acids at temperatures above 150°C (Nabarlatz et al., 2004; Saeman, 1945). The concentrations of initial polygalacturonic acid and reduced molecular size

poly/oligogalacturonic acids were expressed in terms of mg of anhydrous galacturonic acid potentially obtainable during acid hydrolysis per mg of polygalacturonic acid or its derived compounds. Consequently, the concentrations of polygalacturonic acid and selected reactants at a given time were directly reported as mg of galacturonic acid anhydrous equivalents per mL of solution whereas the concentration of the end product (released galacturonic acid monohydrate) was calculated according to Eq. (3.2).

$$[\text{Ga}] = \text{Ga} \times \frac{176.12}{194.14} \quad (\text{Eq. 3.2})$$

where,  $[\text{Ga}]$  is the concentration of galacturonic acid (mg of galacturonic acid anhydrous equivalents/mL of solution),  $\text{Ga}$  is the concentration of released galacturonic acid monohydrate (mg/mL of solution), 194.14 is the molecular weight of galacturonic acid monohydrate, and 176.12 is the molecular weight of galacturonic acid anhydrous. According to the proposed kinetic model, the following differential rate equations were obtained at a constant temperature and pressure:

$$\frac{d[\text{PGa}_{(n>14)}]}{dt} = -k_1[\text{PGa}_{(n>14)}] - k_2[\text{PGa}_{(n>14)}] \quad (\text{Eq. 3.3})$$

$$\frac{d[\text{Ga}_{(2-7)}]}{dt} = k_1[\text{PGa}_{(n>14)}] + k_3[\text{Ga}_{(8-14)}] - k_4[\text{Ga}_{(2-7)}] \quad (\text{Eq. 3.4})$$

$$\frac{d[\text{Ga}_{(8-14)}]}{dt} = k_2[\text{PGa}_{(n>14)}] - k_3[\text{Ga}_{(8-14)}] \quad (\text{Eq. 3.5})$$

$$\frac{d[\text{Ga}]}{dt} = k_4[\text{Ga}_{(2-7)}] \quad (\text{Eq. 3.6})$$

where,  $d[]/dt$  is the reaction rate or the change in the concentration of a reagent or end product with time (mg of galacturonic acid anhydrous equivalents/mL of solution x min) and  $k$  is the rate

constant ( $\text{min}^{-1}$ ). To solve the system of differential equations, the initial conditions indicated in (Eq. 3.7) were set.

$$[\text{PGa}_{(n>14)}] = [\text{PGa}_{(n>14)}]_0, \quad [\text{Ga}_{(2-7)}] = 0, \quad [\text{Ga}_{(8-14)}] = 0, \quad [\text{Ga}] = 0 \quad (\text{Eq. 3.7})$$

where,  $[\text{PGa}_{(n>14)}]_0$  is the concentration of polygalacturonic acid at time 0, which is equal to 4.5 mg/mL.

The concentration of oligogalacturonic acid with 2-7 DP at time  $t$  was estimated by linear regression (least-squares method) using Microsoft Excel. The experimental data were fit to a third order polynomial equation at 135 °C (Eq. 3.8). At 125°C, there was no consumption of Ga (2-7 DP) so the experimental data were fitted to a linear equation (Eq. 3.9). Then, (Eq. 3.8) or (Eq. 3.9) was substituted in (Eq. 3.6). The integration of the set of differential equations was carried out in MATLAB using the Solve stiff differential equations method.

$$[\text{Ga}_{(2-7)}]_t = 9 \times 10^{-6} \times t^3 - 0.0021 \times t^2 + 0.1227 \times t - 0.0878, \quad R^2 = 0.987, \quad (\text{Eq. 3.8})$$

*for 135°C/100 bar*

$$[\text{Ga}_{(2-7)}]_t = 0.0168 \times t - 0.0269, \quad R^2 = 0.981, \quad \text{for } 125^\circ\text{C}/100 \text{ bar} \quad (\text{Eq. 3.9})$$

The unknown rate constants in the model were estimated from the slope of the curve of the natural logarithm of the concentration of the reagents versus reaction time. The curve fitting was performed by linear regression. As the reaction mechanism is complex and involves parallel and consecutive reactions, the obtained curves exhibited positive slopes (formation) and negative slopes (consumption). The initial linear part of the curve corresponding to the formation of products/reactants was considered to estimate the rate constants. In addition, the energy of activation and the pre-exponential factor were also estimated by plotting the natural logarithm of

the rate constants ( $\ln(k)$ ) versus the inverse of temperature ( $1/T$ ) following the temperature dependence of the rate constant described by the Arrhenius model (Eq. 3.10).

$$\ln(k) = \left(-\frac{E_a}{R}\right) \times \frac{1}{T} + \ln(A) \quad (\text{Eq. 3.10})$$

where, A is the pre-exponential factor,  $E_a$  is the activation energy (kJ/mol), R is the ideal gas constant (8.314 kJ/mol·K) and T is the absolute temperature (K). In addition, the conversion of polygalacturonic acid to poly/oligogalacturonic acid fragments with 2-14 DP after 120 min of reaction, and the yield of oligogalacturonic acid fragments with 2-7 DP were quantified according to (Eq. 3.11) and (Eq. 3.12), respectively.

$$\text{Polygalacturonic acid conversion} = \frac{(\text{PGa}_{\text{consumed}})_{t=120}}{(\text{PGa})_{t=0}} \quad (\text{Eq. 3.11})$$

$$\text{Oligogalacturonides 2 – 7 DP Yield (\%)} = \frac{(\text{Ga}_{(2-7)\text{produced}})_t}{(\text{PGa})_{t=0}} \times 100 \quad (\text{Eq. 3.12})$$

where,  $(\text{PGa})_{t=0}$  is the initial amount of polygalacturonic acid loaded in the reactor (mg of galacturonic acid anhydrous equivalents),  $(\text{PGa}_{\text{consumed}})$  is the total amount of polygalacturonic acid consumed after 120 min of reaction (mg of galacturonic acid anhydrous equivalents) and  $(\text{Ga}_{(2-7)})$  is the total amount of oligogalacturonides 2-7 DP produced at time t (mg of galacturonic acid anhydrous equivalents).

### 3.2.5. Statistical analysis

Hydrolysis of polygalacturonic acid at all operating conditions tested as well as the HILIC-ELSD analysis were performed in duplicates. The effects of different reaction media and temperature on polygalacturonic acid hydrolysis performed at 100 bar/60 min were evaluated using a two-way analysis of variance (ANOVA) with a level of significance set at  $\alpha = 0.05$ .

Differences between means were assessed by Tukey's multiple range test ( $p < 0.05$ ) using Minitab software package v.17 (Minitab Inc., State College, PA, USA).

### **3.3 Results and discussion**

#### **3.3.1 Molecular weight distribution of polygalacturonic acid hydrolysates**

The extent of polygalacturonic acid hydrolysis at 125°C/100 bar and aqueous citric acid as the reaction media was monitored by HPSEC-RID. High molecular weight compounds elute close to the exclusion limit ( $E_{XL}$ ) of the column (80 kDa), while medium or low molecular weight compounds elute later. Figs. 3.4a-e show the hydrolysis of polygalacturonic acid into reduced molecular size poly/oligogalacturonic acids based on the appearance of peaks with increasing area at longer elution times as the reaction time approaches 60 min. Generally, polygalacturonic acid is insoluble in hot water and dissolution is necessary prior to hydrolysis. According to Fig. 3.4a and 3.4c, the intensity and symmetry of the peak eluted between 15 and 16 min increased with time and corresponded to compounds with molecular weight range of 4.8 to 9.2 kDa (27 to 52 DP). The absence of peaks at early times suggested that polygalacturonic acid residues with molecular weights higher than 9.2 kDa were insoluble in the reaction media. Indeed, insoluble homogalacturonic fragments with molecular weights between 19 and 24.2 kDa have been obtained from controlled acid hydrolysis of citrus pectin (Thibault et al., 1993). The latter molecular weight range confirmed the absence of peaks before 15 min in Fig. 3.4a. Consequently, dissolution of polygalacturonic acid and its partial hydrolysis into reduced molecular size fragments under sCW conditions was evident; however, further research is needed to better understand solubilization behavior of polygalacturonic acid in sCW. After 30 min, hydrolysis of dissolved galacturonic acid fragments proceeded further (Figs. 3.4d and 3.4e). The areas of the peaks eluted between 15 and 16 min did not increase considerably but shifted towards lower molecular weights, and peaks

eluting later at 16.5 min (3 kDa/18 DP) and 16.8 min (2.4 kDa/14 DP) were identified. In addition, each chromatogram in Figs. 3.4a-e showed a defined peak eluted at 17.3 min, and the intensity of this peak did not change with time. As this peak corresponded to compounds with molecular size of 1.6 kDa (9 DP), which is very close to the permeation limit of the column, it can be assumed that compounds with this molecular size were easily released under sCW conditions within 10 min and were eluted all together at the same time.

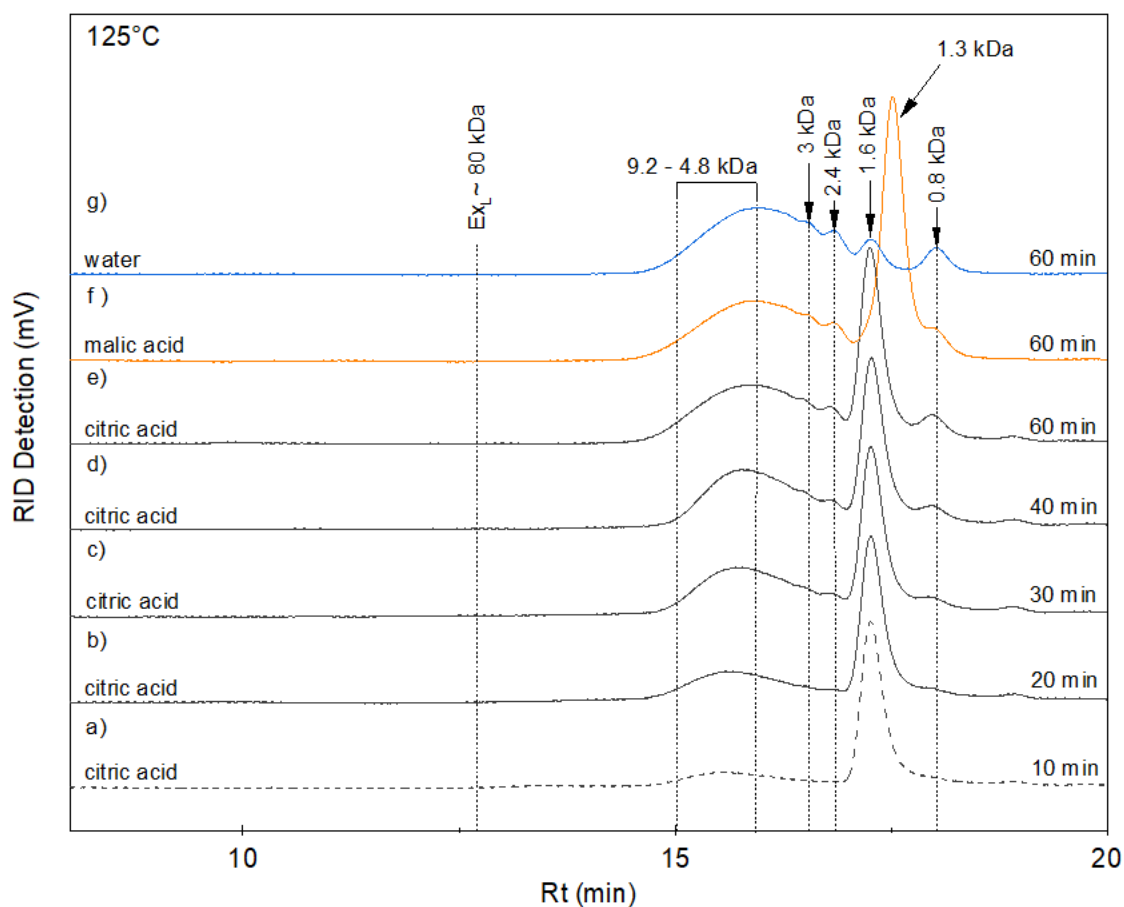


**Fig. 3.4.** HPSEC-RID chromatograms of polygalacturonic acid hydrolysates obtained in aqueous citric acid at 125°C/100 bar and reaction times of: a) 10 min, b) 20 min, c) 30 min, d) 40 min, and e) 60 min, and different reaction media: f) aqueous malic acid, and g) water. EX<sub>L</sub>: column exclusion limit.

Figs. 3.4e-g show the effects of aqueous citric and malic acids and water as reaction media on polygalacturonic acid hydrolysis at 60 min. Malic acid favored hydrolysis, releasing low molecular weight compounds as indicated by the increasing area and peak shift from 17.3 to 17.5 min, that corresponded to compounds with lower molecular weight of 1.3 kDa (7 DP). Although the pH of both aqueous acidic reaction media was 2.6, the nature of the acid and/or the slight difference between the concentrations of acids could have influenced the extent of polygalacturonic acid hydrolysis. Also, the different number of carboxyl functional groups and their corresponding dissociation constants ( $K_a$ ) could have contributed to such an effect as malic acid containing less carboxyl groups and lower  $K_{a1}$  ( $3.84 \times 10^{-4}$ ) led to a high intensity peak for the low molecular weight components compared to citric acid. The elution profile for the hydrolysate obtained with water was different because the peak area at 17.3 min was substantially lower compared to that for citric acid, and no peak was eluted at 17.5 min, which was a singularity for malic acid elution profile (Fig. 3.4f). In addition, a defined peak eluted at 18 min (0.8 kDa/4 DP) was identified for all three media evaluated. In general, water seemed to exert a selective effect on polygalacturonic acid hydrolysis as compounds with molecular sizes between 51-14 DP and 4 DP were produced but compounds between 9 and 7 DP were hindered. Overall, the HPSEC-RID elution profiles confirmed that polygalacturonic acid was hydrolyzed under sCW conditions at a relatively low temperature of 125°C, regardless of the reaction media. Based on these results, a XBridge Amide column with reduced particle size of 3.5  $\mu\text{m}$  was used to further analyze the hydrolysates, in particular to verify the molecular size and composition of fragments ( $\text{MW} \leq 2.4 \text{ kDa}$ ) that eluted close to and beyond the permeation limit of the current Ultrahydrogel 250 column (6  $\mu\text{m}$  particle size).

### 3.3.2 Oligogalacturonides distribution in polygalacturonic acid hydrolysates

The release of oligogalacturonides during polygalacturonic acid hydrolysis at 125 and 135°C/100 bar in aqueous citric acid was determined by HILIC-ELSD analysis. Also, the effects of reaction time (10 – 120 min) and different reaction media (malic acid and water) at 125 and 135°C/100 and 60 min were assessed.

Chromatograms in Fig. 3.5 show that temperature and time influenced the rate of hydrolysis as well as the distribution and concentration of polygalacturonic acid-derived fragments. According to Figs. 3.5a1 and 3.5a2, hydrolysates obtained at 125°C for 10 and 20 min displayed limited peaks associated to polygalacturonic acid fragments of  $DP \leq 14$ , suggesting limited hydrolysis of polygalacturonic acid. Thibault et al. (1993) reported that at  $pH \leq 2$ , O-glycosidic bonds between galacturonic acid residues become more stable, as such, acid-insoluble homogalacturonic acid fragments (21 - 24 kDa) were isolated from pectic matrices (apple, beet and citrus) after 72 h of acid hydrolysis with 0.1 M HCl at 80°C. Hence, studies on the kinetics of hydrolysis of homogalacturonan from apple pectin have shown that acid hydrolysis with 0.2, 1 or 2 M H<sub>2</sub>SO<sub>4</sub> at 80°C for 72 h was insufficient to achieve complete depolymerization to galacturonic acid (Garna et al., 2006).

Conversely, in Fig. 3.5b1, the hydrolysate obtained at 135°C and 10 min already showed peaks corresponding to poly/oligogalacturonic acid fragments within a 2 to 14 DP range. After 20 min of reaction, the area of every peak increased, in particular towards oligogalacturonides with 2-7 DP (Fig. 3.5b2), demonstrating that a 10°C rise in temperature considerably enhanced the rate of hydrolysis. Also, the chromatograms in Figs. 3.5a3-3.5a5 indicate that at 125°C, hydrolysis proceeded gradually between 30 and 60 min, and high peak areas corresponded to 2-7 DP oligogalacturonides at 60 min. Poly/oligogalacturonides with 8-14 DP were further hydrolysed to

mono-, di-, tri- and tetra-galacturonic acids (Fig. 3.5a6). Although longer reaction times favored the release of oligogalacturonides in 2-14 DP range at 125°C, after 60 min of hydrolysis, there was no additional release of intermediates from the backbone but accumulation of 1-4 DP fragments.

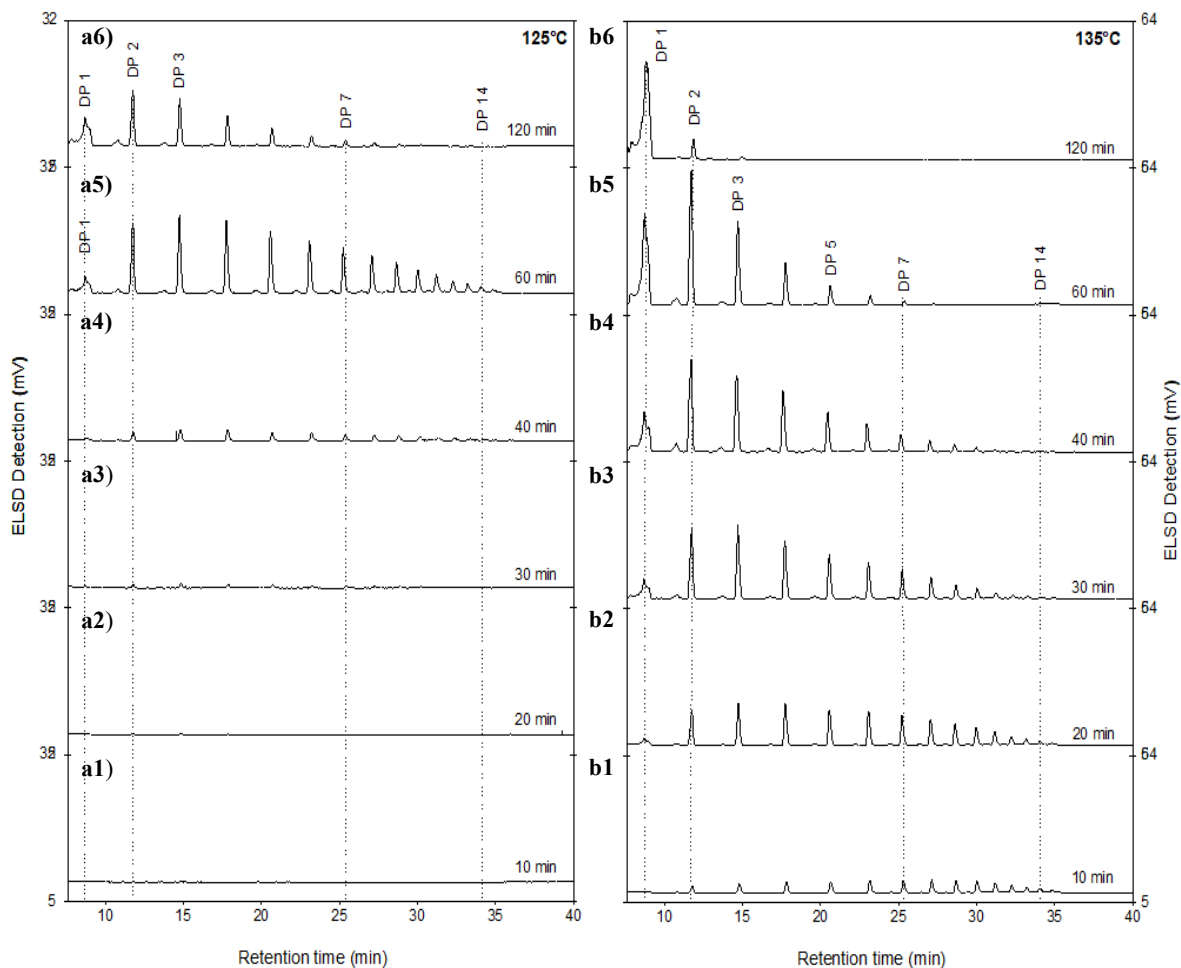


**Fig. 3.5.** Effect of reaction time (10-120 min) on polygalacturonic acid hydrolysis in aqueous citric acid at 100 bar and temperatures of: a) 125°C, and b) 135°C analyzed by HILIC-ELSD. Scale of Fig. 3.5b is 2:1 with respect to Fig. 3.5a.

Interestingly, the cleavage patterns observed during polygalacturonic acid breakdown by either citric acid-catalyzed hydrolysis at sCW conditions or by enzymatic hydrolysis with *endo*-polygalacturonase M2 (*Aspergillus aculeatus*) were similar (Combo et al., 2012). The

endopolygalacturonase activity on polygalacturonic acid is based on a random attack that leads to relatively long galacturonic acid fragments with a subsequent hydrolysis to 1-3 DP oligogalacturonides (Combo et al., 2012), and an analogous trend was also observed for the sCW treatment.

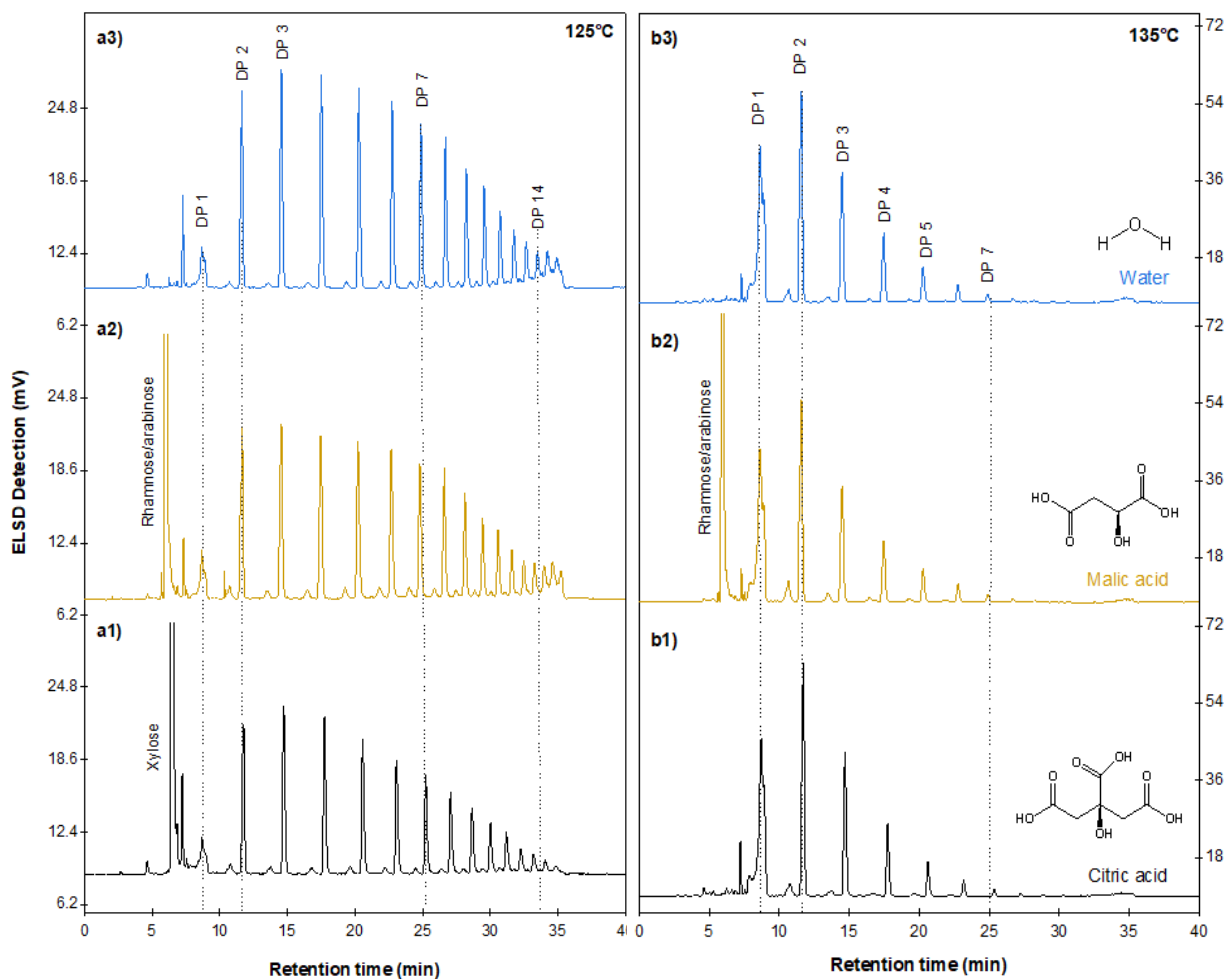
Chromatograms in Figs. 3.5b4-3.5b6 show that at 135°C, a reaction time longer than 30 min favored further hydrolysis of 8-14 DP intermediates but not their release from the backbone. After 120 min of reaction, mainly two peaks corresponding to mono- and di-galacturonic acid were apparent in the chromatogram (Fig. 3.5b6).

Fig. 3.5 indicates that temperature had a considerable effect on the concentrations of produced oligogalacturonides but not the reaction time. Overall, the intensity of peaks obtained at 135°C was approximately 2-fold compared to those obtained at 125°C, regardless of the reaction time. Therefore, the initial breakdown and dissolution of polygalacturonic acid could be considered as the limiting step during polygalacturonic acid hydrolysis under sCW conditions. A temperature rise from 125 to 135°C led to a faster dissolution and breakdown of polygalacturonic acid, increasing the amount of poly/oligogalacturonic acid fragments needed for subsequent oligogalacturonide production. The effect of temperature on polygalacturonic acid breakdown could be associated to its structure. For example, studies on acid hydrolysis of other plant cell wall components, such as cellulose and xylan have also shown a two-stage hydrolysis process, which has been related to the heterogeneous nature of their structures and therefore to the presence of an easy to hydrolyze portion and a resistant portion (Kim et al., 2013; Saeman, 1945). Two linear stages have been also observed during pectic acid breakdown by polygalacturonase, where the rate of the initial stage (30 min) was 44 times faster than the rate of the second stage (10 h) (Delmain and Phaff, 2017). In addition, limited hydrolysis of pectic acids (46%) by exopolygalacturonase

has been reported (Hatanaka and Ozawa, 1964). In general, exopolygalacturonase catalyzes hydrolytic cleavage of  $\alpha$ -(1 $\rightarrow$ 4) glycosidic bonds of pectic acid at its non-reducing end and yields mono-galacturonic acid. Consequently, the existence of unusual O-glycosidic bonds in pectic acids has been suggested as a cause of the limited hydrolysis (Hatanaka and Ozawa, 1964; Stratilová et al., 2005). Based on those findings, sCW hydrolysis at high temperatures could enhance solvation (endothermic process) and breakdown of the structurally different portions of polygalacturonic acid, leading to an increased amount of poly/oligogalacturonic acid fragments for further hydrolysis to oligogalacturonides of lower DP.

Fig. 3.6 shows the effect of different reaction media on polygalacturonic acid hydrolysis when temperature was kept constant at either 125°C or 135°C for 60 min. According to Figs. 3.6a1-3.6a3, the overall influence of the reaction media on hydrolysis at 125°C was negligible as the elution pattern and signal intensity were quite similar for each hydrolysate. Poly/oligogalacturonic acid fragments with 2-7 DP and 8-14 DP were clearly identified regardless of the reaction media. Nonetheless, Figs. 3.6a1 and 3.6a2 showed an additional peak eluted early at either 6 min or 6.5 min when aqueous malic acid or citric acid was used, respectively. The identities of these peaks were determined by injection of neutral sugar standards, which confirmed the presence of rhamnose/arabinose and xylose, eluting at 6 and 6.5 min, respectively. Although polygalacturonic acid has been referred to as a homopolymer, studies of the length of polygalacturonic acid chain in various pectins by acid hydrolysis have revealed that polygalacturonic acid does not exhibit a regular structure and it can be comprised of fragments of 72 - 100 DP in length with intercalated rhamnose (Rha) and xylose (Xyl) residues possibly attached directly to the polygalacturonic acid backbone (Thibault et al., 1993). Therefore, the presence of rhamnose or xylose in the hydrolysates obtained with carboxylic acids could be an indication of the heterogeneity of the polygalacturonic

acid structure as well as the presence of O-glycosidic bonds with different levels of susceptibility to acid hydrolysis.



**Fig. 3.6.** HILIC-ELSD chromatograms of polygalacturonic acid hydrolysates obtained at: a) 125°C and b) 135°C, 100 bar and 60 min in different reaction media: 1) aqueous citric acid, 2) aqueous malic acid, and 3) water.

Consequently, it can be hypothesized that polygalacturonic acid used as substrate in this study could have a structure comprised of O-glycosidic bonds between two galacturonic acid molecules ( $\alpha$ -GalA-(1  $\rightarrow$  4)- $\alpha$ -GalA) and between galacturonic acid and rhamnose ( $\alpha$ -GalA-(1  $\rightarrow$  2)- $\alpha$ -Rha) or rhamnose and galacturonic acid ( $\alpha$ -Rha-(1  $\rightarrow$  4)- $\alpha$ -GalA) (Fig. 3.7). It can also be hypothesized

that O-glycosidic bonds between GalA and Rha or GalA and Xyl could be more susceptible to cleavage in the presence of carboxylic acids compared to water. Solute-solvent interactions can alter intermolecular and intramolecular hydrogen bonding, causing diverse internal electron and steric repulsions between the oxygen atoms, and subsequently influence the final molecular conformation of the solute (Kirschner and Woods, 2001; Mansel et al., 2020). Thus, the solvents used could have influenced differently the molecular conformation preferences of polygalacturonic acid so that cleavage of O-glycosidic bonds between GalA and Rha or Xyl was favored when carboxylic acids were used but not with water alone.

In addition, the effect of polygalacturonic acid-solvent interactions can be also noted on O-glycosidic linkages between two galacturonic acid residues, where the areas of peaks corresponding to polygalacturonic acid fragments with 8-14 DP obtained at 125°C with citric acid were significantly lower compared to those obtained with water or malic acid at the same temperature (Figs. 3.6a1-3.6a3 and Table 3.1). This suggests that the interaction between polygalacturonic acid and citric acid, which is a tri-carboxylic acid, could have modified internal electron and steric repulsions between the oxygen atoms within the polymer, leading to more stable  $\alpha$ -GalA-(1  $\rightarrow$  4)- $\alpha$ -GalA bonds that were less prone to hydrolysis (Thibault et al., 1993).

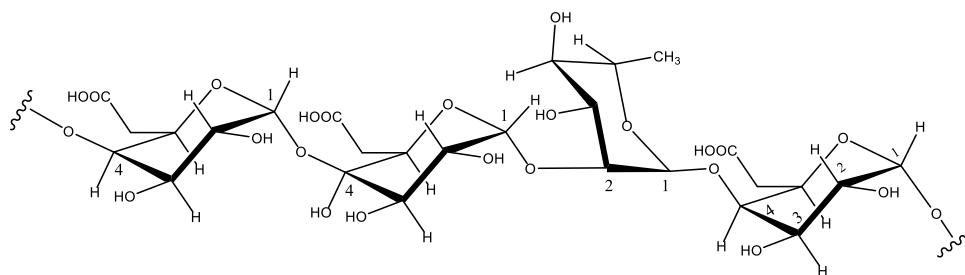


**Fig. 3.7.** O-glycosidic bonds  $\alpha$ -GalA-(1 $\rightarrow$ 4)- $\alpha$ -GalA-(1 $\rightarrow$ 2)- $\alpha$ -Rha-(1 $\rightarrow$ 4)- $\alpha$ -GalA in polygalacturonic acid.

**Table 3.1.** Effects of temperature and reaction media on polygalacturonic acid hydrolysis at 100 bar/60 min.

T (°C)	Reaction media	Degree of polymerization				
		1 DP	2 DP	3 DP	2-7 DP	8-14 DP
(g of galacturonic acid anhydrous equivalents/L)						
125	Citric acid	0.15 ± 0.00 <sup>a</sup>	0.27 ± 0.02 <sup>a</sup>	0.20 ± 0.03 <sup>a</sup>	1.22 ± 0.16 <sup>a</sup>	0.73 ± 0.07 <sup>b</sup>
125	Malic acid	0.16 ± 0.01 <sup>a</sup>	0.29 ± 0.03 <sup>a</sup>	0.22 ± 0.04 <sup>a</sup>	1.38 ± 0.20 <sup>a</sup>	0.90 ± 0.03 <sup>a</sup>
125	Water	0.16 ± 0.01 <sup>a</sup>	0.31 ± 0.02 <sup>a</sup>	0.24 ± 0.01 <sup>a</sup>	1.49 ± 0.01 <sup>a</sup>	1.01 ± 0.04 <sup>a</sup>
135	Citric acid	0.76 ± 0.03 <sup>b</sup>	0.65 ± 0.07 <sup>b</sup>	0.39 ± 0.05 <sup>b</sup>	1.68 ± 0.20 <sup>a</sup>	0.08 ± 0.00 <sup>c</sup>
135	Malic acid	0.78 ± 0.00 <sup>b</sup>	0.68 ± 0.01 <sup>b</sup>	0.40 ± 0.00 <sup>b</sup>	1.78 ± 0.01 <sup>a</sup>	0.10 ± 0.02 <sup>c</sup>
135	Water	0.78 ± 0.01 <sup>b</sup>	0.68 ± 0.04 <sup>b</sup>	0.41 ± 0.04 <sup>b</sup>	1.79 ± 0.17 <sup>a</sup>	0.10 ± 0.01 <sup>c</sup>

<sup>a-c</sup> Means (n=2) in each column followed by different letters are significantly different (Tukey's HSD,  $p < 0.05$ ).

Unlike the broad elution pattern of hydrolysates obtained at 125°C, hydrolysates obtained at 135°C (Figs. 3.6b1-3.6b3) displayed a narrow elution pattern that represents oligogalacturonides with molecular size of 1 and 2-7 DP only. As the elution pattern and signal intensity were similar for each hydrolysate, the reaction media did not have a selective effect on hydrolysis at 135°C, indicating that a 10°C rise in temperature could increase the entropy of the system and the amount of random activity to the point that minimizes the effect of polygalacturonic acid-solvent interactions and therefore decreases the potential selectivity of the reaction media. Temperature had a significant effect ( $p < 0.005$ ) on the rate of hydrolysis. Poly/oligogalacturonic acid fragments with 8–14 DP were hydrolyzed considerably faster at 135°C into 1 and 2-7 DP oligogalacturonides, where mono- and di-galacturonic acids exhibited the highest peak areas. Hence, the amounts of mono-galacturonic acid as well as di- and tri-galacturonic acids obtained at 135°C were 5 and 2-fold, respectively, compared to those obtained at 125°C (Table 3.1). Based on the two-way ANOVA, the interaction effect between temperature and reaction media on the distribution of poly/oligogalacturonic acid fragments was significant (Table 3.1).

The change in the concentrations of released poly/oligogalacturonic acid fragments over time in aqueous citric acid media is presented in Fig. 3.8. The insets of Fig. 3.8 show the overall effect of temperature and reaction time on the yield of polygalacturonic acid fragments obtained with citric acid at 100 bar. The highest yield of 2-7 DP oligogalacturonides was achieved at either 135°C/30 min (41%) or 125°C/120 min (37%), suggesting that temperature and time were inversely proportional, thus a 10°C rise in temperature enhanced the reaction rate and decreased the reaction time 4-fold. At 135°C, the rate of hydrolysis towards smaller fragments also increased. Likewise, the maximum yield of 8-14 DP poly/oligogalacturonides was achieved at either 135°C/10 min (18%) or 125°C/60 min (15%). At 135°C, the reaction time was 1/6<sup>th</sup> of that required at 125°C. As expected, the yield of polygalacturonic acid-derived fragments increased with temperature. Although the temperature range used in this study was relatively low, the yield of 2-7 DP oligogalacturonides obtained with citric acid was comparable to the yield of oligogalacturonides (1-10 DP) obtained at higher temperature by Miyazawa and Funazukuri (2004), who reported a yield of oligogalacturonides and furfural of 33% and 1%, respectively, at 260°C/100 bar and 15 min of reaction in semi-continuous mode.

The composition of the hydrolyzed portion of polygalacturonic acid was elucidated based on the ratio of the yields of 2-7 DP to 8-14 DP fragments, which was approximately 2:1. After 120 min reaction, the conversions of polygalacturonic acid were 0.57 and 0.67 at 125°C and 135°C, respectively. Therefore, 33% of the polygalacturonic acid substrate was not hydrolyzed at 135°C/120 min/100 bar in aqueous citric acid down to the fractions analyzed. But the hydrolyzed portion was 67% and consisted of 2-7 DP and 8-14 DP fragments in a 2:1 ratio.

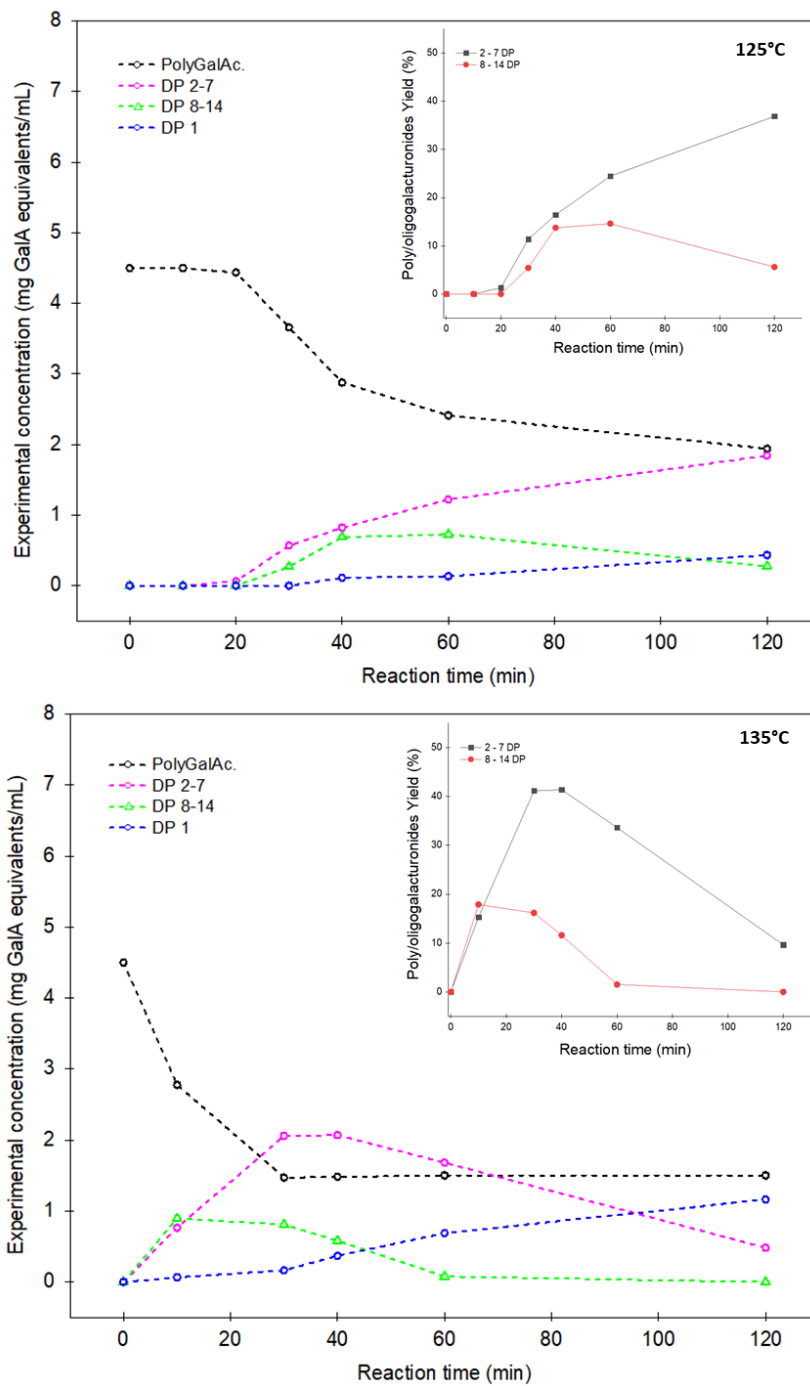


**Fig. 3.8.** Experimental concentrations of released poly/oligogalacturonic acid fragments in aqueous citric acid and their yields at a) 125°C/100 bar, and 135°C/100 bar. The insets show the yield of poly/oligogalacturonides at 125°C and 135°C.

### 3.3.3 Kinetics and modelling of polygalacturonic acid hydrolysis

According to the proposed mechanism for polygalacturonic acid hydrolysis under sCW conditions (Fig. 3.3), the kinetic parameters were estimated and further used to develop a model. Aqueous citric and malic acids exerted a comparable hydrolytic effect on polygalacturonic acid sCW hydrolysis, therefore, the kinetic parameters were only adjusted for citric acid.

The rate constant values obtained at 125 and 135°C as well as the associated activation energy values are summarized in Table 3.2. As expected, the rate constants were higher at 135°C. During the formation of Ga<sub>(2-7)</sub> at 135°C, for example, the increased entropy of the system could have facilitated interaction between reactant molecules, leading to a  $k_1$  value 3-fold higher than that at 125°C. The formation of 8-14 DP poly/oligogalacturonic acid fragments from polygalacturonic acid required the highest energy to achieve enough frequency of collisions between polygalacturonic acid and water molecules to react; therefore, it could be considered as the rate-determining step for the hydrolysis. As well, the higher activation energy corresponded to higher pre-exponential frequency factor. The activation energies for 8-14 DP, 2-7 DP and monogalacturonic acid were 174, 142, and 65 kJ/mol, respectively. These values fall within the activation energy values reported for xylan autohydrolysis into xylo-oligosaccharides (127.3 and 251.7 kJ/mol) and xylose (119.0 kJ/mol) at temperatures between 150 and 190°C, where the highest activation energy corresponded to the hydrolysis of the least reactive xylan portion (Nabarlatz et al., 2004). Like the heterogeneous structure of xylan, polygalacturonic acid backbone seemed to be comprised of fractions that have different susceptibility to acid hydrolysis, where the resistant fraction can be associated to an activation energy probably higher than 174 kJ/mol. Conversely, the relatively lower activation energy required for the hydrolysis of 2-7 DP oligogalacturonides into mono-galacturonic acid suggests that this step is more sensitive to the

treatment than the initial hydrolysis of polygalacturonic acid. Thus, a further temperature increase, or a longer reaction time might not favor the yield of poly/oligogalacturonides (8-14 DP) but depolymerization of 2-7 DP oligogalacturonides to the monomer.

**Table 3.2.** Arrhenius activation energy and rate constants for polygalacturonic acid hydrolysis with citric acid at 125 or 135°C and 100 bar.

	<i>k</i> (min <sup>-1</sup> )				Ln (A) (min <sup>-1</sup> )	Ea (kJ/mol)
	125°C	<i>R</i> <sup>2</sup>	135°C	<i>R</i> <sup>2</sup>		
k <sub>1</sub> (Ga <sub>(2-7)</sub> )	0.2320	0.90	0.6641	1	41.45	142
k <sub>2</sub> (Ga <sub>(8-14)</sub> )	0.1866	0.78	0.6796	1	51.06	174
k <sub>3</sub> (Ga <sub>(2-7)</sub> )	0.0160	1	0.0762	0.99	0.001	0
k <sub>4</sub> (Ga)	0.0080	1	0.0130	0.89	14.98	65

Fig. 3.9 shows the kinetics of polygalacturonic acid hydrolysis obtained by the proposed model. Overall, the model described the trends of the disappearance of polygalacturonic acid due to parallel reactions as well as the appearance of its reduced molecular weight intermediate fragments, and their further decay over time due to consecutive reactions. The effect of temperature on both, reaction rates and concentrations of polygalacturonic acid fragments, was also captured by the model. A temperature rise enhanced the rate of hydrolysis and increased the concentration of the released poly/oligogalacturonic acid fragments, which was aligned to the experimental behavior (Fig. 3.8). However, the proposed model has some limitations as it did not include restrictions associated to the heterogeneity of the polygalacturonic acid backbone such as linked neutral sugars and O-glycosidic bonds with different levels of susceptibility to acid hydrolysis. Therefore, predicted concentration of polygalacturonic acid-derived fragments were based on total polygalacturonic acid conversion, which differed from the experimental conversion values that were 57 and 67% at 125 and 135°C, respectively. The model predicts the general trend of

polygalacturonic acid hydrolysis under sCW conditions, but further work is still required to minimize overestimation in the predicted concentration of oligogalacturonides by taking into account the heterogeneity of the substrate.

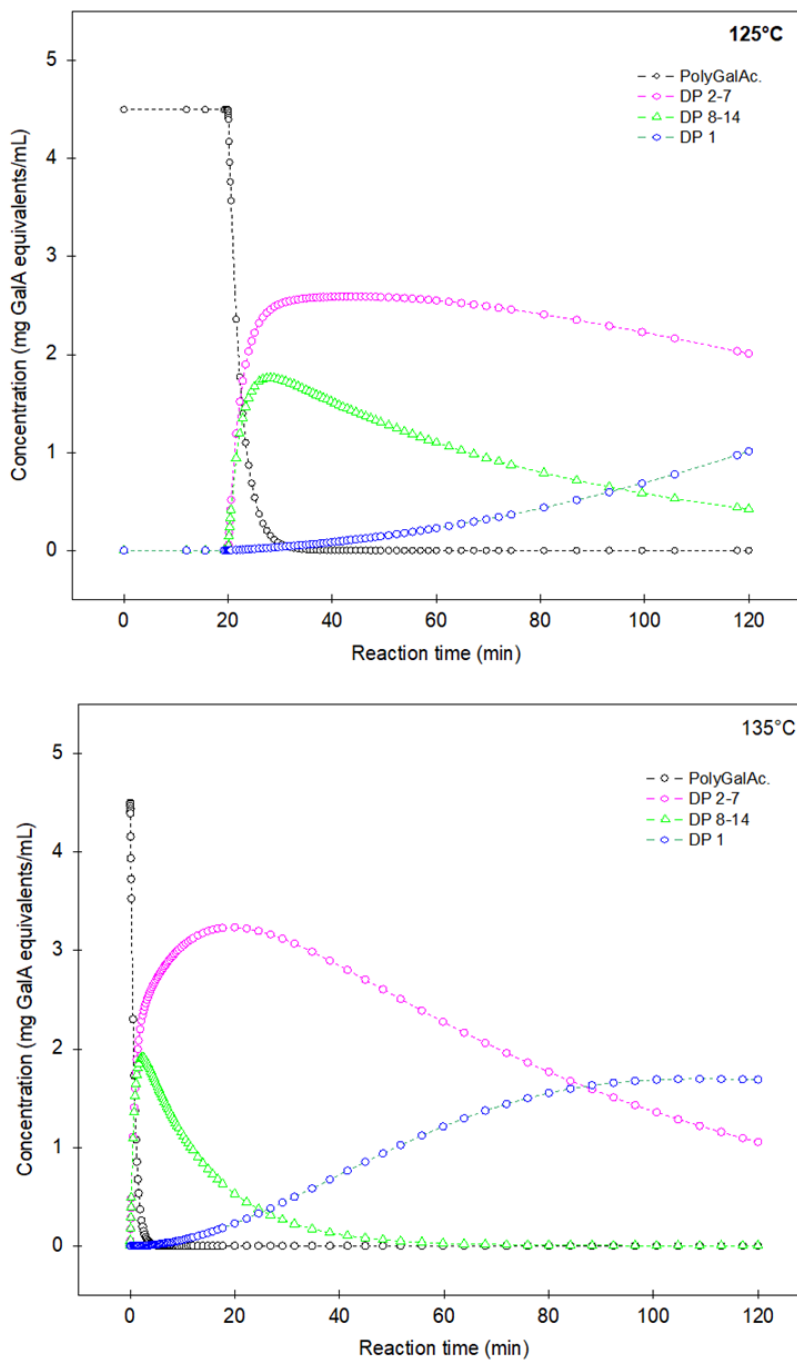


**Fig. 3.9.** Kinetics of polygalacturonic acid hydrolysis with aqueous citric acid at 100 bar predicted by the model at: a) 125°C, and b) 135°C.

### 3.4 Conclusions

For the first time, experimental data obtained in this study showed that *i*) hydrolysis of linear polygalacturonic acid into oligogalacturonides (2-7 DP) was achieved using sCW technology at relatively low temperatures (125 or 135°C) and a short reaction time (30 min), *ii*) di- and tri-carboxylic acids modified the reaction environment via solvent effects, altering the susceptibility of O-glycosidic linkages to acid hydrolysis, particularly at 125°C, *iii*) an easy to hydrolyze portion and a resistant portion were identified as part of the polygalacturonic acid structure, *iv*) the conversions of polygalacturonic acid were 0.57 and 0.67 at 125°C and 135°C, respectively, and *v*) the proposed reaction mechanism and the kinetics model for polygalacturonic acid hydrolysis, assuming a homogeneous structure, involving parallel and consecutive reactions demonstrated the need for a more sophisticated model to reflect the heterogeneous nature of the substrate. These findings provide a foundation for further elucidation of the effects of carboxylic acids under sCW conditions on complex and branched pectic structures comprised of different O-glycosidic linkages like rhamnogalacturonan-I, which is the focus of the next study.

## Chapter 4: Carboxylic acid-catalyzed hydrolysis of rhamnogalacturonan in subcritical water medium\*

### 4.1 Introduction

Rhamnogalacturonans, also referred to as the pectin “hairy regions”, is a very diverse and complex group of pectic polysaccharides found in plant cell walls (Buffetto et al., 2015; Mikshina et al., 2015). Rhamnogalacturonans are branched compounds comprised of neutral and acidic saccharides, including rhamnogalacturonan-I (RG-I) and rhamnogalacturonan-II (RG-II). The chemical composition of RG-I backbone and its main side chains and linkages was described in Chapter 2 (Fig. 2.1).

As rhamnogalacturonans are saccharide-rich pectic structures, they have been used as a source to obtain oligosaccharides of diverse composition. Recently, Zheng et al. (2018) obtained galacto-oligosaccharides with prebiotic effect by acid hydrolysis (0.2M trifluoroacetic acid/80°C/4 h) of potato pectic galactan. However, Khodaei and Karboune (2018) produced prebiotic galacto- and galacto-arabino oligosaccharides by enzymatic digestion (galactanase, arabinanase and rhamnogalacturonase) of potato rhamnogalacturonan-I. Conversely, Schols et al. (1990) isolated heterogeneous oligomers containing a  $[\rightarrow 2)\text{-}\alpha\text{-L-Rhap-(1}\rightarrow 4)\text{-}\alpha\text{-D-GalAp-(1}\rightarrow ]$  backbone by rhamnogalacturonase hydrolysis of apple pectin hairy regions.

The use of diluted mineral acids, multi-enzyme mixtures and their combination has been prevalent to obtain rhamnogalacturonan-derived oligosaccharides as well as to study rhamnogalacturonan fine structure (Buffetto et al., 2015; Huisman et al., 2001; Nakamura et al., 2014). However, neither the use of carboxylic acids nor subcritical water (sCW) technology has

---

\* A version of this Chapter has been submitted to the *Journal of Supercritical Fluids* for consideration for publication as Carla S. Valdivieso Ramirez, Feral Temelli and Marleny D.A. Saldaña. Carboxylic acid-catalysed hydrolysis of rhamnogalacturonan in subcritical water media.

been explored to induce the hydrolysis of rhamnogalacturonan. As part of the ongoing research towards the production of oligosaccharides from complex pectic substrates like pea fiber, the use of di- and tri-carboxylic acids under sCW conditions was initially investigated to induce hydrolysis on polygalacturonic acid, a linear homogalacturonan, as a model substrate in Chapter 3. Therefore, in this study, commercial rhamnogalacturonan from soybean was selected as a model branched pectic compound from legumes to evaluate the hydrolytic effect of aqueous carboxylic acids under subcritical conditions (125, 135, 145, and 155°C/100 bar) as well as to obtain some insight about its structure and hydrolysis mechanism.

## **4.2 Materials and Methods**

### **4.2.1 Materials**

Rhamnogalacturonan from soybean (P-RHAGN, purity of 97%) was purchased from Megazyme (Megazyme Ltd., Bray, Wicklow, Ireland). Reagents for the sCW hydrolysis were citric acid (>99.5%, ACS grade) and malic acid (>99.5%, ACS grade) from Sigma Aldrich (Oakville, ON, Canada), water from the Milli-Q system (18.2 MΩ.cm, Millipore, Billerica, MA, USA) and nitrogen gas (99.9% purity) from Praxair Canada Inc. (Edmonton, AB, Canada).

For the analytical procedures, sodium nitrate, ammonium formate, formic acid, acetonitrile, and standards of mono-galacturonic acid, di-galacturonic acid, tri-galacturonic acid, polygalacturonic acid, glucose, D-galactose, D-arabinose, D-xylose, D-fucose and L-rhamnose were acquired from Sigma Aldrich (Oakville, ON, Canada). Malto-oligosaccharides with a degree of polymerization (DP) of 2 to 7 were purchased from Supelco Inc. (Bellefonte, PA, USA). Low methoxyl pectin (36% degree of esterification) Classic CU 701 was kindly provided by Herbstreith and Fox (Turnstraße, Neuenbürg, Germany). Dextran with molecular weights of 1.2, 3, 5, 25 and

72 kDa were obtained from the American Polymer Standards Corporation (Mentor, OH, USA) and HPLC-grade water was purchased from Fisher Scientific (Ottawa, ON, Canada).

#### **4.2.2 Subcritical water hydrolysis of rhamnogalacturonan**

A Parr 4590 system (Parr Instrument Company, Moline, IL, USA) equipped with a 100 mL reactor, a magnetic drive, a temperature controller, and a computer for data recording was used to hydrolyze rhamnogalacturonan under sCW conditions. The same equipment was also used previously for the hydrolysis of polygalacturonic acid in sCW medium (Chapter 3, Fig. 3.1). The input variables for the sCW hydrolysis of rhamnogalacturonan were temperature (125, 135, 145, and 155°C), reaction time (10, 20, 30, 40, 60, and 120 min), and reaction medium (aqueous citric and malic acids). The aqueous solution consisted of either 0.20% w/w of citric acid or 0.27% w/w of malic acid to reach a pH of 2.6 in both cases. The selected values for reaction time and pH of the reaction medium were the same as in the previous study on sCW hydrolysis of the linear polygalacturonic acid using citric and malic acids (Chapter 3) in an effort to understand the catalytic effect of these acids under sCW conditions on the more complex and branched rhamnogalacturonan. Employing similar conditions would facilitate comparison of results obtained for a linear (polygalacturonic acid) and a branched (rhamnogalacturonan) pectic substrate. The working pressure was set to 100 bar to add energy by compression to the system and favor chemical reactions (Marshall and Frank, 1981; Park and Park, 2002) similar to the reactions performed on the linear polygalacturonic acid model previously (Chapter 3). The experiments were performed in duplicates and water was used as the control reaction medium.

For the sCW hydrolysis, a start-up run was carried out using water only before each set of four experimental runs to ensure the reproducibility of the operating conditions, following the same protocol as described for the linear polygalacturonic acid model system (Chapter 3). A 1% w/w

rhamnogalacturonan solution was used as the starting material for the hydrolysis. Briefly, 400 mg of rhamnogalacturonan and 40 g of citric acid solution (0.2% w/w) were sequentially loaded into the reactor, and after reaching the set temperature and pressure, the reaction time was started. The come-up time for the hydrolysis at 125, 135, 145, and 155 °C were registered as  $5.3\pm 0.2$ ,  $5.8\pm 0.4$ ,  $7.1\pm 0.7$ , and  $6.8\pm 0.5$  min, respectively. At the end of the targeted reaction time, the reactor was cooled down and depressurized. Then, rhamnogalacturonan hydrolysates were collected and stored frozen at  $-18^{\circ}\text{C}$  until further HPLC analysis.

### **4.2.3 Characterization of rhamnogalacturonan hydrolysates**

#### **4.2.3.1 Fourier transform infrared (FT-IR) spectroscopy analysis**

The infrared spectra of rhamnogalacturonan, freeze-dried rhamnogalacturonan hydrolysates, and standards (polygalacturonic acid and low methoxyl pectin) were collected using a Nicolet 8700 Fourier Transform Infrared Spectrometer (Thermo Fisher Scientific Inc, Waltham, MA, USA) equipped with a Smart Speculator for Attenuated Total Reflection (ATR germanium crystal cell). The spectra were recorded from  $350$  to  $4000\text{ cm}^{-1}$  with a resolution of  $4\text{ cm}^{-1}$  and 128 scans using Omnic software (version 7.1).

#### **4.2.3.2 Molecular weight distribution**

High pressure size exclusion chromatography (HPSEC) was used to monitor rhamnogalacturonan hydrolysis under different subcritical conditions. The molecular weight (MW) distribution of rhamnogalacturonan hydrolysates was determined using a Shimadzu 10-A HPLC system (Shimadzu Corporation, Kyoto, Japan) equipped with a refractive index detector RID-10A (Shimadzu Corporation, Kyoto, Japan) and an Ultrahydrogel 250 column ( $7.8 \times 300\text{ mm}$ ,  $6\text{ }\mu\text{m}$  particle size) (Waters, Milford, MA, USA) following the methodology described in Chapter 3 (Section 3.2.3.1).

#### 4.2.3.3 Determination of oligosaccharides

Hydrophilic interaction liquid chromatography (HILIC) was used to study the lower molecular weight fragments derived from rhamnogalacturonan hydrolysis. The analysis was performed on a Shimadzu SPD-20A HPLC system (Shimadzu Corporation, Kyoto, Japan) equipped with an Evaporative Light Scattering detector (3300 Alltech ELSD, BÜCHI Labortechnik. AG, Flawil, Switzerland), using an XBridge Amide column (4.6 x 250 mm, 3.5 µm particle size) (Waters Corp., Milford, MA, USA). The separation was achieved according to the protocol described in Chapter 3 (Section 3.2.3.2).

Standard solutions with concentrations between 0.1 to 1.5 mg/mL of acidic oligosaccharides (mono-, di- and tri-galacturonic acids) as well as of neutral oligosaccharides (malto-oligosaccharides 2-7 DP) were injected to determine their retention times.

#### 4.2.3.4 Neutral sugar analysis

The release of neutral sugars with reaction time was quantified following the HILIC-ELSD method described in Chapter 3 (Section 3.2.3.2), with some modifications. The elution of sugars (D-arabinose, D-xylose, D-fucose and L-rhamnose) was carried out at 40°C and a flow rate of 0.3 mL/min for 35 min. The composition of mobile phases used for the elution were modified to (A) 80:20 (v/v) acetonitrile/water with 0.2% triethanolamine (TEA), and (B) 30:70 (v/v) acetonitrile/water with 0.2% TEA. The elution gradient was: 0-16 min, linear from 5 to 8% B; 16-18 min, linear from 8 to 70% B; 18-22 min, linear from 70 to 8% B; followed by a column re-equilibration elution gradient: 22-22.01 min, linear from 8 to 5% A and, 22.01-35 min, isocratic 5% B. Standard solutions of D-glucose, D-galactose, D-arabinose, D-xylose, D-fucose and L-rhamnose with concentrations between 0.1 and 1.5 mg/mL were injected to determine the retention

times and to obtain the calibration curves. The amounts of individual released neutral sugars and total released sugars were quantified according to Eqs. (4.1) and (4.2), respectively.

$$\text{Released neutral sugar (\%)} = \frac{\text{mass of released sugar (mg)}_t}{\text{mass of sugar in feed (mg)}} \times 100 \quad \text{Eq. (4.1)}$$

where,  $(\text{released sugar})_t$  is the mass of an individual sugar in the free form that is present in the hydrolysate at time  $t$ , and  $(\text{mass of sugar in feed})$  is the total amount of an individual sugar that is initially present in 400 mg of rhamnogalacturonan loaded into the reactor, which is calculated based on the individual sugar composition (% w/w) of rhamnogalacturonan.

$$\text{Total released sugars (\%)} = \frac{\text{mass of released } \sum(\text{Xyl} + \text{Ara} + \text{Fuc} + \text{Rha})_t}{\text{mass of total neutral sugars in feed (mg)}} \times 100 \quad \text{Eq. (4.2)}$$

where,  $\sum(\text{Xyl} + \text{Ara} + \text{Fuc} + \text{Rha})_t$  is the sum of the individual masses of xylose, arabinose, fucose and rhamnose that are in the free form in the hydrolysate at time  $t$ , and  $(\text{total neutral sugar in feed})$  is the total mass of xylose, arabinose, fucose, rhamnose, glucose and galactose that are initially present in 400 mg of rhamnogalacturonan loaded into the reactor. This value was calculated based on the chemical composition of rhamnogalacturonan, where the total neutral sugars was 49% w/w.

## 4.3 Results and discussion

### 4.3.1 Characterization of rhamnogalacturonan by ATR-FTIR analysis

According to the Megazyme product specification, rhamnogalacturonan used in this study was enzymatically produced from soybean pectic fiber, and it was mainly comprised of galacturonic

acid and neutral sugars, 51% and 49% w/w, respectively. The neutral sugars fraction contained xylose (28%), galactose (25%), fucose (21%), rhamnose (13%), arabinose (7%) and other sugars (3%). In addition, it was reported that endo-xylanase (random attack on  $\beta$ -1,4-xylosidic linkage) and  $\alpha$ -L-arabinofuranosidase were not active on neutral sugar side chains of rhamnogalacturonan. Based on this information and the calculated molar ratios of galacturonic acid:rhamnose (6.8:1) and galacturonic acid:xylose (2.9:1) as presented in Table 4.1, the complexity of the rhamnogalacturonan structure can be inferred, where it can also have another pectic fragment rich in galacturonic acid and xylose that can potentially impact its hydrolysis under subcritical conditions.

**Table 4.1.** Sugar composition (mole %) of soybean pectic fragments.

	GalA	Rha	Xyl	Gal	Arb	Fuc	Other sugars	GalA:Xyl ratio
RG + XG (Huisman et al., 2000)	43	11	18	12	7	9	-	2.4:1
RG (This study) <sup>a</sup>	47.3	7	16.5	12.3	4.1	11.3	1.5	2.9:1

<sup>a</sup> Values converted from the w/w % values provided by the supplier to mole %, RG: rhamnogalacturonan, XG:xylogalacturonan, Ara: arabinose, Gal: galactose, Fuc: fucose, Rha: rhamnose, GalA: galacturonic acid, and GalA:Xyl: mole ratio of galacturonic acid to xylose.

ATR-FTIR analysis was performed on rhamnogalacturonan as well as on other pectic structural domains rich in galacturonic acid such as polygalacturonic acid (90% GalA) and low methoxyl pectin (89% GalA) to gain an insight into its complex chemical structure. Fig. 4.1 shows that in the infrared functional group region, the spectra of rhamnogalacturonan exhibited absorption bands similar to those of low methoxyl pectin (i.e., 1600  $\text{cm}^{-1}$ , 1411  $\text{cm}^{-1}$ ) but not of polygalacturonic acid. Interestingly, all analyzed compounds contained galacturonic acid but

differences in their carbonyl group absorption were apparent possibly due to variations in their surrounding functional groups. In general, absorption bands at wavelengths of 1728-1700  $\text{cm}^{-1}$  and 1630-1600/1400  $\text{cm}^{-1}$  correspond to stretching vibrations of the carbonyl group of carboxylic acids (C=O) and asymmetric/symmetric stretching vibrations of carboxylate ion ( $\text{COO}^-$ ), respectively, have been reported (Chylińska et al., 2016; Kacurakova et al., 2000; Marry et al., 2000). Also, spectra in the infrared fingerprint region ( $< 1500 \text{ cm}^{-1}$ ) show that galacturonic acid present in the rhamnogalacturonan molecule indeed has a different chemical structure compared to galacturonic acid that is contained in both, low methoxyl pectin and polygalacturonic acid molecules because its characteristic absorption peaks at frequencies of 1094  $\text{cm}^{-1}$ , 1012  $\text{cm}^{-1}$  and 830  $\text{cm}^{-1}$ , which correspond to pectin ring vibration, galacturonic acid ring vibration and  $\alpha$ -GalA-(1 $\rightarrow$ 4)- $\alpha$ -GalA linkage, respectively, were not well defined in the rhamnogalacturonan spectra (Kacurakova et al., 2000; Szymanska-Chargot and Zdunek, 2012). Consequently, the high galacturonic acid content present in rhamnogalacturonan cannot be associated to the homogalacturonan ( $\alpha$ -GalA-(1 $\rightarrow$ 4)- $\alpha$ -GalA linked backbone) fragment that is characteristic of polygalacturonic acid and low methoxyl pectin, but probably to other heterogeneous pectic fragments such as xylogalacturonan or rhamnogalacturonan-II.

In addition, Huisman et al. (2001) reported that pectic substances obtained from soybean meal by combined acid (0.05 M 1,2-diaminocyclohexane-N,N,N9,N9-tetraacetic acid (CDTA) and 0.05M ammonium oxalate) and enzymatic hydrolysis were mainly comprised of rhamnogalacturonan (RG) and xylogalacturonan (XG).

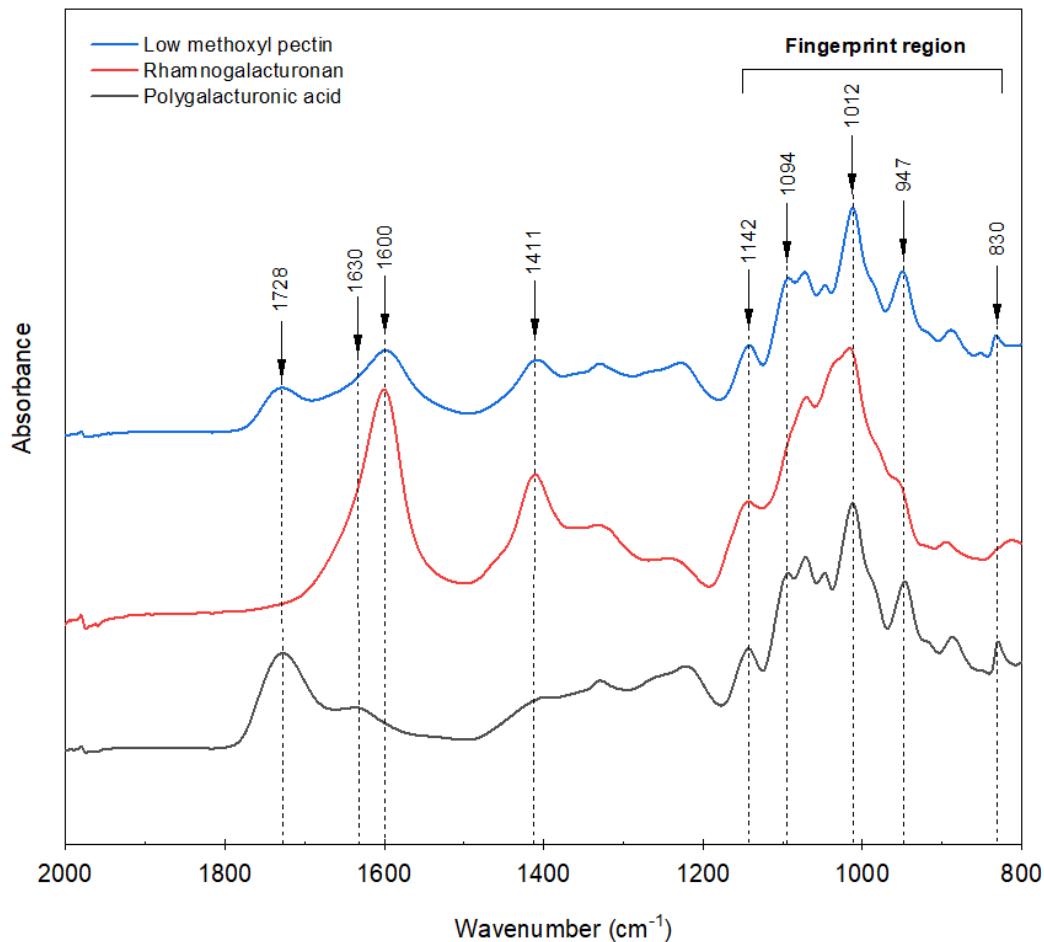


**Fig. 4.1.** ATR-FTIR spectra of rhamnogalacturonan, polygalacturonic acid and low methoxyl pectin.

Interestingly, the molar composition of such pectic fractions as well as their molar ratios of galacturonic acid:rhamnose and galacturonic acid:xylose closely resemble those of the rhamnogalacturonan used in this study as summarized in Table 4.1. Therefore, there is a possibility that the rhamnogalacturonan used as the substrate for hydrolysis in this study also contained xylogalacturonan as part of its structure.

## 4.3.2 Characterization of rhamnogalacturonan hydrolysates

### 4.3.2.1 Molecular weight distribution

The extent of hydrolysis of rhamnogalacturonan at temperatures between 125°C and 155°C and a pressure of 100 bar in aqueous citric acid and reaction times of up to 60 min was monitored by HPSEC-RID analysis. The elution profile of the starting rhamnogalacturonan in aqueous citric acid (Fig. 4.2a) showed two differentiated molecular weight fractions, one considerably higher than the exclusion limit of the column of 80 kDa and the other one of 1.6 kDa as indicated by the peaks with elution volumes of 5.85 mL (or 11.7 min) and 8.6 mL (or 17.2 min), respectively. At 125°C, a molecular weight reduction of the rhamnogalacturonan was apparent within 20 min of reaction (Figs. 4.2b-4.2c) as the broad peak eluted at 11.7 min got more defined, sharper and more intense, indicating possible sequential hydrolysis of the side branched chains of the polymer, which contained glycosidic bonds that are more sensitive to acid hydrolysis. In fact, the result of HILIC-ELSD neutral sugar analysis of hydrolysates obtained at 125°C (Fig. 4.3) showed a fast release of arabinose (67%), followed by fucose (28%) and xylose (12%) within that same time frame (20 min). In Figs. 4.2d-4.2f, as the reaction time approached 60 min, the intensity of the peak eluted at 11.7 min decreased considerably, leading to the formation of a new broad peak eluted between 12.6 min (exclusion limit of the column at 6.3 mL elution volume) and 16.4 min (3.4 kDa at 8.2 mL elution volume), with a peak maximum at 14.6 min (5.8 mL) that corresponded to 11.6 kDa compounds. At 60 min of reaction, low intensity but defined peaks that corresponded to 2.5 kDa, 1.6 kDa, and compounds eluted beyond the column permeation limit of 17.7 min (8.9 mL elution volume) were also identified. Similarly, Huisman et al. (2001) reported a similar HPSEC elution pattern for soybean meal pectic polysaccharides (RG + XG) obtained after 24 h of acid hydrolysis

(0.1M HCl/80°C), with main peaks corresponding to approximately 11 kDa compounds and oligosaccharides.

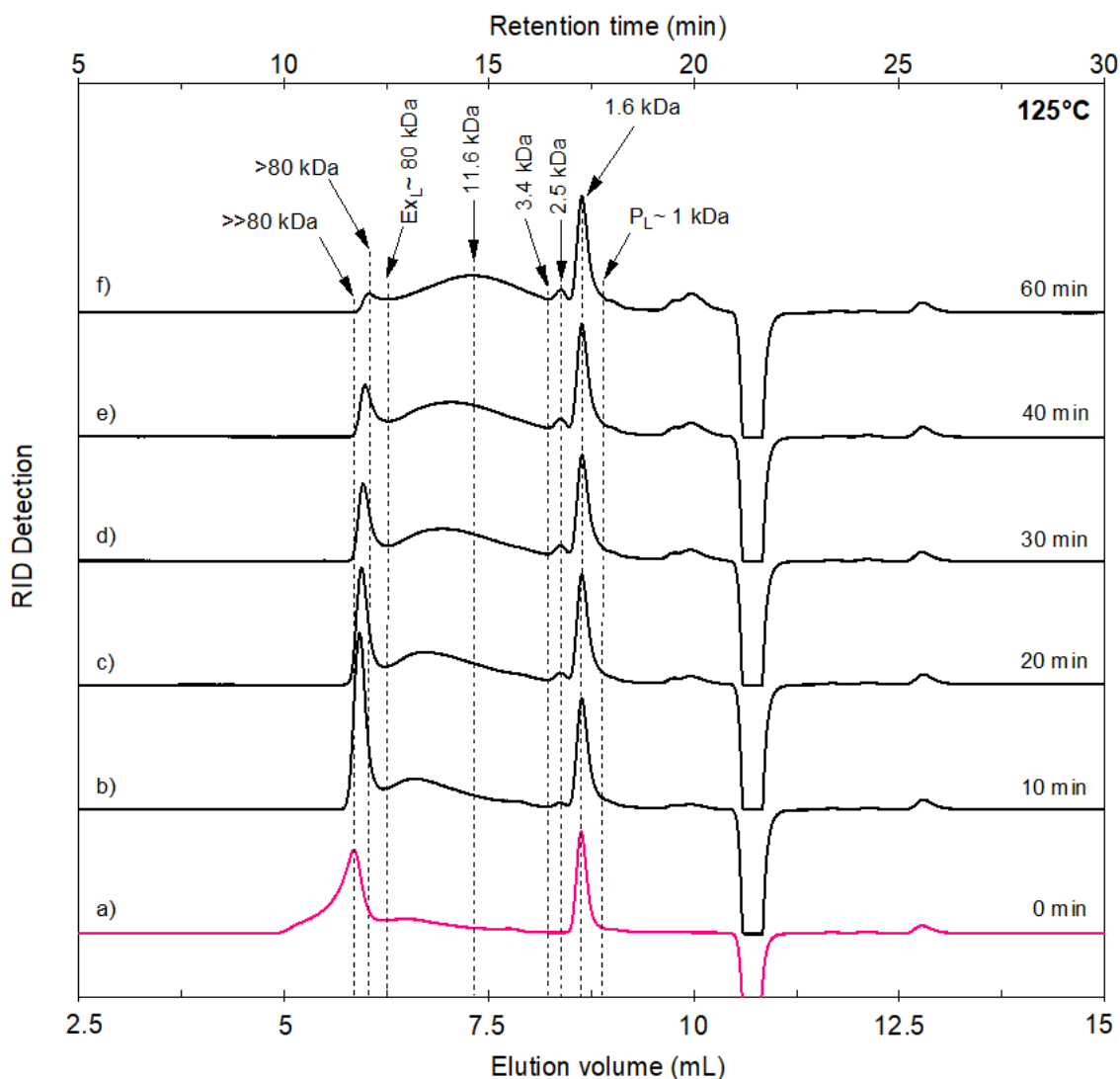


**Fig. 4.2.** HPSEC-RID molecular weight distribution profiles of rhamnogalacturonan hydrolysates obtained in aqueous citric acid at 125°C/100 bar and reaction times of: a) 0 min, b) 10 min, c) 20 min, d) 30 min, e) 40 min, and f) 60 min. Ex<sub>L</sub>: column exclusion limit, and P<sub>L</sub>: column permeation limit.

In addition, at 125°C/60 min, the total released Xyl+Ara+Fuc reached 14.45% (Eq. 4.2), revealing that cleavage of glycosidic bonds corresponding to sugar residues of side chains was predominant as rhamnose release (backbone sugar) was not detected. Also, differences in the rate

of individual sugars release were apparent. Release of xylose and arabinose, for example, decreased after the first 20 min of reaction, whereas fucose release was faster (Fig. 4.3). As such, released fucose reached 41%, 1.5 times the amount released at 20 min (28%). Conversely, the absence of rhamnose in the hydrolysate obtained after 60 min of reaction at 125°C/100 bar suggest that there was no breakdown of the rhamnogalacturonan backbone under these conditions. Therefore, it can be hypothesized that the compounds eluted between 6.3 mL (or 12.6 min) and 8.2 mL (or 16.4 min) (Fig. 4.2f), with an average molecular weight of 11.6 kDa, can correspond to linear or branched structures depleted of fucose and arabinose as in 60 min, 41% fucose and 78% arabinose were already released (Fig. 4.3).

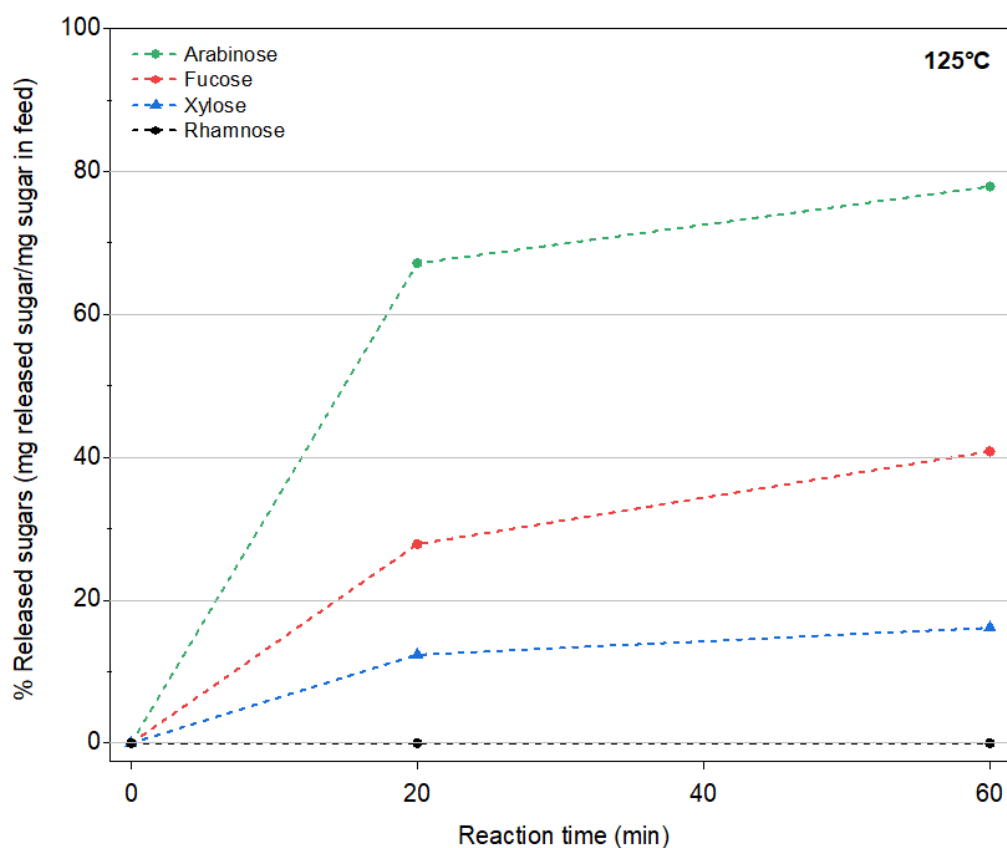


**Fig. 4.3.** Released sugars during rhamnogalacturonan hydrolysis with aqueous citric acid at 125°C/100 bar over 60 min of reaction.

Figs. 4.4a-4.4f shows that the hydrolysis of rhamnogalacturonan with aqueous citric acid was enhanced at 135°C compared to that at 125°C (Fig. 4.2). As observed in Fig. 4.4, the intensity of the first eluting peak (Fig. 4.4a) that corresponded to molecular weight compounds considerably higher than the exclusion limit of the column of 80 kDa (5.64 mL elution volume), dramatically decreased within 20 min of reaction (Fig. 4.4c). Interestingly, the HPSEC-RID elution profile of hydrolysates obtained after 20 min of reaction at 135°C resembled its analog obtained in aqueous citric acid after 60 min at 125°C/100 bar (Fig. 4.2f). Moreover, after 20 min of reaction at 135°C, the weight percentages of released sugars (Fig. 4.5) such as xylose (16%), arabinose (73%) and fucose (41%) were also close to those values obtained at 125°C/100 bar and 60 min (Fig. 4.3). Therefore, a 10°C temperature rise shortened the reaction time down to 1/3 of its level without any loss of the hydrolytic effect.

Fig. 4.4d-4.4f depicts the effect of time on further rhamnogalacturonan hydrolysis. As reaction time approached 60 min, the broad peak eluted between 12.4 min (6.2 mL elution volume) and 15.3 min (7.6 mL elution volume), which corresponded to compounds in the range of 26.6 kDa and 2.9 kDa, respectively, became narrower and its peak maxima shifted towards low molecular weight compounds of 4.7 kDa at 60 min (Fig. 4.4f). Also, peaks corresponding to compounds eluted beyond the permeation limit were more evident. Likewise, total released sugars calculated using Eq. (4.2) reached a maximum of 33% after 60 min of reaction at 135°C with citric acid. Conversely, the main individual released sugar calculated using Eq. (4.1) was arabinose (79%), followed by fucose (57%), rhamnose (40%) and xylose (34%) (Fig. 4.5). Therefore, sCW hydrolysis of rhamnogalacturonan with citric acid at 135°C/100 bar and reaction times longer than 30 min could be associated with further cleavage of sugar residues of substituted side chains as well as to the breakdown of rhamnogalacturonan backbone.

The effect of reaction medium (aqueous citric acid, aqueous malic acid, or water) on the extent of rhamnogalacturonan hydrolysis at 135°C/100 bar/60 min is shown in Fig. 4.4f-4.4h. Hydrolysates obtained with either aqueous citric or malic acids exhibited peaks of comparable areas at the same elution times, which corresponded to 4.7 kDa, 2.1 kDa, 1.4 kDa, and compounds eluted beyond the permeation limit of 1 kDa (8.25 mL elution volume).

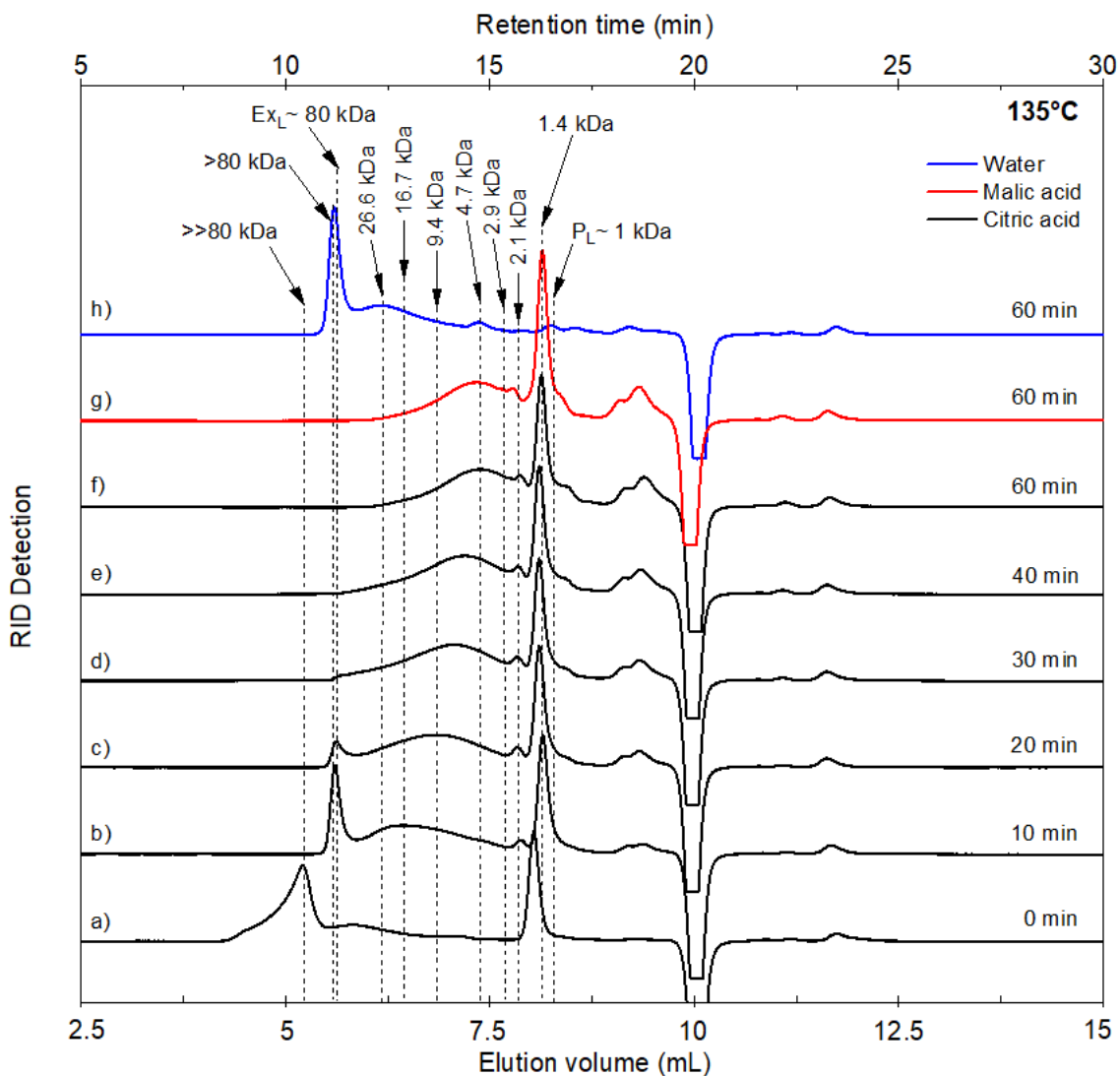


**Fig. 4.4.** HPSEC-RID molecular weight distribution profiles of rhamnogalacturonan hydrolysates obtained in aqueous citric acid at 135°C/100 bar and reaction times of: a) 0 min, b) 10 min, c) 20 min, d) 30 min, e) 40 min, f) 60 min, and different reaction media of: g) malic acid, and h) water. ExL: column exclusion limit, and PL: column permeation limit.

The released sugar contents of hydrolysates obtained with aqueous malic acid at 135°C/100 bar/60 min resembled those obtained with aqueous citric acid. As such, the percentages of individual released sugars (Eq. 4.1) like arabinose, fucose, rhamnose, and xylose in aqueous malic acid were 83%, 60%, 40% and, 36.7%, respectively. Consequently, there was no difference between the use of tri- or di-carboxylic acids in terms of their hydrolytic effect. However, the elution profile of the hydrolysate obtained with water showed signs of limited hydrolysis compared to those obtained with aqueous citric or malic acids, as indicated by the high intensities of the first eluting peak corresponding to compounds with molecular weights > 80 kDa and the following broad peak corresponding to 26.6 kDa compounds, as well as the absence of peaks at later elution volumes corresponding to smaller molecular weights (Fig. 4.4h). Similarly, the release of neutral sugars was reduced when water was used as the reaction medium. As such, xylose was the only neutral sugar identified and quantified using Eq. (1) that reached 12.8% after 60 min of reaction. The absence of the high intensity peak corresponding to compounds of 1.4 kDa when water alone is used as the reaction medium demonstrate that the addition of citric or malic acids indeed exerted a catalytic effect on rhamnogalacturonan hydrolysis compared to water.

The sugar release at 135°C over time in the presence of citric acid, depicted in Fig. 4.5, provides some insight on the mechanism of rhamnogalacturonan hydrolysis. For example, a fast release (steeper lines) of neutral sugar residues from the side chains (arabinose and fucose) was apparent during the first 20 min of reaction, while the release of neutral sugars that belong to XG or RG-I backbones (xylose and rhamnose) was predominant after that time period, suggesting sequential hydrolysis starting from the branched portion followed by the backbone of the molecule. The type of glycosidic bond (alpha or beta), as well as the type of sugar (pentose or hexose) involved in the linkage, could also influence the susceptibility of the glycosidic bond to sCW

hydrolysis. According to Fig. 4.5, for example, xylose was the most difficult to be released within 60 min among the sugars from side chains, as depicted by its increasing release with time (linear trendline), suggesting that the xylose containing structure was strongly bound and therefore more resilient to sCW hydrolysis than the structures containing the other sugar side chains such as arabinose and fucose.

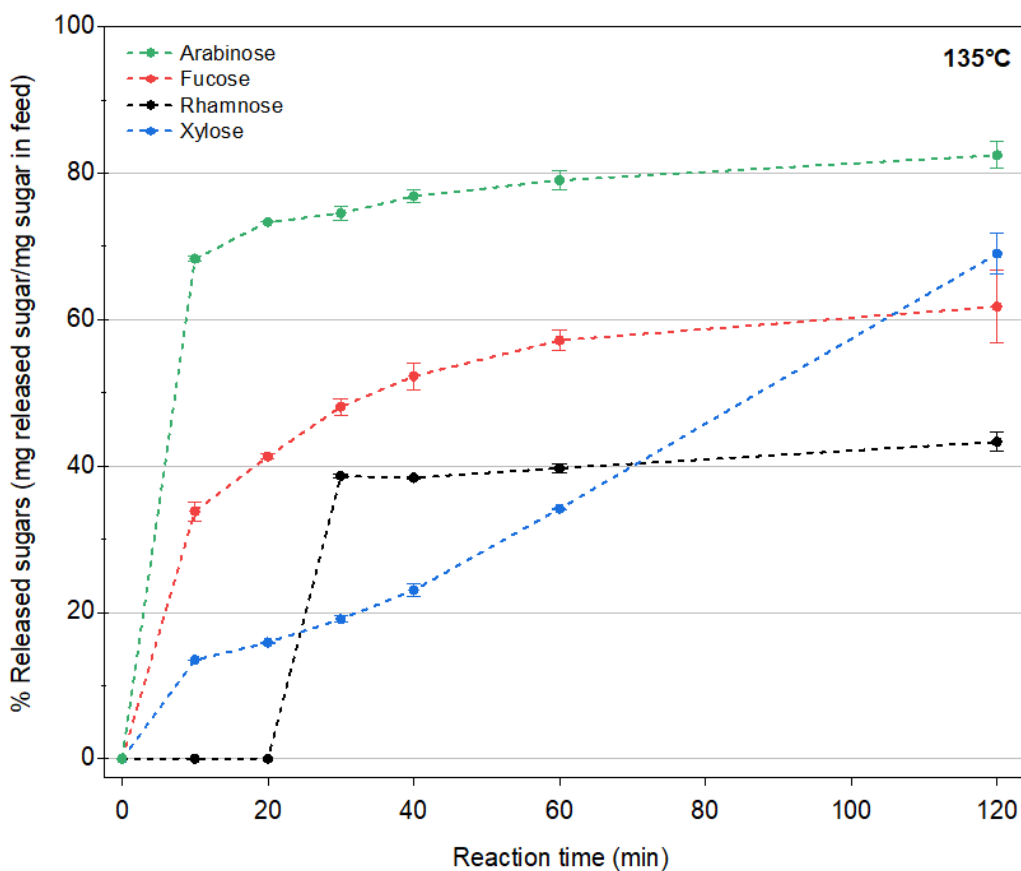


**Fig. 4.5.** Sugars released during rhamnogalacturonan hydrolysis with aqueous citric acid at 135°C/100 bar over 120 min of reaction.

Fig. 4.6a-4.6c shows the HPSEC-RID elution pattern of hydrolysates obtained with aqueous citric acid at 145°C and 155°C/100 bar. According to Fig. 4.6a, rhamnogalacturonan was substantially hydrolyzed at 145°C/100 bar within 60 min of reaction as major peaks were apparent at longer elution times and even beyond the permeation limit of the column. Such peaks

corresponded to rhamnogalacturonan-derived fragments of 3.1 kDa, 1.6 kDa, and compounds eluted beyond the permeation limit (8.9 mL elution volume). Also, the high percentages of released xylose (76.8%) and rhamnose (86.7%) at 145°C/100 bar/60 min (Eq. 4.1) indicate a considerable breakdown of the rhamnogalacturonan backbone and therefore the predominance of low molecular weight compounds.

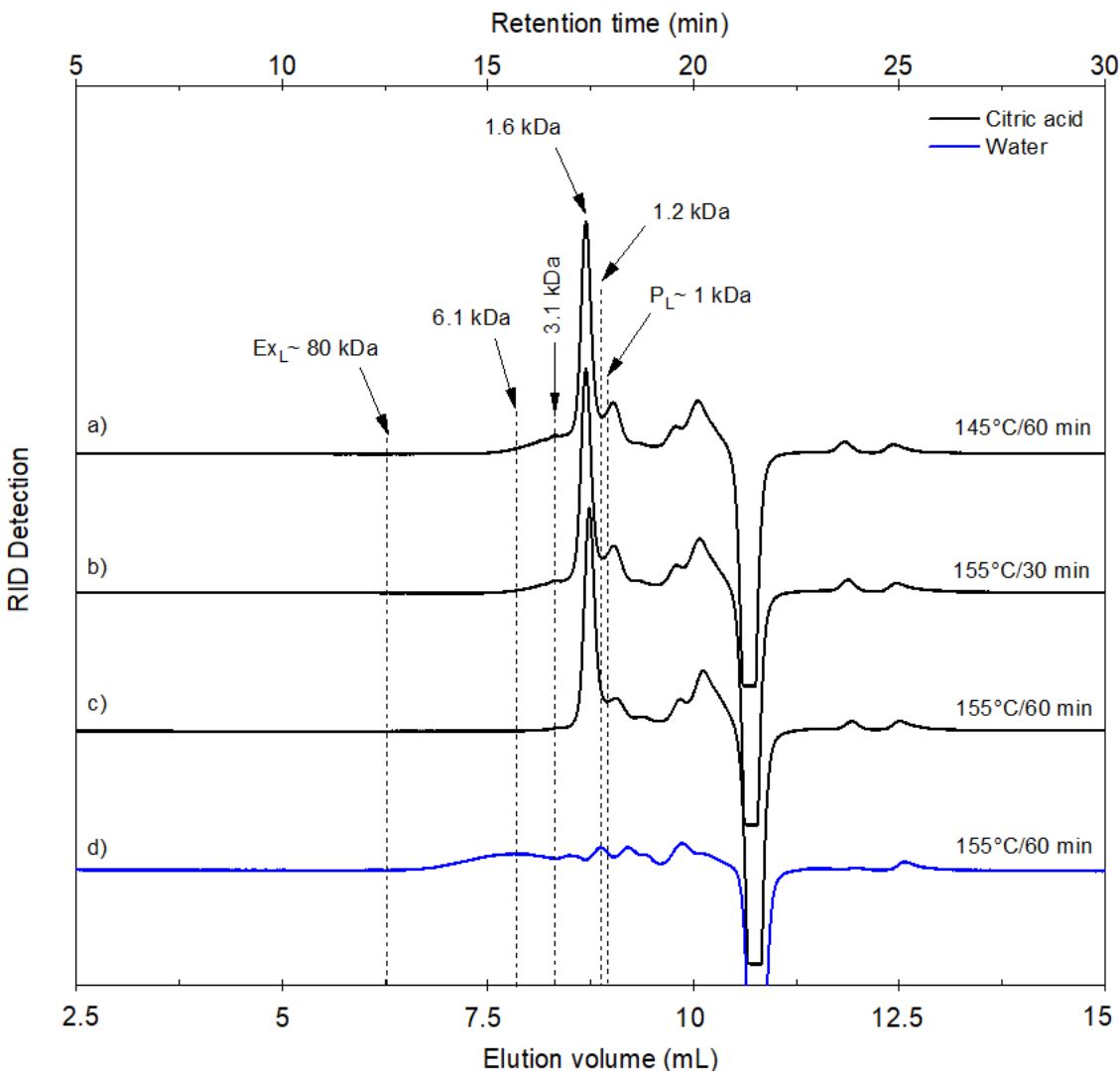


**Fig. 4.6.** HPSEC-RID elution profiles of rhamnogalacturonan hydrolysates obtained at 145°C and 155°C/100 bar/60 min within different reaction media: a-c) aqueous citric acid, and d) water. Ex<sub>L</sub>: column exclusion limit, and P<sub>L</sub>: column permeation limit.

Fig. 4.6b shows that a combination of high temperature (155°C) and short reaction time (30 min) also led to rhamnogalacturonan-derived fragments with reduced molecular weights comparable to those obtained at 145°C/100 bar but 60 min (Fig. 4.6a) as evidenced by the similarities of their HPSEC elution profiles. Thus, a 10°C rise in temperature was able to shorten the reaction time approximately by half. Besides the temperature rise, a long reaction time also favored hydrolysis. The HPSEC elution profile of the hydrolysate obtained at 155°C and 60 min (Fig. 4.6c) showed the disappearance of a peak eluted at 8.3 mL (6.1 kDa) but the prevalence of peaks at longer times that corresponded to 1.6 kDa fragments and other compounds that eluted beyond the permeation limit. The disappearance of 6.1 kDa fragments could be associated with further cleavage of xylose residues from the XG backbone as the percentage of released xylose increased from 76.8% at 145°C/60 min to 87.4% at 155°C/60 min (Table 4.2). Likewise, further hydrolysis of rhamnogalacturonan backbone-derived fragments could have also occurred as released rhamnose increased from 87% to 112%. The unusual high percentage of rhamnose, however, could be the result of epimerization of sugars at 155°C (Ohno and Ward, 1961)

The effect of water as reaction medium on rhamnogalacturonan hydrolysis at 155°C/100 bar and 60 min is depicted in Fig. 6d. The presence of a broad peak eluted between 6.7 mL and 8.3 mL, with a peak maximum at 7.8 mL (6.1 kDa) and a peak eluted at 8.8 mL (1.2 kDa) show that water indeed exerted a substantial hydrolytic effect on rhamnogalacturonan molecule. However, the low intensity of peaks and its different elution pattern, compared to its analog obtained with aqueous citric acid (Fig. 6c), suggests that the hydrolysis mechanism in water differs from the one in aqueous citric acid. The presence of diverse glycosidic bonds with different susceptibility to acid hydrolysis could be a contributing factor that led to different mechanisms. For example, glycosidic bonds between neutral sugars have been found to be more susceptible to acid hydrolysis

than glycosidic bonds between sugar acids like galacturonic acid (Locatelli et al., 2012). Therefore, diluted acids have been used to exert a controlled hydrolytic effect to obtain neutral sugar residues from biopolymers like pectin, without further damage to the backbone (Coenen et al., 2007; Zhang et al., 2018). Moreover, in the previous study on the hydrolysis of polygalacturonic acid under sCW conditions reported in Chapter 3, O-glycosidic bonds between galacturonic acid residues were found to be less susceptible to cleavage by aqueous citric acid compared to water. Similarly, aqueous citric acid seemed to exert a controlled hydrolytic effect on the side chains of rhamnogalacturonan as sugars were released progressively with temperature rise, which did not occur at the same rate when water was used as the reaction medium (Table 4.2).

**Table 4.2.** Released sugars during hydrolysis of rhamnogalacturonan at 135°C, 145°C and 155°C/100 bar/60 min with aqueous citric acid or water.

Temperature/ time	Reaction media	Released neutral sugars (% , Eq. (1))			
		Arabinose	Fucose	Xylose	Rhamnose
135°C/60 min	Citric acid	79.1 ± 1.4	57.2 ± 1.4	34.2 ± 0.1	39.7 ± 0.7
145°C/60 min	Citric acid	144.3 ± 0.9	68.8 ± 1.7	76.8 ± 1.9	86.6 ± 0.2
155°C/60 min	Citric acid	147.9 ± 2.0	71.3 ± 3.5	87.4 ± 3.8	111.9 ± 1.7
155°C/60 min	Water	127.5 ± 0.1	46.1 ± 1.1	28.7 ± 0.3	75.4 ± 1.3

According to Table 4.2, released arabinose at either 145 or 155°C in citric acid medium exceeded 100%. Such unusual values can be an indication of galacturonic acid degradation as arabinose can result from decarboxylation of galacturonic acid (Conrad, 1931). L-Arabinose or 4,5-unsaturated 4-deoxy-L-arabinose has been proposed as intermediates in the degradation pathway of galacturonic acid in a pH range of 3 to 8 and temperatures higher than 100°C (Bornik and Kroh, 2013). Considering that degradation reactions occurred at 155°C/60 min, the effect of reaction medium on the extent of rhamnogalacturonan degradation can be visually assessed by the

difference in the color of hydrolysates (Fig. 4.7). For example, the hydrolysate obtained with aqueous citric acid at 155°C/60 min was brown in color (Fig. 4.7C), whereas the hydrolysate obtained with water was close to black (Fig. 4.7D), suggesting that citric acid prevented further degradation reactions to some extent. Usuki et al. (2008) studied the degradation of pentoses and galacturonic acid in sCW at temperatures between 140°C and 240°C and reported that pentoses were more resistant to degradation than galacturonic acid. Degradation of pentoses like xylose and arabinose was observed at 200°C/1 min while degradation of galacturonic acid occurred at 140°C/1 min. Also, Bornik and Kroh (2013) reported that concentrations of the main degradation products generated during galacturonic acid thermal treatment at 100°C for 2 h, such as reductic acid, 4,5-dihydroxy-2-cyclopenten-1-one, furan-2-carbaldehyde and norfuraneol, were pH dependent. At pH 3, for example, galacturonic acid degradation reached 31% and the concentration of degradation products was the highest, except for norfuraneol that was negligible. At pH 5, however, galacturonic acid degradation reached 42% and the concentration of degradation products was reduced, except for norfuraneol that was the highest. As these degradation products contain reactive groups, they have been associated with non-enzymatic browning due to their capacity to form chromophoric structures (Bornik and Kroh, 2013). Interestingly, the degree of browning was also reported to be the highest at pH 5 (Bornik and Kroh, 2013). In the present study, the hydrolysate obtained with water at 155°C/60 min exhibited lower levels of released fucose, xylose and rhamnose compared to those obtained with aqueous citric acid (Table 4.2), suggesting further degradation of these released neutral sugars, possibly due to their interactions with the reactive degradation products generated from galacturonic acid decomposition. Therefore, it can be hypothesized that: i) hydrolysis of rhamnogalacturonan in water proceeded in a random manner, where cleavage of glycosidic bonds between two galacturonic acid residues was favored over

cleavage of neutral sugar residues from side chains, and ii) released galacturonic acid was further degraded to arabinose and other compounds contributing to the brown color.

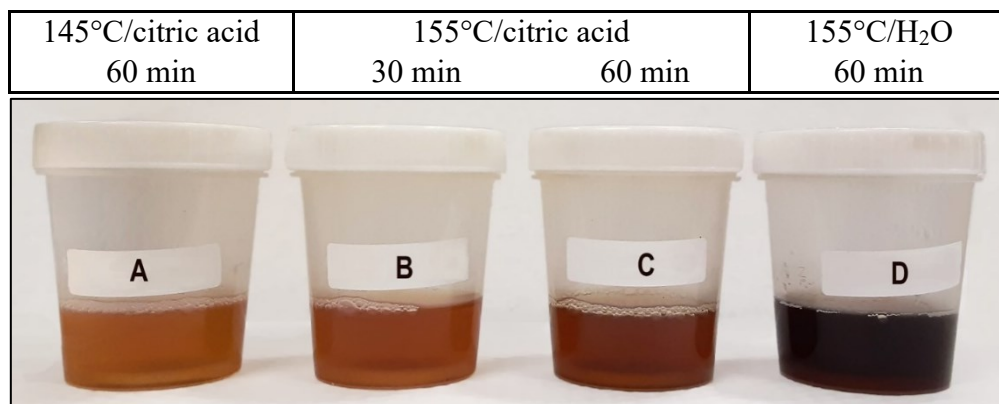


**Fig. 4.7.** Rhamnogalacturonan hydrolysates obtained at 145°C and 155°C/100 bar/60 min within different reaction media: A-C) aqueous citric acid, and D) water.

Further, an XBridge Amide column with a reduced particle size of 3.5  $\mu\text{m}$  was used to determine the molecular size and composition of rhamnogalacturonan derived-fragments with molecular weight  $\leq 2.5$  kDa as they were eluted close to and beyond the permeation limit of the current Ultrahydrogel 250 column (6  $\mu\text{m}$  particle size).

#### 4.3.2.2 Determination of oligosaccharides

Rhamnogalacturonan hydrolysates obtained with citric acid at 125°C and 135°C/100 bar and reaction times of 10 to 120 min were analyzed to determine the presence of oligosaccharides. Overall, Fig. 4.8a-4.8b shows that hydrolysates obtained at either 125°C or 135°C were comprised of oligogalacturonides of 2 to 9 DP and neutral oligosaccharides of 5, 8 and 10 DP. Identification of neutral oligosaccharides, however, was based on the retention times of gluco-oligosaccharide standards.

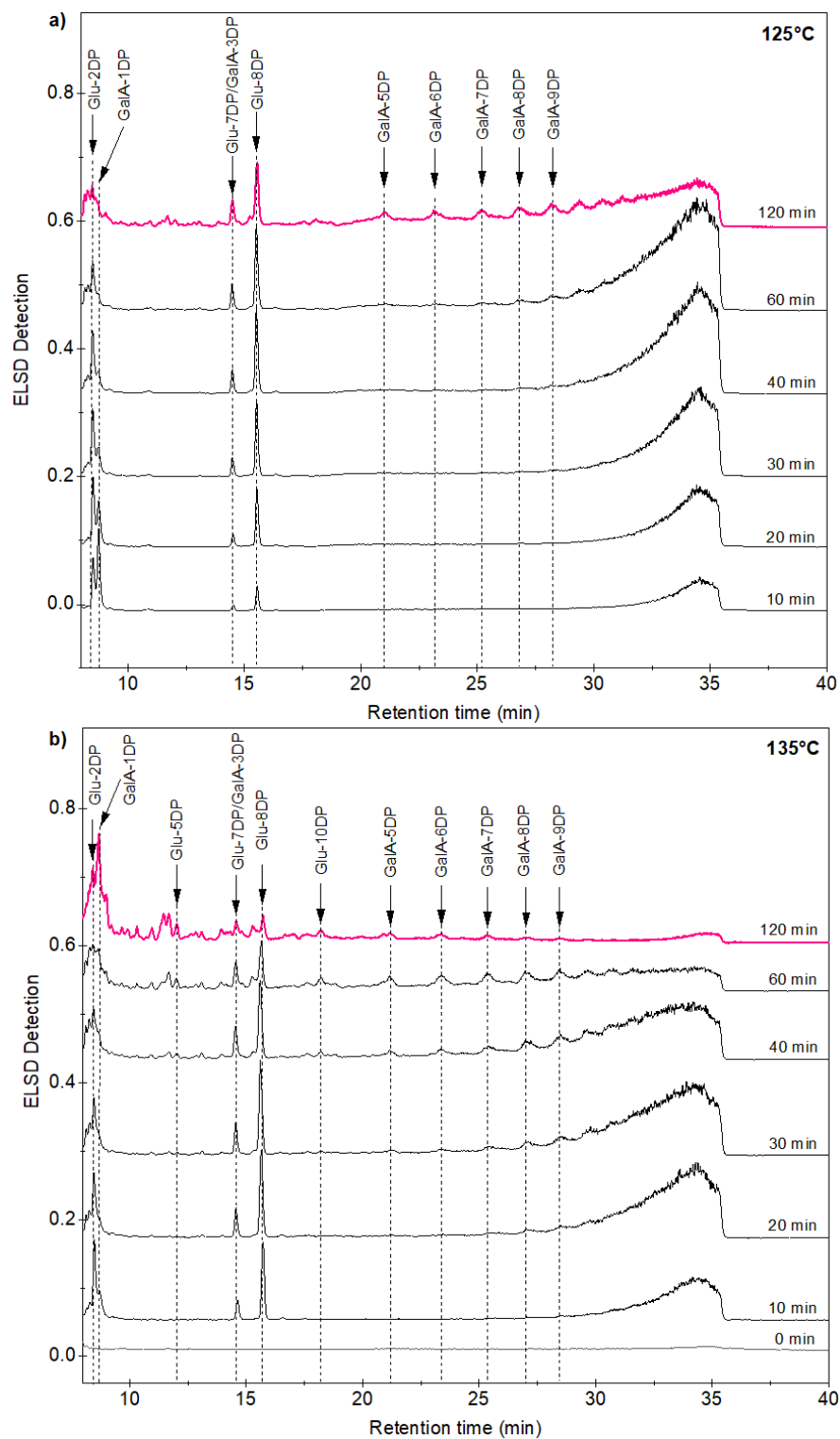


**Fig. 4.8.** Effect of reaction time (10-120 min) on rhamnogalacturonan hydrolysis in aqueous citric acid at 100 bar and temperatures of: a) 125°C and b) 135°C, analyzed by HILIC-ELSD.

Considering that rhamnogalacturonan used in this study is comprised of 12% of galactose and no glucose, and the fact that separation of glucose and galactose was not possible using the current HILIC-ELSD method as they eluted at the same time, it can be assumed that the identified neutral oligosaccharides would probably not be gluco-oligosaccharides but galacto-oligosaccharides (GOS).

According to Fig. 4.8a, at 125°C, GOS of 8 DP and tri-galacturonic acid were released from the rhamnogalacturonan within 10 min and were predominant over time. Conversely, oligogalacturonides of 5 to 9 DP were apparent only at 120 min of reaction. Such behavior supports the fact that under mild acid conditions, neutral sugar residues are first cleaved from the rhamnogalacturonan side chains, releasing mono- and oligosaccharides whereas the backbone structure is preserved (Zhang et al., 2018). In addition, Makio (1965) found that hot water extractable polysaccharides from defatted and deproteinized soybean flour were mainly comprised of arabinogalactan with an arabinose to galactose molar ratio of 1:2. Based on that, it can be inferred that rhamnogalacturonan (from soybean) used in this study can also include arabinogalactan as part of its complex structure. Moreover, the fact that at 125°C and 10 min, released arabinose reached 67%, also indicating that there was a fast initial cleavage of arabinose residues probably from arabinogalactan side chains, containing arabinose and galactose at a molar ratio of 1:3 (Table 4.2), that led to more accessible linear  $\beta$ -galactan chains that were further acid hydrolyzed into galacto-oligosaccharides of 8-DP in length. Identified oligogalacturonides, however, could be associated with RG-I scission as galacturonan fragments containing 4 to 10 galacturonic acid residues have been reported as linker portions between two RG units, where an RG unit ( $[-4)\text{-}\alpha\text{-D-GalpA-(1}\rightarrow\text{2)-}\alpha\text{-L-Rhap-(1-)]$ ) can have 15, 28 or 100 DP in length (Nakamura et al., 2014). Therefore, the presence of oligogalacturonides of 5 to 9 DP at 120 min of reaction

(Fig. 4.8a) could be indicative of partial hydrolysis of the RG backbone at the RG-RG junctions. Overall, the low intensity of peaks that corresponded to oligogalacturonides of 5 to 9 DP can be attributed to limited hydrolysis of RG backbone as was also depicted by the HPSEC-RID elution profile obtained at 125°C (Fig. 4.2f) where fragments of an average molecular weight of 11.6 kDa were predominant.

Fig. 4.8b shows that at 135°C, hydrolysis of rhamnogalacturonan was enhanced as the intensities of peaks corresponding to GOS and oligogalacturonides were considerably higher compared to those displayed at 125°C (Fig. 4.8a). However, as the rate of reactions increased with temperature, further hydrolysis of GOS was also favored at 135°C and 30 min of reaction as indicated by the reduced intensity of 8 DP GOS and the simultaneous increased intensity of peak corresponding to galactose-2 DP. Likewise, at 135°C, a reaction time longer than 60 min also induced further hydrolysis of rhamnogalacturonan. Then, depolymerization of oligogalacturonides of 5 to 9 DP (linker portion) into galacturonic acid (GalA-1 DP) was noticed between 60 and 120 min of reaction as the intensity of peak corresponding to galacturonic acid increased.

Based on the information obtained from oligosaccharide and sugar analyses, it can be hypothesized that after 60 min of reaction at 135°C/100 bar in citric acid, depolymerization of oligogalacturonides released from rhamnogalacturonan was favored over cleavage of xylogalacturonan backbone into oligogalacturonides. The intensity of oligogalacturonides signal decreased between 60 min and 120 min, and released arabinose, fucose and rhamnose remained constant while xylose release increased from 34% to 69% within that time frame (Fig. 4.5), suggesting that there was cleavage of xylose residues from xylogalacturonan that led to homogalacturonan regions.

The difference in the extent of hydrolysis of rhamnogalacturonan at 135°C/60 min/100 bar according to the reaction medium is shown in Fig. 4.9. Elution patterns of hydrolysates obtained with both, aqueous malic and citric acids were analogous and exhibited defined peaks that corresponded to galacto-oligosaccharides with 5, 8, and 10 DP as well as to oligogalacturonides of 3 DP and 5 to 9 DP (Fig. 4.9). Conversely, the elution pattern of the hydrolysate obtained with water differed from those obtained with aqueous malic and citric acids as it did not exhibit peaks that corresponded to either galacto-oligosaccharides or oligogalacturonides. Therefore, aqueous malic and citric acids exhibited a catalytic effect on rhamnogalacturonan hydrolysis at 135°C/60 min/100 bar compared to water at the same processing conditions (Fig. 4.9).

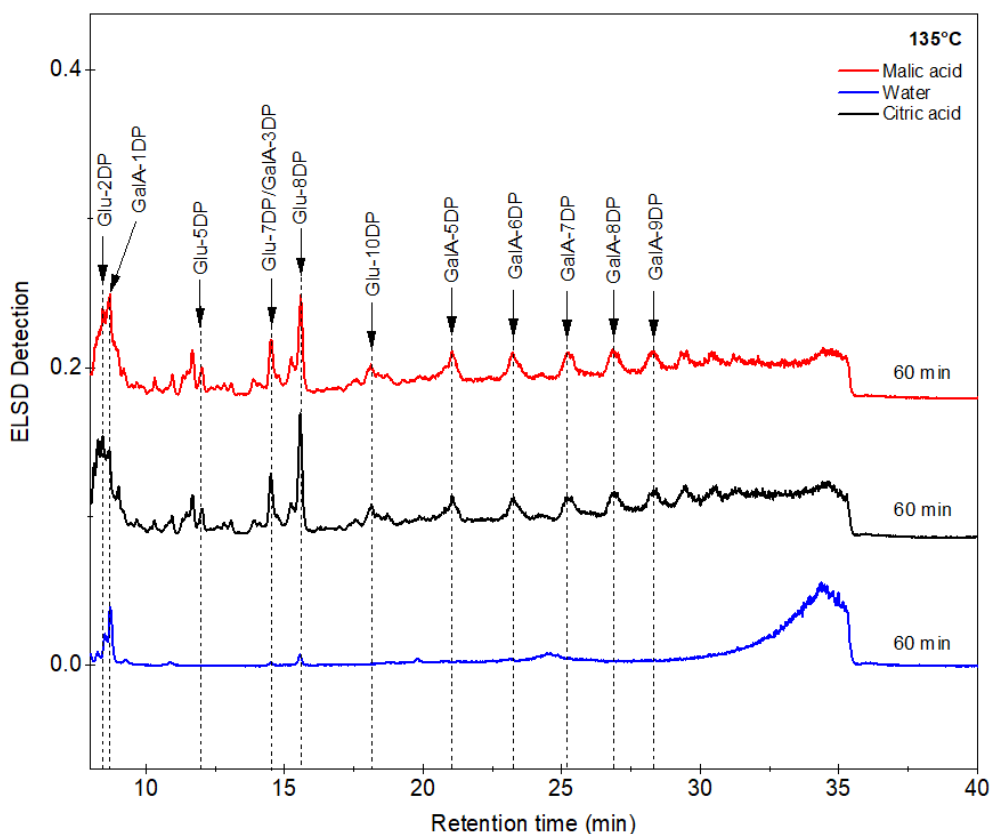


**Fig. 4.9.** HILIC-ELSD chromatograms of rhamnogalacturonan hydrolysates obtained at 135°C/100 bar/60 min in different reaction media. Glu stands for 2 –10 DP gluco-oligosaccharides that elute at the same time as galacto-oligosaccharides.

According to the results discussed above, the structure of rhamnogalacturonan substrate used in this study could correspond to a rhamnogalacturonan + xylogalacturonan complex, where rhamnogalacturonan fragments are linked together via oligogalacturonide regions as proposed in Fig. 4.10. Pectic structures such as RG-I, RG-II and  $\alpha$ -galactosides have been reported in soybean meal (Choct et al., 2010). In addition, the hydrolytic pathway of rhamnogalacturonan + xylogalacturonan complex at 135°C/100 bar in citric acid can be summarized in multi-step sequential hydrolysis, as highlighted in Fig. 4.10, that begins with the simultaneous cleavage of arabinose and fucose residues from arabinogalactan side chains (1-2) and scission of de-branched  $\beta$ -galactan (3). It is followed by partial hydrolysis of rhamnogalacturonan backbone at the linker junction (4), with subsequent release of rhamnose and oligogalacturonides. Next, a parallel reaction takes place as released oligogalacturonides are progressively depolymerized into monogalacturonic acid (5) and xylose residues are cleaved from the xylogalacturonan region (6). Finally, the galacturonan backbone is further hydrolyzed into reduced molecular weight compounds and monogalacturonic acid (7). Interestingly, enzymatic hydrolysis of rhamnogalacturonan requires various enzymes with different acting sites to hydrolyze rhamnogalacturonan into low molecular weight fragments, including exo- $\beta$ -1,4 galactanase,  $\alpha$ -arabinofuranosidase, endo-rhamnogalacturonase, hemicellulases, and pectinase (Nakamura et al., 2014). Therefore, aqueous citric acid under sCW conditions could also be an alternative medium to induce controlled and progressive hydrolysis of rhamnogalacturonan to its acidic and neutral monomers.



#### 4.4 Conclusions

In this study, carboxylic acids under subcritical water conditions (125°C to 155°C and 100 bar) were used for the first time as reaction medium to induce hydrolysis of the branched pectic structure rhamnogalacturonan. The chemical structure of rhamnogalacturonan was elucidated based on its molar composition of neutral and acidic monosaccharides as a rhamnogalacturonan-I and xylogalacturonan complex. The analysis of molecular weight distribution, neutral sugars and oligosaccharides of rhamnogalacturonan sCW hydrolysates showed that: *i*) aqueous citric (0.20%) or malic acid (0.27%) under sCW conditions at pH 2.6 exerted better catalytic effect on the hydrolysis of glycosidic bonds compared to sCW alone, *ii*) progressive cleavage of neutral sugar residues from side branched chains and scission of rhamnogalacturonan backbone were favored in aqueous citric acid at 125°C and 135°C C/100 bar, respectively, *iii*) glycosidic bonds in xylogalacturonan were less sensitive to acid hydrolysis compared to those present in rhamnogalacturonan, *iv*) aqueous citric acid hydrolysis at 135°C/100 bar/60 min led to compounds with molecular weights of 4.7 kDa, 2.1 kDa, and 1.4 kDa, *v*) oligogalacturonides of 2 to 9 DP and galacto-oligosaccharides of 5, 8 and 10 DP were identified in fractions with  $\leq 2.1$  kDa, and *vi*) a mechanistic insight based on a multi-stage sequential hydrolysis was provided for sCW hydrolysis of rhamnogalacturonan within aqueous citric acid medium. These findings demonstrate that pressurized aqueous carboxylic acids at relatively low temperatures can exert a controlled and selective hydrolytic effect on different pectic fragments like rhamnogalacturonan, which can consequently be utilized for the development of a novel green process to obtain bioactive oligosaccharides from pectin-rich agro-industrial by-products.

## **Chapter 5: Production of soluble pea fiber-derived oligosaccharides using subcritical water with carboxylic acids\***

### **5.1 Introduction**

Production of peas as an economic field crop has dramatically increased in Canada (4.2 million tons in 2019), particularly due to its high-quality protein content (Nosworthy et al., 2017; Wu et al., 2018). Industrial manufacture of pea protein, however, generates substantial amounts of underutilized pea hull fiber as a co-product after the dehulling process (90 kg hull/ton whole pea) (Ali-Khan, 1993). In recent years, efforts towards valorization of this co-product has led to its utilization as a dietary fiber. In 2017, pea fiber was labelled as a ‘novel fiber’ by Health Canada due to its proven physiological laxative effect, which has been associated with its high insoluble dietary fiber content (Health-Canada, 2017). Nonetheless, the soluble dietary fiber fraction of pea hull can be further studied in terms of its physicochemical properties and extractability towards its further utilization to obtain value-added oligosaccharides with diverse mechanisms of action and health-promoting effects (Moskovitz and Kim, 2004).

Pectic polysaccharides, also known as pectin, is a very complex group of plant cell wall components, composed of the major fractions homogalacturonan (HG), rhamnogalacturonan-I (RG-I) and rhamnogalacturonan-II (RG-II). Functionally, pectin is widely known as a valuable soluble dietary fiber. Interestingly, studies on plant physiology have shown that cotyledon cell walls of Leguminosae family members like soybean, also contain pectic polysaccharides, in particular the RG-I pectic fraction (Huisman et al., 2001; Nakamura et al., 2014). For example, a recent study on the deconstruction of pea pectin using various pectinolytic enzymes has revealed

---

\* A version of this Chapter has been submitted for consideration for publication as Carla S. Valdivieso Ramirez, Feral Temelli and Marleny D.A. Saldaña. Production of soluble pea fiber-derived oligosaccharides using subcritical water with carboxylic acids.

that the chemical structure of pectin obtained from dehulled pea cotyledons at pH 6/120°C/90 min was mainly comprised of homogalacturonan, xylogalacturonan (XG) and RG-I with associated molecular weights of 7, 46 and 67 kDa, respectively (Noguchi et al., 2020). In addition, the XG fragment was 12% xylosylated, and that rhamnose residues of RG-I backbone were highly substituted with side chains of branched (1→5)- $\alpha$ -L-arabinan, (1→4)- $\beta$ -D-galactans, galacto-oligosaccharides and galactose. The chemical structure of pectic fragments and the main side chains found in pea pectin according to Le Goff et al. (2001) and Noguchi et al. (2020) were described in Chapter 2 (Fig. 2.1, xylogalacturonan, rhamnagalacturonan-I, arabinan and arabinogalactan).

Pectic oligosaccharides (POS) are produced via enzymatic, chemical, or thermal partial hydrolysis of pectin (Babbar et al., 2016). Due to pectin's rich and complex structure, acidic and neutral oligosaccharides can be obtained, such as acid oligogalacturonides from homogalacturonan breakdown, and neutral arabino-, galacto- and rhamnagalacturonan-oligosaccharides from RG-I hydrolysis (Moskovitz and Kim, 2004). In general, prior to POS production, pectin is isolated from plant sources using enzymes, hot diluted inorganic acids, or chelating agents, which influences the length and chemical structure of the isolated pectin. Subsequently, multi-enzyme complexes, inorganic acids, or their combination as well as extended reaction times are required for pectin hydrolysis into POS (Babbar et al., 2016). Lately, subcritical water (sCW) technology has been explored as an eco-friendly alternative to obtain oligosaccharides directly from agro-industrial residues. For example, xylo-oligosaccharides from corncob, manno-oligosaccharides from coconut meal, pectic oligosaccharides from orange peel waste and olive by-products, and others have been produced with sCW at temperatures between 140 and 200°C within short reaction times (Khuwijitjaru et al., 2014; Martínez et al., 2010; Nabarlantz et al., 2007). As agro-industrial residues

are complex substrates containing various macro components (i.e. protein, carbohydrates and fat), their processing at very high temperatures generates oligosaccharides together with undesired products such as furfural and acids, which become a challenge for downstream purification processes (Pinelo et al., 2009). The use of di-carboxylic acids (i.e. malic and oxalic acids) has been explored as an alternative to inorganic acids in homogeneous catalysis to induce selectivity in hydrothermal treatments towards production of fermentable sugars from lignocellulosic biomass (Kim et al., 2013; Lu and Mosier, 2007). In addition, reduced degradation rates of arabinose in aqueous maleic and fumaric acids at 150°C and 170°C/60 min have been reported compared to that in water only, indicating that the addition of di-carboxylic acids can potentially modify the selectivity in reactions where water at high temperature was used as a reaction medium (Kootstra et al., 2009). Nevertheless, neither sCW nor carboxylic acid catalyzed sCW-systems have been investigated for pectin extraction from pea fiber or its conversion into POS. In a systematic approach to this main goal, hydrolysis of pure model pectic structures such as linear polygalacturonic acid (Chapter 3) and branched rhamnogalacturonan (Chapter 4) was investigated in the previous studies using carboxylic acids under sCW conditions to gain more insight prior to tackling a complex substrate like pea fiber. Building on those model pure substrate studies (Chapters 3 and 4), the overall objective of this study was to investigate whether the addition of di- or tri-carboxylic acids to a sCW system can exert a catalytic effect on pea fiber hydrolysis into oligosaccharides and its reaction mechanism. First, soluble pectic polysaccharides were extracted from pea fiber using sCW, and then their further hydrolysis into oligosaccharides was carried out at relatively low temperatures of 125, 135, 145, and 155°C within 10 to 120 min of reaction time to evaluate the hydrolytic effect of citric and malic acids on glycosidic bond cleavage. A possible

mechanism for pea fiber pectic polysaccharides hydrolysis under sCW conditions was also proposed.

## **5.2 Materials and Methods**

### **5.2.1 Materials**

Pea fiber was kindly provided by AGT Food and Ingredients Inc. (Saskatoon, SK, Canada). Reagents for the subcritical water extraction/hydrolysis were citric acid (>99.5%, ACS grade) and malic acid (>99.5%, ACS grade) from Sigma Aldrich (Oakville, ON, Canada), water from the Milli-Q system (18.2 M $\Omega$ .cm, Millipore, Billerica, MA, USA) and nitrogen gas (99.9% purity) from Praxair (Edmonton, AB, Canada).

For the analytical methods, the chemicals used were of analytical grade. Sodium nitrate, ammonium formate, formic acid, acetonitrile, dichloromethane, 1-methylimidazole, acetic anhydride, sodium borohydride, myo-inositol, 12 M sulfuric acid, glacial acetic acid and ammonia anhydrous as well as mono-galacturonic acid, di-galacturonic acid and tri-galacturonic acid, glucose, D-galactose, D-arabinose, D-xylose, D-fucose and L-rhamnose were acquired from Sigma Aldrich (Oakville, ON, Canada). Malto-oligosaccharides with a degree of polymerization (DP) of 2 to 7, raffinose and stachyose from Supelco Inc. (Bellefonte, PA, USA), and xylo-hexose from Megazyme Ltd. (Bray, Wicklow, Ireland) were used. Dextran with molecular weights of 1.2, 3, 5, 25 and 72 kDa were obtained from the American Polymer Standards Corp. (Mentor, OH, USA) and HPLC-grade water was purchased from Fisher Scientific (Ottawa, ON, Canada).

### **5.2.2 Characterization of raw material**

#### **5.2.2.1 Proximate composition analysis**

Macro-components of pea fiber were determined as follows: a) crude protein by the Dumas combustion method using a LECO TruSpec nitrogen analyser (LECO Instruments Ltd.,

Mississauga, ON, Canada). Rye flour and ethylenediaminetetraacetic acid (EDTA) were used as standards to obtain the calibration curves. Nitrogen released from combustion of samples was quantified and used to calculate crude protein with a conversion factor of 6.25, which represents an average nitrogen content of proteins being equal to 16% w/w, b) crude fat using a Goldfish continuous solid-liquid extraction unit (Labconco Co., Kansas, MO, USA) using petroleum ether for 4 h. Total extracted crude fat was quantified gravimetrically as a percentage of the amount of sample used, c) moisture content using a convection oven set at 110°C for 2 h. The change in total weight of samples was determined gravimetrically, d) crude ash according to the National Renewable Energy Laboratory (NREL) protocol using a muffle furnace at 550°C for 18 h (Sluiter et al., 2008) and e) total carbohydrates by difference between 100% and the total of moisture, protein, fat and ash contents.

#### **5.2.2.2 Total starch and dietary fiber analyses**

Total dietary fiber and starch contents of pea fiber were determined using commercial assay kits for total dietary fiber (K-TDFR-100A/K) and total starch (K-TSTA-100A), respectively, from Megazyme Ltd. (Bray, Wicklow, Ireland).

#### **5.2.2.3 Neutral sugars analysis**

The neutral sugars content of pea fiber was determined by pre-column derivatization followed by Gas Chromatography (GC) analysis, according to a methodology previously described by Englyst and Cummings (1984) with some modifications. As such, starch and protein were enzymatically removed from pea fiber using a commercial assay kit for total dietary fiber (K-TDFR-100A/K), using heat-stable  $\alpha$ -amylase (100°C/30 min) and amyloglucosidase (60°C/30 min), and protease (65°C/30 min), respectively. Then, the enzymatically pre-purified and oven dried pea fiber (50 mg) was sequentially hydrolyzed to monosaccharides according to the protocol

described by Englyst and Cummings (1984) using sulfuric acid (12 M H<sub>2</sub>SO<sub>4</sub>/35°C/1 h and 1 M H<sub>2</sub>SO<sub>4</sub>/100°C/2 h). Myo-inositol was added to the hydrolysates as internal standard prior to conversion of monosaccharides into alditol acetate volatile derivatives. Next, monosaccharides were reduced with sodium borohydride at 45°C for 1 h. Glacial acetic acid, 1-methylimidazole (catalyst) and acetic anhydride were added and mixed thoroughly. Water was added to decompose excess acetic anhydride and to aid in phase separation, then dichloromethane was added to extract the produced alditol acetates. This mixture was placed at 4°C overnight and then centrifuged at 1250 g for 10 min. The upper aqueous phase was removed by aspiration with a Pasteur pipette, and dichloromethane was evaporated from the lower phase using a gentle flow of nitrogen. Extracted alditol acetates were then transferred to GC capped vials. Alditol acetates were analyzed according to the procedure detailed by Englyst and Cummings (1984) using an Agilent 7890A/MSD GC system (Agilent, Santa Clara, CA, USA) coupled to an Agilent 5975C EI/CI mass selective detector. The separation was performed on a SPB-17 column (30 m x 0.25 mm ID x 0.25 µm) (Supelco Inc., Bellefonte, PA, USA) using helium gas as the carrier. The column was heated from 50 to 190°C at 30°C /min and held for 3 min, then ramped to 270°C at 5°C/min and held for 5 min. The temperature of the detector was 300°C and the total run time was 28 min (Englyst and Cummings, 1984). Neutral sugars were identified and quantified based on the retention times and peak areas obtained from derivatized sugar standards, including glucose, galactose, arabinose, xylose, rhamnose and fucose.

#### **5.2.2.4 Galacturonic acid analysis**

Galacturonic acid content of pea fiber was determined by HPLC analysis after acid hydrolysis, following the methodologies described by Locatelli et al. (2012) and Pettolino et al. (2012) with some modification. Briefly, pea fiber was first enzymatically treated for starch and protein removal

using a commercial assay kit for total dietary fiber (K-TDFR-100A/K) containing  $\alpha$ -amylase, amyloglucosidase and protease. Then, 50 mg of purified and oven dried pea fiber were hydrolyzed with 8 mL of 2.5 M trifluoroacetic acid (TFA) at 121°C for 90 min in a convection oven. TFA was evaporated under a nitrogen stream at 50°C. The dried hydrolysate was re-solubilized in 4 mL of HPLC water and the resulting solution was used for further HPLC analysis. Galacturonic acid was quantified using a Shimadzu 10-A system (Shimadzu Corp., Kyoto, Japan) equipped with a refractive index detector RID-10A. An Aminex HPX-87H column (300 x 7.8 mm, 9  $\mu$ m particle size) (Bio-Rad Laboratories Ltd., Mississauga, ON, Canada) at 45°C was used to achieve the separation. The mobile phase was 0.005M H<sub>2</sub>SO<sub>4</sub>, the flow rate was 0.3 mL/min and the run time was 60 min. Galacturonic acid standards with concentrations between 0.1 and 1.5 mg/mL were used to obtain the calibration curve.

### **5.2.3 Subcritical water extraction and characterization of soluble polysaccharides from pea fiber**

#### **5.2.3.1 sCW extraction**

The Parr 4590 system (Parr Instrument Company, Moline, IL, USA) described in Chapter 3 (Section 3.2.2) with a slightly different configuration was used for the extraction of soluble polysaccharides from pea fiber under sCW conditions. The Parr 4590 system was equipped with a 600 mL batch stirred reactor, a 780 W heating mantle, and a temperature controller. The parameters of the controller were fine tuned to minimize the temperature fluctuation. The optimized proportional (P), integral (I) and derivative (D) parameters for the controller were P = 21, I = 500 and D = 71. The heating setting was on minimum power position and the stirring speed was on 1½ position.

For the sCW extraction of soluble polysaccharides from pea fiber, a methodology previously described by Valdivieso-Ramirez (2016) at optimized parameters of 120°C/50 bar/30 min with 0.2% w/w aqueous citric acid was adopted. The reactor was loaded at 50% of its capacity to prevent overpressure due to thermal expansion of water. Briefly, 25 g of pea fiber and 300 g of citric acid solution (0.2% w/w) were loaded sequentially into the reactor. The reactor was closed and assembled into the system. Next, nitrogen gas was used to flush out entrapped air from the reaction vessel. Once the mixture was purged for 12 min under constant stirring, it was semi-pressurized with nitrogen gas to 38 bar and then heated up to 120°C. After reaching the set temperature and pressure (50 bar), the extraction time (30 min) was started. The come-up time for the extraction at 120 °C was 25.8±1.9 min. At the end of the extraction time, the heating mantle was turned off and the reactor was immediately quenched to 50°C using a cold-water bath and depressurized slowly. The resulting pea fiber extract was centrifuged at 3,250 g for 15 min to aid in the separation of extracted soluble polysaccharides from the remaining insoluble fraction (denatured protein and insoluble fiber fraction). The filtered supernatant containing the soluble fraction was collected and further purified by ethanol precipitation at 4°C for 12 h. Ethanol (96%) was used at a ratio of 4:1 (v/v) ethanol/supernatant. After the precipitation time, the ethanolic mixture was centrifuged at 3,250 g for 15 min and the precipitate collected. Distilled water was used to re-solubilize the precipitate prior to freeze drying. The dried soluble polysaccharides were stored at 22°C for further characterization and subsequent sCW hydrolysis to oligosaccharides. The overall extraction protocol is depicted in Fig. 5.1 and the extraction yield of pea fiber soluble polysaccharides from pea fiber substrate was quantified according to Eq. (5.1).

$$\text{Extraction yield (\%)} = \frac{\text{pea fiber soluble polysaccharides extracted (g)}}{\text{pea fiber substrate used as feed (g)}} \times 100 \quad (\text{Eq. 5.1})$$

In addition, a batch liquid extraction of soluble polysaccharides from pea fiber (40 g) was also carried out under atmospheric pressure at 90°C/90 min with aqueous citric acid (1000 mL of 0.2% w/w) as a control. A digital hot plate stirrer (SP142020-33Q Cimarec, Thermo Scientific Inc, Waltham, MA, USA) and a 2000 mL Pyrex glass beaker was used for the control extraction. The obtained fiber extract was further processed following the steps 2 to 7 shown in Fig. 5.1.

### **5.2.3.2 Characterization of sCW pea fiber extract and residue**

Protein, total dietary fiber and starch contents as well as neutral sugar profile and galacturonic acid content were determined on pea fiber soluble polysaccharides extracted at 120°C/50 bar/30 min with aqueous citric acid, according to the methodologies described in Sections 5.2.2.1-5.2.2.4, respectively.

#### **5.2.3.2.1 Fourier transform infrared (FT-IR) spectroscopy analysis**

The FT-IR spectra of freeze-dried pea fiber soluble polysaccharides extract and pectic standards were collected using a Nicolet 8700 FT-IR Spectrometer (Thermo Fisher Scientific Inc, Waltham, MA, USA) equipped with a Smart Speculator for Attenuated Total Reflection (ATR germanium crystal cell). The spectra were recorded from 350 to 4000  $\text{cm}^{-1}$  with a resolution of 4  $\text{cm}^{-1}$  and 128 scans using Omnic software (version 7.1).

#### **5.2.3.2.2 Morphology analysis**

The morphology of the starting pea fiber and the residue obtained after sCW extraction were observed by scanning electron microscopy (SEM). The images were collected using a field emission scanning electron microscope (S4700 FE-SEM, Hitachi, Tokyo, Japan) with a secondary electron detector at 10 kV electron beam energy.

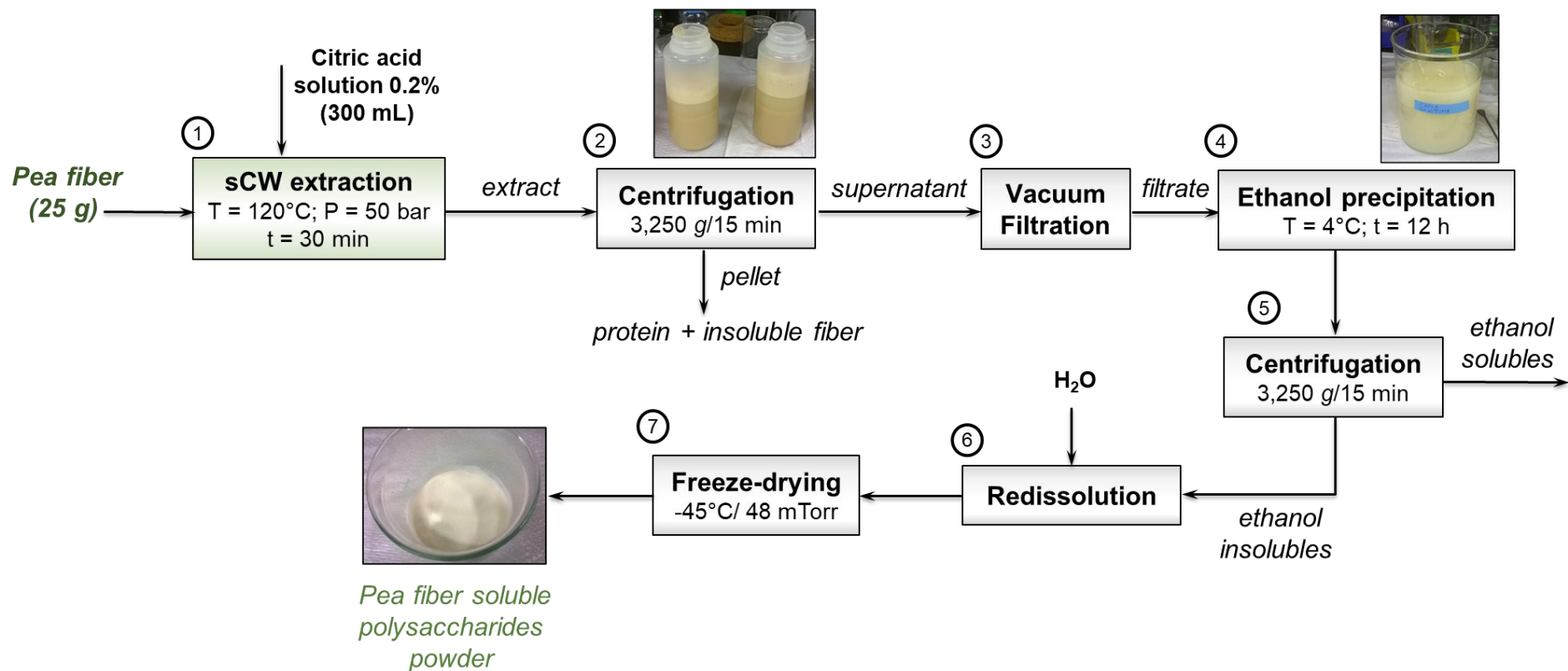


**Fig. 5.1.** Extraction of soluble polysaccharides from pea fiber under sCW conditions with aqueous 0.2% w/w citric acid at  $120^{\circ}\text{C}/50\text{ bar}/30\text{ min}$ .

The powdered samples were deposited as a thin layer on a double-sided carbon tape and carbon coated (Desk V HP TSC, Denton Vacuum LLC, Moorestown, NJ, USA) prior to the analysis.

The morphology of sCW extracted and freeze-dried pea fiber soluble polysaccharides was observed by helium ion microscopy (HIM) using a Zeiss Orion Helium Ion Microscope (Ostalbkreis, BW, Germany). Sample imaging was carried out directly on uncoated sample as previously described by Liu (2019).

#### **5.2.3.2.3 Degree of esterification analysis**

The degree of esterification (DE) represents the ratio between esterified carboxyl groups and total carboxyl groups that are present in the sample (Boчек et al., 2001). DE of sCW extracted pea fiber soluble polysaccharides was determined by titrimetric analysis as described by Boчек et al. (2001) and Pinheiro et al. (2008). Briefly, 200 mg of freeze-dried sample was dispersed in 20 mL of Milli-Q water at 40°C for 2 h under constant stirring. To neutralize the free carboxylate ion groups of galacturonic acid present in the sample, a 0.1 M NaOH solution was used as titrant in the presence of phenolphthalein to reach the neutralization point (pale rose color) and the volume used was recorded as the initial titre ( $V_1$ ). Then, 10 mL of 0.1 M NaOH was used to induce ester hydrolysis. After 2 h of saponification under constant stirring (120 rpm), 10 mL of 0.1 M HCl was added and excess HCl was determined by titration with 0.1 M NaOH. The volume of NaOH used to reach the neutralization point was recorded as the saponification titre ( $V_2$ ). The degree of esterification was calculated using Eq. (5.2).

$$DE (\%) = \frac{V_2}{V_1 + V_2} \times 100 \quad (\text{Eq. 5.2})$$

## **5.2.4 Subcritical water hydrolysis of pea fiber soluble polysaccharides into oligosaccharides and their characterization**

### **5.2.4.1 sCW hydrolysis**

Hydrolysis of the sCW extracted pea soluble polysaccharides into oligosaccharides was carried out using the same Parr 4590 system (Parr Instrument Company, Moline, IL, USA) described in Chapter 3 (Section 3.2.2). The input variables for the sCW hydrolysis were temperature (125, 135, 145 and 155°C), reaction time (10, 20, 30, 40, 60 and 120 min) and the number of carboxyl groups of the organic acids used in the reaction medium (tri-carboxylic acid (citric acid) and di-carboxylic acid (malic acid)). As such, a 0.2% w/w aqueous citric acid solution or a 0.27% w/w aqueous malic acid solution was used as the reaction medium at pH 2.6 in both cases. An Accumet XL25 pH meter (Fisher Scientific, Ottawa, ON, Canada) was used for the pH measurements. The pH of the reaction medium was selected based on Lu and Mosier (2007), who reported the use of di-carboxylic acids as an alternative to inorganic acids in homogeneous catalysis to obtain fermentable sugars from lignocellulosic biomass. For example, aqueous malic acid at pH 1.7-2.2 and aqueous oxalic acid at pH 1.5-2.2 were used to hydrolyze hardwood-derived xylo-oligosaccharides into xylose at temperatures of 140°C to 180°C/30 h, where sulphuric acid at pH 1.3-2.2 was used as the control (Kim et al., 2013). In the present study a slightly higher pH of 2.6 was selected as the starting point due to the different nature of the substrate and the unknown behavior of the di- and tri-carboxylic acids under sCW conditions. In addition, due to the reported enhancing effect of pressure on chemical reactions that involve ionic mechanism (Eldik et al., 1989; Martinez-Monteagudo and Saldaña, 2014) such as hydrolysis (Park and Park, 2002), the pressure of the reaction system was kept constant at 100 bar. The experimental runs were performed in duplicates and MilliQ-water was used as the control reaction medium.

For the sCW hydrolysis, the methodology described in Chapter 3 (Section 3.2.2) was used, with minor modifications. The concentration of the starting pea soluble polysaccharides solution was kept constant at 1% w/w. Pea soluble polysaccharides (400 mg) and 40 g of either 0.2% w/w of citric acid or 0.27% w/w of malic acid solution were loaded sequentially into the 100 mL reactor vessel. Then, the reactor was semi-pressurized with nitrogen gas to either 83, 80, 76 or 73 bar and then heated up to 125, 135, 145 or 155 °C, respectively. The come-up times for the hydrolysis at 125, 135, 145 and 155 °C were registered as 5.3±0.2, 5.8±0.4, 7.1±0.7 and 6.8±0.5 min, respectively. The resulting pea soluble polysaccharide hydrolysates were collected in plastic containers and stored frozen at -18°C until further HPLC analysis.

#### **5.2.4.2 Characterization of sCW hydrolysates**

##### **5.2.4.2.1 Molecular weight distribution**

The molecular weight (MW) distribution profile of sCW extracted pea fiber soluble polysaccharides and, the corresponding sCW hydrolysates were analyzed by high pressure size exclusion chromatography (HPSEC). The analysis was carried out using a Shimadzu 10-A HPLC system (Shimadzu Corp., Kyoto, Japan) equipped with a LC-10AD pump, autosampler SIL-10A, and a refractive index detector RID-10A all from the Shimadzu Corp. (Kyoto, Japan) and a Ultrahydrogel 250 column (7.8 x 300 mm, 6 µm particle size) (Waters, Milford, MA, USA). Dextrans were selected as standards and separation was achieved following the methodology described in Chapter 3 (Section 3.2.3.1).

##### **5.2.4.2.2 Determination of oligosaccharides**

Acidic and neutral oligosaccharides released during sCW hydrolysis of pea fiber soluble polysaccharides were further characterized by hydrophilic interaction liquid chromatography (HILIC) as described in Chapter 3 (Section 3.2.3.2). Mono-, di- and tri-galacturonic acids, 2- 7 DP

malto-oligosaccharides, raffinose, stachyose and xylo-hexose were used as standards to obtain the calibration curves, which were fitted to a power model regression curve. In addition, the yield of gluco-oligosaccharides with 2-6 DP was quantified according to Eq. (5.3).

$$\text{Yield of GluOS of 2-6 DP(\%)} = \frac{(\text{GluOS}_{(2-6)} \text{ produced})_t}{(\text{Pea soluble polysaccharides})_{t=0}} \times 100 \quad (\text{Eq. 5.3})$$

where,  $(\text{Pea soluble polysaccharides})_{t=0}$  is the initial mass of extracted pea soluble polysaccharides loaded in the reactor (400 mg), and  $(\text{GluOS}_{(2-6)} \text{ produced})_t$  is the total mass of galacto-oligosaccharides of 2-6 DP in mg produced at time t.

## 5.3 Results and discussion

### 5.3.1 Pea fiber characterization

Table 5.1 shows that the pea fiber used in this study is mainly comprised of carbohydrates, followed by protein, moisture, ash, and fat. Other studies on the composition of fiber from pea hull have shown values for crude protein that fluctuate between 3.8–5.3% and 18% (Dalgetty and Baik, 2006; Leterme et al., 1996; Ralet et al., 1993). However, consistent values for ash (1.7 - 3.3%) have been reported. Variations in composition could be due to the different fiber isolation processes (i.e. dry fractionation, wet fractionation, or chemical/enzymatic post-treatments) as well as the pea variety or degree of maturity when harvested (Dalgetty and Baik, 2006; Leterme et al., 1996; Ralet et al., 1993). Among the total carbohydrates present in pea fiber, insoluble fiber represented the major fraction, followed by starch and soluble fiber. Similarly, Leterme et al. (1996) reported insoluble and soluble fiber contents of yellow pea hull as 66.4% and 16%, respectively, based on the method of Englyst and Hudson (1987). Also, early studies have reported a starch content for pea hull in the range of 0-2.6% and 30% (Dalgetty and Baik, 2006; Leterme et

al., 1996; Ralet et al., 1993). The starch content of pea fiber used in this study was  $11.70 \pm 2.00\%$ , that lies within that range.

**Table 5.1.** Proximate composition and neutral sugars profile of pea fiber used in this study.

Proximate composition		Neutral sugars and GalA (in non-starch polysaccharides)	
	% (w/w)		% (w/w)
Crude protein	$13.26 \pm 0.20$	Glucose	$50.64 \pm 6.14$
Fat	$0.64 \pm 0.04$	Arabinose	$6.46 \pm 0.59$
Ash	$2.81 \pm 0.18$	Xylose	$4.43 \pm 0.55$
Moisture	$6.20 \pm 0.04$	Mannose	nd
Total carbohydrates	$77.09 \pm 0.41$	Galactose	$2.35 \pm 0.15$
Dietary fiber <sup>a</sup>	$67.01 \pm 0.07$	Rhamnose	$1.91 \pm 0.23$
<i>Insoluble</i>	$60.17 \pm 0.23$	Fucose	nd
<i>Soluble</i>	$6.84 \pm 0.15$	Total <sup>b</sup>	$65.80 \pm 7.67$
Starch	$11.70 \pm 2.00$	GalA	$6.37 \pm 0.13$

GalA: Galacturonic acid, <sup>a</sup>: AOAC method; <sup>b</sup>: Method of Englyst and Cummings (1984), nd: not detected.

The method of Englyst and Cummings (1984) for fiber determination of non-starch polysaccharides was used to study the neutral sugars profile of the pea fiber. Results presented in Table 5.1 showed that cellulosic glucose is the major component, followed by arabinose, xylose, galactose and rhamnose. Leterme et al. (1996) reported a similar neutral sugar profile for pea hull, including cellulosic glucose (53.9%), xylose (7.5%), arabinose (3.2%), mannose (1.7%), galactose (1.1%), rhamnose (0.6%) and fucose (0.2%). Some minor neutral sugars, however, were not detected in the present study, possibly due to peak overlap between rhamnose and fucose during the GC analysis. Ralet et al. (1993), for example, reported a low mannose content (1%), and rhamnose and fucose together as 0.9%. Reichert (1981) reported that pea hull from Saskatchewan smooth field pea contained cellulose (68.9%) predominantly followed by pectic substances (16.8%), hemicellulose (7.5%) and lignin (1.4%). Based on the reported neutral sugar profile and

uronic acid content (14%) of pea hull, studies have also suggested the presence of xylose- and arabinose-containing polysaccharides such as arabinose-rich hemicelluloses and pectic fragments (Leterme et al., 1996). In addition, a galacturonic acid content between 10.9 and 11.7% has been reported for hulls from six different pea varieties (Gutöhrlein et al., 2018). Although, galacturonic acid (6.37%) and soluble dietary fiber (6.84%) contents were consistent for the pea fiber used in this study, both values were lower compared to the previously reported results.

Based on the proximate composition results, it can be inferred that protein and residual starch that are present in pea fiber can lead to caramelization and Maillard reaction products during pea fiber hydrolysis to convert them to oligosaccharides, hindering the downstream processes. Therefore, sCW technology was used first to extract soluble polysaccharides from pea hull fiber and minimize the protein level in the extract to be used as the feed material for the hydrolysis reaction.

### **5.3.2 Subcritical water extraction of soluble polysaccharides from pea hull fiber**

The sCW extraction was carried out with aqueous citric acid (0.2% w/w) at 120°C/50 bar/30 min to recover soluble polysaccharides (rich in pectin) from pea hull fiber, whereas the conventional extraction process (control) was done with aqueous citric acid (0.2% w/w) at 90°C for 90 min at atmospheric pressure. The extracted soluble polysaccharides were further analyzed for soluble fiber, starch, and protein contents.

The sCW extraction yielded 11.8% w/w of soluble polysaccharides, which was 2.1-fold of that obtained by the conventional extraction method (5.6%). Such a difference could be attributed to enhanced dissolution and partial extraction of starch, also included in the pea hull fiber, together with pectic polysaccharides under sCW conditions compared to that of hot aqueous citric acid at atmospheric pressure. Gutöhrlein et al. (2018), however, reported a yield of 9.8% for the extraction

of pectic polysaccharides from pea hulls with aqueous citric acid (pH 2) at 90°C/3 h under atmospheric pressure. Although the reported extraction yield was relatively high compared to the control yield reported in this study, the reported extraction time was also 2-fold of that used in this study, suggesting that long extraction times can be favorable for pectic polysaccharides extraction at atmospheric pressure.

The chemical analysis of the sCW extracted soluble polysaccharides showed that their major macronutrients were soluble dietary fiber ( $49.2\pm 0.3\%$ ), starch ( $34.9\pm 1.2\%$ ) and protein ( $5.43\pm 0.0\%$ ), indicating the heterogeneous composition of the extracted soluble polysaccharides as well as the relatively low purity of the sCW extracted soluble fiber. In addition, based on the initial soluble dietary fiber content (6.84%) of the pea hull fiber, the sCW extraction yield, and the soluble dietary fiber content (49.2%) of the sCW extracted polysaccharides, the recovery of soluble dietary fiber by the sCW method was 85%. Further optimization of the operating processing parameters of the sCW method to increase the recovery of soluble dietary fiber is suggested.

Also, partial extraction of starch and protein together with soluble polysaccharides by sCW extraction was confirmed as the starch and the protein recovery in the sCW extract was 35.2% and 4.83%, respectively. The low protein recovery suggested that the sCW extraction method was a feasible approach not only for extraction of soluble polysaccharides from pea hull fiber but for reduction of the protein level in the extract via protein denaturation, as denatured protein was removed from the extract after centrifugation together with the insoluble components (i.e., cellulose and lignocellulose).

### **5.3.3 Characterization of pea hull fiber soluble polysaccharides extract and residue**

#### **5.3.3.1 Morphology analyses**

The morphology of the starting pea fiber and pea fiber solid residue obtained after sCW treatment was observed by SEM. Fig. 5.2a shows that pea fiber had a heterogeneous morphology as indicated by the fibrous material differing in size and shape as well as the presence of round starch granules. Fig. 5.2b shows the surface of the inner part of the fibrous material in higher magnification. This coated surface can be associated to the innermost layer of pea hull known as the nutrient layer, which is comprised of 5 to 12 parenchyma cell layers that are in direct contact with the endosperm (Smýkal et al., 2014). This parenchymal layer is not related to water impermeability as the outer layers (cuticle and palisade cell) are (Smýkal et al., 2014). Conversely, Fig. 5.2c shows the microstructure of the pea fiber residue obtained after sCW extraction, where disruption of the tightly packed palisade cells that are characterized by thick cell walls and radially elongated disposition can be observed (Smýkal et al., 2014). In Fig. 5.2d, showing the pea fiber residue in higher magnification, more exposed microfibril-like structures were apparent, suggesting that parenchymal cell layers were solubilized and removed during sCW treatment.

In addition, sCW pea fiber extract was freeze-dried, ground using a porcelain mortar and pestle, and the whitish and extremely light material obtained was analysed by HIM. Fig. 5.3a shows a material with irregular shape and various particle sizes, whereas the higher magnification in Fig. 5.3b shows a material with a continuous matrix appearance with some porosity associated to the freeze-drying process.

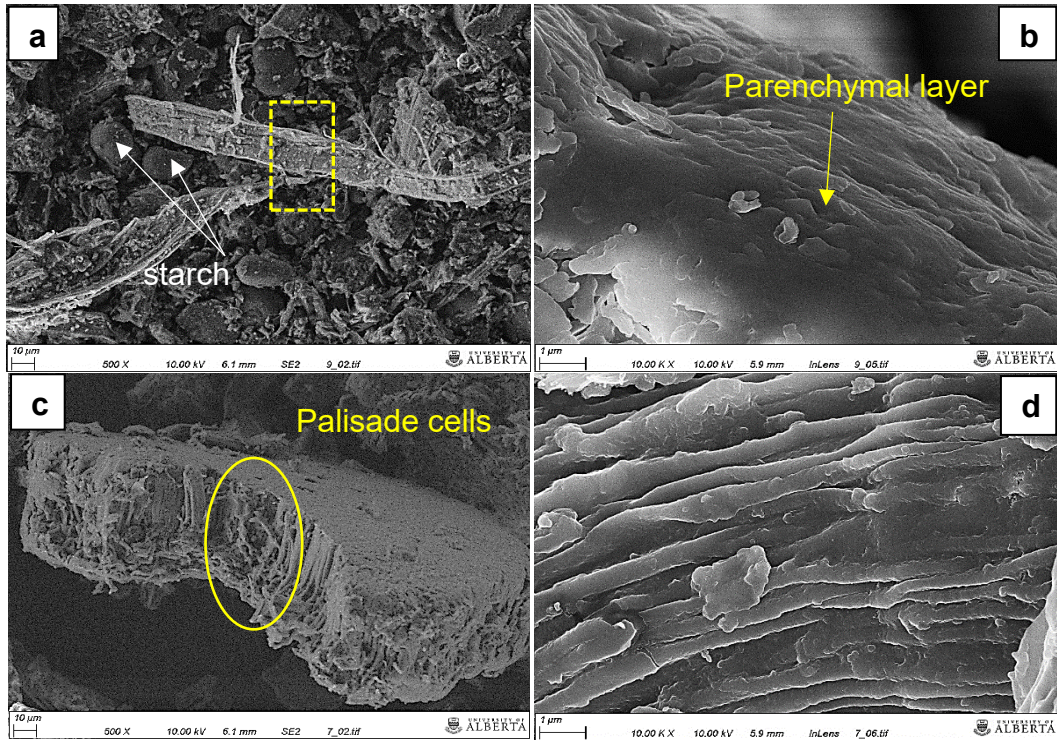


**Fig. 5.2.** Scanning electron microscopy images of: (a, b) pea fiber and (c, d) pea fiber residue after sCW extraction with aqueous citric acid at 120°C/50bar/30 min. Scale bars represent 10µm in a) and c), and 1µm in b) and d).

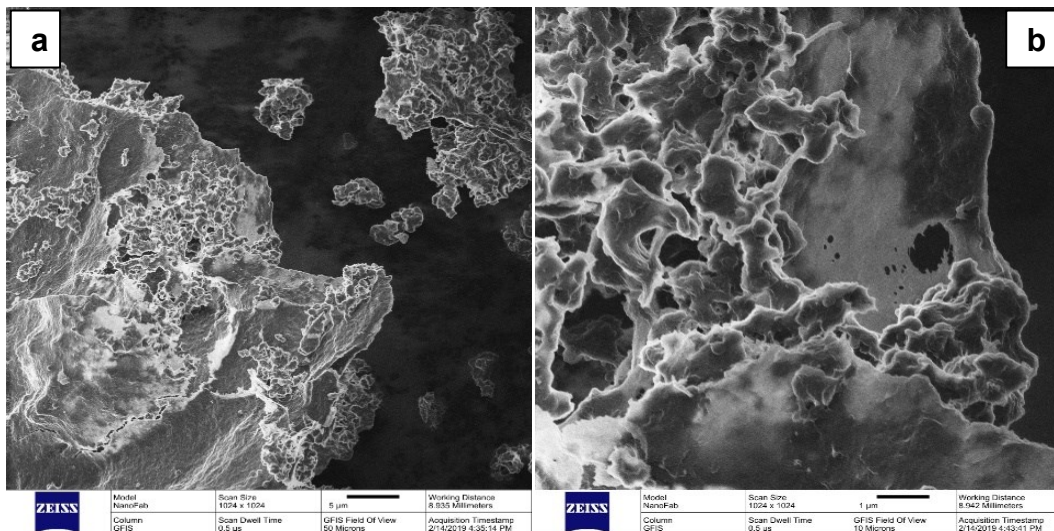


**Fig. 5.3.** Helium ion microscopy images of sCW pea fiber dried extract. Scale bars represent 5µm in (a), and 1µm in (b).

### 5.3.3.2 ATR-FTIR and degree of esterification analyses

ATR-FTIR analysis was performed on sCW pea fiber extract as well as on the standards of low methoxyl (LM) pectin, arabinogalactan and rhamnogalacturonan for comparison purposes. According to Fig. 5.4, typical absorption bands in the functional-group region (2000-1500  $\text{cm}^{-1}$ ) were apparent for pea fiber soluble polysaccharides, LM-pectin, arabinogalactan and rhamnogalacturonan. In pectin, absorption bands at wavenumbers of 1750-1735  $\text{cm}^{-1}$  and 1630-1600  $\text{cm}^{-1}$  correspond to stretching vibrations of the carboxylic ester (C=O) and carboxylate ion ( $\text{COO}^-$ ), respectively (Chylińska et al., 2016). The intensity of these absorption bands is also an indication of pectin's degree of esterification, where a high intensity peak corresponding to the carboxylate ion is predominant in low esterified pectin (Fellah et al., 2009). Interestingly, a high intensity peak at 1599  $\text{cm}^{-1}$  was also characteristic of rhamnogalacturonan from soybean (Fig. 5.4).

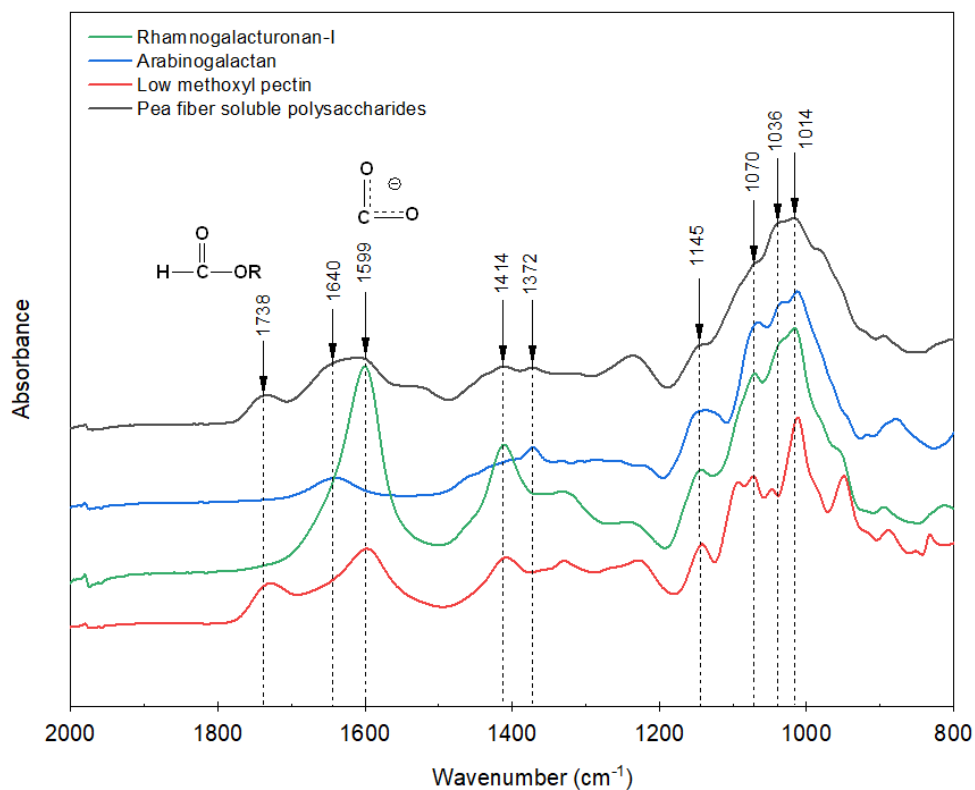


**Fig. 5.4.** ATR-FTIR spectra of sCW pea fiber extract and standards of rhamnogalacturonan, arabinogalactan and low methoxyl pectin.

The intensity ratio between peaks at  $1738\text{ cm}^{-1}$  and  $1599\text{ cm}^{-1}$  indicate that pea fiber soluble polysaccharides contain LM pectin, which was also confirmed by the DE analysis as  $50.9\pm 1.3\%$ . Similarly, in a recent study by Gutöhrlein et al. (2018) on pectin extraction from pea hulls using nitric or citric acid solutions at temperatures between  $70^{\circ}\text{C}$  and  $90^{\circ}\text{C}$ , pH of 1 to 2, and reaction times of 3 h to 6 h at atmospheric pressure, DE values between 36.4-48.9% were reported, where extraction temperature and pH had the most effect on DE. Moreover, absorption bands at frequencies of  $1640\text{-}1600\text{ cm}^{-1}$  and  $1420\text{ cm}^{-1}$  that correspond to deprotonated carboxylic acid are also distinctive in polysaccharides containing uronic acids as it is in the case of rhamnogalacturonan and pectin (Lopez-Torrez et al., 2015). Although the fingerprint region of infrared spectra ( $< 1500\text{ cm}^{-1}$ ) shows a unique absorption pattern for each analyzed sample, pea fiber polysaccharides, pectin, rhamnogalacturonan and arabinogalactan exhibited similar absorption peaks at frequencies of  $1145\text{ cm}^{-1}$ ,  $1070\text{ cm}^{-1}$  and  $1014\text{ cm}^{-1}$ , which have been assigned to glycosidic linkage vibration (C-O-C), rhamnogalacturonan ring vibration (C-C) and galacturonic acid ring vibration in the pectin molecule, respectively (Kacurakova et al., 2000). Therefore, it is concluded that the sCW extracted pea fiber soluble polysaccharides are comprised of a heterogeneous group of pectic fragments, including rhamnogalacturonan and homogalacturonan.

### **5.3.3.3 Neutral sugars and galacturonic acid contents**

The sCW extracted pea fiber soluble polysaccharides was mainly comprised of xylose, rhamnose, galactose, arabinose, and glucose (Table 5.2). Total neutral sugars and galacturonic acid contents were  $35.7\pm 1.3$  and  $17.4\pm 0.2\%$  w/w, respectively. Gutöhrlein et al. (2020) reported that total neutral sugars (19.6 to 35.7%) and galacturonic acid content (45.5 to 67.4%) of pea pectic polysaccharides isolated from pea hull with citric acid varied according to the extraction conditions

of temperature (70 and 90°C) and pH (1 and 2). As such, pectic polysaccharides with the lowest amount of total neutral sugars and the highest content of galacturonic acid were obtained at 90°C/pH 1/180 min (Gutöhrlein et al., 2020). Although the total neutral sugars quantified in this study falls within the previously reported range, the galacturonic acid content is much lower, suggesting that citric acid employed under sCW conditions can cleave different linkages within the substrate that led to a pea fiber extract with a high concentration of the RG-I fragment rather than the homo- or xylo-galacturonan fragments that are richer in galacturonic acid.

**Table 5.2.** Neutral sugars and galacturonic acid contents of pea fiber soluble polysaccharides extracted using sCW with aqueous citric acid (0.2% w/w) at 120°C/50 bar/30 min.

Neutral sugars and GalA (in non-starch polysaccharides)	Weight (%)	Mole (%)
Glucose	5.0 ± 0.0	8.9 ± 0.0
Arabinose	4.7 ± 0.2	10.0 ± 0.3
Xylose	12.9 ± 0.6	27.3 ± 0.9
Galactose	6.4 ± 0.1	11.4 ± 0.1
Rhamnose	6.6 ± 0.4	12.9 ± 0.5
Galacturonic acid	17.4 ± 0.2	28.5 ± 0.6

Total neutral sugars and GalA accounted for 53.0±1.1%, which was comparable to the determined soluble dietary fiber content of 49.2±0.3%. Moreover, based on the molar composition of the sCW pea fiber extract (Table 5.2), its chemical structure can be estimated. For example: *i*) the molar ratio of GalA/Rha of >2:1 can indicate that besides the RG-I fragment, for which the backbone is characterized by a molar ratio of GalA/Rha (1:1), GalA is also a part of other pectic fragments like xylogalacturonan, *ii*) considering the GalA that is not a part of RG-I (i.e. 28.5 - 12.9 = 15.6), the molar ratio of Xyl/GalA of >1.75:1 suggests the presence of other structures rich in xylose like the hemicellulose xyloglucan, and *iii*) the ratios of Ara/Rha (0.8:1) and Gal/Rha (0.9:1)

suggest that the RG-I fragment could be highly substituted with side chains of arabinans and galactans. As such, Le Goff et al. (2001) isolated xylogalacturonan from pea hull-derived polysaccharides obtained from acid hydrolysis with 0.1M HCl/80°C/24 h, whereas Noguchi et al. (2020) reported that RG-I, homogalacturonan and xylogalacturonan in a molar ratio of 3:3:4 were the main pectic fragments present in pectin extracted from pea cotyledons at pH 6/120°C/90 min. As the pea fiber used in this study comes from pea hull and it is comprised of 50.64% cellulose, it is more likely that xyloglucan ( $\beta$ -Glup-(1→4)- $\beta$ -Glup + Xyl side chains) was also present as a cell wall component. However, fiber that comes from cotyledon cell debris may not include significant amounts of neither cellulose nor xyloglucan. In addition, the intensity of the sCW treatment used in this study could have favored xyloglucan extraction together with pectic fragments, which may not have occurred at the extraction conditions previously reported.

### **5.3.4 Characterization of subcritical water hydrolysates of pea hull fiber soluble polysaccharides**

The sCW pea fiber extract with the composition described above, which was low in protein, was used for oligosaccharides production in this hydrolysis step. Hydrolysis was carried out under sCW conditions and hydrolysates were characterized.

#### **5.3.4.1 Molecular weight distribution**

The extent of hydrolysis of pea fiber soluble polysaccharides obtained at 125°C/100 bar in aqueous citric acid over time was monitored by HPSEC (Figs. 5.5a-5.5d). According to Fig. 5.5a, pea fiber soluble polysaccharides had a broad molecular weight range represented by three major peaks eluted at 5.8 mL (beyond the exclusion limit of the column, 80 kDa), 6.5 mL, and 8.8 mL. These peaks corresponded to compounds with molecular weights of  $\gg 80$  kDa, 46 kDa and 1.65 kDa, respectively. Similarly, Le Goff et al. (2001) obtained a pea hull-derived pectin fragment

(rich in xylogalacturonans) containing molecular weight fractions of 287 kDa and 31.9 kDa after pea hull hydrolysis with 0.1 M HCl at 80°C for 24 h and further purification with rhamnogalacturonan hydrolase for 24 h. Figs. 5.5a-5.5c depict: *i*) a decrease in the concentration of major high molecular weight fractions based on the substantial reduction in the intensity of these peaks as the reaction time approached 60 min, and *ii*) the release of smaller molecular weight fragments based on the appearance of peaks at longer elution times with an increase in reaction time.

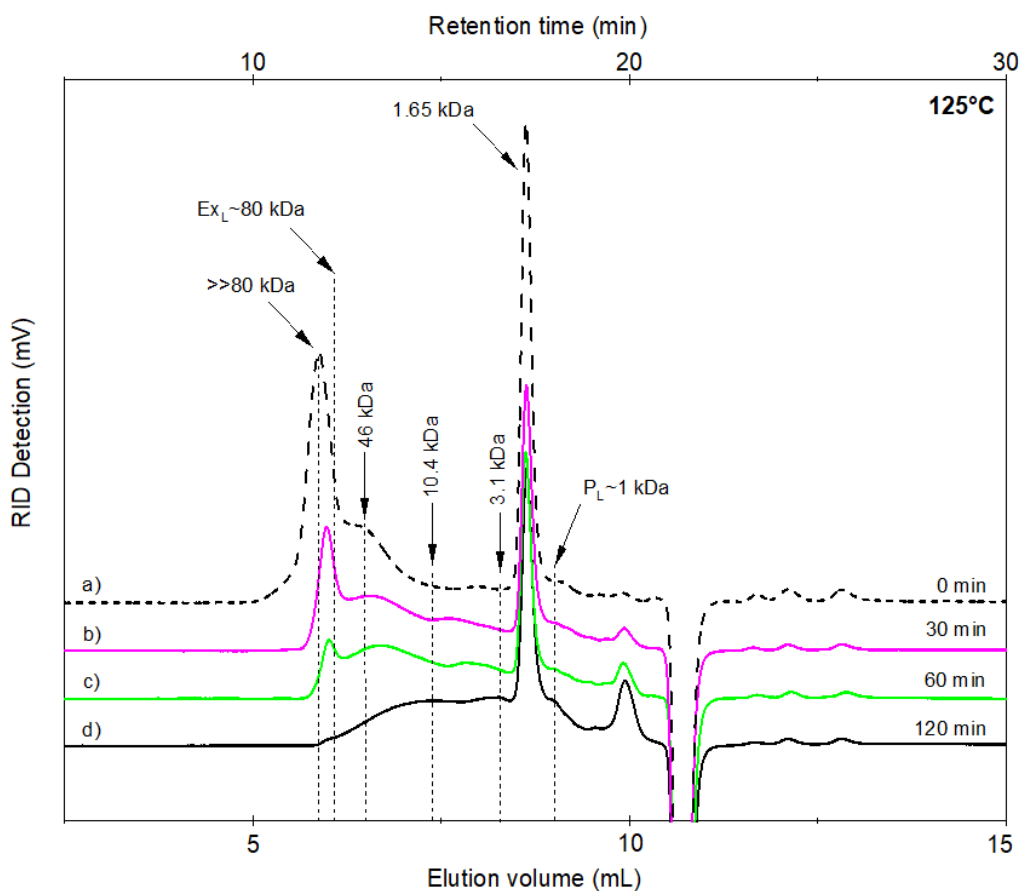


**Fig. 5.5.** HPSEC molecular weight distribution profile of pea fiber soluble polysaccharides hydrolysates obtained in aqueous citric acid at 125°C/100 bar and reaction times of: a) 0 min, b) 30 min, c) 60 min, and d) 120 min. Ex<sub>L</sub>: column exclusion limit, and P<sub>L</sub>: column permeation limit.

After 60 min, however, the hydrolysis of pea fiber soluble polysaccharides proceeded further as the elution profile at 120 min of reaction time (Fig. 5.5d) showed the complete disappearance of the two major peaks eluted at 5.8 mL (11.7 min) and 6.5 mL (13 min), and the reduced intensity of the peak eluted at 8.8 mL, which corresponded to the lowest molecular weight fraction that was present initially. In addition, Fig. 5.5d depicts the appearance of broad peaks eluted at 7.4 mL (14.8 min) and 8.2 mL (16.5 min), corresponding to compounds with reduced molecular weights of 10.4 kDa and 3.1 kDa, respectively. Also, a sharp peak eluting at 9.9 mL beyond the permeation limit of the column (9 mL) was identified.

Structural studies on other Leguminosae members like soybeans have shown that soluble polysaccharides from soybean cotyledons also contain pectic polysaccharides, in particular: *i*) galacturonans with 4 to 10 DP in length (0.72-1.78 kDa) partially branched with xylose residues located in between rhamnogalacturonan regions, *ii*) galacturonans with 7 to 9 DP in length (1.25-1.6 kDa) located at the reducing end of the polysaccharide, *iii*) rhamnogalacturonan containing side chains of  $\beta$ -1,4-galactans branched with fucose and arabinose, and *iv*) long side-chain  $\beta$ -1,4-galactans with approximately 43 to 47 DP in length (7-7.6 kDa) (Nakamura et al., 2014).

Based on the neutral sugar composition (Table 5.2) of pea soluble polysaccharides and the molecular weight distribution profile of the hydrolysate obtained at 120 min reaction (Fig. 5.5d), it can be hypothesized that the peaks corresponding to molecular weights of 10.4 kDa and 1.65 kDa could represent  $\beta$ -1,4-galactans (43-47 DP) and galacturonans (7-9 DP), respectively, similar to soybean soluble polysaccharides.

The molecular weight distribution profile of pea fiber soluble polysaccharide hydrolysates confirmed that hydrolysis was achieved using aqueous citric acid at mild sCW conditions (125°C/100 bar), and suggested that the hydrolysis pathway involved two parallel reactions, where

high molecular weight fractions ( $>>80$  and 46 kDa) were cleaved into fragments with molecular weights between 10.4 and 3.2 kDa, and simultaneously, the low molecular weight fraction (1.65 kDa) was further broken down into oligosaccharides with molecular weights of  $\leq 1$  kDa. Next, a XBridge Amide column with reduced particle size of 3.5  $\mu\text{m}$  was used to further analyze the hydrolysates, in particular, to verify the molecular size and composition of fragments ( $\text{MW} \leq 2.4$  kDa) that were eluted close to and beyond the permeation limit of the current Ultrahydrogel 250 column (6  $\mu\text{m}$  particle size).

#### 5.3.4.2 Determination of oligosaccharides

The oligosaccharide contents of hydrolysates obtained from pea fiber soluble polysaccharides with citric acid at 125 to 155°C/100 bar and reaction times of 10 to 120 min were analyzed by HILIC-ELSD. According to Fig. 5.6, hydrolysates obtained at either 125°C or 135°C were mainly comprised of neutral oligosaccharides (gluco-oligosaccharides) and a minor fraction of acidic saccharides (di- and tri-galacturonic acids); however, several peaks corresponding to low molecular weight fragments ( $\text{DP} > 7\text{DP}$ , based on gluco-oligosaccharide standards) but unknown composition were also detected at 125°C and 135°C. Therefore, hydrolysis of pea soluble polysaccharides under sCW could be associated with cleavage of rhamnogalacturonan side chains, which are generally composed of arabinose (i.e. (1 $\rightarrow$ 5)- $\alpha$ -L-arabinan) or galactose (i.e. (1 $\rightarrow$ 4)- $\beta$ -D-galactans), and the subsequent release of various types of oligosaccharides (i.e. galacto- and arabino-oligosaccharides). Nonetheless, sCW conditions could also favor the hydrolysis of starch fraction ( $34.9 \pm 1.2\%$  wet basis) present in the sample.

As expected, chromatograms in Figs. 5.6a-5.6b show that temperature and reaction time influenced the rate of hydrolysis. At 135°C, the intensity of peaks corresponding to gluco-

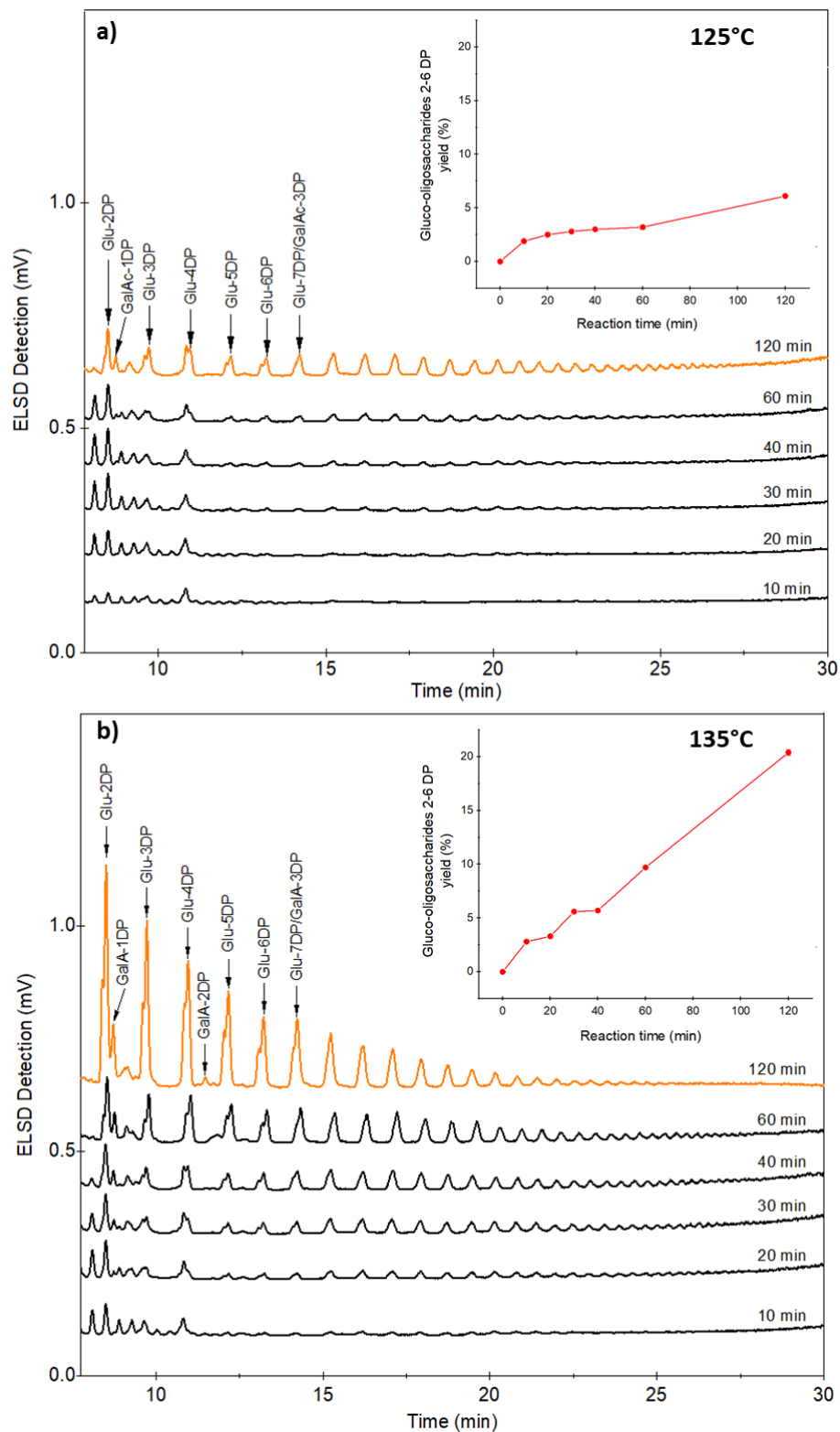


**Fig. 5.6.** Effect of reaction time (10-120 min) on pea fiber soluble polysaccharides hydrolysis in aqueous citric acid at 100 bar and 2-6 DP gluco-oligosaccharides yield (insets) at temperatures of: a) 125°C and b) 135°C analyzed by HILIC-ELSD.

oligosaccharides with 2-6 DP and oligogalacturonides with 2-3 DP was considerably higher compared to those displayed at 125°C. After 120 min of reaction, the yields of gluco-oligosaccharides (GluOS) with 2-6 DP obtained at 125°C and 135°C were  $6.1 \pm 0.1$  and  $20.4 \pm 0.3\%$  (Eq. 5.3), respectively. Then, the overall yield of oligosaccharides was the highest (2.4%, based on the original pea hull fiber substrate) at 135°C/120 min.

As expected, at a constant temperature, longer reaction times favored hydrolysis. At 125°C, however, a considerably longer reaction time was required to achieve a similar extent of hydrolysis to that at 135°C. A combination of 125°C and 120 min, for example, could lead to results comparable to that at 135°C and 40 min (GluOS yield of  $5.7 \pm 0.1\%$ ). Thus, a 10°C rise in temperature shortened the reaction time by 3-fold.

Fig. 5.7a shows the effect of the reaction medium (i.e., aqueous malic and citric acids and water) on the hydrolysis of pea soluble polysaccharides at 135°C and 60 min by the difference in the elution pattern and signal intensity of peaks. For example, chromatograms of hydrolysates obtained with both, aqueous malic and citric acids exhibited defined peaks that corresponded to gluco-oligosaccharides with 2-6 DP as well as to mono- and tri-galacturonic acids. However, low intensity peaks that corresponded to raffinose and xylohexaose were also identified in the hydrolysate obtained with aqueous citric acid. The yields of gluco-oligosaccharides with 2-6 DP obtained at 135°C/60 min/100 bar with aqueous malic and citric acids were  $11.7 \pm 0.5$  and  $9.7 \pm 0.1\%$ , respectively. Conversely, water at 135°C/100 bar had a minimal hydrolytic effect on pea fiber soluble polysaccharides compared to aqueous malic and citric acids as indicated by the overall fewer peaks and small intensity of gluco-oligosaccharides peaks, which corresponded to a yield of only  $1.9 \pm 0.0\%$ .

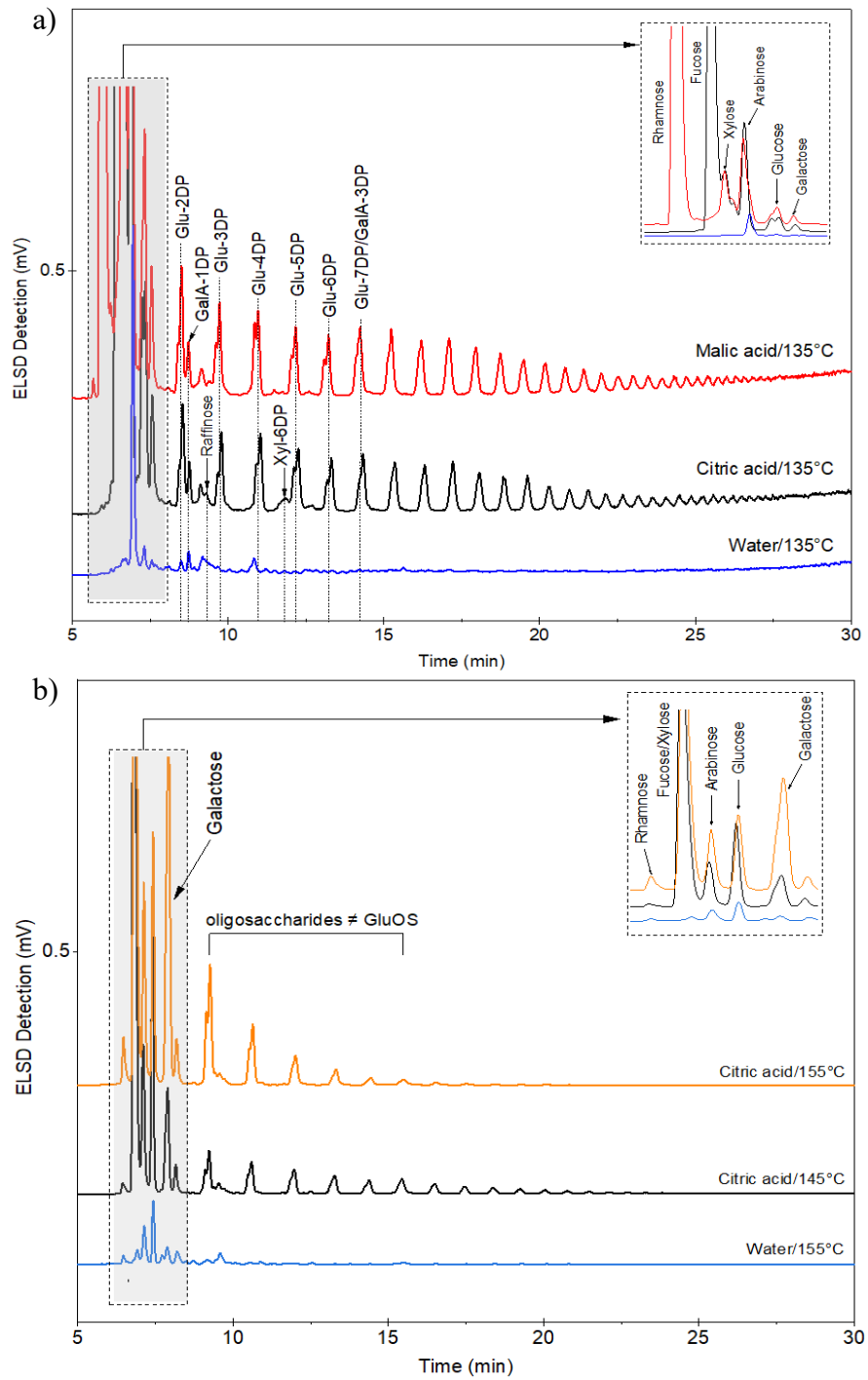


**Fig. 5.7.** HILIC-ELSD chromatograms of pea fiber soluble polysaccharides hydrolysates obtained at 100 bar and 60 min in different reaction media at a) 135°C, b) 145°C and 155°C. (GluOS: gluco-oligosaccharides).

Chromatograms in the inset of Fig. 5.7a show peaks eluted at early times, which corresponded to neutral monosaccharides. Aqueous malic acid, for example, favored the release of arabinose, xylose, glucose and rhamnose. This suggests that hydrolysis of rhamnogalacturonan pectic fragment in the presence of malic acid proceeded in a random manner, where side branches containing arabinose, xylose, and glucose were hydrolysed in addition to the rhamnogalacturonan backbone that released rhamnose. Conversely, aqueous citric acid favored fucose, xylose and arabinose release but not rhamnose, suggesting that hydrolysis occurred in a stepwise manner, as fucose and arabinose residues that are present in the side chains of rhamnogalacturonan were cleaved first prior to the backbone scission.

According to Fig. 5.7b, hydrolysis with aqueous citric acid at higher temperatures of 145°C and 155°C led to chromatograms with different elution patterns compared to those at 135°C (Fig. 5.7a). The chromatogram at 155°C was characterized by high intensity peaks but low in number, whereas at 145°C, various lower intensity peaks were present. In addition, peaks at either 145°C or 155°C had retention times different from those that corresponded to GluOS standards, suggesting that temperatures higher than 135°C can favor cleavage of (1→4)-β-D-galactans into galacto-oligosaccharides with retention times closer to GluOS. In fact, the chromatograms in the inset of Fig. 5.7b show that at 155°C, the intensity of the galactose peak increased, possibly due to further hydrolysis of the released galacto-oligosaccharides into the galactose monomer. Moreover, such temperatures could also induce complete hydrolysis of GluOS into glucose, as suggested by the increased intensity of the glucose peak at either 145°C or 155°C. On the contrary, the hydrolytic effect of water at 155°C on oligosaccharides production was still limited compared to that of aqueous citric acid at the same temperature.

Overall, the addition of citric and malic acids to a sCW system had a selective catalytic effect on pea fiber soluble polysaccharides hydrolysis. Also, based on the results above, it can be hypothesized that: *i)* pea fiber soluble polysaccharides are comprised of a branched pectic fragment like rhamnogalacturonan-I, *ii)* side chain branches hinder the hydrolysis of pectic-backbone, *iii)* gluco-oligosaccharides can result from starch hydrolysis in the presence of carboxylic acids at 135°C/100 bar, and *iv)* hydrolysis of (1→4)-β-D-galactans into galacto-oligosaccharides could be favored at either 145°C or 155°C/60 min/100 bar with aqueous citric acid.

Additionally, data obtained from the previous studies on the hydrolysis of pure linear polygalacturonic acid (Chapter 3) and branched rhamnogalacturonan (Chapter 4) were compared with the current data for pea fiber polysaccharides in Fig. 5.8 to get an overall understanding of the hydrolytic effect of aqueous citric acid at 135°C/100 bar/60 min on different pectic structures. According to Fig. 5.8, the extent of hydrolysis of linear polygalacturonic acid was extensive as indicated by the high intensity and well-defined peaks that corresponded to 2-7 DP oligogalacturonides and the monomeric galacturonic acid (Chapter 3). However, the extent of hydrolysis of branched rhamnogalacturonan was limited as the representative peaks were less intense and eluted later than those of polygalacturonic acid (Chapter 4). As such, 5-8 DP oligogalacturonides prevail suggesting that side chains can exert a protective effect on the backbone and slowdown its hydrolysis. Conversely, pea fiber soluble polysaccharides hydrolysate exhibited several well-defined peaks, including those corresponding to 3-7 DP gluco-oligosaccharides and 6-7 DP oligogalacturonides. Various peaks eluted after 15 min were also apparent, but their chemical identity was undetermined. As expected, the chromatogram of hydrolysate from pea fiber soluble polysaccharides reflects the complexity of the pea fiber pectic substrate. Additional analytical techniques such as glycosidic linkage analysis, tandem mass

spectrometry with collision induced dissociation, and nuclear magnetic resonance spectroscopy are suggested for their structural identification.

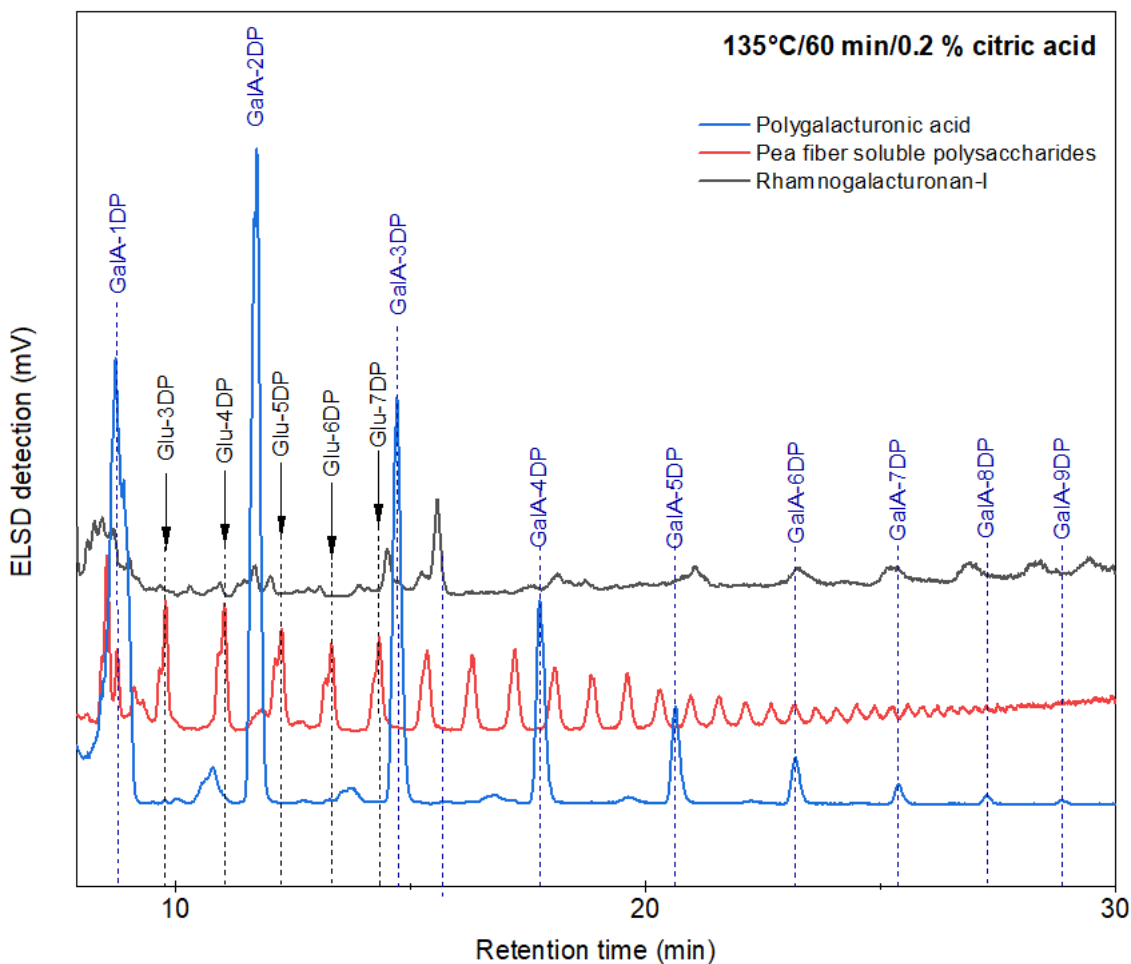


**Fig. 5.8.** HILIC-ELSD chromatograms of hydrolysates obtained with citric acid at 135°C, 100 bar and 60 min from linear polygalacturonic acid (Chapter 3), branched rhamnogalacturonan-I (Chapter 4), and pea fiber soluble polysaccharides.

## 5.4 Conclusions

In this study, a sequential approach based on subcritical water technology and the use of carboxylic acids was carried out for the extraction of soluble polysaccharides from pea fiber as

well as their hydrolysis to obtain oligosaccharides. Pea soluble polysaccharides extract (yield 11.8%) obtained with aqueous citric acid at 120°C/30 min/50 bar was comprised of pectic fragments with an esterification degree of 50.9%. Based on its sugar composition, the major chemical structures of the isolated pea soluble polysaccharides were estimated as rhamnogalacturonan-I, xylogalacturonan and xyloglucan. Further sCW hydrolysis of the pea fiber extracts into oligosaccharides showed that *i*) aqueous citric (0.20%) or malic acid (0.27%) at pH 2.6 and 100 bar exerted a catalytic effect on glycosidic bonds cleavage at a relatively low temperature range of 125°C to 155°C, *ii*) aqueous citric acid under sCW conditions favored a stepwise hydrolysis where rhamnogalacturonan-I side chains were first cleaved followed by their breakdown into oligosaccharides, *iii*) the yields of gluco-oligosaccharides with 2-6 DP were 6.1% and 20.4% at 125°C and 135°C/120 min/100 bar, respectively, and *iv*) aqueous citric acid at 145°C and 155°C/100 bar led to oligosaccharides with chemical composition that differed from gluco-oligosaccharides. These findings provide an insight about the potential catalytic effect of carboxylic acids under sCW conditions on the hydrolysis of complex polysaccharide-rich substrates that are comprised of different types of glycosidic linkages as in the case of pectic substances.

## **Chapter 6: Scale-up of soluble pea fiber-derived oligosaccharides production and drying**

### **6.1 Introduction**

Pectic oligosaccharides are generally obtained from partial hydrolysis of pectin-rich substrates such as apple pomace (Chen et al., 2013), sugar beet (Combo et al., 2013), and orange peel (Martínez et al., 2010), among others (Babbar et al., 2015; Khuwijitjaru et al., 2014). Pectic oligosaccharides have been studied for their promising prebiotic effect and efforts have focused on gaining more insight about their complex structure and quantification (Remoroza et al., 2012). Due to the multicomponent nature of the resulting pectic hydrolysates, their fractionation and purification have also been investigated to isolate and concentrate the pectic oligosaccharides fraction (Pinelo et al., 2009). As such, the use of membrane reactors (Pinelo et al., 2009), ultra- and nanofiltration (Akin et al., 2012; Gómez et al., 2014) and electrofiltration (Dudziak et al., 2008) have been reported for purification of pectic oligosaccharides. However, the challenge of drying pectic hydrolysates rich in low molecular weight neutral and acidic saccharides remains (Muzaffar, 2015). Hence, spray drying of mono-, di- and tri-saccharides as well as supercritical fluid drying of polysaccharides, including dextran, cyclodextrin and monosaccharides have been reported with low yields (Bouchard et al., 2008; Wrzosek et al., 2013). Supercritical drying of aqueous solutions using CO<sub>2</sub> is challenging due to the low solubility of water in supercritical CO<sub>2</sub>.

Pectic oligosaccharides have not been commercialized yet in contrast to their homologue types of prebiotics (i.e., fructo-, galacto- and xylo-oligosaccharides) and more research is needed to establish processes for their production at large scale as well as for their purification and drying. Therefore, the objectives of this study were to carry out the scale-up of the subcritical water (sCW) production of soluble pea fiber-derived oligosaccharides within bench scale (600 mL reactor) as

well as to purify the resulting pectic hydrolysate using a tangential flow ultrafiltration unit. In addition, spray drying, freeze drying, and Pressurized Gas eXpanded (PGX) liquid drying technologies were explored to obtain pectic oligosaccharides in powder form. PGX drying was selected as it is an emerging technology that allows drying of high molecular weight water-soluble biopolymers by spraying the biopolymer aqueous solution through a coaxial nozzle into CO<sub>2</sub>+ethanol at 40°C and 100 bar, where the ternary mixture forms a single phase gas-expanded liquid (Couto et al., 2020). However, PGX drying has not been explored for drying of small molecular weight water-soluble oligomers as in the case of oligosaccharides targeted here.

## **6.2 Materials and Methods**

### **6.2.1 Materials**

Pea fiber soluble polysaccharides used for oligosaccharides production were previously isolated from pea fiber provided by AGT Food and Ingredients Inc. (Saskatoon, SK, Canada) as described in Chapter 5 (Section 5.2.3). Reagents used for the sCW treatment were citric acid (>99.5%, ACS grade) from Sigma Aldrich (Oakville, ON, Canada), water from the Milli-Q system (18.2 MΩ.cm, Millipore, Billerica, MA, USA) and nitrogen gas (99.9% purity) from Praxair Canada Inc. (Edmonton, AB, Canada). In addition, for PGX drying, anhydrous ethanol (> 99.5%; Greenfield Global Inc., Brampton, ON, Canada) and carbon dioxide (99.9% purity, < 3 ppm H<sub>2</sub>O; from Praxair Canada Inc. (Edmonton, AB, Canada)) were used.

For analytical procedures, sodium nitrate, triethanolamine (TEA), acetonitrile, D-glucose, D-galactose, D-arabinose, D-xylose, D-fucose and L-rhamnose were acquired from Sigma Aldrich (Oakville, ON, Canada). Malto-oligosaccharides with a degree of polymerization (DP) of 2 to 6 were obtained from Supelco Inc. (Bellefonte, PA, USA), and xylo-oligosaccharides PreticXTM (AIDP Inc., City of Industry, CA, USA) were used as standards. Dextran with molecular weights

of 1.2, 3, 5, 25 and 72 kDa were obtained from the American Polymer Standards Corp. (Mentor, OH, USA) and HPLC-grade water was purchased from Fisher Scientific (Ottawa, ON, Canada).

### **6.2.2 Production of soluble pea fiber-derived oligosaccharides**

The overall approach used in this study for the production, characterization and drying of soluble pea fiber-derived oligosaccharides is summarized in Fig. 6.1. The sCW production of soluble fiber-derived oligosaccharides was performed at large scale using a reactor vessel of 600 mL (as opposed to the 100 mL reactor used in the previous study reported in Chapter 5) and the resulting hydrolysate was characterized by high pressure size exclusion chromatography (HPSEC) with refractive index detection (RID) and hydrophilic interaction liquid chromatography (HILIC) coupled with an evaporative light scattering detector (ELSD) for size distribution and oligosaccharides determination, respectively. In addition, the sCW hydrolysate was purified using an ultrafiltration membrane system, and its retentate and permeate fractions were analyzed for determination of free sugars recovery. Finally, sCW hydrolysate was dried by spray drying, freeze drying, and PGX drying and the resulting powders were characterized.

#### **6.2.2.1 Subcritical water hydrolysis scale-up**

The scale-up of oligosaccharides production was performed using a Parr 4590 system (Parr Instrument Company, Moline, IL, USA) equipped with a 600 mL batch stirred reactor. The configuration of the reactor system and the PID parameters of the temperature controller were detailed in Chapters 3 (Section 3.2.2.2) and 5 (Section 5.2.4.1), respectively. Also, the heating setting was adjusted to maximum power position to minimize the come-up time.

Hydrolysis of pea fiber soluble polysaccharides into oligosaccharides was carried out according to the methodology previously established for the 100 mL reactor vessel as described in

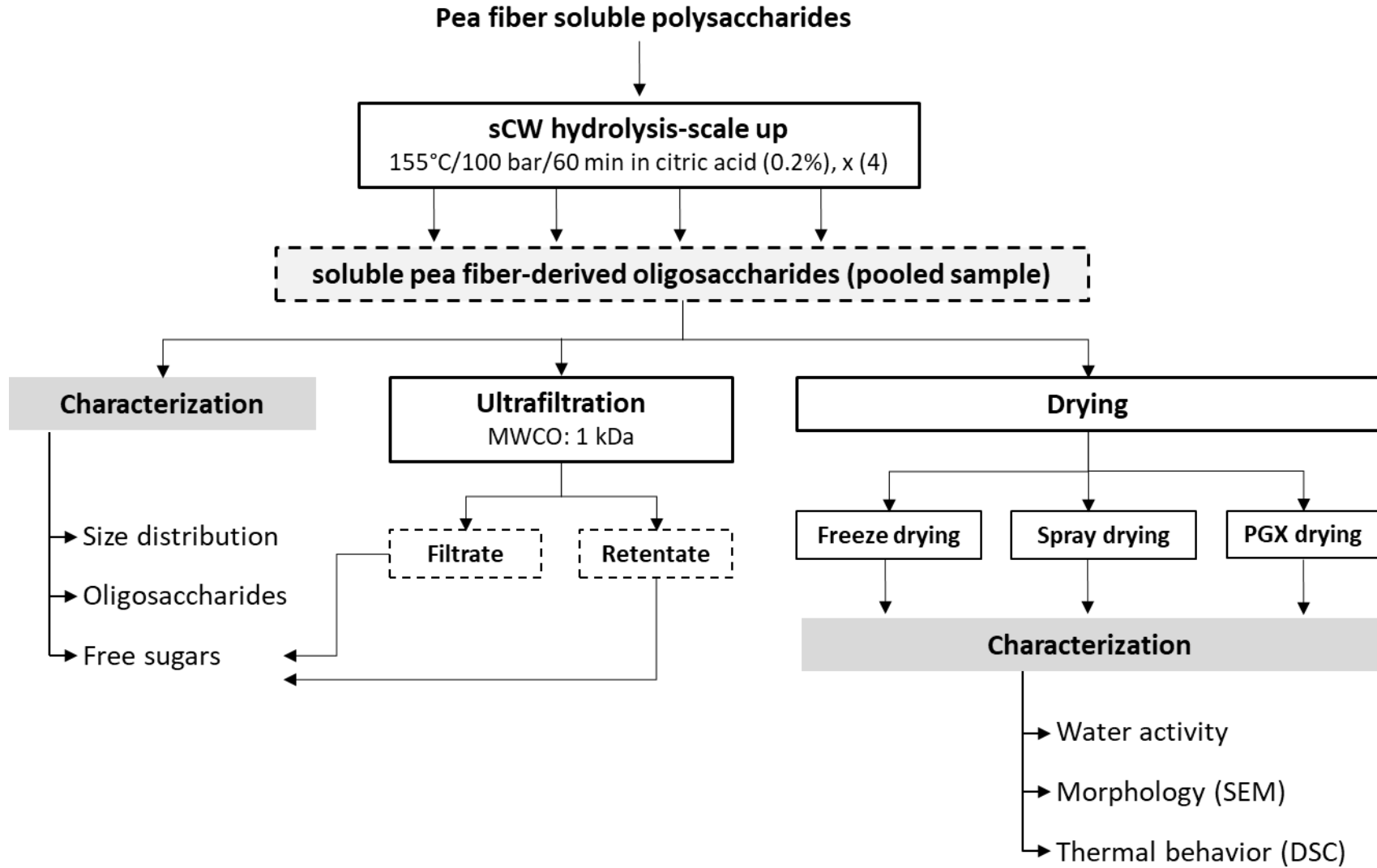


**Fig. 6.1.** Scheme for the production, drying and characterization of soluble pea fiber-derived oligosaccharides.

Chapter 5 (Section 5.2.4.1) at the optimized conditions of 155°C, 100 bar and 60 min in aqueous citric acid. Briefly, 3 g of pea fiber soluble polysaccharides and 300 g of citric acid solution (0.2% w/w) were loaded sequentially into the reactor and the resulting mixture was purged with N<sub>2</sub> gas for 12 min under constant stirring. Then, the reactor was partially pressurized with N<sub>2</sub> gas to 74 bar and heated up to 155°C. After reaching the set temperature and pressure (100 bar), the 60 min reaction time was started. At the end of the reaction time, the reactor was quenched to 60°C prior to its slow depressurization. The experiment was performed in quadruplicate and the resulting hydrolysates were collected, pooled as one sample, and stored frozen at -18°C for further characterization, purification and drying.

#### **6.2.2.2 Purification**

The hydrolysate obtained from the sCW treatment (pooled sample) was passed through a tangential flow filtration unit (Minimate, Pall Canada Ltd., Mississauga, ON, Canada), previously described by Aghashahi (2019), and equipped with an ultrafiltration membrane (Omega, polyethersulfone (PES)) of 1 kDa molecular weight cut-off (Pall Canada Ltd., Mississauga, ON, Canada) to concentrate and purify the oligosaccharides fraction. A tangential flow filtration unit was selected as it has been reported to minimize fouling during oligosaccharides production (Pinelo et al., 2009). A PES membrane was used due to its hydrophobic nature, which was utilized for the purification of pectic-oligosaccharides (Rodriguez-Nogales et al., 2008b) and fructo-oligosaccharides (Olano-Martin et al., 2001). The ultrafiltration temperature was selected based on the Omega membrane specifications as well as the temperature range (40-50°C) reported for oligosaccharide fractionation (Pinelo et al., 2009). The unit was set up in constant volume diafiltration mode by recirculating the retentate at 40°C at the same rate as the feed was pumped into the system. There was no addition of fresh solvent. The speed of the peristaltic pump and the

transmembrane pressure were set to 56 rpm and 1.2 bar, respectively. sCW hydrolysate (280 mL) was continuously pumped for 7 h and the permeate was collected at 0.166 mL/min. The resulting permeate and retentate were further analyzed by HILIC-ELSD for their free sugar contents.

### **6.2.3 Characterization of pea soluble fiber hydrolysate**

#### **6.2.3.1 Molecular weight distribution analysis**

The molecular weight distribution of the pea soluble fiber hydrolysate (pooled sample) as well as the xylo-oligosaccharides standard was determined by HPSEC-RID following the methodology described in Chapter 3 (Section 3.2.3.1).

#### **6.2.3.2 Free sugars analysis**

The pea soluble fiber hydrolysate as well as its permeate and retentate fractions (Fig. 6.1) were analyzed for free sugars using an Agilent 1200 Series HPLC system (Agilent, Santa Clara, CA, USA) coupled with an Agilent 1200 Evaporative Light Scattering detector (ELSD), following the methodology described in Chapter 4 (Section 4.2.3.4). The percentage of free sugars present in the pooled sample was quantified according to Eq. (6.1).

$$\text{Free sugar in sCW hydrolysate (\%)} = \frac{\text{mass of free sugar (mg)}_{t=60 \text{ min}}}{\text{mass (mg) of pea fiber soluble polysaccharides}} \times 100 \quad (\text{Eq. 6.1})$$

where,  $(\text{free sugar})_{t=60 \text{ min}}$  is the mass of an individual sugar in the free form that is present in the hydrolysate after 60 min of reaction, and  $(\text{pea fiber soluble polysaccharides})$  is the initial mass of pea fiber soluble polysaccharides (3000 mg) loaded into the 600 mL reactor. Also, the percentage of free sugars that were recovered in the retentate and permeate resulting from the membrane purification were determined according to Eq. (6.2).

$$\text{Free sugar recovery (\%)} = \frac{\text{mass of free sugar (mg) in retentate or permeate fraction}}{\text{mass (mg) of initial total free sugar in the feed}} \times 100$$

(Eq. 6.2)

where, (free sugar) is the mass of an individual sugar in free form that was retained as part of the retentate or the mass of an individual sugar that passed through to the permeate, and (Total free sugar in the feed) is the initial mass of an individual sugar in free form that was present in the sCW hydrolysate (pooled sample) fed to the ultrafiltration unit.

### 6.2.3.3 Neutral oligosaccharides analysis

The sCW hydrolysate obtained from pea fiber soluble polysaccharides using the 600 mL reactor vessel (pooled sample) as well as the hydrolysate previously obtained using the 100 mL reactor vessel (Chapter 5, Section 5.2.4.1) were analyzed for neutral oligosaccharides by HILIC on an Agilent 1200 Series HPLC system (Agilent, Santa Clara, CA, USA) equipped with an Agilent 1200 ELSD detector. The methodology described in Chapter 4 (Section 4.2.3.4) was followed with some modifications. As such, the separation of oligosaccharides was carried out at 40°C and a flow rate of 0.8 mL/min for 40 min. The composition of mobile phases was not altered where (A) was 80:20 (v/v) acetonitrile/water with 0.2% triethanolamine (TEA), and (B) was 30:70 (v/v) acetonitrile/water with 0.2% TEA. However, the elution gradient was modified as follows: 0-20 min, linear from 10 to 70% B; 20-20.1 min, linear from 70 to 10% B; and 20.1-30 min, isocratic 10% B for column re-equilibration. Also, the injection volume was set to 10 µL, and malto-oligosaccharides (2 – 6 DP) were used as standards for identification and quantification. The percentage of neutral oligosaccharides present in the sCW hydrolysate was quantified according to Eq. (6.3).

$$\text{Neutral oligosaccharides (\%)} = \frac{\text{mass of } \sum(2 \text{ to } 6 \text{ DP) oligosaccharides}_{t=60 \text{ min}}}{\text{mass of pea fiber soluble polysaccharides}} \times 100$$

(Eq. 6.3)

where,  $\sum(2 \text{ to } 6 \text{ DP oligosaccharides})_{t=60 \text{ min}}$  is the sum of individual mass of oligosaccharides that are present in the hydrolysate after 60 min of reaction, and (pea fiber soluble polysaccharides) is the initial mass of pea fiber soluble polysaccharides (3000 mg) loaded into the 600 mL reactor.

## 6.2.4 Drying of soluble pea fiber-derived oligosaccharides

### 6.2.4.1 Preparation of dried powders

The pea fiber hydrolysate obtained from the reactor (pooled sample) that contained the soluble pea fiber-derived oligosaccharides was directly subjected to drying by spray-, freeze- and PGX-drying methods. The pooled sample was not purified by ultrafiltration as its amount was limited and the volume needed for the drying processes was large. In addition, the available limited quantity of the dried polysaccharides obtained by sCW extraction from pea fiber substrate prevented the generation of more sCW hydrolysate for purification and drying.

#### 6.2.4.1.1 Spray drying

Spray drying was explored as a potential method to dry the sCW hydrolysate rich in oligosaccharides into a powder form. Spray drying process was carried out based on the methodology and parameters reported by Wrzosek et al. (2013). Briefly, the sCW hydrolysate (492 mL) with a total solids content of 1.07% was pumped into a SD-06A Spray drier (Lab plant, Filey, North Yorkshire, UK) at 5 rpm, corresponding to a feed flow rate of 280 mL/h. The air inlet and outlet temperatures were set to 125°C and 65°C, respectively. The drying air speed was 4.3 m/s. After 2 h of spray drying, the collected powder was removed from the collection vessel and stored

frozen at -18°C for further physical and thermal characterization. The spray drying process is summarized in Fig. 6.2.

#### **6.2.4.1.2 Pressurized Gas eXpanded liquid (PGX) drying**

PGX drying was explored to obtain a dry powder rich in pea fiber-derived oligosaccharides. A modified laboratory-scale Thar SFE 500 unit (Waters, Milford, MA, USA) equipped with a 500 mL collection vessel was used. The drying process was carried out according to the methodology previously described by Couto et al. (2020), with some modifications. As such, a reverse osmosis membrane SG (GE Osmonics Inc., Minnetonka, MN, USA) with a covalently cross-linked structure, that was previously shown to withstand SC-CO<sub>2</sub> processing conditions (Akin and Temelli, 2012), was placed at the bottom of the collection vessel to aid with the retention of the precipitated particles (MW < 1.7 kDa) throughout the PGX drying process.

Briefly, the PGX unit was assembled including the collection vessel, then heated up to 40°C and pressurized to 100 bar by pumping CO<sub>2</sub> and ethanol at flow rates of 10 g/mL and 30 g/mL, respectively. Next, the soluble pea fiber hydrolysate (492 mL) was pumped into the system at a flow rate of 10 g/mL together with ethanol and CO<sub>2</sub>, maintaining a mass flow rate ratio of 1: 3: 1. Once the complete volume of the feed solution was delivered, the aqueous feed pump was stopped and ethanol and CO<sub>2</sub> were pumped for approximately 1 h more to ensure water removal from the collection vessel. Then, the ethanol pump was stopped, and only CO<sub>2</sub> was pumped at an increased flow rate of 40 g/mL for 30 min for ethanol removal. Finally, the PGX unit was cooled down, slowly depressurized and the dry sample was removed from the collection vessel and stored frozen at -18°C for further analysis.

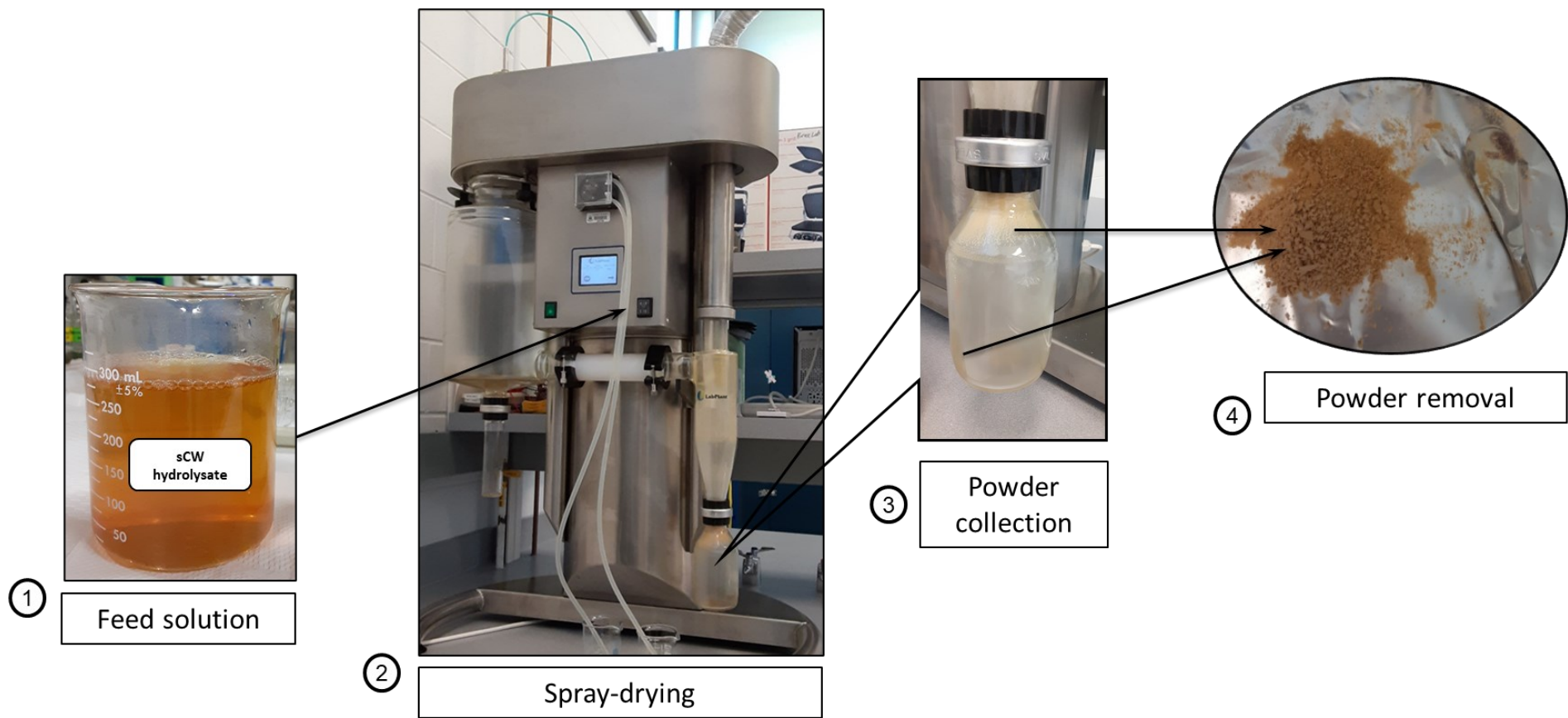


**Fig. 6.2.** Scheme of the spray drying process of the soluble pea fiber sCW hydrolysate

### **6.2.4.1.3 Freeze drying**

The sCW hydrolysate rich in pea fiber-derived oligosaccharides was also subjected to freeze drying to obtain a dry powder by sublimation of the freezable water present in the hydrolysate. Briefly, 200 mL of sCW hydrolysate were frozen at  $-18^{\circ}\text{C}$  for 24 h and further freeze dried using a Labconco FreeZone 6 L freeze dry system (Labconco, Kansas City, MO, USA) set at  $-46^{\circ}\text{C}$  and  $6.4 \times 10^{-5}$  bar (48 mTorr) for 3 days. Finally, the dried powder was collected in a glass container and stored frozen at  $-18^{\circ}\text{C}$  for further characterization.

### **6.2.4.2 Characterization of hydrolysate powders**

#### **6.2.4.2.1 Morphology and water activity**

The influence of the type of drying technique on the morphology of the obtained dried powders was observed using a scanning electron microscope ZEISS EVO 10 (Carl Zeiss, Oberkochen, Jena, Germany). First, as powder samples were not conductive, they were deposited as a thin layer on the carbon tabs of SEM pin stubs for gold coating. Then, SEM pin stubs containing the gold-coated samples were placed inside the SEM chamber at  $2.25 \times 10^{-6}$  mbar and subsequently scanned with a 15 kV electron beam. The images were collected with a secondary electron detector at magnifications of 2000, 5000 and 10,000x.

Water activity ( $a_w$ ) of the dried powders was measured using a water activity meter (AQUALAB 4TE, METER Food, Pullman, WA, USA). The water activity meter was calibrated at  $25^{\circ}\text{C}$  using a 13.41 mol/kg of LiCl in  $\text{H}_2\text{O}$  verification standard of 0.250  $a_w$ , prior to sample measurements.

#### **6.2.4.2.2 Differential scanning calorimetry analysis**

The thermal transitions (i.e. glass transition, melting and decomposition) of the dried powders were analyzed by differential scanning calorimetry (DSC) to determine whether the type of drying

technique had an effect on them. The analysis was carried out using a differential scanning calorimeter (Q100, TA Instruments, New Castle, DE, USA) following the methodology described by Combo et al. (2013), with some modifications. Briefly, for sample preparation, 5 to 10 mg of the corresponding dried powders were loaded into the DSC aluminium pans and then hermetically sealed with the lid using a pan sealing press. Then, samples were subjected to a heating cycle from 25°C to 300°C at a heating rate of 5°C/min. The data analysis was done using the TA Universal Analysis software (TA Instruments, New Castle, DE, USA).

#### **6.2.4.2.3 X-ray diffraction analysis**

X-ray diffraction (XRD) analysis was performed on the dried powders to investigate whether the type of drying method had an influence on their microstructure and crystallinity. The analysis was performed using a Rigaku Ultima IV diffractometer (Rigaku Corporation, Tokyo, Japan), equipped with a cobalt tube at 38 kV and 38 mA as the radiation source and a D/Tex Ultra detector with a Fe filter. The samples were scanned in a continuous mode within a range of 5 to 90° at 2°/min. The data were converted to .txt files with Jade MDI 9.6 software and plotted using Origin2019b (Academic) software.

### **6.3 Results and discussion**

#### **6.3.1 Production of soluble pea fiber-derived oligosaccharides**

##### **6.3.1.1 sCW hydrolysis scale-up and neutral oligosaccharides determination**

To evaluate the impact of the increase in reactor size on oligosaccharides production, heating and pressure profiles were recorded throughout the sCW hydrolysis process carried out in 100 mL (detailed experimental information presented in Chapter 5) and 600 mL reactor vessels. According to Fig. 6.3, heating profiles recorded from the 100 mL and 600 mL reactor vessels were similar, suggesting that a homogeneous well stirred reaction occurred in both cases as no abrupt

temperature oscillation was exhibited for the 600 mL vessel. The similarity of heating profiles was also indicative of an adequate temperature control from the temperature controller as the same PID parameters were kept constant for all the runs regardless of the volume of the reactor used. As expected, however, there was an increase in the come-up time of 7 min for the 600 mL reactor compared to that of the 100 mL reactor. As such, for the 600 mL reactor, the average come-up time to reach  $155.40 \pm 0.85^\circ\text{C}$  was  $13.66 \pm 0.58$  min, whereas for the 100 mL reactor the average come-up time to reach  $151.20 \pm 0.05^\circ\text{C}$  was registered as  $6.75 \pm 0.35$  min.

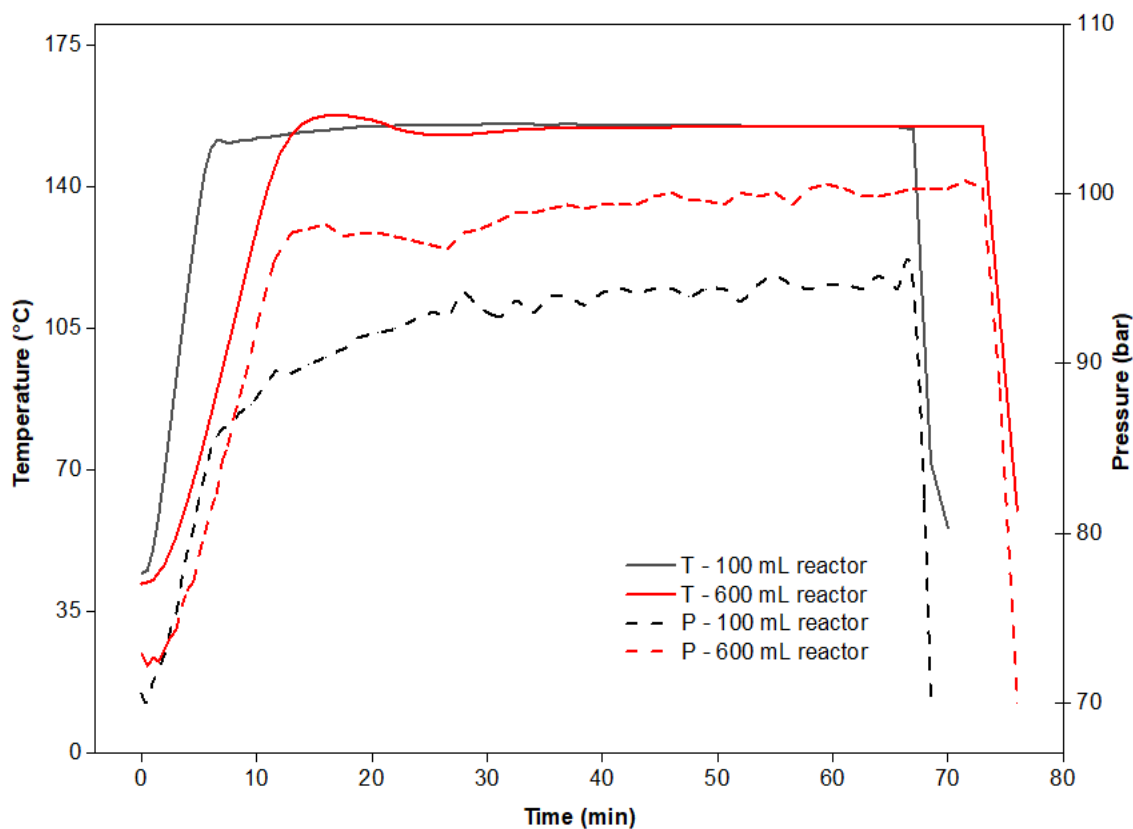


**Fig. 6.3.** Heating and pressure profiles of the Parr 4590 system set at  $155^\circ\text{C}/100$  bar up to 80 min using reactor vessels of 100 mL and 600 mL volume.

As the volume of the reaction solution increased from 40 mL in the 100 mL reactor to 300 mL in the 600 mL reactor, an increase of 7 min in the come-up time was considered acceptable for a 7.5-fold increase in the volume of the reaction solution. In addition, the pressure profile recorded for the 100 mL reactor showed that the system did not reach the set pressure of 100 bar similar to that of the 600 mL reactor. The average pressure in the 100 mL reactor was 91 bar, which suggests that the initial pressurization to 70 bar was not enough to reach the set pressure of 100 bar; however, for the 600 mL reactor, the initial pressurization to 72 bar was adequate to reach 100 bar. Although the difference in the initial pressure was 2 bar, it had an effect on the final pressure of the system, possibly due to the expansion of water with temperature (volume expansion coefficient) (Dinçer and Zamfirescu, 2006). Therefore, the additional pressure generated by heating 300 mL of the aqueous solution in 600 mL reactor was higher than the pressure generated by heating 40 mL of the same solution in a 100 mL reactor.

The impact of the scale-up on the chemical composition of the resulting hydrolysates was evaluated based on the yield of 2-6 DP gluco-oligosaccharides as well as the yield of individual gluco-oligosaccharides. Results of the HILIC-ELSD analysis of sCW hydrolysates showed that the total yields of 2-6 DP gluco-oligosaccharides produced in the 100 mL and 600 mL reactors were 17.1% and 14.9%, respectively (Fig. 6.4). This difference in yield could be attributed to the 7 min increase in the come-up time for the 600 mL reactor compared to the 100 mL reactor. The extended come up time could have favored further hydrolysis of oligosaccharides into monosaccharides, leading to a lower yield of gluco-oligosaccharides in the case of 600 mL reactor. In addition, Fig. 6.4 shows the yield of individual gluco-oligosaccharides present in the sCW hydrolysates obtained in the 100 mL and 600 mL reactor vessels. According to Fig. 6.4, the overall distribution of individual gluco-oligosaccharides in both hydrolysates exhibited the same trend,

where 2-4 DP gluco-oligosaccharides were predominant, followed by 6 DP and 5 DP gluco-oligosaccharides. However, the sCW hydrolysate produced in the 600 mL reactor exhibited slightly lower yields of individual gluco-oligosaccharides compared to the hydrolysate produced in the 100 mL reactor.

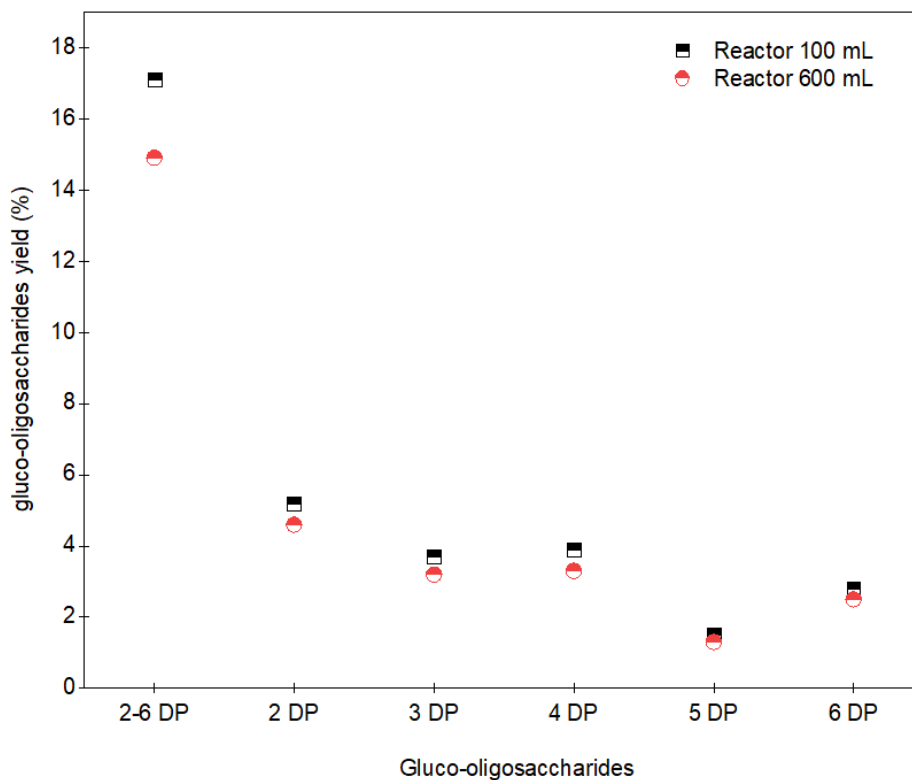


**Fig. 6.4.** Yield of individual and total gluco-oligosaccharides present in the sCW hydrolysates obtained at 155°C/100 bar/60 min using a reactor vessel of 100 mL (black square) and 600 mL (red circle).

Based on the above, it can be concluded that the scale-up process allowed obtaining the desired product at a larger scale without compromising its yield or chemical composition. Therefore, it can be hypothesized that the 7 min increment of come-up time for the hydrolysis reaction in the 600 mL vessel did not randomly alter the hydrolysis mechanism as the slight reduction in the total

yield of 2-6 DP gluco-oligosaccharides was due to the reduced yield of individual gluco-oligosaccharides, which took place following an orderly fashion.

### **6.3.1.2 Characterization of sCW hydrolysate**

#### **6.3.1.2.1 Molecular weight distribution and free sugars analyses**

The molecular weight distribution profiles of the pea soluble fiber hydrolysate obtained at 155°C/100 bar/60 min within the 600 mL reactor and the xylo-oligosaccharide standard were determined by HPSEC-RID analysis for comparison purposes. According to the chromatogram shown in Fig. 6.5, sCW hydrolysate was comprised of various low molecular weight fragments as indicated by the well-defined peak eluted at 17.6 min that corresponded to compounds of 1.38 kDa molecular weight, and the peaks eluted at 18.2 min and 19.2 min, which corresponded to compounds with a molecular weight < 1 kDa. The molecular weights of the later peaks were not defined as they were eluted beyond the permeation limit (1 kDa) of the column. Conversely, the elution profile of the xylo-oligosaccharide standard showed two main peaks at 18.7 and 19.2 min, which corresponded to compounds with a molecular weight < 1 kDa. Based on the chromatograms in Fig. 6.5, sCW hydrolyte was indeed comprised of low molecular weight fragments including oligosaccharides.

The amounts of free sugars present in the sCW hydrolysate were determined for further purification purposes. The HILIC-RID analysis of the sCW hydrolysate showed a total free-sugars (Arb+Xyl+Rha) content of 14.7%, where arabinose was the major component (7.8%), followed by rhamnose (3.7%) and xylose (3.2%). These results suggest that a considerable amount of monosaccharides was also generated during the sCW hydrolysis of the branched pea fiber soluble polysaccharides. In fact, as indicated in Chapter 5 (Section 5.3.2.1.3), the neutral sugar composition of pea fiber soluble polysaccharides (non-starch polysaccharides) include not only

arabinose, xylose and rhamnose but also galactose and glucose. Therefore, the total free sugars percentage reported here could be underestimated as galactose and glucose could not be quantified using the current HILIC method due to the peak overlap.

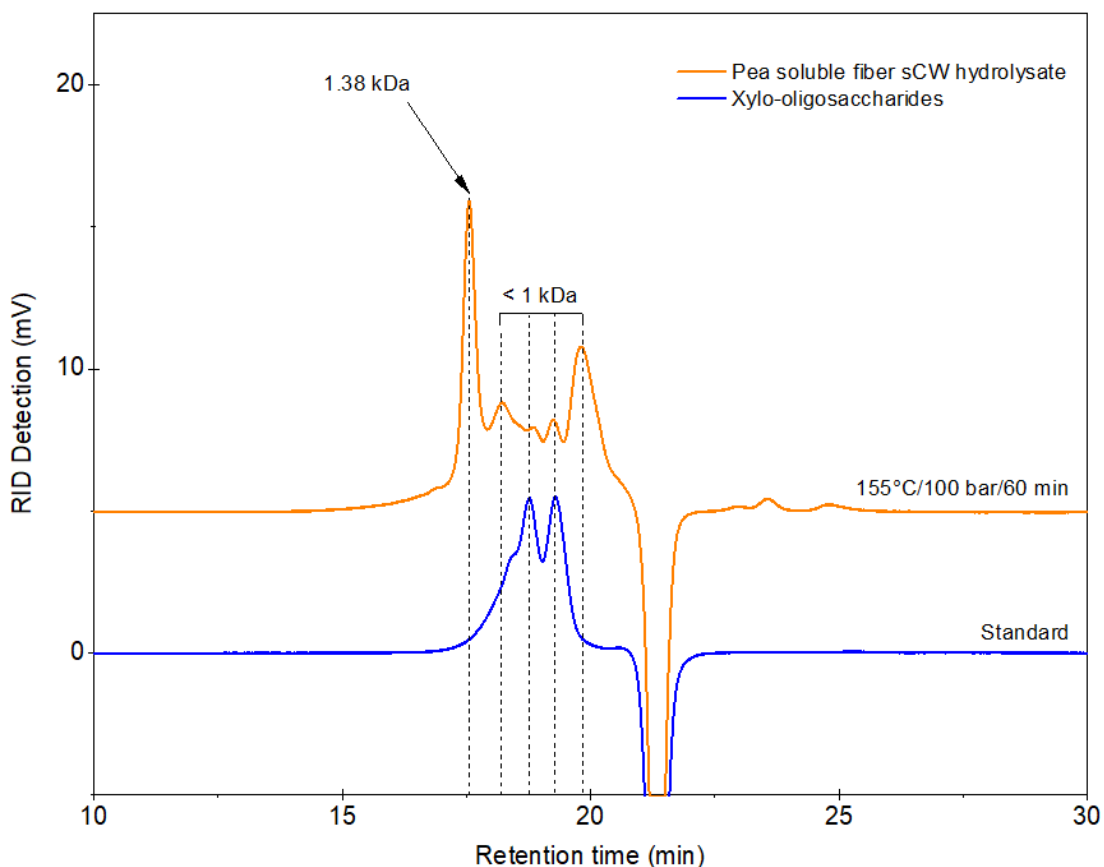


**Fig. 6.5.** HPSEC-RID elution profiles of pea soluble fiber hydrolysate obtained at 155°C/100 bar/60 min using a reactor vessel of 600 mL (orange), and xylo-oligosaccharide standard (blue).

Based on the molecular weight distribution of the soluble pea fiber sCW hydrolysate, membrane filtration was used next as the first step for monosaccharides removal and concentration of soluble pea fiber-derived oligosaccharides.

### 6.3.1.3 Purification

To evaluate the efficiency of the tangential-flow ultrafiltration process (1 kDa membrane, 40°C, 7 h) for monosaccharides removal from the sCW hydrolysate, the free sugar recovery was determined for the resulting retentate and permeate. According to Fig. 6.6, the individual sugar recovery in the retentate was lower than that in the permeate as expected. The recovery of rhamnose, xylose and arabinose in the retentate was 49.2%, 42.1% and 38.3%, respectively. However, the total sugars (Rha+Xyl+Ara) recovery in the retentate and permeate was 40.3% and 51.8%, respectively. Therefore, it can be inferred that due to fouling effect, approximately 60% of monosaccharides were removed from the hydrolysate. In addition, among the individual sugars, total arabinose recovery was lower than those of xylose and rhamnose. As such, the total arabinose recovery (permeate + retentate) was 85.8% and not 100% as for the other two sugars, suggesting that sugars can interact differently with the ultrafiltration PES membrane surface. Also, it can be inferred that arabinose was more prone to be adhered onto the PES membrane surface compared to xylose and rhamnose, inducing membrane fouling and therefore loss of arabinose.

The physical aspect of the retentate and permeate obtained by ultrafiltration of pea soluble fiber sCW hydrolysate using a 1 kDa membrane for 7 h is also shown in Fig. 6.6, where the retentate rich in oligosaccharides was darker in color compared to that of the permeate rich in monosaccharides.

Although the available Minimate tangential-flow ultrafiltration system aided concentration of oligosaccharides in the retentate, complete removal of monosaccharides as targeted was not possible, which is a limitation of this ultrafiltration system.

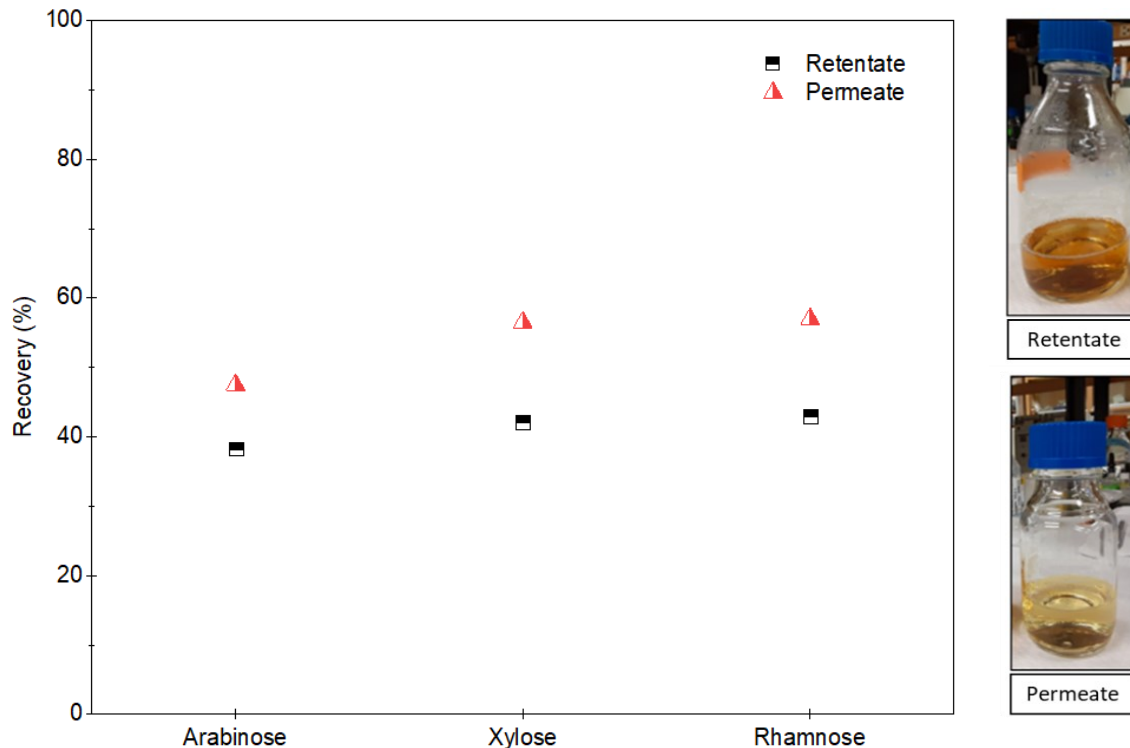


**Fig. 6.6.** Recovery of free sugars in the retentate and permeate obtained by ultrafiltration of pea soluble fiber sCW hydrolysate using a 1 kDa membrane for 7 h.

### 6.3.2 Drying of soluble pea fiber-derived oligosaccharides

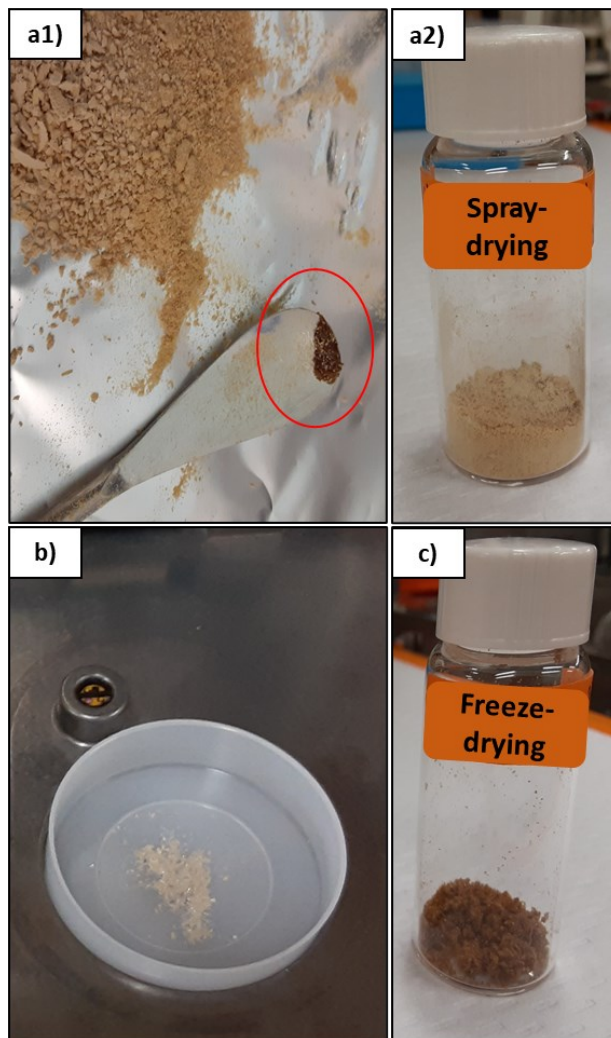
#### 6.3.2.1 Preparation of dried powders

Fig. 6.7 shows the physical appearance of the dried powders obtained from the soluble pea fiber sCW hydrolysate by spray drying, freeze drying and PGX drying. According to Figs. 6.7a1-6.7a2, spray drying of the sCW hydrolysate produced a light brown expanded powder (major fraction) as well as a dark brown viscous and sticky liquid (minor fraction) deposited at the bottom of the collection vessel, suggesting that spray drying temperature favored water evaporation from oligosaccharides and slightly higher molecular weight compounds while monosaccharides formed a viscous liquid due to their low glass transition temperatures. For example, Simperler et al. (2006) reported glass transition temperatures of 23°C, 60°C and 107°C for amorphous microstructures of

glucose, sucrose, and trehalose, respectively. Also, Syamaladevi et al. (2015) reported glass transition temperatures of 34.5°C, 78.5°C and 128.8°C for amorphous glucose, maltose and maltotriose, respectively. Conversely, freeze-drying process (Fig. 6.7c) led to a darker and more compact powder compared to that of spray drying (Fig. 6.7a2). Such color variation could be due to the formation different morphologies. For example, spray-drying process can favor the formation of expanded and aerated microstructures due to atomization and hot air contact leading to powders with bigger surface area and lighter in color, whereas freeze-drying process can induce the formation of more compact microstructures due to the slow freezing step (bigger ice crystal formation) and drying at reduced pressure (sublimation of ice crystals) leading to powders with smaller surface area, minimally aerated and darker in color (Assegehegn et al., 2019). PGX drying also led to an expanded powder (Fig. 6.7b) similar to that of spray drying, suggesting that the spraying step included in both processes could have favored the formation of less compact structures. However, the powder obtained by PGX drying was lighter in color, indicating that the color compounds could have been solubilized in the ternary mixture of CO<sub>2</sub>+ethanol+water used in the process and removed.

In terms of yield, substantial differences were apparent between each drying technique. The highest drying yield was obtained by freeze drying (87.8%), followed by spray drying (23%). This variation of yield could be due to powder stickiness and adherence on the spray drying chamber, cyclone, and collection vessel, making it difficult to collect all the material, which was not an issue during the freeze-drying process. Similarly, Wrzosek et al. (2013) reported a yield of 16% after spray drying of a fructo-oligosaccharide mixture (also containing sucrose and glucose) at optimum conditions of inlet temperature of 120°C, feed flow rate of 1.4 mL/min, and air flow rate of 100

L/h. The reported low yield was attributed to the high stickiness of the resulting product and its further deposition on the walls of the drying cylinder, which hindered its recovery.



**Fig. 6.7.** Dry powders obtained from soluble pea fiber sCW hydrolysate (containing pea fiber-derived oligosaccharides) using a1-a2) spray drying, b) PGX drying, and c) freeze drying.

The yield was the lowest (2.1%) for PGX drying. Factors such as the low molecular weight of oligosaccharides and their solubility in  $\text{CO}_2$ +ethanol+water ternary mixture as well as the small size of the precipitated particles and their poor retention on the RO membrane located at the bottom of the collection vessel could have contributed to the low yield as it was not possible to recover

the precipitated particles from various parts of the system and some were lost in the exhaust stream. PGX drying has been successfully used to obtain powders with increased surface area of high molecular weight water-soluble polysaccharides like sodium alginate (Liu, 2019) and gum arabic (Couto et al., 2020) due to the action of CO<sub>2</sub>+ethanol in the gas-expanded liquid region as anti-solvent. In the present study, however, low molecular weight saccharides soluble in water+ethanol were used for the first time to explore the scope of the PGX-drying technology. For this purpose, an optimized operating condition adopted from a previous study was used (aqueous solution:ethanol:CO<sub>2</sub> mass flow ratio of 1:3:1) (Liu, 2019) where CO<sub>2</sub>+ethanol act as an antisolvent to precipitate the polysaccharides but as a solvent for water removal. Therefore, based on the extremely low yield, some modification can be suggested to improve the powder recovery, such as increasing the solid content of the aqueous solution as well as modifying the flow rate ratios to change the composition of the ternary mixture to maximize the precipitation of the oligosaccharides, possibly by increasing the level of ethanol as the solubility of saccharides decrease in concentrated ethanol solutions (Bouchard et al., 2008). Also, different types of membranes like organic-inorganic hybrid membranes can be tested to improve the retention of precipitated particles (Sarrade et al., 2002).

### **6.3.2.2 Characterization of powders**

#### **6.3.2.2.1 Morphology and water activity**

Fig. 6.8 shows the SEM images of the dry powders from the soluble pea fiber sCW hydrolysate obtained by spray drying, freeze drying, and PGX drying. According to Fig. 6.8a1, the powder produced by spray drying was comprised of particles of heterogeneous morphology but mostly spherical shaped particles with a wide range of particle sizes.

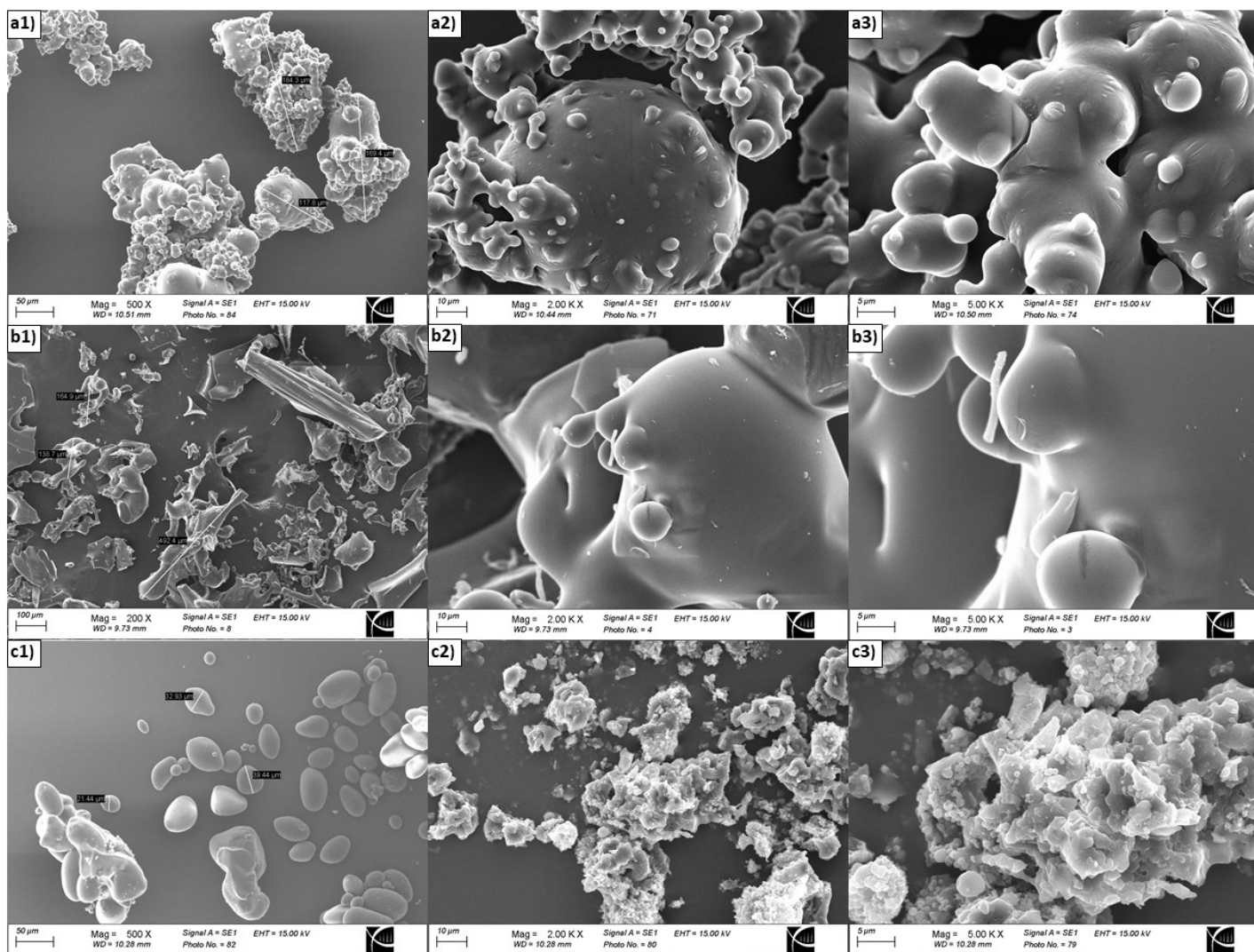


**Fig. 6.8.** Scanning electron microscopy images of dry powders from pea fiber-derived oligosaccharides obtained by a) spray drying, b) freeze drying, and c) PGX drying. Scale bars represent 50  $\mu\text{m}$  in a1) and c1), 100  $\mu\text{m}$  in b1), 10  $\mu\text{m}$  in a2-c2), and 5  $\mu\text{m}$  in a3-c-3).

At a higher magnification, Fig. 6.8a2-9a3, the sticky nature of the spray dried powders can be inferred as particles were not separated but self-agglomerated (particle cohesion). However, some vacancies in between the agglomerated particles were also observed, which can explain its more voluminous and light weight appearance (Fig. 6.8a2) compared to the powder obtained by freeze-drying (Fig. 6.8c). Particle cohesion and particle adhesion on the dryer walls have been reported during spray drying of sugars and sugar-containing foods, such as lactose (Chiou et al., 2008), sugarcane juice (Nishad et al., 2017) and fruit juices (Goula and Adamopoulos, 2010; Muzaffar, 2015; Papadakis et al., 2007; Truong et al., 2005). Low glass transition temperatures associated to their low molecular weight and amorphous microstructure as well as to hygroscopicity have been attributed to such phenomenon (Boonyai et al., 2004; Jaya and Das, 2009). Conversely, the powder obtained by freeze drying (Fig. 6.8b1) was characterized by particles with very irregular morphology, including sharp edges, and various sizes. Such heterogeneity of the sample could be due to the irregular ice crystal formation during the freezing step, which later form the pores upon sublimation, and the lack of a dispersion step, so that particles did not have a uniform shape pattern. In addition, Fig. 6.8b2-b3 show the highly sticky nature and the compact microstructure of the powder as their particles were very close and fused to each other, forming clumps with little space remaining between them. Likewise, stickiness or loss of structure of freeze-dried sucrose and carbohydrate solutions has been reported due to plasticization of particles surface by water (Boonyai et al., 2004; te Booy et al., 1992; Tsourouflis et al., 1976). In Fig. 6.8c1-c3, however, individual round shaped particles as well as defined structures made of these small individual particles were apparent for the PGX-dried powder. Also, it can be observed that particles were not very attached to each other at the point of fusion as was the case for particles obtained by freeze drying. Overall, PGX-dried powder exhibited an expanded microstructure with the lowest

stickiness, possibly due to good dispersion of the solution through the co-axial nozzle and removal of monosaccharides in the exhaust stream. SC-CO<sub>2</sub>+ethanol drying of monosaccharides like glucose has been a challenge due to its low glass transition temperature and solubility in water+ethanol (Bouchard et al., 2008).

Water activity ( $a_w$ ) values of the powders obtained by freeze drying, spray drying and PGX drying were 0.3702, 0.3885 and 0.4067, respectively. Although  $a_w$  values were similar for the three powders, SEM analysis provided some insights that suggest different microstructures among the powders, particularly, of the freeze-dried product.

#### **6.3.2.2.2 Differential scanning calorimetry analysis**

Fig. 6.9 shows the thermal transitions of the dried powders when heated from 25°C to 300°C at 5°C/min under nitrogen gas. Overall, it can be observed that powders obtained by spray drying, freeze drying, and PGX drying did not exhibit a glass transition step but melting/decomposition endotherms. Although sugars are commonly found as crystalline structures, they can also exhibit amorphous structures when subjected to cooling and heating cycles or to rapid removal of solvent when they are in solution (i.e. spray drying and freeze drying) (Lappalainen, 2010; Saleki-Gerhardt and Zografí, 1994; Simperler et al., 2006; Booy et al., 1992). When sugars are in the amorphous state, they lack crystal order, and their molecular mobility and kinetic energy are higher compared to that of the crystalline state (Lappalainen, 2010). As such, upon heating, the DSC profile of amorphous sugars is characterized by a glass transition endotherm, followed by a crystallization exotherm and a thermodynamic melting endotherm (Saleki-Gerhardt et al., 1994).

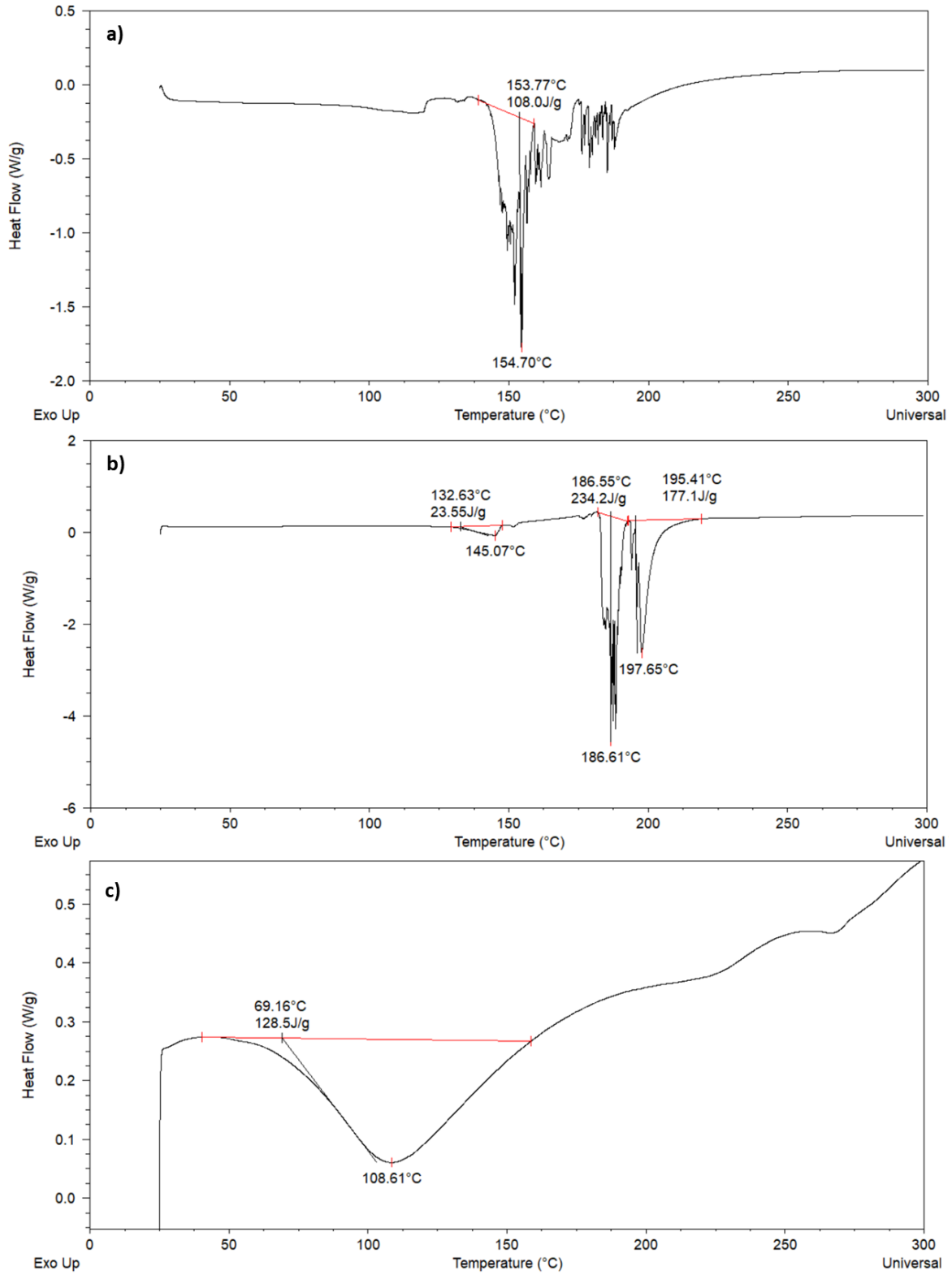


**Fig. 6.9.** DSC thermograms of dried sCW hydrolysates obtained by: a) freeze drying, b) spray drying, and c) PGX drying.

Thus, the absence of glass transition endotherm and crystallization in the DSC thermograms displayed in Figs. 6.9a-c, suggests that either the dried pea fiber derived-oligosaccharides and monosaccharides have crystalline structures or that amorphous sugars and saccharides had a  $T_g < 25^\circ\text{C}$ , which was out of the temperature range used for the present DSC analysis, or that such saccharides were not able to crystallize due to the presence of a mixture of components with a wide range of molecular weights. In fact, te Booy et al. (1992) found that crystallization of amorphous sucrose was hindered by dextran and buffer salts (dibasic sodium phosphate and citric acid). Likewise, Combo et al. (2013) did not report a glass transition temperature for freeze-dried sugar beet pectin-derived oligosaccharides obtained by enzymatic hydrolysis. A hidden glass transition due to the sample complexity was hypothesized in that case (Combo et al., 2013).

The thermograms of powders obtained by freeze drying and spray drying showed multiple endothermic peaks (Figs. 6.9a-b) with enthalpies in the range of 23.55 J/g to 177.1 J/g, that represent the loss of crystalline structure due to thermodynamic melting and/or apparent melting. Apparent melting refers to the loss of crystalline structure due to chemical processes (i.e. chemical interactions, desolvation, dissociation, thermal decomposition) (Lee et al., 2011). If thermodynamic melting of pea fiber-derived mono/oligosaccharides was the case, multiple endothermic peaks could represent melting of crystalline structures of mono/oligosaccharides, which possibly exhibited different crystal morphologies (polymorphism). However, if apparent melting had occurred, multiple endothermic peaks could represent thermal degradation of different monosaccharides (arabinose, xylose and rhamnose) as well as 2-7 DP gluco-oligosaccharides. Hence, multiple endothermic peaks could also represent a combination of both thermodynamic and apparent melting as the corresponding temperatures can be close to each other. Saavedra-Leos et al. (2012), for example, reported glucose (amorphous structure) melting and degradation at

temperatures of 159°C and 225°C, respectively. Thus, endotherms in the DSC thermogram of the freeze-dried sample (Fig. 6.9a) with onset temperatures higher than 153.77°C and endotherms for the spray dried sample (Fig. 6.9b) with onset temperatures higher than 186.55°C could correspond to thermodynamic melting and thermal degradation of mono- and oligo-saccharides. Based on the information provided by the DSC thermograms, it can be inferred that the powder obtained via spray drying could be more stable than that obtained by freeze drying as its onset temperatures and enthalpy values of endotherms were higher compared to those of the freeze-dried powder.

Conversely, the thermogram of the powder obtained by PGX drying exhibited a different trend compared to those of freeze drying and spray drying as only one broad endothermic peak with an onset temperature of 69.16°C was apparent. As the onset temperature of the endotherm was relatively low compared to the onset temperature reported for thermodynamic melting of monosaccharides like fructose (136°C) (Lee et al., 2011), it is more likely that such an endotherm could represent apparent melting due to chemical interactions and desolvation. Bouchard et al. (2008), for example, reported that at temperatures between 65°C and 75°C, release of water, CO<sub>2</sub> and ethanol was detected in supercritical-dried (SC-CO<sub>2</sub>+ethanol) di- and tri-saccharides by thermogravimetric analysis coupled with FT-IR. Then, the endotherm in Fig. 6.9c could indicate possible desolvation. However, thermogravimetric analysis coupled with gas chromatography can be used to confirm such phenomenon. However, it should be considered that the thermodynamic melting temperatures of the individual saccharides can be influenced by the presence of other components, water, salts, etc. present in the complex mixture under consideration. In addition, the unsteady baseline in Fig. 6.9c could represent conformational energy associated to less stable molecular orientations. Heating and cooling cycles at different heating rates could be included in

the DSC analysis to aid relaxation of molecules into a minimum energy configuration and to obtain a more linear baseline, and therefore more accurate thermal information.

### 6.3.2.2.3 X-ray diffraction analysis

Fig. 6.10 shows the XRD diffraction pattern of sCW hydrolysate powders obtained by spray drying, freeze drying and PGX drying. According to Fig. 6.10, the powders obtained by spray drying and freeze drying exhibited a similar XRD pattern, with broad peaks at  $13^\circ$  and  $21^\circ$ , suggesting that semi-crystalline microstructures were formed during such drying processes.

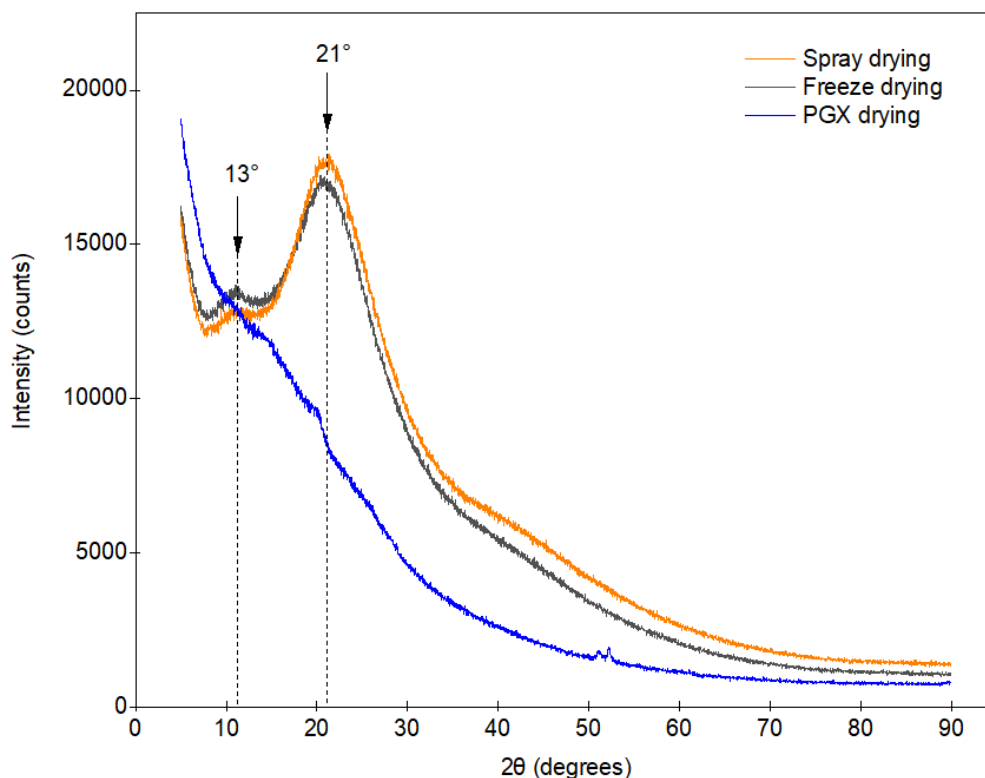


**Fig. 6.10.** XRD diffraction pattern of sCW hydrolysate powders obtained by spray drying (orange), freeze drying (black) and PGX drying (blue).

A fast removal of water from sprayed droplets during spray drying or water freezing during freeze drying could have facilitated interactions between the solutes of low molecular weight and their organization to some extent, leading to semicrystalline structures. Conversely, no peak was

apparent in the XRD pattern of the powder obtained by PGX drying, indicating its amorphous microstructure. As oligosaccharides are comprised of saccharides with different degrees of polymerization and structure, the literature lacks information about XRD patterns of oligosaccharides for comparison purposes. In addition, the microstructure variation between powders obtained by spray and freeze drying compared to PGX drying could rely on their saccharide composition. Powders from spray and freeze drying, for example, were expected to have approximately 14.1% of total free mono sugars as in the initial feed, whereas in the powder obtained by the PGX process the percentage of monosaccharides was expected to be low due to their solubility in aqueous ethanol and removal in the exhaust stream. As mono sugars can be more prone to crystallize than higher molecular weight compounds, powders obtained by spray and freeze drying exhibited a more organized structure compared to that of PGX drying. The powder from PGX drying could represent the fraction of saccharides with higher molecular weight and low solubility in ethanol that were precipitated very fast with no time for organization, leading to an amorphous microstructure.

#### **6.4 Conclusions**

In this study, a bench level scale-up of the process for the sCW production of soluble pea fiber-derived oligosaccharides was carried out as well as their further membrane purification and powder formation by spray-, freeze- and PGX-drying techniques. The scale-up process was successfully achieved as a product with the desired chemical composition (2-6 DP gluco-oligosaccharides) was obtained at a larger scale (600 mL reactor) without compromising its yield (14.9%). In addition, the use of a tangential-flow ultrafiltration system equipped with a 1 kDa PES membrane allowed removal of 60% of monosaccharides from the pea soluble fiber hydrolysate, leading to a fraction enriched in oligosaccharides. Further drying of the pea soluble fiber

hydrolysate showed that according to the drying method applied, powders with different color, microstructure and thermal behavior can be obtained. Drying yields varied as 87.8%, 23% and 2.1% for freeze drying, spray drying, and PGX drying, respectively. Spray drying at inlet and outlet temperatures of 125°C and 65°C, respectively, led to a powder with semicrystalline microstructure whereas PGX drying resulted in a powder in amorphous form. Among the drying methods tested, spray drying led to a powder with the highest melting and decomposition temperatures. These findings provide an insight about the feasibility of sCW technology scale-up for the production of oligosaccharides from agro-industrial residues at a relatively mild temperature with the use of citric acid as the acid catalyst as well as the possibility to continue exploring the membrane and drying technologies for purification and drying of sCW hydrolysates from various biomass.

## Chapter 7: Conclusions and recommendations

### 7.1 Summary of key findings

Subcritical water (sCW) technology uses pressurized liquid water at temperatures higher than its boiling point but below its critical temperature of 374°C to facilitate solvation and extraction of diverse bioactives from biomass as well as to act as a reaction media in acid-base catalyzed reactions. As the physicochemical properties of water vary in the subcritical region, its polarity, for example, can be tuned to target the solvation and extraction of either polar or non-polar compounds, which is advantageous as the use of conventional organic solvents and inorganic acids is avoided. Therefore, sCW has been considered as an eco-friendly and GRAS solvent for extraction and hydrolysis processes. In this PhD thesis research, sCW technology was used as an alternative method for the extraction and conversion of a co-product into value-added compounds like oligosaccharides. Canadian pea hull fiber was selected as a substrate of study as it is a co-product of industrial pea protein manufacture, which is currently underutilized. In addition, production of pea hull fiber-derived oligosaccharides was the target in this study as oligosaccharides are known for their prebiotic effect.

In an effort to minimize formation of toxic products resulting from undesired reactions that occur within the upper sCW temperature range required for biomass hydrolysis, the use of di- and tri-carboxylic acids under mild sCW conditions (125-155°C/100 bar) was investigated as homogeneous organic acid catalysts. However, before tackling the carboxylic acid-catalyzed sCW hydrolysis of the complex pea fiber substrate, sCW hydrolysis of model systems of linear polygalacturonic acid and branched rhamnogalacturonan was studied as a proof-of-concept. Next, a sequential approach based on sCW technology and the use of carboxylic acids was carried out for the extraction of soluble polysaccharides from pea fiber as well as their hydrolysis to obtain

oligosaccharides. Finally, the bench level scale-up of the process for the sCW production of pea soluble fiber-derived oligosaccharides as well their downstream processing was investigated.

The first study (Chapter 3) investigated the hydrolytic effect of aqueous citric and malic acids, and water at 125-135°C/100 bar on a model system of linear polygalacturonic acid. The hydrolysis of polygalacturonic acid into oligogalacturonides successfully occurred at either 125°C or 135°C regardless of the sCW reaction medium. The catalytic effect of aqueous carboxylic acids under sCW was not clearly evident due to the acidic nature of polygalacturonic acid as it contains ionizable carboxylic groups that could also be released in the sCW medium alone. However, the use of sCW technology to hydrolyze polygalacturonic acid into oligosaccharides as an alternative to inorganic acids in homogeneous acid catalysis was demonstrated. The highest yield of oligogalacturonides (41%) was obtained with aqueous citric acid at 135°C/100 bar within 30 min, which was higher than that reported in literature by fast sCW hydrolysis at temperatures higher than 180°C.

The hydrolytic pattern of polygalacturonic acid at sCW conditions was characterized by poly/oligogalacturonic acid intermediates with a degree of polymerization (DP) of 8-14 that were subsequently hydrolyzed to oligogalacturonides of 2-7 DP. Interestingly, the observed O-glycosidic bond cleavage pattern was similar to that reported for endo-polygalacturonase. A possible reaction mechanism and a kinetic model for sCW hydrolysis of linear polygalacturonic acid based on parallel and consecutive reactions were also proposed to facilitate future optimization of the reaction process.

The second study (Chapter 4) investigated the hydrolytic effect of aqueous citric and malic acids, and water at 125-155°C/100 bar on a more complex model system of branched rhamnogalacturonan from soybean. Hydrolysis of rhamnogalacturonan was clearly evident at

either 125°C/40 min or 135°C/20 min within the aqueous carboxylic acid medium. Aqueous carboxylic acids at either 125°C or 135°C showed a remarkable catalytic effect on rhamnogalacturonan hydrolysis compared to sCW alone, in contrast to their negligible enhancement effect on polygalacturonic acid hydrolysis compared to sCW alone (Chapter 3). The use of citric and malic acids under sCW conditions as an alternative to inorganic acids in homogeneous acid catalysis was also demonstrated for the hydrolysis of a branched pectic substrate like rhamnogalacturonan. In addition, temperature had a considerable effect on rhamnogalacturonan hydrolysis, where cleavage of neutral sugar residues from the side chains of rhamnogalacturonan was favored at 125°C, while scission of rhamnogalacturonan backbone was evident at temperatures higher than 135°C. For example, hydrolysis of rhamnogalacturonan at 135°C/100 bar/60 min with aqueous carboxylic acids led to compounds with a broad range of molecular weight ( $\leq 4.7$  kDa), including oligogalacturonides of 2 to 9 DP and galacto-oligosaccharides of 5, 8 and 10 DP. Also, diverse glycosidic bonds with different susceptibility to carboxylic acid-catalyzed hydrolysis were observed. Thus, the potential use of aqueous carboxylic acids under sCW conditions as an alternative to conventional processes that use alkali and acid treatments in combination with various enzymes to obtain rhamnogalacturonan-derived fragments and oligomers was also demonstrated. Finally, an overall mechanistic insight on rhamnogalacturonan sCW hydrolysis by aqueous carboxylic acids was proposed, considering the catalytic effect of aqueous carboxylic acids at mild sCW conditions.

Based on the results of the two model systems in the previous studies, the third study (Chapter 5) investigated the catalytic effect of aqueous citric and malic acids, and water at 125-155°C/100 bar on the hydrolysis of a real agro-industrial co-product. Pea fiber generated as a co-product of commercial pea protein production was selected for its conversion into oligosaccharides. The

starting pea fiber was comprised of starch, protein, and soluble and insoluble fibers. Pea soluble polysaccharides were successfully extracted with aqueous citric acid at mild sCW conditions (120°C/50 bar/30 min) prior to its further sCW hydrolysis into oligosaccharides. Pea soluble polysaccharides were mainly comprised of pectic compounds (17.4% galacturonic acid) and their molar sugar composition indicated the presence of rhamnogalacturonan-I and xylogalacturonan. The extraction of pectic polysaccharides from legume co-products using citric acid under sCW conditions as a GRAS solvent was demonstrated. In addition, similar to the rhamnogalacturonan sCW hydrolysis (Chapter 4), aqueous carboxylic acids at temperatures above 125 °C and 100 bar also showed a remarkable catalytic effect on the hydrolysis of pea soluble polysaccharides into oligosaccharides compared to sCW alone. As such, the highest yield of released gluco-oligosaccharides (2-6 DP) was 20.4% at 135°C/100 bar/120 min with citric acid. The main hydrolysis mechanism of pea soluble polysaccharides exhibited a stepwise pattern, where rhamnogalacturonan side chains were cleaved first followed by their breakdown into reduced molecular weight compounds and oligosaccharides, demonstrating the potential use of citric acid as a homogeneous catalyst for controlled hydrolytic cleavage of different glycosidic bonds present in complex pectic substrates like pea fiber.

The last study (Chapter 6) focused on the scale up of the process for the sCW production of pea soluble fiber-derived oligosaccharides at lab scale as well as on the downstream processing of oligosaccharides. Pea soluble fiber-derived oligosaccharides were successfully produced on a large-scale (600 mL reactor) as their chemical composition and yield were not compromised. Concentration of oligosaccharides by partial removal of monosaccharides was achieved by tangential-flow ultrafiltration. Conventional freeze drying and spray drying as well as PGX drying

led to pea soluble fiber-derived oligosaccharide powders with semicrystalline and amorphous microstructures, respectively.

In conclusion, these studies on the use of carboxylic acid-catalyzed sCW systems for the hydrolysis of pure model systems and complex pectic substrates have generated new fundamental and applied knowledge on the use of unconventional, nontoxic, and non-flammable pressurized fluid systems at mild sCW conditions for conversion of pectin-rich agro-industrial co-products into potential functional ingredients or dietary supplements. This approach was demonstrated for the case of obtaining novel oligosaccharides from the soluble fraction of the pea hull fiber with anticipated prebiotic effect and health benefits. As such, the use of carboxylic acid-catalyzed sCW systems were shown to be a feasible alternative to obtain oligosaccharides from legume co-products at relatively low temperatures compared to those of conventional hydrothermal treatments, minimizing further breakdown of sugars into toxic compounds, which is a limitation of treatments at high temperatures as reported in other studies. In addition, these systems facilitate the downstream processing of oligosaccharides as the resulting hydrolysates are expected to contain minimal levels of toxic degradation compounds due to side reactions and avoid the use of additional neutralization steps of inorganic alkalis or acids. Therefore, the generated fundamental knowledge can be used for the prediction of sCW processing parameters to obtain pectic oligosaccharides from similar other agro-industrial co-products, to design a cost effective semi-continuous process as well as to scale-up from bench to pilot plant scale. The different unit operations (extraction, reaction, membrane separation, and drying) investigated in this thesis research can be integrated as proposed in Fig 7.1 towards the development of a pea fiber biorefinery where all the fractions can be utilized and generate additional value. For example, cellulose can be converted into nanocellulose for tissue engineering applications as reported in

previous studies in our laboratory, protein can be converted into bioactive peptides, and fermentable sugars can be used for ethanol production; however, such approaches require further research before the envisioned pea biorefinery can become a reality.

Finally, the outcomes of the present thesis can benefit the pea processing industry as it provides a new and environmentally-friendly process (minimum environmental burden as the use of toxic chemicals was avoided) for value addition to a co-product of pea protein manufacture and its conversion into oligosaccharides with anticipated prebiotic effect and health benefits. Such an approach can contribute to the diversification of the economy in Alberta as the global demand for prebiotics and functional ingredients continues to grow.

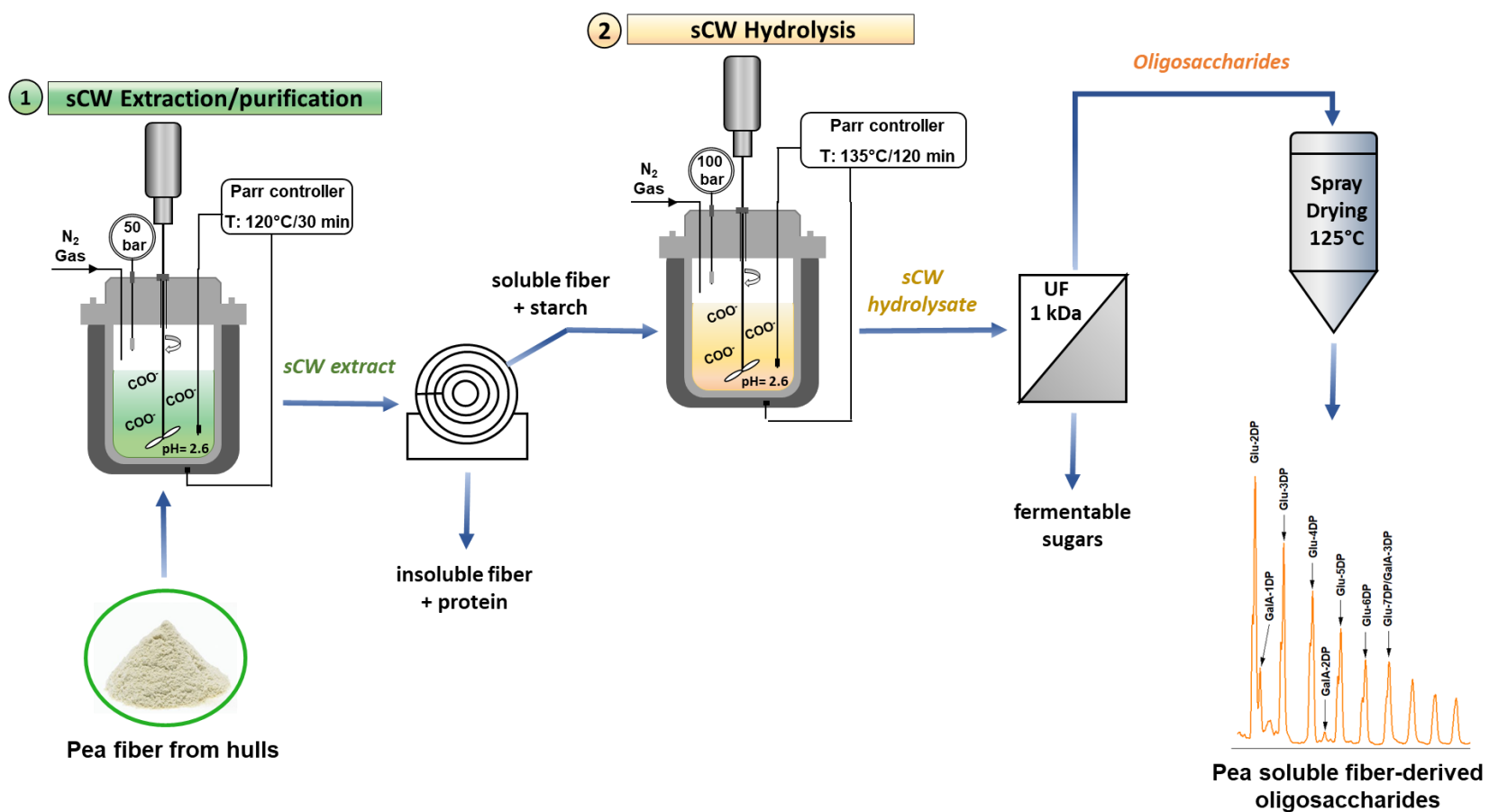


**Fig. 7.1.** Scheme of proposed integrated sCW process for the production of pea soluble fiber-derived oligosaccharides followed by ultrafiltration (UF) and drying.

## 7.2 Recommendations

The use of carboxylic acid-catalyzed sCW systems showed great potential for selective hydrolysis of pectin-rich agro-industrial co-products into value-added products; however, complementary, and future investigations are suggested as follows:

- For the model systems, the use of additional analytical methods to quantify various neutral and acidic compounds is required using tandem mass spectrometry with collision induced dissociation and nuclear magnetic resonance spectroscopy to further improve the kinetic model.
- A more robust model for the sCW water hydrolysis of polygalacturonic acid could be developed, incorporating the effect of temperature, pressure and come-up time or a severity factor that facilitates its extrapolation to other pectic substrates.
- For pea fiber pre-treatment, starch removal from pea fiber substrate by a dry fractionation process can be investigated to facilitate sCW extraction of pea soluble polysaccharides with a higher purity.
- More sCW research is needed to investigate the catalytic effect of carboxylic acids at concentrations above 0.2% w/w and pressures above 100 bar to gain more information of the phenomena under sCW conditions.
- Pressure, temperature and pH of carboxylic acid-catalyzed sCW systems could be tuned in such a way that the properties of the medium eventually lead to oligosaccharides with targeted chemical composition and degree of polymerization.
- The use of anion exchange solid phase extraction cartridges like Oasis Max for separation of neutral and acidic oligosaccharides present in the sCW hydrolysates could aid HILIC-ELSD analysis and further determination of catalyst selectivity.

- The use of additional analytical methods and techniques such as glycosidic linkage analysis, tandem mass spectrometry with collision induced dissociation, and nuclear magnetic resonance spectroscopy are suggested for characterization and fine structure determination of extracted pectic oligosaccharides.
- More research on oligosaccharides purification is needed, in particular on monosaccharides removal to minimize problems of sticky and burnt particles during spray drying.
- Use of nanofiltration membranes with low salt rejection could favor monosaccharides removal and increase the purity of retained soluble pea fiber-derived oligosaccharides.
- A particle-size analysis of dried powders obtained from the soluble pea fiber sCW hydrolysis is recommended to determine the effect of the drying technique on the size distribution and heterogeneity of the powders.
- To improve the powder recovery during PGX drying of pea soluble fiber sCW hydrolysates, the solid content of the hydrolysate can be increased by sequential membrane purification. Also, the level of ethanol can be increased to modify the composition of the ternary mixture to favor precipitation of the oligosaccharides.
- *In vitro* and *in vivo* studies on the bioactivity and prebiotic effect of sCW extracted pea soluble fiber polysaccharides and its derived oligosaccharides can be of great interest for their potential commercial utilization as functional ingredients.
- Future economic feasibility studies of semi-continuous or continuous sCW production of pea fiber-derived oligosaccharides are of interest for their potential manufacture at commercial scale.

## References

- Aghashahi, A. (2020). *Oligosaccharides production and purification from barley bran using sequential supercritical CO<sub>2</sub> extraction, subcritical water hydrolysis and membrane filtration*. MSc thesis, University of Alberta, Edmonton, AB, Canada. <https://doi.org/10.7939/R3-8FB7-2W30>
- Ahuja, K., and Mamtani, K. (2020). *Pea Protein Market Share Forecasts 2020-2026 | Global Report*. <https://www.gminsights.com/industry-analysis/pea-protein-market-report>
- Akin, O., and Temelli, F. (2012). Effect of supercritical CO<sub>2</sub> pressure on polymer membranes. *Journal of Membrane Science*, 399–400, 1–10. <https://doi.org/10.1016/j.memsci.2012.01.017>
- Akin, O., Temelli, F., and Köseoğlu, S. (2012). Membrane applications in functional foods and nutraceuticals. *Critical Reviews in Food Science and Nutrition*, 52(4), 347–371. <https://doi.org/10.1080/10408398.2010.500240>
- Ali-Khan, S. T. (1993). Seed hull content in field pea. *Canadian Journal of Plant Science*, 73(2), 611–613. <https://doi.org/10.4141/cjps93-082>
- Amrutha, N., Hebbar, H. U., Prapulla, S. G., and Raghavarao, K. S. M. S. (2014). Effect of additives on quality of spray-dried fructooligosaccharide powder. *Drying Technology*, 32(9), 1112–1118. <https://doi.org/10.1080/07373937.2014.886257>
- Assegehegn, G., Brito-de la Fuente, E., Franco, J. M., and Gallegos, C. (2019). The importance of understanding the freezing step and its impact on freeze-drying process performance. *Journal of Pharmaceutical Sciences*. 108(4), 1378–1395. <https://doi.org/10.1016/j.xphs.2018.11.039>
- Babbar, N., Dejonghe, W., Gatti, M., Sforza, S., and Elst, K. (2015). Pectic oligosaccharides from agricultural by-products: production, characterization and health benefits. *Critical Reviews in Biotechnology*, 36(4), 1–13. <https://doi.org/10.3109/07388551.2014.996732>
- Bačáková, L., Novotná, K., and Pařzek, M. (2014). Polysaccharides as cell carriers for tissue engineering: The use of cellulose in vascular wall reconstruction. *Physiological Research*. 63(Suppl.1), 29-47. <https://doi.org/10.33549/physiolres.932644>
- Baker, R. W. (2004). Ultrafiltration. In *Membrane Technology and Applications* (pp. 237–274). John Wiley and Sons, Ltd. <https://doi.org/10.1002/0470020393.ch6>
- Baldassarre, S., Babbar, N., Van Roy, S., Dejonghe, W., Maesen, M., Sforza, S., and Elst, K. (2018). Continuous production of pectic oligosaccharides from onion skins with an enzyme membrane reactor. *Food Chemistry*, 267, 101–110. <https://doi.org/10.1016/j.foodchem.2017.10.055>
- Balu, A. M., Budarin, V., Shuttleworth, P. S., Pfaltzgraff, L. A., Waldron, K., Luque, R., and Clark, J. H. (2012). Valorisation of orange peel residues: waste to biochemicals and nanoporous materials. *Chemistry Sustainability Energy Materials*, 5(9), 1694–1697. <https://doi.org/10.1002/cssc.201200381>
- Benali, M., and Boumghar, Y. (2014). Supercritical fluid-assisted drying. In *Handbook of industrial drying*. A. Mujumdar, Ed., CRC Press.
- Berk, Z., and Berk, Z. (2009). Chapter 10 – Membrane processes. In *Food Process Engineering*

- and Technology*, 233–257. Academic Press. <https://doi.org/10.1016/B978-0-12-373660-4.00010-7>
- Biermann, C. J. (1988). Hydrolysis and other cleavages of glycosidic linkages in polysaccharides. *Advances in Carbohydrate Chemistry and Biochemistry*, 46(C), 251–271. [https://doi.org/10.1016/S0065-2318\(08\)60168-7](https://doi.org/10.1016/S0065-2318(08)60168-7)
- Bocek, A. M., Zabivalova, N. M., and Petropavlovskii, G. A. (2001). Determination of the esterification degree of polygalacturonic acid. *Russian Journal of Applied Chemistry*, 74(5), 796–799. <https://doi.org/10.1023/A:1012701219447>
- Bonnin, E., Garnier, C., and Ralet, M. C. (2014). Pectin-modifying enzymes and pectin-derived materials: applications and impacts. *Applied Microbiology and Biotechnology*. 98(2), 519–532. <https://doi.org/10.1007/s00253-013-5388-6>
- Boonyai, P., Bhandari, B., and Howes, T. (2004). Stickiness measurement techniques for food powders: a review. *Powder Technology*, 145, 34–46. <https://doi.org/10.1016/j.powtec.2004.04.039>
- Bornik, M. A., and Kroh, L. W. (2013). D-galacturonic acid as a highly reactive compound in nonenzymatic browning. 1. Formation of browning active degradation products. *Journal of Agricultural and Food Chemistry*, 61(14), 3494–3500. <https://doi.org/10.1021/jf303855s>
- Bouchard, A., Jovanović, N., Hofland, G. W., Jiskoot, W., Mendes, E., Crommelin, D. J. A., and Witkamp, G. J. (2008). Supercritical fluid drying of carbohydrates: Selection of suitable excipients and process conditions. *European Journal of Pharmaceutics and Biopharmaceutics*, 68(3), 781–794. <https://doi.org/10.1016/j.ejpb.2007.06.019>
- Bourdoux, S., Li, D., Rajkovic, A., Devlieghere, F., and Uyttendaele, M. (2016). Performance of drying technologies to ensure microbial safety of dried fruits and vegetables. *Comprehensive Reviews in Food Science and Food Safety*, 15(6), 1056–1066. <https://doi.org/10.1111/1541-4337.12224>
- Buffetto, F., Cornuault, V., Rydahl, M. G., Ropartz, D., Alvarado, C., Echasserieau, V., Le Gall, S., Bouchet, B., Tranquet, O., Verherbruggen, Y., Willats, W. G. T., Knox, J. P., Ralet, M.-C., and Guillon, F. (2015). The deconstruction of pectic rhamnogalacturonan I unmasks the occurrence of a novel arabinogalactan oligosaccharide epitope. *Plant and Cell Physiology*, 56(11), 2181–2196. <https://doi.org/10.1093/pcp/pcv128>
- Burana-osot, J., Soonthornchareonnon, N., Hosoyama, S., Linhardt, R. J., and Toida, T. (2010). Partial depolymerization of pectin by a photochemical reaction. *Carbohydrate Research*, 345(9), 1205–1210. <https://doi.org/10.1016/j.carres.2010.04.007>
- Butt, J. B. (1964). Catalytic selectivity in complex systems. *The Canadian Journal of Chemical Engineering*, 42(5), 211–215.
- Byg, I., Diaz, J., Øgendal, L. H., Harholt, J., Jørgensen, B., Rolin, C., Svava, R., and Ulvskov, P. (2012). Large-scale extraction of rhamnogalacturonan I from industrial potato waste. *Food Chemistry*, 131(4), 1207–1216. <https://doi.org/10.1016/j.foodchem.2011.09.106>
- Canadian Grain Commission. (2020). *Quality of western Canadian peas 2019 - Production*. <https://grainscanada.gc.ca/en/grain-research/export-quality/pulses/peas/2019/3production.html>

- Cano, M. E., García-Martin, A., Comendador Morales, P., Wojtusik, M., Santos, V. E., Kovensky, J., and Ladero, M. (2020). Production of oligosaccharides from agrofood wastes. *Fermentation*, 6(1), 31. <https://doi.org/10.3390/fermentation6010031>
- Cantu-Jungles, T. M., Maria-Ferreira, D., Da Silva, L. M., Baggio, C. H., Werner, M. F. D. P., Iacomini, M., Cipriani, T. R., and Cordeiro, L. M. C. (2014). Polysaccharides from prunes: gastroprotective activity and structural elucidation of bioactive pectins. *Food Chemistry*, 146, 492–499. <https://doi.org/10.1016/j.foodchem.2013.09.093>
- Chen, B., Hoffmann, R., and Cammi, R. (2017). The effect of pressure on organic reactions in fluids—a new theoretical perspective. *Angewandte Chemie - International Edition*. 56(37), 11126–11142. <https://doi.org/10.1002/anie.201705427>
- Chen, J, Liang, R. H., Liu, W., Li, T., Liu, C. M., Wu, S. S., and Wang, Z. J. (2013). Pectic-oligosaccharides prepared by dynamic high-pressure microfluidization and their in vitro fermentation properties. *Carbohydrate Polymers*, 91(1), 175–182. doi: 10.1016/j.carbpol.2012.08.021
- Chiou, D., Langrish, T. A. G., and Braham, R. (2008). The effect of temperature on the crystallinity of lactose powders produced by spray drying. *Journal of Food Engineering*, 86(2), 288–293. <https://doi.org/10.1016/j.jfoodeng.2007.10.005>
- Choct, M., Dersjant-Li, Y., McLeish, J., and Peisker, M. (2010). Soy oligosaccharides and soluble non-starch polysaccharides: a review of digestion, nutritive and anti-nutritive effects in pigs and poultry. *Asian-Australasian Journal of Animal Sciences*, 23(10), 1386–1398. <https://doi.org/10.5713/ajas.2010.90222>
- Chylińska, M., and Szymańska-Chargot, M, Zdunek, A. (2016). FT-IR and FT-Raman characterization of non-cellulosic polysaccharides fractions isolated from plant cell wall. *Carbohydrate Polymers*, 154, 48–54. <https://doi.org/https://doi.org/10.1016/j.carbpol.2016.07.121>
- Ciftci, D., and Saldaña, M. D. A. (2015). Hydrolysis of sweet blue lupin hull using subcritical water technology. *Bioresource Technology*, 194, 75–82. <https://doi.org/10.1016/j.biortech.2015.06.146>
- Cipriani, T. R., Mellinger, C. G., Bertolini, M. L. C., Baggio, C. H., Freitas, C. S., Marques, M. C. A., Gorin, P. A. J., Sasaki, G. L., and Iacomini, M. (2009). Gastroprotective effect of a type I arabinogalactan from soybean meal. *Food Chemistry*, 115(2), 687–690. <https://doi.org/10.1016/j.foodchem.2008.12.017>
- Ciriminna, R., Chavarría-Hernández, N., Inés Rodríguez Hernández, A., and Pagliaro, M. (2015). Pectin: a new perspective from the biorefinery standpoint. *Biofuels, Bioproducts and Biorefining*, 9(4), 368–377. <https://doi.org/10.1002/bbb.1551>
- Coenen, G. J., Bakx, E. J., Verhoef, R. P., Schols, H. A., and Voragen, A. G. J. (2007). Identification of the connecting linkage between homo- or xylogalacturonan and rhamnogalacturonan type I. *Carbohydrate Polymers*, 70(2), 224–235. <https://doi.org/10.1016/j.carbpol.2007.04.007>
- Combo, A., Aguedo, M., Goffin, D., and Wathelet, B. (2012). Enzymatic production of pectic oligosaccharides from polygalacturonic acid with commercial pectinase preparations. *Food Bioproducts Process*, 90, 588–596. <https://doi.org/doi:10.1016/j.fbp.2011.09.003>

- Combo, A., Aguedo, M., Quiévy, N., Danthine, S., Goffin, D., Jacquet, N., Blecker, C., Devaux, J., and Paquot, M. (2013). Characterization of sugar beet pectic-derived oligosaccharides obtained by enzymatic hydrolysis. *International Journal of Biological Macromolecules*, 52(1), 148–156. <https://doi.org/10.1016/j.ijbiomac.2012.09.006>
- Conrad, C. M. (1931). The decarboxylation of d-galacturonic acid with special reference to the hypothetical formation of l-arabinose. *Journal of the American Chemical Society*, 53(6), 2282–2287. <https://doi.org/10.1021/ja01357a036>
- Cordes, E. H., and Bull, H. G. (1974). Mechanism and catalysis for hydrolysis of acetals, ketals, and ortho esters. *Chemical Reviews*, 74(5), 581–603. <https://doi.org/10.1021/cr60291a004>
- Couto, R., Wong, E., Seifried, B., Yépez, B., Moquin, P., and Temelli, F. (2020). Preparation of PGX-dried gum arabic and its loading with coQ10 by adsorptive precipitation. *Journal of Supercritical Fluids*, 156, 104662. <https://doi.org/10.1016/j.supflu.2019.104662>
- Cybulska, J., Brzyska, A., Zdunek, A., and Woliński, K. (2014). Simulation of Force Spectroscopy Experiments on Galacturonic Acid Oligomers. *PLoS ONE*, 9(9), e107896. <https://doi.org/10.1371/journal.pone.0107896>
- Dalgetty, D. D., and Baik, B. K. (2006). Fortification of bread with hulls and cotyledon fibers isolated from peas, lentils, and chickpeas. *Cereal Chemistry*, 83(3), 269–274. <https://doi.org/10.1094/CC-83-0269>
- De Marco, I., and Reverchon, E. (2012). Supercritical carbon dioxide+ethanol mixtures for the antisolvent micronization of hydrosoluble materials. *Chemical Engineering Journal*, 187, 401–409. <https://doi.org/10.1016/j.cej.2012.01.135>
- Demain, A., and Phaff, H. J. (1954). Hydrolysis of the oligogalacturonides and pectic acid by yeast polygalacturonase. *Journal of Biology Chemistry*, 210, 381–393. <http://www.jbc.org/>
- Demazeau, G. (2006). High pressure and chemical bonding in materials chemistry. *ChemInform*, 37(39), 799-807. <https://doi.org/10.1002/chin.200639228>
- Diaz, J. V., Anthon, G. E., and Barrett, D. M. (2007). Nonenzymatic degradation of citrus pectin and pectate during prolonged heating: effects of pH, temperature, and degree of methyl esterification. *ACS Publications*, 55(13), 5131–5136. <https://doi.org/10.1021/jf0701483>
- Dinçer, İ., and Zamfirescu, C. (2006). *Drying Phenomena: Theory and Applications* (First Edit). John Wiley and Sons Ltd.
- Do Nascimento, G. E., Iacomini, M., and Cordeiro, L. M. C. (2017). New findings on green sweet pepper (*Capsicum annuum*) pectins: rhamnogalacturonan and type I and II arabinogalactans. *Carbohydrate Polymers*, 171, 292–299. <https://doi.org/10.1016/j.carbpol.2017.05.029>
- Dudziak, G., Traving, M., and Mutter, M. (2008). *Electrofiltration method* (Patent No. US 2008/0156648 A1).
- Durling, N. E., Catchpole, O. J., Tallon, S. J., and Grey, J. B. (2007). Measurement and modelling of the ternary phase equilibria for high pressure carbon dioxide-ethanol-water mixtures. *Fluid Phase Equilibria*, 252(1–2), 103–113. <https://doi.org/10.1016/j.fluid.2006.12.014>
- Eldik, R. Van, Asano, T., and Le Noble, W. J. (1989). Activation and reaction volumes in solution. 2. *Chemical Reviews*, 89(3), 549–688. <https://doi.org/10.1021/cr00093a005>

- Elst, K., Babbar, N., Van Roy, S., Baldassarre, S., Dejonghe, W., Maesen, M., and Sforza, S. (2018). Continuous production of pectic oligosaccharides from sugar beet pulp in a cross flow continuous enzyme membrane reactor. *Bioprocess and Biosystems Engineering*, 41(11), 1717–1729. <https://doi.org/10.1007/s00449-018-1995-z>
- Englyst, H., and Cummings, J. (1984). Simplified method for the measurement of total non-starch polysaccharides by gas - liquid chromatography of constituent sugars as alditol acetates. *The Analyst*, 109(7), 937–942. <https://doi.org/10.1039/an9840900937>
- Englyst, H. N., and Hudson, G. J. (1987). Colorimetric method for routine measurement of dietary fibre as non-starch polysaccharides. A comparison with gas-liquid chromatography. *Food Chemistry*, 24(1), 63–76. [https://doi.org/10.1016/0308-8146\(87\)90084-7](https://doi.org/10.1016/0308-8146(87)90084-7)
- Fellah, A., Anjukandi, P., Waterland, M. R., and Williams, M. a K. (2009). Determining the degree of methylesterification of pectin by ATR/FT-IR: Methodology optimisation and comparison with theoretical calculations. *Carbohydrate Polymers*, 78(4), 847–853. <https://doi.org/10.1016/j.carbpol.2009.07.003>
- Galkin, A., and Lunin, V. (2005). Subcritical and supercritical water: a universal medium for chemical reactions, *Russian Chemical Reviews*, 74 (1), 21–35. <https://doi.org/10.1070/RC2005v074n01ABEH001167>
- Garna, H., Mabon, N., Nott, K., Wathelet, B., and Paquot, M. (2006). Kinetic of the hydrolysis of pectin galacturonic acid chains and quantification by ionic chromatography. *Food Chemistry*, 96(3), 477–484. <https://doi.org/10.1016/j.foodchem.2005.03.002>
- Ghai, K., Gupta, A. K., and Gupta, P. K. (2012). Pectin: a versatile biopolymer with numerous health benefits and medical uses. *Journal of Biologically Active Products from Nature*, 2(4), 250–255. <https://doi.org/10.1080/22311866.2012.10719132>
- Gómez, B., Gullón, B., Remoroza, C., Schols, H. A., Parajó, J. C., and Alonso, J. L. (2014). Purification, characterization, and prebiotic properties of pectic oligosaccharides from orange peel wastes. *Journal of Agricultural and Food Chemistry*, 62(40), 9769–9782. <https://doi.org/10.1021/jf503475b>
- Gómez, B., Gullón, B., Yáñez, R., Parajó, J. C., and Alonso, J. L. (2013). Pectic oligosaccharides from lemon peel wastes: production, purification, and chemical characterization. *Journal of Agricultural and Food Chemistry*, 61(42), 10043–10053. <https://doi.org/10.1021/jf402559p>
- Goula, A., and Adamopoulos, K. (2010). A new technique for spray drying orange juice concentrate. *Innovative Food Science and Emerging Technologies*, 11(2), 342–351. <https://doi.org/10.1016/j.ifset.2009.12.001>
- Guggenbichler, J. P., D. B. tignies Dutz, A., Meissner, P., Schellmoser, S., and Jurenitsch, J. (1997). Acidic oligosaccharides from natural sources block adherence of *Escherichia coli* on uroepithelial cells. *Pharmaceutical and Pharmacological Letters*, 7(1), 35–38.
- Gullón, B., Gómez, B., Martínez-Sabajanes, M., Yáñez, R., Parajó, J. C., and Alonso, J. L. (2013). Pectic oligosaccharides: manufacture and functional properties. *Trends in Food Science and Technology*, 30(2), 153–161. <https://doi.org/10.1016/j.tifs.2013.01.006>
- Gutöhrlein, F., Drusch, S., and Schalow, S. (2018). Towards by-product utilisation of pea hulls: isolation and quantification of galacturonic acid. *Foods*, 7(203), 1–7.

<https://doi.org/10.3390/foods7120203>

- Gutöhrlein, F., Drusch, S., and Schalow, S. (2020). Extraction of low methoxylated pectin from pea hulls via RSM. *Food Hydrocolloids*, 102, 105609. <https://doi.org/doi:10.1016/j.foodhyd.2019.105609>.
- Hanna, M., and York, P. (1996). *Method and apparatus for the formation of particles* (Patent No. WO / 1996/000610).
- Hatanaka, C., and Ozawa, J. (1964). Enzymic degradation of pectic acid part i. limited hydrolysis of pectic acids by carrot exopolysaccharidase. *Agr. Biol. Chem.*, 28(9), 627–632. <https://doi.org/10.1080/00021369.1964.10858279>
- Health-Canada. (2017). *List of Dietary Fibres Reviewed and Accepted by Health Canada's Food Directorate* - Canada.ca. <https://www.canada.ca/en/health-canada/services/publications/food-nutrition/list-reviewed-accepted-dietary-fibres.html>
- Holck, J., Hotchkiss Jr., Arland T. Meyer, A. S., Mikkelsen, J. D., and Rastall, R. A. (2014). Production and bioactivity of pectic oligosaccharides from fruit and vegetable biomass. In *Food oligosaccharides: Production, analysis and bioactivity*. F. J. Moreno and M. L. Sanz (Eds.), John Wiley and Sons, Ltd., 76-86
- Holck, J., Lorentzen, A., Vignæs, L. K., Licht, T. R., Mikkelsen, J. D., and Meyer, A. S. (2011). Feruloylated and nonferuloylated arabinosaccharides from sugar beet pectin selectively stimulate the growth of *bifidobacterium spp.* in human fecal in vitro fermentations. *Journal of Agricultural and Food Chemistry*, 59(12), 6511–6519. <https://doi.org/10.1021/jf200996h>
- Huisman, M. M. H., Fransen, C. T. M., Kamerling, J. P., Vliegenthart, J. F. G., Schols, H. A., and Voragen, A. G. J. (2001). The CDTA-soluble pectic substances from soybean meal are composed of rhamnogalacturonan and xylogalacturonan but not homogalacturonan. *Biopolymers*, 58(3), 279–294. [https://doi.org/10.1002/1097-0282\(200103\)58:3<279::AID-BIP1005>3.0.CO;2-1](https://doi.org/10.1002/1097-0282(200103)58:3<279::AID-BIP1005>3.0.CO;2-1)
- Iwasaki, K. I., and Matsubara, Y. (2000). Purification of pectate oligosaccharides showing root-growth-promoting activity in lettuce using ultrafiltration and nanofiltration membranes. *Journal of Bioscience and Bioengineering*, 89(5), 495–497. [https://doi.org/10.1016/S1389-1723\(00\)89104-5](https://doi.org/10.1016/S1389-1723(00)89104-5)
- Jaya, S., and Das, H. (2009). Glass transition and sticky point temperatures and stability/mobility diagram of fruit powders. *Food and Bioprocess Technology*, 2(1), 89–95. <https://doi.org/10.1007/s11947-007-0047-5>
- Jiménez-Maldonado, M. I., Tiznado-Hernández, M. E., Rascón-Chu, A., Carvajal-Millán, E., Lizardi-Mendoza, J., and Troncoso-Rojas, R. (2018). Analysis of rhamnogalacturonan I fragments as elicitors of the defense mechanism in tomato fruit. *Chilean Journal of Agricultural Research*, 78(3), 339–349. <https://doi.org/10.4067/S0718-58392018000300339>
- Jouppila, K., and Roos, Y. H. (1994). Glass transitions and crystallization in milk powders. *Journal of Dairy Science*, 77(10), 2907–2915. [https://doi.org/10.3168/jds.S0022-0302\(94\)77231-3](https://doi.org/10.3168/jds.S0022-0302(94)77231-3)
- Jung, J., and Perrut, M. (2001). Particle design using supercritical fluids: literature and patent survey. In *Journal of Supercritical Fluids*. 20(3), 179–219. [https://doi.org/10.1016/S0896-8446\(01\)00064-X](https://doi.org/10.1016/S0896-8446(01)00064-X)

- Kacurakova, M., Capek, P., and Sasinkova, V, Wellner, N, Ebringerova, A. (2000). FT-IR study of plant cell wall model compounds: pectic polysaccharides and hemicelluloses. *Carbohydrate Polymers*, 52(2), 195–203. [https://doi.org/10.1016/S0144-8617\(00\)00151-X](https://doi.org/10.1016/S0144-8617(00)00151-X)
- Kamada, T., Nakajima, M., Nabetani, H., Saglam, N., and Iwamoto, S. (2002). Availability of membrane technology for purifying and concentrating oligosaccharides. *European Food Research and Technology*, 214(5), 435–440. <https://doi.org/10.1007/s00217-001-0486-6>
- Khodaei, N., and Karboune, S. (2018). Optimization of enzymatic production of prebiotic galacto/galacto(arabino)-oligosaccharides and oligomers from potato rhamnogalacturonan I. *Carbohydrate Polymers*, 181, 1153–1159. <https://doi.org/10.1016/j.carbpol.2017.11.011>
- Khuwijitjaru, P., Pokpong, A., Klinchongkon, K., and Adachi, S. (2014). Production of oligosaccharides from coconut meal by subcritical water treatment. *International Journal of Food Science and Technology*, 49(8), 1946–1952. <https://doi.org/10.1111/ijfs.12524>
- Kim, Y., Kreke, T., and Ladisch, M. R. (2013). Reaction mechanisms and kinetics of xylo-oligosaccharide hydrolysis by dicarboxylic acids. *AIChE Journal*, 59(1), 188–199. <https://doi.org/10.1002/aic.13807>
- Kirschner, K. ., and Woods, R. . (2001). Solvent interactions determine carbohydrate conformation. *National Academy of Sciences of the United States of America*, 98(19), 10541–10545. <https://www.pnas.org/content/98/19/10541.short>
- Klinchongkon, K., Khuwijitjaru, P., Wiboonsirikul, J., and Adachi, S. (2017). Extraction of oligosaccharides from passion fruit peel by subcritical water treatment. *Journal of Food Process Engineering*, 40(1), e12269. <https://doi.org/10.1111/jfpe.12269>
- Kootstra, A. M. J., Mosier, N. S., Scott, E. L., Beftink, H. H., and Sanders, J. P. M. (2009). Differential effects of mineral and organic acids on the kinetics of arabinose degradation under lignocellulose pretreatment conditions. *Biochemical Engineering Journal*, 43(1), 92–97. <https://doi.org/10.1016/j.bej.2008.09.004>
- Lama-Muñoz, A., Rodríguez-Gutiérrez, G., Rubio-Senent, F., and Fernández-Bolaños, J. (2012). Production, characterization and isolation of neutral and pectic oligosaccharides with low molecular weights from olive by-products thermally treated. *Food Hydrocolloids*, 28(1), 92–104. <https://doi.org/10.1016/j.foodhyd.2011.11.008>
- Lappalainen, M. (2010). *Melting behaviour and quantification of low amorphous levels in sugars and sugar alcohols with DSC techniques*. PhD thesis, Aalto University School of Science and Technology, Espoo, Finland.
- Le Goff, A., Renard, C. M. G. C., Bonnin, E., and Thibault, J. F. (2001). Extraction, purification and chemical characterisation of xylogalacturonans from pea hulls. *Carbohydrate Polymers*, 45(4), 325–334. [https://doi.org/10.1016/S0144-8617\(00\)00271-X](https://doi.org/10.1016/S0144-8617(00)00271-X)
- Leclere, L., Cutsem, P. Van, and Michiels, C. (2013). Anti-cancer activities of pH- or heat-modified pectin. *Frontiers in Pharmacology*. 4 (128), 1-8 . <https://doi.org/10.3389/fphar.2013.00128>
- Lee, J. W., Thomas, L. C., and Schmidt, S. J. (2011). Investigation of the heating rate dependency associated with the loss of crystalline structure in sucrose, glucose, and fructose using a

- thermal analysis approach (Part I). *Journal of Agricultural and Food Chemistry*, 59(2), 684–701. <https://doi.org/10.1021/jf1042344>
- Leijdekkers, A. G. M., Sanders, M. G., Schols, H. A., and Gruppen, H. (2011). Characterizing plant cell wall derived oligosaccharides using hydrophilic interaction chromatography with mass spectrometry detection. *Journal of Chromatography A*, 1218(51), 9227–9235. <https://doi.org/10.1016/j.chroma.2011.10.068>
- Leivas, C. L., Iacomini, M., and Cordeiro, L. M. C. (2015). Structural characterization of a rhamnogalacturonan I-arabinan-type I arabinogalactan macromolecule from starfruit (*Averrhoa carambola* L.). *Carbohydrate Polymers*, 121, 224–230. <https://doi.org/10.1016/j.carbpol.2014.12.034>
- Leterme, P., Théwis, A., Van Leeuwen, P., Monmart, T., and Huisman, J. (1996). Chemical composition of pea fibre isolates and their effect on the endogenous amino acid flow at the ileum of the pig. *Journal of the Science of Food and Agriculture*, 72, 127–134. [https://doi.org/https://doi.org/10.1002/\(SICI\)1097-0010\(199609\)72:1<127::AID-JSFA637>3.0.CO;2-C](https://doi.org/https://doi.org/10.1002/(SICI)1097-0010(199609)72:1<127::AID-JSFA637>3.0.CO;2-C)
- Li, T., Li, S., Du, L., Wang, N., Guo, M., Zhang, J., Yan, F., and Zhang, H. (2010). Effects of haw pectic oligosaccharide on lipid metabolism and oxidative stress in experimental hyperlipidemia mice induced by high-fat diet. *Food Chemistry*, 121(4), 1010–1013. <https://doi.org/10.1016/j.foodchem.2010.01.039>
- Li, Z., Wang, K., and Zhang, Y. (2018). Eco-friendly separation and purification of soybean oligosaccharides via nanofiltration technology. *Separation Science and Technology*, 53(5), 777–785. <https://doi.org/10.1080/01496395.2017.1405983>
- Liu, Z. (2019). *Pressurized Gas eXpanded (PGX) liquid drying of sodium alginate and its loading with coenzyme Q10 by adsorptive precipitation*. MSc thesis, University of Alberta, Edmonton, AB, Canada. <https://doi.org/https://doi.org/10.7939/r3-g8g6-dh98>
- Locatelli, G., Da Silva, G. D., Finkler, L., and Finkler, C. L. L. (2012). Acid hydrolysis of pectin for cell growth of cupriavidus necator. *Biotechnology*, 11(1), 29–36. <https://doi.org/10.3923/biotech.2012.29.36>
- Lopez-Torrez, L., Nigen, M., and Williams, P, Doco, T, Sanchez, C. (2015). Acacia senegal vs. Acacia seyal gums—Part 1: composition and structure of hyperbranched plant exudates. *Food Hydrocolloids*, 51, 41–53. <https://doi.org/https://doi.org/10.1016/j.foodhyd.2015.04.019>
- Lu, Y., and Mosier, N. S. (2007). Biomimetic catalysis for hemicellulose hydrolysis in corn stover. *Biotechnology Progress*, 23(1), 116–123. <https://doi.org/10.1021/bp060223e>
- Lubrano, C., Flavet, L., Saintigny, G., and Jean-Renaud. (2004). Oligosaccharides in cosmetic or dermatological compositions for stimulating adhesion of keratinocytes to major proteins of the dermoepidermal junction and restoration of epidermal cohesion (Patent No. US 2004224892).
- Maguire, O. R., and O'Donoghue, A. C. (2015). *Chapter 3. Homogeneous Acid Catalysis in Nonasymmetric Synthesis*. In Sustainable catalysis: without metals or other endangered elements, Part 1, Royal Society of Chemistry Publishing, 38–64. <https://doi.org/10.1039/9781782622093-00038>

- Makio, M. (1965). Polysaccharides of soybean seeds. *Agricultural and Biological Chemistry*, 29(6), 564–573. <https://doi.org/10.1080/00021369.1965.10858424>
- Mansel, B. W., Chen, H.-L., Ryan, T. M., Lundin, L., and Williams, M. A. K. (2020). Polysaccharide conformations measured by solution state x-ray scattering. *Chemical Physics Letters*, 739, 136951. <https://doi.org/10.1016/j.cplett.2019.136951>
- Marry, M., McCann, M. C., Kolpak, F., White, A. R., Stacey, N. J., and Roberts, K. (2000). Extraction of pectic polysaccharides from sugar-beet cell walls. *Journal of the Science of Food and Agriculture*, 80(1), 17–28. [https://doi.org/10.1002/\(SICI\)1097-0010\(20000101\)80:1<17::AID-JSFA491>3.0.CO;2-4](https://doi.org/10.1002/(SICI)1097-0010(20000101)80:1<17::AID-JSFA491>3.0.CO;2-4)
- Marshall, W. L., and Frank, E. U. (1981). Ion product of water substance, 0-1000 c, 1-10,000 bars new international formulation and its background. *Journal of Physical and Chemical Reference Data*, 10, 295–304.
- Martinez-Montegudo, S. I., and Saldaña, M. D. . (2014). Chemical Reactions in Food Systems at High Hydrostatic Pressure. *Food Engineering Reviews*, 6, 105–126. <https://doi.org/10.1007/s12393-014-9087-6>
- Martínez, M., Yáñez, R., Alonsó, J. L., and Parajó, J. C. (2010). Chemical production of pectic oligosaccharides from orange peel wastes. *Industrial and Engineering Chemistry Research*, 49(18), 8470–8476. <https://doi.org/10.1021/ie101066m>
- McNaught, A. D. (1996). Nomenclature of carbohydrates (IUPAC recommendations 1996). *Pure and Applied Chemistry*, 68(10), 1925. <https://doi.org/10.1351/pac199668101919>
- Mikshina, P. V., Petrova, A. A., and Gorshkova, T. A. (2015). Functional diversity of rhamnogalacturonans I. *Russian Chemical Bulletin*, 64(5), 1014–1023. <https://doi.org/10.1007/s11172-015-0970-y>
- Miyazawa, T., and Funazukuri, T. (2004). Hydrothermal production of mono(galacturonic acid) and the oligomers from poly(galacturonic acid) with water under pressures. *Industrial and Engineering Chemistry Research*, 43(10), 2310–2314. <https://doi.org/10.1021/ie0202672>
- Mohnen, D. (2008). Pectin structure and biosynthesis. *Current Opinion in Plant Biology*, 11(3), 266–277. <https://doi.org/10.1016/j.pbi.2008.03.006>
- Möllér, M., Nilges, P., Harnisch, F., Schröder, U. (2011). Subcritical water as reaction environment: fundamentals of hydrothermal biomass transformation. *ChemSusChem*, 4(5), 566-579. <https://doi.org/10.1002/cssc.201000341>
- Molnár, Á. (2011). Acids and Acid Catalysis-Homogeneous. In *Encyclopedia of Catalysis*. John Wiley and Sons, Inc. <https://doi.org/10.1002/0471227617.eoc002.pub2>
- Moskovitz, D., and Kim, Y. (2004). Dietary fiber. In *Encyclopedia of Gastroenterology* (pp. 597–612). <https://doi.org/10.1016/B0-12-386860-2/00184-2>
- Moss, G. P., Smith, P. A. S., & Tavernier, D. (1995). Glossary of class names of organic compounds and reactive intermediates based on structure (IUPAC recommendations 1995). *Pure and Applied Chemistry*, 67(8–9), 1307–1375. <https://doi.org/10.1351/pac199567081307>

- Mulder, M. (1996). Materials and material properties. In *Basic Principles of Membrane Technology*. Springer Netherlands, 22–70. [https://doi.org/10.1007/978-94-009-1766-8\\_2](https://doi.org/10.1007/978-94-009-1766-8_2)
- Munarin, F., Tanzi, M. C., and Petrini, P. (2012). Advances in biomedical applications of pectin gels. *International Journal of Biological Macromolecules*, 51, 681–689. <https://doi.org/10.1016/j.ijbiomac.2012.07.002>
- Muñoz-Almagro, N., Valadez-Carmona, L., Mendiola, J. A., Ibáñez, E., and Villamiel, M. (2019). Structural characterisation of pectin obtained from cacao pod husk. comparison of conventional and subcritical water extraction. *Carbohydrate Polymers*, 217, 69–78. <https://doi.org/10.1016/j.carbpol.2019.04.040>
- Muralidhara, H. S. (2010). Challenges of membrane technology in the XXI century. In *Membrane Technology*. Elsevier Ltd., 19–32. <https://doi.org/10.1016/B978-1-85617-632-3.00002-1>
- Muzaffar, K. (2015). Stickiness problem associated with spray drying of sugar and acid rich foods: a mini review. *Journal of Nutrition and Food Sciences*, s12(003), 1-3 <https://doi.org/10.4172/2155-9600.s12-003>
- Nabarlatz, D., Ebringerová, A., and Montané, D. (2007). Autohydrolysis of agricultural by-products for the production of xylo-oligosaccharides. *Carbohydrate Polymers*, 69(1), 20–28. <https://doi.org/10.1016/j.carbpol.2006.08.020>
- Nabarlatz, D., Farriol, X., and Montané, D. (2004). Kinetic modeling of the autohydrolysis of lignocellulosic biomass for the production of hemicellulose-derived oligosaccharides. *Industrial and Engineering Chemistry Research*, 43(15), 4124–4131. <https://doi.org/10.1021/ie034238i>
- Nakamura, A., Furuta, H., Maeda, H., Takao, T., and Nagamatsu, Y. (2014). Structural studies by stepwise enzymatic degradation of the main backbone of soybean soluble polysaccharides consisting of galacturonan and rhamnogalacturonan. *Bioscience, Biotechnology, and Biochemistry*, 66(6), 1301–1313. <https://doi.org/10.1271/bbb.66.1301>
- Nesterenko, V., Nesterenko, A., Babenko, V., Yerkovich, T., and Babenko, I. (2004). Reducing the 137Cs-load in the organism of “Chernobyl” children with apple-pectin. *Swiss Medical Weekly*, 134(1–2), 24–27. <https://doi.org/2004/01/smw-10223>
- Nishad, J., Selvan, C. J., Mir, S. A., and Bosco, S. J. D. (2017). Effect of spray drying on physical properties of sugarcane juice powder (*Saccharum officinarum L.*). *Journal of Food Science and Technology*, 54(3), 687–697. <https://doi.org/10.1007/s13197-017-2507-x>
- Noguchi, M., Hasegawa, Y., and Suzuki, S, Nakazawa, M. (2020). Determination of chemical structure of pea pectin by using pectinolytic enzymes. *Carbohydrate Polymers*, 231, 115738. <https://doi.org/10.1016/j.carbpol.2019.115738>
- Nosworthy, M. G., Neufeld, J., Frohlich, P., Young, G., Malcolmson, L., and House, J. D. (2017). Determination of the protein quality of cooked Canadian pulses. *Food Science and Nutrition*, 5(4), 896–903. <https://doi.org/10.1002/fsn3.473>
- Øbro, J., Harholt, J., Scheller, H. V., and Orfila, C. (2004). Rhamnogalacturonan I in *Solanum tuberosum* tubers contains complex arabinogalactan structures. *Phytochemistry*, 65(10), 1429–1438. <https://doi.org/10.1016/j.phytochem.2004.05.002>
- Ochoa-Villarreal, M, Aispuro-Hernández, E, Vargas-Arispuro, I, Martinez-Tellez, M., and 2012.

- (2012). Plant cell wall polymers: function, structure and biological activity of their derivatives. In *Polimerization*. A. De Souza-Gomez (Ed.), InTech publisher. <https://doi.org/10.5772/46094>
- Ohno, Y., and Ward, K. (1961). Acid epimerization of d-glucose. *Journal of Organic Chemistry*, 26(10), 3928–3931. <https://doi.org/10.1021/jo01068a070>
- Olano-Martin, E., Gibson, G. R., and Rastall, R. A. (2002). Comparison of the in vitro bifidogenic properties of pectins and pectic-oligosaccharides. *Journal of Applied Microbiology*, 93(3), 505–511. <https://doi.org/10.1046/j.1365-2672.2002.01719.x>
- Olano-Martin, E., Mountzouris, K. C., Gibson, G. R., and Rastall, R. A. (2001). Continuous production of pectic oligosaccharides in an enzyme membrane reactor. *Journal of Food Science*, 66(7), 966–971. <https://doi.org/10.1111/j.1365-2621.2001.tb08220.x>
- Olano-Martín, E., Rimbach, G., Gibson, G., and Rastall, R. (2003). Pectin and pectic-oligosaccharides induce apoptosis in in vitro human colonic adenocarcinoma cells. *Anticancer research*, 23(1A), 341–346.
- Olano-Martin, Estibaliz, Williams, M. R., Gibson, G. R., and Rastall, R. A. (2003). Pectins and pectic-oligosaccharides inhibit Escherichia coli O157:H7 Shiga toxin as directed towards the human colonic cell line HT29 . *FEMS Microbiology Letters*, 218(1), 101–105. <https://doi.org/10.1111/j.1574-6968.2003.tb11504.x>
- Onumpai, C., Kolida, S., Bonnin, E., and Rastall, R. A. (2011). Microbial utilization and selectivity of pectin fractions with various structures. *Applied and Environmental Microbiology*, 77(16), 5747–5754. <https://doi.org/10.1128/AEM.00179-11>
- Palanivelu, P. (2006). Polygalacturonases: active site analyses and mechanism of action. *Indian Journal of Biotechnology*, 5, 148-162.
- Papadakis, S. E., Gardeli, C., and Tzia, C. (2007). Drying technology spray drying of raisin juice concentrate spray drying of raisin juice concentrate. *Drying Technology*, 24(2), 173–180. <https://doi.org/10.1080/07373930600559019>
- Park, J. H., and Park, S. Do. (2002). Kinetics of cellobiose decomposition under subcritical and supercritical water in continuous flow system. *Korean Journal of Chemical Engineering*, 19(6), 960–966. <https://doi.org/10.1007/BF02707218>
- Paulionis, L., Walters, B., and Li, K. (2015). Authorised EU health claims on pectins. *Foods, Nutrients and Food Ingredients with Authorised EU Health Claims*, 2, 153–174. <https://doi.org/10.1016/B978-1-78242-382-9.00009-8>
- Pettolino, F., Walsh, C., Fincher, G., Protocols, A. B.-N., and 2012, U. (2012). Determining the polysaccharide composition of plant cell walls. *Nature Protocols*, 7, 1590–1607. <https://doi.org/https://doi.org/10.1038/nprot.2012.081>
- Pinelo, M., Jonsson, G., and Meyer, A. S. (2009). Membrane technology for purification of enzymatically produced oligosaccharides: Molecular and operational features affecting performance. *Separation and Purification Technology*, 70 (1), 1–11. <https://doi.org/10.1016/j.seppur.2009.08.010>
- Pinheiro, E. R., Silva, I. M. D. A., Gonzaga, L. V., Amante, E. R., Teófilo, R. F., Ferreira, M. M. C., and Amboni, R. D. M. C. (2008). Optimization of extraction of high-ester pectin from

- passion fruit peel (*Passiflora edulis flavicarpa*) with citric acid by using response surface methodology. *Bioresource Technology*, 99(13), 5561–5566. <https://doi.org/10.1016/j.biortech.2007.10.058>
- Polamarasetty, J., Das, M., and Das, S. K. (2009). Effect of moisture content on glass transition and sticky point temperatures of sugarcane, palmyra-palm and date-palm jaggery granules. *International Journal of Food Science and Technology*, 45(1), 94–104.
- Proseus, T. E., and Boyer, J. S. (2012). Pectate chemistry links cell expansion to wall deposition in *Chara corallina*. *Plant Signaling and Behavior*, 7 (11), 1490. <https://doi.org/10.4161/psb.21777>
- Ralet, M. C., Buffetto, F., Capron, I., and Guillon, F. (2016). Cell wall polysaccharides of potato. In *Advances in Potato Chemistry and Technology: Second Edition*, Elsevier Inc., 33–56. <https://doi.org/10.1016/B978-0-12-800002-1.00002-9>
- Ralet, M., Della-Valle, G., and Thibault, J. (1993). Raw and extruded fibre from pea hulls. Part I: Composition and physico-chemical properties. *Carbohydrate Polymers*, 20(1), 17–23. [https://doi.org/https://doi.org/10.1016/0144-8617\(93\)90028-3](https://doi.org/https://doi.org/10.1016/0144-8617(93)90028-3)
- Reichert, R. D. (1981). Quantitative isolation and estimation of cell wall material from dehulled (*Pisum Sativum*) flours and concentrates. *Cereal Chemistry (USA)*, 58, 266–70.
- Remoroza, C., Cord-Landwehr, S., Leijdekkers, A. G. M., Moerschbacher, B. M., Schols, H. A., and Gruppen, H. (2012). Combined HILIC-ELSD/ESI-MS enables the separation, identification and quantification of sugar beet pectin derived oligomers. *Carbohydrate Polymers*, 90(1), 41–48. <https://doi.org/10.1016/j.carbpol.2012.04.058>
- Renard, C. M. G. C., Lahaye, M., Mutter, M., Voragen, F. G. J., and Thibault, J. F. (1997). Isolation and structural characterisation of rhamnogalacturonan oligomers generated by controlled acid hydrolysis of sugar-beet pulp. *Carbohydrate Research*, 305(2), 271–280. [https://doi.org/10.1016/S0008-6215\(97\)10028-3](https://doi.org/10.1016/S0008-6215(97)10028-3)
- Rodriguez-Nogales, J. M., Ortega, N., Perez-Mateos, M., and Busto, M. D. (2008). Pectin hydrolysis in a free enzyme membrane reactor: an approach to the wine and juice clarification. *Food Chemistry*, 107(1), 112–119. <https://doi.org/10.1016/j.foodchem.2007.07.057>
- Rogalinski, T., Liu, K., Albrecht, T., and Brunner, G. (2008). Hydrolysis kinetics of biopolymers in subcritical water. *Journal of Supercritical Fluids*, 46(3), 335–341. <https://doi.org/10.1016/j.supflu.2007.09.037>
- Saavedra-Leos, M. Z., Alvarez-Salas, C., Esneider-Alcalá, M. A., Toxqui-Terán, A., Pérez-García, S. A., and Ruiz-Cabrera, M. A. (2012). Towards an improved calorimetric methodology for glass transition temperature determination in amorphous sugars. *CyTA - Journal of Food*, 10(4), 258–267. <https://doi.org/10.1080/19476337.2011.639960>
- Saeman, J. F. (1945). Kinetics of Wood Saccharification - Hydrolysis of cellulose and decomposition of sugars in dilute acid at high temperature. *Industrial and Engineering Chemistry*, 37(1), 43–52. <https://doi.org/10.1021/ie50421a009>
- Saldaña, M. D. A., dos Reis Coimbra, J. S., and Cardozo-Filho, L. (2015). Recovery, encapsulation and stabilization of bioactives from food residues using high pressure techniques. *Current Opinion in Food Science*, 5, 76–85. <https://doi.org/10.1016/j.cofs.2015.09.001>

- Saldaña, M. D. A., and Valdivieso-Ramírez, C. S. (2015). Pressurized fluid systems: Phytochemical production from biomass. *Journal of Supercritical Fluids*, 96, 228–244. <https://doi.org/10.1016/j.supflu.2014.09.037>
- Salak Asghari, F., and Hiroyuki Yoshida. (2006). Acid-catalyzed production of 5-hydroxymethyl furfural from D-fructose in subcritical water. *Industrial & Engineering Chemistry Research*, 45(7), 2163–2173. <https://pubs.acs.org/doi/10.1021/ie051088y>
- Saleki-Gerhardt, A., Ahlneck, C., and Zografí, G. (1994). Assessment of disorder in crystalline solids. *International Journal of Pharmaceutics*, 101(3), 237–247. [https://doi.org/10.1016/0378-5173\(94\)90219-4](https://doi.org/10.1016/0378-5173(94)90219-4)
- Saleki-Gerhardt, A., and Zografí, G. (1994). Non-isothermal and isothermal crystallization of sucrose from the amorphous state. *Pharmaceutical Research: An Official Journal of the American Association of Pharmaceutical Scientists*, 11(8), 1166–1173. <https://doi.org/10.1023/A:1018945117471>
- Sarrade, S., Guizard, C., and Rios, G. M. (2002). Membrane technology and supercritical fluids: chemical engineering for coupled processes. *Desalination*, 144(1–3), 137–142. [https://doi.org/10.1016/S0011-9164\(02\)00302-8](https://doi.org/10.1016/S0011-9164(02)00302-8)
- Schols, H. A., Posthumus, M. A., and Voragen, A. G. J. (1990). Structural features of hairy regions of pectins isolated from apple juice produced by the liquefaction process. *Carbohydrate Research*, 206(1), 117–129. [https://doi.org/10.1016/0008-6215\(90\)84011-I](https://doi.org/10.1016/0008-6215(90)84011-I)
- Seymour, G., and Knox, J. (2002). *Pectins and their manipulation*. Blackwell Publishing Ltd.
- Shishir, M. R. I., and Chen, W. (2017). Trends of spray drying: a critical review on drying of fruit and vegetable juices. *Trends in Food Science and Technology*, 65, 49–67. <https://doi.org/10.1016/j.tifs.2017.05.006>
- Simperler, A., Kornherr, A., Chopra, R., Bonnet, P. A., Jones, W., Motherwell, W. D. S., and Zifferer, G. (2006). Glass transition temperature of glucose, sucrose, and trehalose: An experimental and in silico study. *Journal of Physical Chemistry B*, 110(39), 19678–19684. <https://doi.org/10.1021/jp063134t>
- Sluiter, A., Hames, B., Ruiz, R., and Scarlata, C, Sluiter, J, Templeton, D. (2008). *Determination of ash in biomass laboratory analytical procedure*.
- Smýkal, P., Vernoud, V., Blair, M. W., Soukup, A., and Thompson, R. D. (2014). The role of the testa during development and in establishment of dormancy of the legume seed. *Frontiers in Plant Science*, 5, 1–19. <https://doi.org/10.3389/fpls.2014.00351>
- Sosa, N., Gerbino, E., Golowczyc, M. A., Schebor, C., Gómez-Zavaglia, A., and Tymczyszyn, E. E. (2016). Effect of galacto-oligosaccharides: maltodextrin matrices on the recovery of lactobacillus plantarum after spray-drying. *Frontiers in Microbiology*, 7, 584. <https://doi.org/10.3389/fmicb.2016.00584>
- Staples, M., and Rolke, J. (2015). *Modified pectins, compositions and methods related thereto* (Patent No. US 9181354 B2).
- Stratilová, E., Ria Džú Rová, M., Malovíková, A., and Omelková, J. (2005). Oligogalacturonate hydrolase from carrot roots. *Zeitschrift für Naturforschung*, 60, 900–905. <http://www.znaturforsch.com>

- Sun, L., Ropartz, D., Cui, L., Shi, H., Ralet, M. C., and Zhou, Y. (2019). Structural characterization of rhamnogalacturonan domains from *Panax ginseng* C. A. Meyer. *Carbohydrate Polymers*, 203, 119–127. <https://doi.org/10.1016/j.carbpol.2018.09.045>
- Suzuki, T., Tomita-Yokotani, K., Yoshida, S., Takase, Y., Kusakabe, I., and Hasegawa, K. (2002). Preparation and isolation of oligogalacturonic acids and their biological effects in Cockscomb (*Celosia argentea* L.) seedlings. *Journal Plant Growth Regulation*, 21(3), 209–215. <https://doi.org/10.1007/s003440010060>
- Syamaladevi, R. M., Barbosa-Cánovas, G. V., Schmidt, S. J., and Sablani, S. S. (2015). *Molecular weight effects on enthalpy relaxation and fragility of amorphous carbohydrates*. In: Water Stress in Biological, Chemical, Pharmaceutical and Food Systems. Gutiérrez-López G., Alamilla-Beltrán L., del Pilar Buera M., Welti-Chanes J., Parada-Arias E., Barbosa-Cánovas G. (eds), Food Engineering Series. Springer, New York, 161–174. 161NY. [https://doi.org/10.1007/978-1-4939-2578-0\\_13](https://doi.org/10.1007/978-1-4939-2578-0_13)
- Szymanska-Chargot, M., and Zdunek, A. (2012). Use of FT-IR spectra and PCA to the bulk characterization of cell wall residues of fruits and vegetables along a fraction process. *Food Biophysics*, 8, 29–42. <https://doi.org/10.1007/s11483-012-9279-7>
- Takahashi, A., Suetsugu, T., Tanaka, M., Hoshino, M., Sasaki, M., and Goto, M. (2011). *Facilitatory effect of dissolved carbon dioxide in subcritical water for pectin hydrolysis*. [https://www.researchgate.net/profile/Munehiro\\_Hoshino/publication/260448689\\_Facilitatory\\_effect\\_of\\_dissolved\\_carbon\\_dioxide\\_in\\_subcritical\\_water\\_for\\_pectin\\_hydrolysis/data/0a85e5315811f82349000000/Facilitatory-effect-of-dissolved-carbon-dioxide-in-subcritical-water-for-pectin-hydrolysis.pdf](https://www.researchgate.net/profile/Munehiro_Hoshino/publication/260448689_Facilitatory_effect_of_dissolved_carbon_dioxide_in_subcritical_water_for_pectin_hydrolysis/data/0a85e5315811f82349000000/Facilitatory-effect-of-dissolved-carbon-dioxide-in-subcritical-water-for-pectin-hydrolysis.pdf)
- Te Booy, M., de Ruiter, R. A., and de Meere, A. (1992). Evaluation of the physical stability of freeze-dried sucrose-containing formulations by differential scanning calorimetry. *Pharmaceutical Research: An Official Journal of the American Association of Pharmaceutical Scientists*, 9(1), 109–114. <https://doi.org/10.1023/A:1018944113914>
- Temelli, F. (2018). Perspectives on the use of supercritical particle formation technologies for food ingredients. *Journal of Supercritical Fluids*, 134, 244–251. <https://doi.org/10.1016/j.supflu.2017.11.010>
- Temelli, F., and Seifried, B. (2016). *Supercritical fluid treatment of high molecular weight biopolymers* (Patent No. 9,249,266).
- Thakur, B. R., Singh, R. K., and Handa, A. K. (1997). Chemistry and uses of pectin - a review. *Critical Reviews in Food Science and Nutrition*, 37(1), 47–73. <https://doi.org/10.1080/10408399709527767>
- Thibault, J. F., Renard, C. M. G. C., Axelos, M. A. V., Roger, P., and Crepeau, M. J. (1993). Studies of the length of homogalacturonic regions in pectins by acid hydrolysis. *Carbohydrate Research*, 238, 271–286. [https://doi.org/10.1016/0008-6215\(93\)87019-O](https://doi.org/10.1016/0008-6215(93)87019-O)
- Thibault, J., Renard, C., Axelos, M., and Roger, P. (1993). Studies of the length of homogalacturonic regions in pectins by acid hydrolysis. *Carbohydrate Research*, 238, 271–286. <https://www.sciencedirect.com/science/article/pii/000862159387019O>
- Tingirikari, J. M. R. (2018). Microbiota-accessible pectic poly- and oligosaccharides in gut health. *Food and Function*, 9 (10), 5059–5073. Royal Society of Chemistry.

<https://doi.org/10.1039/c8fo01296b>

- Truong, V., Bhandari, B. R., and Howes, T. (2005). Optimization of co-current spray drying process of sugar-rich foods. Part I-Moisture and glass transition temperature profile during drying. *Journal of Food Engineering*, 71(1), 55–65. <https://doi.org/10.1016/j.jfoodeng.2004.10.017>
- Tsourouflis, S., Flink, J. M., and Karel, M. (1976). Loss of structure in freeze-dried carbohydrates solutions: Effect of temperature, moisture content and composition. *Journal of the Science of Food and Agriculture*, 27(6), 509–519. <https://doi.org/10.1002/jsfa.2740270604>
- Ueno, H., Tanaka, M., Hosino, M., Sasaki, M., and Goto, M. (2008). Extraction of valuable compounds from the flavedo of Citrus junos using subcritical water. *Separation and Purification Technology*, 62(3), 513–516. <https://doi.org/10.1016/j.seppur.2008.03.004>
- Usuki, C., Kimura, Y., and Adachi, S. (2008). Degradation of pentoses and hexouronic acids in subcritical water. *Chemical Engineering and Technology*, 31(1), 133–137. <https://doi.org/10.1002/ceat.200700391>
- Valdivieso-Ramirez, C. S. (2016). *Subcritical water extraction and reaction of bioactive pectic polysaccharides*. MSc thesis, University of Alberta, Edmonton, AB, Canada. <https://doi.org/https://doi.org/10.7939/R37659T2F>
- Van Aubel, G., Buonatesta, R., and Van Cutsem, P. (2014). COS-OGA: A novel oligosaccharidic elicitor that protects grapes and cucumbers against powdery mildew. *Crop Protection*, 65, 129–137. <https://doi.org/10.1016/j.cropro.2014.07.015>
- Verma, P., Shah, N. G., and Mahajani, S. M. (2020). A novel technique to characterize and quantify crystalline and amorphous matter in complex sugar mixtures. *Food Analytical Methods*, 13(11), 2087–2101. <https://doi.org/10.1007/s12161-020-01789-1>
- Voragen, A. G. J., Coenen, G. J., Verhoef, R. P., and Schols, H. A. (2009). Pectin, a versatile polysaccharide present in plant cell walls. *Structural Chemistry*, 20(2), 263–275. <https://doi.org/10.1007/s11224-009-9442-z>
- Wang, H., Shi, S., Bao, B., Li, X., and Wang, S. (2015). Structure characterization of an arabinogalactan from green tea and its anti-diabetic effect. *Carbohydrate Polymers*, 124, 98–108. <https://doi.org/10.1016/j.carbpol.2015.01.070>
- Wang, X., Chen, Q., and Lü, X. (2014). Pectin extracted from apple pomace and citrus peel by subcritical water. *Food Hydrocolloids*, 38, 129–137. <https://doi.org/10.1016/j.foodhyd.2013.12.003>
- Wrzosek, K., Moravčík, J., Antošová, M., Illeová, V., and Polakovič, M. (2013). Spray drying of the mixtures of mono-, di-, and oligosaccharides. *Acta Chimica Slovaca*, 6(2), 177–181. <https://doi.org/10.2478/acs-2013-0028>
- Wu, L., Chang, K. F., Conner, R. L., Strelkov, S., Fredua-Agyeman, R., Hwang, S. F., and Feindel, D. (2018). *Aphanomyces euteiches*: A threat to Canadian field pea production. *Engineering*, 4(4), 542–551. <https://doi.org/10.1016/j.eng.2018.07.006>
- Zhang, L., Qiu, J., Cao, X., Zeng, X., Tang, X., Sun, Y., and Lin, L. (2019). Drying methods, carrier materials, and length of storage affect the quality of xylooligosaccharides. *Food Hydrocolloids*, 94, 439–450. <https://doi.org/10.1016/j.foodhyd.2019.03.043>

- Zhang, L., Zeng, X., Fu, N., Tang, X., Sun, Y., and Lin, L. (2018). Maltodextrin: A consummate carrier for spray-drying of xylooligosaccharides. *Food Research International*, *106*, 383–393. <https://doi.org/10.1016/j.foodres.2018.01.004>
- Zhang, S., Hu, H., Wang, L., Liu, F., and Pan, S. (2018). Preparation and prebiotic potential of pectin oligosaccharides obtained from citrus peel pectin. *Food Chemistry*, *244*, 232–237. <https://doi.org/doi:10.1016/j.foodchem.2017.10.071>.
- Zhao, J., Zhang, F., Liu, X., St. Ange, K., Zhang, A., Li, Q., and Linhardt, R. J. (2017). Isolation of a lectin binding rhamnogalacturonan-I containing pectic polysaccharide from pumpkin. *Carbohydrate Polymers*, *163*, 330–336. <https://doi.org/10.1016/j.carbpol.2017.01.067>
- Zhao, Y., and Saldaña, M. D. A. (2019). Hydrolysis of cassava starch, chitosan and their mixtures in pressurized hot water media. *Journal of Supercritical Fluids*, *147*, 293–301. <https://doi.org/10.1016/j.supflu.2018.11.013>
- Zheng, Y., Li, L., Feng, Z., Wang, H., Mayo, K. H., Zhou, Y., and Tai, G. (2018). Preparation of individual galactan oligomers, their prebiotic effects, and use in estimating galactan chain length in pectin-derived polysaccharides. *Carbohydrate Polymers*, *199*, 526–533. <https://doi.org/10.1016/j.carbpol.2018.07.048>